Chronic Radiation Doses to Aquatic Biota

Thesis submitted in partial fulfilment of the requirements for the award of the degree of Doctor of Philosophy of the University of Portsmouth

Vithit Pungkun

January 2012

Abstract

Chronic Radiation Doses to Aquatic Biota

On 26 April 1986, the worst nuclear accident in the history of the nuclear industry occurred at Unit 4 of the Chernobyl nuclear power plant (ChNPP) in the Ukraine (at that time a Republic of the Soviet Union) resulting a large amount of radioactive nuclides released into the environment in Russia, Ukraine, Belarus and other European countries. The chronic radiation doses from radioactive nuclides released from the accident are still significant in the freshwater aquatic environment of the 30 km Exclusion Zone around Chernobyl.

In this study, current methods of estimating radiation doses have been further developed by model inter-comparison and testing against empirical data. This research also supports previous work on the effects of radiation on aquatic biota by accurately measuring the external radiation dose in the littoral zone of Svyatoye and Perstok lakes in Belarus.

The testing and critical analysis of five dose assessment models (RESRAD, FASSET, ERICA, R&D128 and the D-Max model) was carried out in order to understand the key factors which influence predictions of both internal and external doses. For the internal dose, studies of the relationship between modelled dose and organism mass showed that mass is a more important factor than organism shape. The predictions of external dose were generally more variable than those for internal dose. The most important factor causing variation in external dose was the assumed habitat of the organism and the occupancy factor.

The Monte Carlo method was used to estimate the uncertainty in internal dose rate caused by the variability of fish mass and fish concentration in real environments. It was found that the variability in Cs-137 activity concentration in different fish was the most important factor contributing to the uncertainty of predictions of internal dose rate. Organism size at different life stages also has a large influence on dose. For young, small, fish, the internal dose is lower than the range of internal doses estimated by the different models, whilst the external dose could be greater than that estimated by models, especially in cases where part of the life cycle is spent on the sediment surface.

Using measured values of tissue activity concentration, the model predictions of doses in Svyatoye and Perstok lakes, show good agreement with each other. In cases when tissue activity concentration data are not available, these have to be estimated from the tissue-water Concentration Ratio (CR). In this case, the predicted internal dose rates (using radionuclide concentration in the water) are more uncertain because of the variation of CR in the models. The model where CR is estimated depending on water chemistry gives the best prediction in this case.

Measurements were made of the beta- and gamma- dose rate in three lakes (Perstok, Svyatoye and Dvorishche) giving profiles of dose as a function of depth. The method for gamma dose rate measurement worked well and a simple model for external gamma dose rate with depth above and below the sediment surface was found to give reasonable agreement with measured values. The beta in situ measurement was not successful and the method would need further investigation.

The modelling studies carried out showed that internal dose rates to fish in Svyatoye and Perstok lakes are lower than or close to the 40 $\mu Gy\ hr^{-1}$ recommended limit for possible impacts from radiation .The external dose rate to insect larvae and benthic fish is much higher than to pelagic fish because the former live in or on the sediment which has a much higher activity concentration than the water. None of the estimated external dose rates in these lakes was higher than 10 $\mu Gy\ hr^{-1}$.

It is concluded that the external dose rates to benthic biota and large fish in these closed lakes are still significant at this long time after the Chernobyl accident. But, radiation effects on these organisms may not be clearly seen, since the dose rates are below or close to guideline limits.

Table of Contents

Declaration

Whilst registered as a candidate for the above degree, I have not been registered for any other research award. The results and conclusions embodied in this thesis are the work of the named candidate and have not been submitted for any other academic award.

List of Tables

List of Figures

Abbreviations

ADC; Analog Output Converter

Ba-137; Barium-137

BCG; Biota Concentration Guide Level

BIV; Bioaccumulation factor

Bq; Becquerels

C; Coulomb

Ca-40; Calcium-40

CaF_2; Calcium Fluoride

C_{air}; air concentration

$CaSO_4$; Calcium Sulphate

CF; Concentration Factor

ChNPP; Chernobyl Nuclear Power Plant

C_{min}; minimum concentration

CR; Concentration ratio

C_s; soil concentration

Cs-137; Caesium-137

C_t; Tissue Activity Concentration

d.w.; dry weight

D; Absorbed Dose

d; day

DCC; Dose Conversion Coefficient

DCF; Dose Conversion Factor

D_{ext}; External Dose Rate

D_{int}; Internal Dose Rate

DNA; Deoxyribonucleic Acid

DOE; Department of Energy

DPUC; Dose Per Unit Concentration Factor

DSTL; Defence Science and Technology Laboratory

EPA; Environmental Protection Agency

eV; Electron Volt

Fe^{2+}; Ferrous ions

Fe^{3+}; Ferric ion

FWHM; Full With at Half Maximum

Ge(Li); Germanium semiconductor detector

Gy; Grey

H; Equivalent Dose

H_0; centroid

H_2O; water

He; Helium

$H_p(0.07)$; personal dose equivalent at 0.07 mm depth

$H_p(10)$; personal dose equivalent at 10 mm depth

HV; High Voltage Power Supply

I; Iodine

IAEA; International Atomic Energy Agency

ICRP; International Commission on Radiological Protection

J; Joule

K; Kerma

K^+; potassium ion

K-40; Potassium-40

KCl; potassium chloride

Kg; Kilogram

Km; Kilometre

km; kilometre

l; litre

LET; Linear Energy Transfer

LiF; Lithium Fluoride

LLD; Lower Level Discriminator

MCA; Multichannel Analyser

Mg; Magnesium

mg; milligram

Mn; Manganese

NaI; Sodium iodide scintillation detector

NH_4^+; Ammonium ion

NRC; Nuclear Regulatory Commission

O_2; Oxygen

PMT; Photomultiplier Tube

R; Range

R; Roentgen

rad; radiation absorbed dose

RAP; Reference Animals and Plants

rem; Roentgen Equivalent Man

SI; International System of Units

Sr-90; strontium-90

Sv; Sievert

TL; Thermoluminescent

TLD; Thermoluminescence Dosimetry

USSR; Soviet Union

w.w.; wet weight

W_R; Radiation Weighting Factor

W_T; Tissue Weighting Factor

X; Exposure

Y-90; Yttrium-90

yr; year

Z_{eff}; The photon effective atomic number

Zr-90; Zirconium-90

Acknowledgement

First and foremost, I owe my deepest gratitude to my supervisors, Dr. Jim Smith and Dr. Chris Dewdney, especially Dr. Jim Smith for the valuable guidance, supervision and support during this project. His willingness to motivate me contributed tremendously to my project. Also, special thanks are expressed to Jim for his patience when reading my struggling English and for taking role the first supervisor following Dr. David Timms who passed away in September 2007. Without him this thesis would not have been possible.

It is honour for me to thanks Belarusian Scientists, Anatoly V. Kudelsky and Vasily I. Pashkevich, for their assistance and taking care of me during field trip in Belarus and contribution useful information during this project. Also, many thanks to Vasily for sediment sampling and taking TLDs back to U.K. In addition, I would like to thank collaborators at the Belarusian State University, Minsk for beta and gamma measurement.

I am grateful to thank Dr. Roger Stokes from Defence Science and Technology Laboratory (DSTL) for reading and evaluating TLDs.

My appreciation is expressed to Robert Mortlock, Gamma Spectrometry specialist, University of Portsmouth for his teaching gamma spectrometry.

I would like to thank the Thai Government for their financial support and for providing me a good opportunity to study and gain my knowledge in a wonderful country.

Many thanks to Jarupa Vipoopinyo, Namphon Khampilang, Mallika Nillorm and Kittisak Chaisan for the wonderful environment in England when I am far away from home. Also I really appreciate all of them for supporting and making my thesis looking better.

I would like to show my gratitude to Somboon Meepoo for his support in a number of ways and for taking care my parents when I stay here.

Last but not least, I would like to show my gratitude to my parents and my aunt for their continued support, their love and encouragement throughout this project. Without all of them, I would never have done so far.

Chapter 1

General Introduction to Radiation and Radiation Dosimetry

1.1 Introduction

On 26 April 1986, the worst nuclear accident in the history of the nuclear industry occurred at Unit 4 of the Chernobyl nuclear power plant (ChNPP) in the Ukraine (at that time a Republic of the Soviet Union) (Anspaugh, Catlin, & Goldman, 1988; IAEA, 2006a, 2006b; J. T. Smith & Beresford, 2005; UNSCEAR, 2000). The explosion of the reactor vessel and the consequent fire continued over 10 days (IAEA, 2006a) and a large amount of radioactive nuclides were released into the environment (IAEA, 2006b; UNSCEAR, 1996). The effect of ionizing radiation from radioactive nuclides released from the accident is still significantly important, especially long half-life radionuclides (IAEA, 2006b). In the past, studies of radioactivity in the environment have primarily been focused on the impact on humans. However, recently there has been a change of emphasis to the protection of the environment from ionising radiation (IAEA, 2003).

The hypothesis of the International Commission on Radiation Protection (ICRP) states that: “If humans are protected from the effects of ionizing radiation, then flora and fauna are also adequately protected” (ICRP, 1977). This approach is no longer considered appropriate because some situations humans are not present or have been removed, or non-human biota (animals and plants) receive much higher doses than humans (Holm, 2004). Few studies have been able to assess the effects of chronic radiation exposure on animal and plant life in its natural environment. The freshwater aquatic environments of the 30 km Exclusion Zone around Chernobyl present a unique opportunity to quantify the effects of chronic radiation doses from ionising radiation on biota (IAEA, 2006b).

In order to assess the effects of chronic radiation on biota, it is necessary to develop effective methods of estimating radiation doses. This research will focus on the in-situ measurement of the radiation exposure received by aquatic organisms and compare these values with predictions of new and existing methods for calculating radiation dose.

1.2 Ionising radiation, radiation quantities and units

Radiation is the energy that comes from a radioactive source or radioactive material. There are two main categories of radiation; non-ionising radiation and ionising radiation. Non-ionising radiation is the radiation that does not have enough energy to remove an electron from an atom or molecule. Examples of non-ionising radiation are ultraviolet, visible light and microwave. Ionising radiation is the radiation that has enough energy to remove an electron from atom. The results of the ionisation process formulate into two fragments: the atom with a positive charge and the free negative charge electron (U.S.EPA, 2009b). The crucial distinction between ionising radiation and non-ionising radiation is their physiological effects. Ionising radiation may cause cancer and other health effects (Boice, 2010), whilst non-ionising radiation has not yet been shown to produce any direct health effects. Currently, there is no conclusive evidence for non-ionising radiations such as Radio Frequency Fields to lead to an increase in cancer in humans (EuropianCommission, 2009). However, further studies of non-ionising radiation effects are necessary to identify the long term human cancer risk. Ionising radiations can occur both as electromagnetic rays, such as X-rays and gamma rays, and particles, such as alpha and beta particles. The ionisations they can produce in plant or animal cells can lead to cellular damage, for example cancer induction by either direct or indirect damage to DNA.

1.2.1 Types of ionising radiation

The most common emissions from radioactive decay are alpha particles, beta particles and gamma rays, whilst positrons, x-rays and neutrons may also be found.

1.2.1.1 Alpha particles

Alpha particles are generally emitted from unstable heavy nuclei which consist of two protons and two neutrons (^{4}He nucleus) (Knoll, 1989). Atomic mass and charge of the alpha particles are 4u and +2 respectively (IAEA & ANSTO, 2004b). The velocity of the alpha particle is about 1/20 of the speed of light when travelling in air (U.S.EPA, 2009a). The alpha particle is a high linear energy transfer (LET) particle because the alpha particles densely deposit their energy in a short track within cells, whilst low-LET radiations such as x rays, gamma rays and beta particles sparsely deposit their energy across their ionization track (UNSCEAR, 2000). Alpha particles (high-LET radiation)

can damage DNA more than low-LET radiation. Low-LET radiations mostly ionise a single strand of DNA (normally DNA has 2 strands) which can be relatively easily repaired by enzymes whilst the “cluster” of several ionisations of high-LET are likely to occur in both strand of DNA which are more difficult to repair (UNSCEAR, 2000). A typical alpha decay is in the following:

$$^{235}_{92}\mathrm{U} \rightarrow {}^{232}_{90}\mathrm{Th} + \alpha$$

In general: $$^{A}_{Z}\mathrm{X} \rightarrow {}^{A-4}_{Z-2}\mathrm{Y} + \alpha$$

1.2.1.2 Beta particles

Beta particles are fast electrons which have been ejected from the nucleus of a radioisotope (Knoll, 1989). Beta emissions are generated when a neutron in the unstable nucleus changes into a proton and an electron. The electron (beta particle) is emitted, whilst the proton remains in the nucleus. The same as electrons, beta particles have small atomic mass (approximately 1/1840 u) and have negative charge (–1e) (IAEA & ANSTO, 2004b). As stated above, beta particles are much lighter than alpha particles and they travel at close to the speed of light. The beta particles have a much lower rate of LET than alpha particles because they lose their energy over a longer distance than alpha particles. However, the beta particles are more penetrating than alpha particles and so are more important in contributing to external dose. A typical beta decay is in the following:

$$^{14}_{6}\mathrm{C} \rightarrow {}^{14}_{7}\mathrm{N} + \beta + \bar{\nu}$$

In general: $$^{A}_{Z}\mathrm{X} \rightarrow {}^{A}_{Z+1}\mathrm{Y} + \beta + \bar{\nu}$$

Where $\bar{\nu}$ is a particle called the anti neutrino, necessary to conserve momentum

1.2.1.3 Gamma and X-rays

Gamma rays (**γ)** are electromagnetic radiation emitted from the excited nucleus of an atom and therefore travel at the speed of light. Gamma rays have no mass and no charge. X-rays are also electromagnetic radiation but gamma rays are produced by changes in the nucleus of an atom, whereas X-rays are produced when atomic electrons undergo a change in orbit or decelerate rapidly (Bremsstrahlung X-rays).

1.2.2 Radiation quantities and units

This work concerns the measurement and estimation of radiation dose received by biota. In this section, a number of relevant terms and definitions are given for the quantities which describe the radiation field (known as radiometric quantities) and the effects produced by the radiation dose (known as dosimetric quantities). The properties of radiation quantities and units are described in various texts and reports (Greening, 1985; IAEA & ANSTO, 2004b; NPL, 2010; Stabin, 2008; UNSCEAR, 1996) and are summarized below.

1.2.2.1 Radiometric quantities

The radiation field (particles or rays) and the quantity of ionization produced by the radiation can be described by the following radiometric quantities.

Energy

The SI unit of energy is the joule. However, when considering particle or electromagnetic ray energies, one joule is a very large unit of energy. The traditional unit of energy of ionising radiation is measured in terms of electronvolts (eV), one electronvolt being the amount of kinetic energy gained by an electron when it is accelerated through one volt of potential difference. In terms of joules:

$$1\ \text{eV} = 1.6 \times 10^{-19}\ \text{J} \qquad (1.1)$$

Fluence (Φ)

Fluence, the number of particles (or photons) passing through unit area, is the quotient of *dN* and *da*, where *dN* is the number of particles incident on a sphere of cross-sectional area *da*; thus

$$\Phi = \frac{dN}{da} \qquad (1.2)$$

Unit: m^{-2}

Exposue (X)

The exposure, the amount of ionisation that gamma and X-rays produce in air**,** is the quotient of *dQ* by *dm* where the value of *dQ* is the total charge of the ions of one sign produced in air when all the electrons (negatrons and positrons) liberated by photons in air of mass *dm* are completely stopped in air. It is noted that this unit is only used for gamma and X-rays and only defined in air.

$$X = \frac{dQ}{dm} \quad (1.3)$$

Unit: $C.kg^{-1}$, The special unit of exposure was originally called the roentgen (R)

$$1R = 2.58x10^{-4}\ C.kg^{-1} \quad (1.4)$$

Kerma (K)

Kerma, the **k**inetic **e**nergy **r**eleased per unit **m**ass of **a**bsorber is a measurement of the kinetic energy of charged particles produced in an absorbing medium by uncharged radiations (photons and neutrons), is the quotient of *dEtr* and *dm*, where *dEtr* is the sum of the initial kinetic energies of all the charged ionizing particles released by uncharged ionizing particles in a material of mass *dm*; thus

$$K_a = \frac{dEtr}{dm} \quad \text{or} \quad (1.5)$$

$$K_a = a\,X \quad (1.6)$$

Where a is the conversion factor applicable for most photon energies between 0.1 and 4 MeV, 33.85 Gy per C kg^{-1}

Unit: $J.kg^{-1}$, The special name for the unit of kerma is gray (Gy)

1.2.2.2 Dosimetric quantities

Dosimetric quantities describe the amount of energy deposited when radiation passes through a material.

Absorbed dose (D)

Absorbed dose, a measure of the energy deposited in any medium by any type of radiation, is the quotient of *dM* and *dm*, where *dM* is the mean energy imparted by ionizing radiation to matter of mass *dm*, thus

$$D = \frac{dM}{dm} \quad (1.7)$$

In the case of radiation equilibrium, D_{org}, the absorbed dose in an organism, is equal to K_{org}, the tissue kerma at the same point, thus

$$D_{org} = K_{org} = s\,K_a \quad (1.8)$$

Where s is the ratio of the mass energy absorption coefficients of the tissue of the organism and the air (photon energies 0.1-4 MeV, s = 1.10), thus

$$D_{org} = s\,a\,X \quad (1.9)$$

Unit: $J.kg^{-1}$, The special unit name of absorbed dose is gray (Gy) where one gray is equal to 100 rad.

$$1\ Gy = 1\ J.kg^{-1} = 100\ rad$$

Equivalent dose (H)

Equivalent dose is used for measuring the biological effect of a particular type of radiation on organs or tissues. It can be calculated by multiplying the absorbed dose to an organ or tissue (in gray) by the radiation weighting factor (W_R) (**Table 1.1**). Equivalent dose is defined in the following equation.

$$H_{TR} = D_{TR} \times W_R \quad (1.10)$$

Where H_{TR} is the equivalent dose to an organ or tissue T delivered by radiation type R

D_{TR} is the absorbed dose to an organ or tissue T delivered by radiation type R

W_R is the radiation weighing factor for radiation type R

Table 1.1 Radiation weighting factors recommended by ICRP.

Type and Energy Range	Radiation Weighting Factor (W_R)
Alpha particles, all energies	20
Beta particles, all energies	1
Gamma and x-rays, all energies	1
Neutrons:	
<10 keV	5
10 keV to 100 keV	10
> 100 keV to 2 MeV	20
> 2 MeV to 20 MeV	10
> 20 MeV	5

The SI unit for the equivalent dose is joule per kilogram which is the same as the absorbed dose but the equivalent dose has the special name which is Sievert (Sv) to distinguish it from the absorbed dose. The original unit of equivalent dose is rem (Roentgen Equivalent Man) where one Sievert is equal to 100 rem.

$1\ Sv = 1\ J\ kg^{-1} = 100\ rem$

Currently, there is no international agreement on an appropriate value for weighting doses to non-human biota (Chambers, Osborne, & Garva, 2006). Generally, radiation protection standards for non-human biota have been used in terms of absorbed dose (Kocher & Trabalka, 2000). For calculating doses to biota, the stochastic radiation weighting factor for alpha particles is often assumed to be 20, whilst the deterministic radiation weighting factor is in the range of 5-10 (Kocher & Trabalka, 2000).

Effective dose (E)

Effective dose is defined in terms of the sensitivity of some tissues or organs to the radiation. Some tissues or body organs are more sensitive to radiation than others. The equivalent doses in each organ and tissue are different, depending on their radio-sensitivity. The ICRP recommends tissue weighting factors (W_T) (**Table 1.2**) to apply to

specific body organs. The effective dose to an organ or tissue can be calculated by multiplying the equivalent dose by the appropriate tissue weighting factor as shown in the following equation.

$$E_T = H_T \times W_T \quad (1.11)$$

Where E_T is the effective dose to an organ or tissue type T

H_T is the equivalent dose to an organ or tissue type T

W_T is the tissue weighing factor for an organ or tissue type T

The effective dose units are the same as the equivalent dose units (Sv or rem). The conversion factor between the old units (rem) and SI units (Sv) is still the same.

Table 1.2 Tissue weighting factors recommended by ICRP (IAEA & ANSTO, 2004b).

Tissue	Tissue Weighting Factor (W_T)
Gonads	0.20
Bone marrow (red)	0.12
Colon	0.12
Lung	0.12
Stomach	0.12
Bladder	0.05
Breast	0.05
Liver	0.05
Oesophagus	0.05
Thyroid	0.05
Skin	0.01
Bone Surface	0.01
Remainder	0.05

1.3 Radiation protection of non-human biota

Previously, radiation protection focused on humans with the assumption that if humans were protected from the effects of ionising radiation, then non-human biota were also protected as stated by the International Commission on Radiological Protection (ICRP) Publication 26 (ICRP, 1977). In 1991, ICRP 60 stated that "The commission believes that the standards of environmental control needed to protect man to the degree currently thought desirable will ensure that other species are not put at risk" (ICRP, 1991). This statement only considers the effects of ionising radiation on the environment when those effects directly affect humans (R.J. Pentreath, 1998). Recently, radiation protection from the effects of ionising radiation to the environment has received increased attention by many researchers and organisations (Copplestone & et al., 2010; Delistraty, 2008; Holm, 2004; R. J. Pentreath, 2002; R. J. Pentreath & Woodhead, 2001; J.T. Smith, 2005).

The current dose limit for humans (members of the public) is 1 mSv yr^{-1}, as recommended by ICRP, whist a dose limit for the protection of non-human species of 1 mGy d^{-1} has been suggested (IAEA, 1992; UNSCEAR, 1996). This is much higher than for humans. This is mainly because for humans, radiation protection is based on a stochastic effects, whilst for non-human biota, radiation protection is based on deterministic effects (Holm, 2004). Stochastic effects (cancer induction and genetic effects) are effects that may or may not occur, have no threshold dose, the probability of the effect increases with dose The effect is typically delayed and not definitively associated with the radiation exposure (Delistraty, 2008; Stabin, 2008). Deterministic effects (organ and tissue impairment often due to cell death) are effects that occur above a threshold dose, the severity of the effect increases with dose. They result from acute exposure to high doses and are definitively associated with the radiation exposure (Delistraty, 2008; Stabin, 2008).

Several regulatory limits have been set to protect wildlife from ionising radiation, as shown in **Table 1.3** (Copplestone, et al., 2009).

Table 1.3 Values of dose rate used by regulators to demonstrate that organisms are protected from the effects of ionising radiation (Copplestone, et al., 2009).

Regulator	Numeric value
Environment Agency, England & Wales	5 µGy h^{-1} - screening value for all biota groups
	40 µGy h^{-1} - action level for all biota groups
DOE, US	40 µGy h^{-1} - benchmarks for terrestrial animals
	400 µGy h^{-1} - benchmarks for terrestrial plants
	400 µGy h^{-1} - dose limit for aquatic animals
Canada	20 µGy h^{-1} - screening dose rates for fish
	110 µGy h^{-1} - screening dose rates for other freshwater organisms
	220 µGy h^{-1} - screening dose rates for terrestrial organisms

1.4 Method of dosimetry

Radiation Dosimetry is the measurement of radiation dose by using a dosimeter. There are 4 main types of measurements (Attix, Roesch, & Tochilin, 1968); (1) measurement of the absorbed dose in the matter (2) measurement of the energy released from indirect ionising particles per unit mass of reference material (exposure and kerma) (3) measurement of the number of particles or their energy occurring at a given point (flux, fluence) and (4) measurement of some function of the number and energy of particles occurring at a given point.

The method of dosimetry depends on the dosimeter that is used to measure the radiation dose. There are a lot of methods to measure the radiation dose which are suitable for different purposes (Greening, 1985); (1) Calorimeters are a basic method to measure an absorbed dose. The temperature of the absorbing medium can be increased by ionising radiation. By measuring the increasing of the temperature the radiation dose can be estimated. This method is usually used in standard works or research applications. It is not suitable to use in routine work because it is not very sensitive: even a large radiation dose results in only a small temperature rise; (2) The Ionisation Chamber has widely

been used for most of accurate dosimetry. The number of Ion pairs which are produced from ionisations within the matter in an ionisation chamber can be related to the amount of ionising radiation. The ionisation chamber equipment is simple and portable.

The differentiation between the ionisation chamber and Geiger-Muller counter is the applied voltage into the detector. The applied voltage to use in the ionisation chamber is lower than the Geiger-Muller counter. The voltage in the ionisation chamber is just large enough to generate the ions reach to the cathode, whilst the voltage in the Geiger-Muller is very high to produce gas multiplication causing a very large pulse (IAEA & ANSTO, 2004a; Knoll, 1989); (3) Chemical Dosimetry has been used for high-dose measurement. Ionising radiation can change the chemical mechanism in matter: this is used in equipment such as the Fricke, or ferrous sulphate, dosimeter. In this system, Ferrous ions, Fe^{2+}, are oxidised by ionising radiation to ferric ion, Fe^{3+} (Greening, 1985). The number of ferric ions can be observed and related to number of ionising radiations that come through matter; (4) Thermoluminescence Dosimetry (TLD) has been used for monitoring personal doses and environmental doses (these will be described further in Section 1.3.1); (5) Photographic Dosimetry is one kind of chemical dosimetry. Photographic film consists of silver halide crystals (mainly silver bromide) suspended in gelatine and supported on a thin cellulose acetate film (Greening, 1985; Knoll, 1989). The radiation dose can be determined by the optical density which is proportional to the absorbed dose in silver halide crystals; (6) Scintillation Detector has been used for radiation monitoring. When radiation comes through the scintillation detector, electrons in scintillator which normally fill in lower energy orbits will raise into higher energy orbits by excitation process. The light will be released after electrons from higher energy orbits move down to the lower energy orbits. The light can be converted to an electrical signal which relates to the amount of radiation absorbing in the scintillator.

1.4.1 Thermoluminescence dosimetry

A TLD is a passive dosimeter that can record dose information. It can be used to obtain dose equivalent values of personal dose equivalent at 10 mm depth ($H_p(10)$) for penetrating radiation such as gamma and x-rays radiation and personal dose equivalent at 0.07 mm depth ($H_p(0.07)$) for low penetrating radiation such as beta radiation (Greening, 1985; IAEA & ANSTO, 2004b). Thermoluminescent (TL) materials are doped inorganic compounds. The electrons in TL materials are moved up to higher

energy level when the energy from incident radiation is absorbed by TL materials. These electrons remain trapped at these higher levels until the material is heated by a specific heating pattern. The energy is then released as light. This light can be changed into an electrical signal which is related to the amount of incident radiation (**Figure 1.1**).

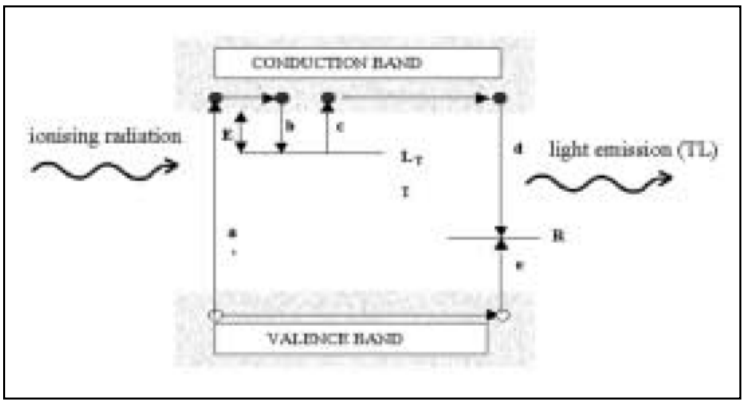

Figure 1.1 Illustration of processes produced in the crystal by irradiation and a successive heat treatment (Ranogajec-Komor, 2003).

The type of thermoluminescent materials chosen depends on the application. Lithium-based TLDs are used for personal dosimetry because they are closely the same atomic composition as the human tissue (The photon effective atomic number (Z_{eff}) of biological tissue = 7.42) (C. Furetta, Prokic, Salamon, Prokic, & Kitis, 2001). The types of Lithium-based TLDs have been used for dosimetry such as LiF:Mg (Z_{eff} = 8.2), $Li_2B_4O_7$:Cu (Z_{eff} = 7.4) and $Li_2B_4O_7$:Mn (Z_{eff} = 7.3) (C. Furetta, et al., 2001; McKinlay, 1981). On the other hand, calcium based TLDs are suitable to use for environmental monitoring because of their high sensitivity material because they have a high effective atomic number such as $CaSO_4$ (Z_{eff} =15.3), CaF_2 (Z_{eff} = 16.3) (McKinlay, 1981). The principal applications of TLDs are (1) for personal dosimetry: LiF:Mn, (2) for radiotherapy and diagnostic radiology dosimetry: $Li_2B_4O_7$:Mn, (3) for high or low absorbed dose measurement: CaF_2:Mn, CaF_2:Dy and (4) for environmental and short-term dosimetry: $CaSO_4$:Mn, $CaSO_4$:Dy and $CaSO_4$:Tm (McKinlay, 1981).

TLD reading consists of 3 main parts: (1) heating, (2) conversion from light to electrical pulse part and (3) electronic data processing. When the TLDs are heated in a specific heat pattern, a light signal is produced. This light signal is amplified and converted to an electrical signal by a photomultiplier tube (PMT). The output can be presented as a graph of number of light photons emitted against the time of heating. This graph is known as a glow curve (**Figure 1.2**). By using parameters determined by calibration TLDs, it is then possible to determine the actual dose received by TLDs.

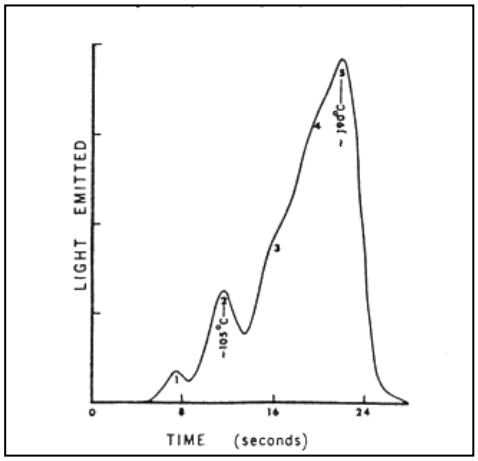

Figure 1.2 Illustration of Typical Glow Curve of LiF: Mn after Irradiation to 1 Sv (IAEA & ANSTO, 2004b).

The main algorithm which can be used to convert the light emission obtained during the readout of a thermoluminescent detector to the absorbed dose (D) can be expressed by the following relationship (C Furetta, 2003).

$$D = M.F_C$$

where M is the TL signal (integral light or peak height), and

F_C is the individual calibration factor of the detector.

1.4.2 Choice of dosimetric system

The choice of dosimetric system (absolute method, Calorimeter or ionisation) depends on the application that will be used. The range of absorbed doses should be taken into account because some dosimeters can be used only for high-dose rate measurement, for example, the Calorimeter, Fricke dosimeter and Plastic dosimeter (see **Figure 1.3**). Some of them, such as the Scintillation detector, are suitable only for low-dose

measurement. In addition, the size of detector is also important because of ease of use. The TLD is suitable for this research because it is small, easy to arrange in designed-equipment, has a wide dose range (10^{-5} to 10^{4} Gy) and can measure both gamma and beta radiation.

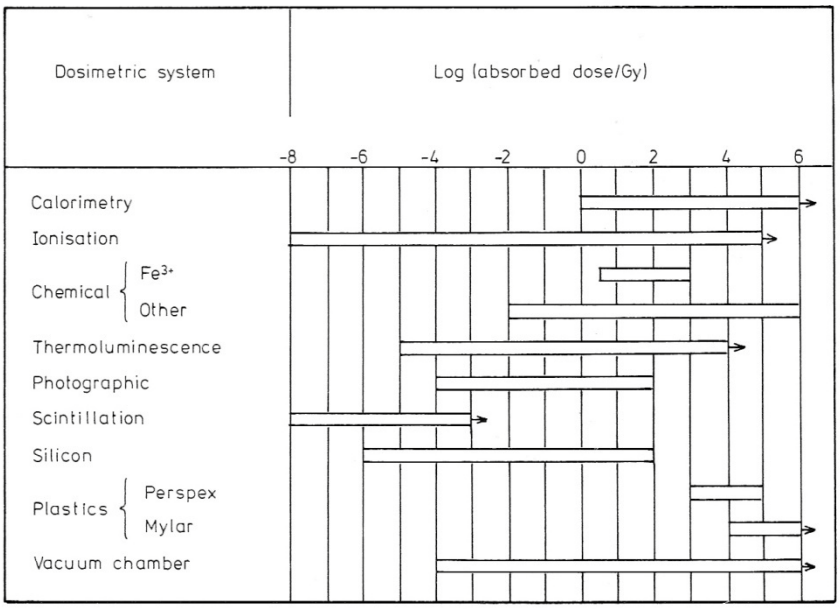

Figure 1.3 Approximate rage of absorbed doses measurable with different dosimetric systems (Greening, 1985).

1.5 The Chernobyl Nuclear Power Plant (ChNPP) Accident

On 26 April 1986, the explosion at Reactor 4 of the Chernobyl nuclear power plant which is located 100 km from Kiev in Ukraine (at that time part of the USSR) was occurred. The explosion of the reactor vessel and the consequent fire continued over 10 days (IAEA, 2006b). A large number of radioactive material from a nuclear reactor released to the public and the environment (IAEA, 2006b). A plume of radioactive fallout drifted over the European continent (**Figure 1.4**), Scandinavia, Asia and eastern North America (OECD/NEA, 2002).

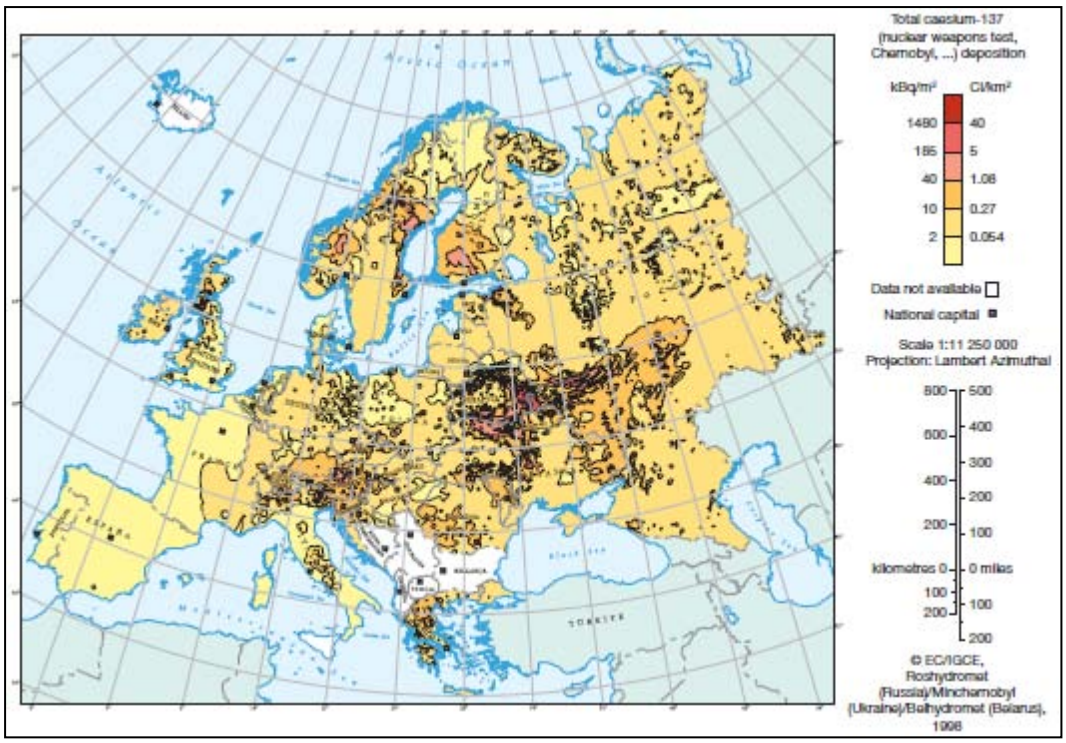

Figure 1.4 The deposition of Cs-137 throughout Europe as a result of the Chernobyl accident (IAEA, 2006b).

Large areas of Ukraine, Belarus, and Russia were badly contaminated (IAEA, 2006a, 2006b; OECD/NEA, 2002) (**Figure 1.5**). Many radioisotopes of numerous elements were released, for example, noble gases (including Argon and Xenon), Iodine, Strontium and Caesium. Most had short physical half-lives and have since decayed away. The release of radioactive isotopes of iodine caused great concern immediately after the accident. Firstly, large quantities of radioiodines (I-131 ~1760 PBq, I-133 2500 PBq) were released (IAEA, 2006b) and secondly, as iodine is accumulated in the human thyroid gland, the release resulted in large radiation doses to thyroids of the local population (Fairlie & Sumner, 2006). Now, twenty years on, only isotopes with half lives exceeding a decade remain in the environment in significant quantities. Cs-137 (half life =30.17 y) and Sr-90 (half life = 28.8 y) remain the contaminants of greatest importance whereas over the longer term (hundreds to thousands of years) the long half life contaminants of plutonium isotopes and americium-241 will remain (IAEA, 2006b).

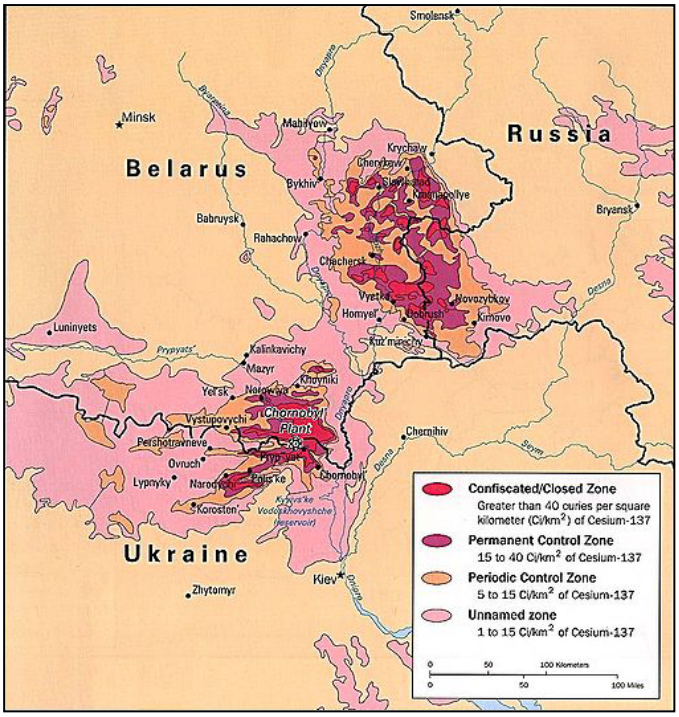

Figure 1.5 Radiation Hotspots Resulting from the Chernobyl Nuclear Power Plant accident ("Belarus Maps," 2008).

The radioisotopes released by the accident can be grouped into two categories; beta gamma emitters or alpha emitters. Nuclear fission splits the nucleus of the atom into two unequal parts and as the neutron:proton ratio is highest for heavy elements the fission fragments that result are neutron rich.

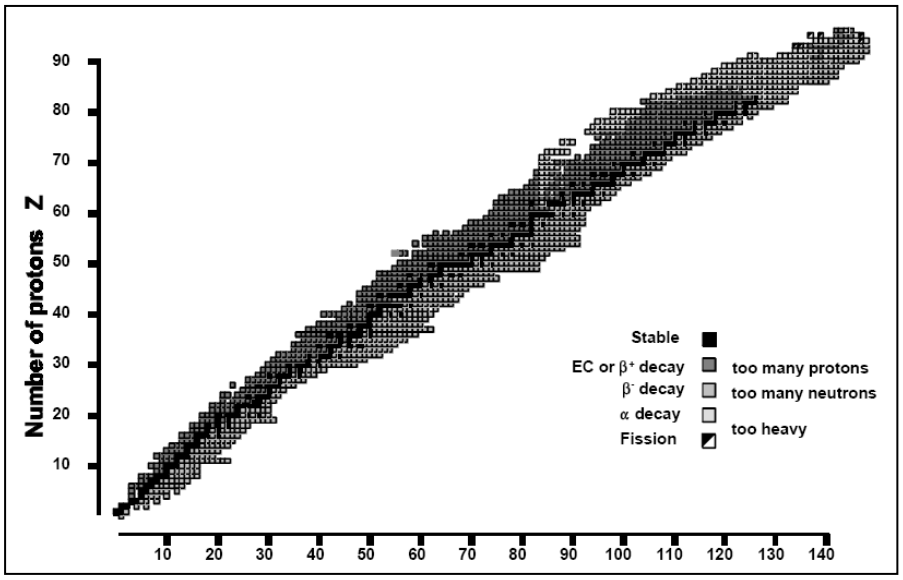

Figure 1.6 Neutron:Proton Plot of the stable nuclides (Lawson, 1999).

The neutron:proton ratio of the nucleus of the stable isotopes (**Figure 1.6**) increases from unity to a maximum of 1.5 for the heaviest isotopes. Any isotope with an excess of neutrons or protons will be unstable and decay with the emission of alpha, beta or gamma radiation, or a combination of these, until a stable nuclear configuration is reached. As the fission fragments are neutron rich, they decay by the emission of beta and gamma radiation. Absorption of neutrons by the uranium nuclear fuel leads to the production of numerous isotopes of the transuranic elements. These heavy mass elements are also radioactive and decay with the emission of high energy, high mass, helium nuclei called alpha particles. The radiological risk factor from exposure to alpha radiation is high but the abundance of this type of radioisotope was significantly lower than that of the fission fragments.

Much of the proposed work will concern the environmental behaviour and radiological risk associated with the radioisotopes Caesium-137 (Cs-137) and Strontium-90 (Sr-90).

Cs-137 is a radioactive isotope which is formed mainly by nuclear fission, for example

$$^{235}_{92}\mathrm{U} \rightarrow {}^{137}_{55}\mathrm{Cs} + {}^{95}_{37}\mathrm{Rb} + 3{}^{1}_{0}\mathrm{n}$$

It has a half-life of 30.17 years. Cs-137 disintegrates with a probability of 5.6% of going directly to the Ba-137 ground state and the remainder decaying via the intermediate, the metastable Barium-137m. The metastable Ba-137 disintegrates with a physical half-life of 2.55 minutes releasing gamma rays (0.662 MeV) (KAERI, 2000). The decay scheme of the nuclide is presented in **Figure 1.7**. The nuclear decay formula of Cs-137 is shown below.

$$^{137}_{55}\mathrm{Cs} \rightarrow {}^{137}_{56}\mathrm{Ba} + {}^{0}_{-1}\mathrm{e} + \gamma$$

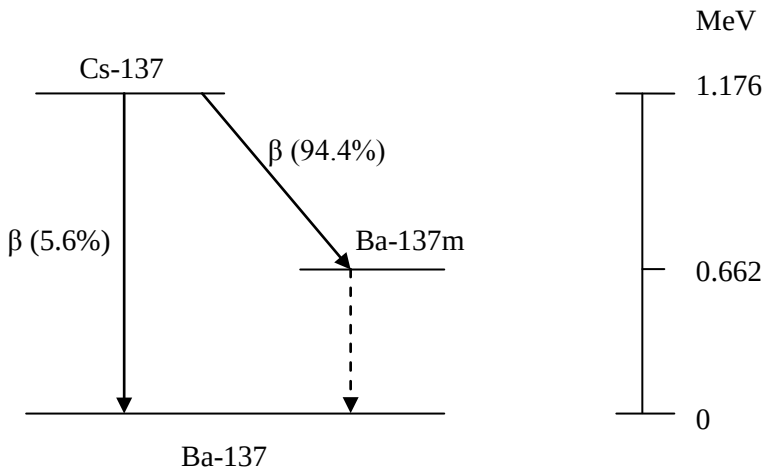

Figure 1.7 Decay scheme of Caesium-137.

Strontium-90 (Sr-90) has a half life of 28.8 years. The decay of the parent Sr-90 produces 100% beta particles with a maximum energy 0.546 MeV to the daughter Yttrium-90 (Y-90). Y-90 produces 100% beta particles with a maximum energy 2.280 MeV to the stable nuclide Zirconium-90 (Zr-90) (KAERI, 2000). The decay scheme of the nuclide is presented in **Figure 1.8**.

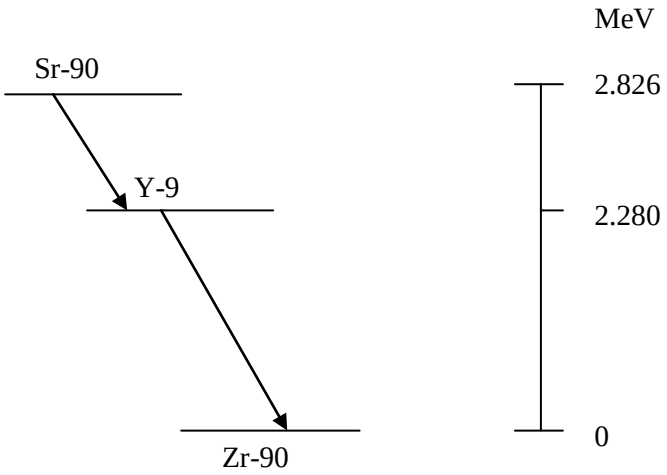

Figure 1.8 Decay scheme of Strontium-90

1.6 General description of the study lakes

The surrounding area of the ChNPP has several types of aquatic system including rivers, reservoirs, open lakes and closed lakes. The radionuclide fallout on the water and the transfer of radionuclides from the surrounding catchment areas caused these aquatic

systems to become contaminated. Radionuclide concentrations in water decreased rapidly in rivers, reservoirs and open lakes from several reasons: the decay of short half life radioisotopes, the absorption of radionuclides to catchment soil and lake sediments, and loss of radioactivity through the water outflow (Jim T. Smith, Voitsekhovitch, Konoplev, & Kudelsky, 2005). Radio-caesium in closed lake systems (lakes with little inflow and outflow of water) have much higher activity concentrations in water and aquatic biota than open lakes and rivers because of remobilization from sediments in closed lakes (IAEA, 2006b).

Seven closed lakes located in Belarus and Ukraine were considered as potential study sites. These are: the cooling pond of the Chernobyl power station, Glubokoye, Perstok, Dvorishche, Svyatoye No.3, Svyatoye No.7 and Svyatoye No.8 (**Figure 1.9**). Perstok and Svyatoye No.3 in Belarus were chosen for this study because of their high contamination of Cs-137 (and Sr-90 in the case of Perstok). It is noted that the cooling pond of the Chernobyl NPP also has high contamination, but it is too big for this study.

1.6.1 Svyatoye lake No.3

The Svyatoye No.3 lake is a closed lake, located 225 km from ChNPP and 30 km southeast of Kostyukovichy town in Belarus. The lake has a surface area and watershed area of 0.25 and 1.02 km^2 respectively (**Table 1.4**). It contains approximately 717,950 m^3 of water (**Table 1.4**). The maximum depth is 5.1 m in the centre of the lake (**Figure 1.13**). The density of Cs-137 contamination in the watershed area was 1.753×10^9 kBq km^{-2} in 1986 (1.779×10^9 kBq for the Cs-137 inventory in 1986). The external dose rate in air at 1 m above the ground around this lake was about 1 $\mu Sv\ hr^{-1}$ in June 2007, measured by the author using a portable dose-rate gamma survey meter (Mini-Monitor Series 900 made by Mini Instruments Inc.). There are two main texture classes of the bottom sediments in Svyatoye lake: fine sand and silty loam (Kudelsky, et al., 2005). The concentration of Cs-137 in the solid phase of silty loam and fine sand from 0-0.2m layer was 30.882 kBq kg^{-1} d.w. in 1999 and 30.413 kBq kg^{-1} dw in 2000 respectively (Kudelsky, et al., 2005). The lake bank is covered by both terrestrial and aquatic plants (**Figure 1.10**).

In 1997, (James T. Smith, Kudelsky, Ryabov, Hadderingh, & Bulgakov, 2003) selected Svyatoye lake for a field experiment consisting of an introduction of potassium chloride fertilizer into the water mass as a countermeasure to Cs-137 accumulation in fish.

During 1996-1997, the K^+ and NH_4^+ concentration of the lake water ranged between 0.95 to 1 mg l^{-1} and from 0.2 to 0.6 mg l^{-1}, respectively (Kudelsky, et al., 2005). The Cs-137 concentration ranged between 3.8 to 4.9 Bq l^{-1} and in the one case only was as high as 7.2 Bq l^{-1} (Kudelsky, et al., 2005). When KCl fertilizer was added, the concentration of both K^+ and Cs-137 in the water increased up to 10 mg l^{-1} and 12.36 Bq l^{-1} respectively (Kudelsky, et al., 2005). As a result of the increase in K^+ in the water, the Cs-137 activity in fish decreased significantly. In Rudd, for example, the Cs-137 declined from 15 kBq kg^{-1} ww in 1997 to 5 kBq kg^{-1} Cs-137 ww in 2004 (Kudelsky, et al., 2005). In 2002, Cs-137 radioactivity in the water was estimated to be 10.74 Bq l^{-1} (**Table 1.5**). The increasing of Cs-137 in water and the decreasing of Cs-137 in fish were the results of the remobilization of activity from the bottom sediments as a result of competition for sorption sites in sediment between Cs-137 and K^+.

In 2002, the value of pH, K^+, NH_4^+ and organic carbon in the water were 7.51, 7.00 mg l^{-1}, 0.1 mg l^{-1} and 4.32 mgC l^{-1} respectively. A total of 15 fish species were identified in the catches in the years 2001-2004: Pike (*Esox lucius L.*), Roach (*Rutilus rutilus L.*), Rudd (*Scardinius erythrophthalmus L.*), Belica (*Leucaspius delineatus Heck.*), Tench (*Tinca tinca L.*), Gudgean (*Gobio gobio L.*), Bitterling (*Rhodeus sericeus amarus Bloch.*), Gold fish (*Carassius auratus gibelio Bloch.*), Perch (*Perca fluviatilus L.*), Ruff (*Gymnocephalus cernuus L.*), Bream (*Abramis brama L.*), Silver Bream (*Blicca bjoerkna L.*), Shchipovka (*Sabanejewia caspia*), Bleak (*Alburnus alburnus L.*) and Crayfish (*Decapoda L.*).

1.6.2 Perstok lake

Perstok lake (mostly undrained, but periodically flooded) is located 13 km northwest of the ChNPP **(Figure 1.9**). The water surface area of the lake is approximately 0.176 km^2 with a maximum depth of 2 m (**Figure 1.14**), and a volume of 257,800 m^3 of water (**Table 1.4**). The lake is illustrated in **Figure 1.11**. The lake edge is heavily vegetated in comparison with the other study lakes. The main type of the lake bottom sediment is silt with a high content of organic matter. In 2002, the Cs-137 and Sr-90 activity of the organic slit from 0-0.2m layer was 55.0662 kBq kg^{-1} and 92.2 kBq kg^{-1} dw respectively (Kudelsky, et al., 2005). The maximum Cs-137 contamination was 3,700 kBq m^{-2} and Sr-90 contamination was 110 kBq m^{-2} (Kudelsky, et al., 2005). The total inventory of Cs-137 and Sr-90 was estimated to be $5.2x10^9$ kBq and 1.6×10^8 kBq respectively. The external dose rate in air at 1 m above the ground around this lake was about 2 μSv hr^{-1}

in June 2007, measured using portable dose-rate gamma survey meter (Mini-Monitor Series 900 made by Mini Instruments Inc.). Although unconnected to the river system, Perstok lake is occasionally flooded during spring flood. During the rest of the year, the lake obtains water from rain and subsurface runoff, whilst evaporation and subsurface discharge control the water discharge of the lake water. The Cs-137 and Sr-90 radioactivity in the water was measured to have a value 14.09 Bq l^{-1} and 22 Bq l^{-1} respectively in 2002 (**Table 1.4**).

In 2002, the value of pH, K^+, NH_4^+ and organic carbon in the water were 7.75, 6.1 mg l^{-1}, 0.18 mg l^{-1} and 12.6 mgC l^{-1} respectively (**Table 1.5**). A total of 9 fish species were identified in the catches in the years 2001-2004: Pike, Roach, Rudd, Gold fish, Perch, Ruff, Bream, Tench and Belica (Kudelsky, et al., 2005). The Cs-137 activity of fish varied from 2.752 kBq kg^{-1} to 14.728 kBq kg^{-1} ww (Kudelsky, et al., 2005).

1.6.3 Dvorishche lake

Dvorishche lake is located 95 km north-west of ChNPP (**Figure 1.9**) in the valley of Pripyat river, Kalinkovichi district, Gomel region. The distance between the lake and Pripyat river is about 4-5 km. Dvorishche lake is not connected with the active river channel. The lake is extremely flooded in spring by high water level in the Pripyat river (Kudelsky, et al., 2005). The Cs-137 activity concentrations in the water column were between 4.81 and 6.51 Bq l^{-1} in 2004. The density of Cs-137 contamination in the watershed area was 2.38×10^8 kBq km^{-2} in 1986. Dvorishche lake has an oblong shape. The water surface area of the lake is approximately 0.128 km^2 with a maximum depth of 3.5 m (**Figure 1.15**), and a volume of 256,000 m^3 of water (**Table 1.4**) The main types of bottom sediments are fine sands and lacustrine silts with high content of organic matter (Kudelsky, et al., 2005). The catchment area of the lake is covered by wet meadow used as a natural pasture and the lake shores are swampy (**Figure 1.12**).

Fish species were caught between 2003 and 2004 in this lake consist of Roach, Perch, and Belica. The Cs-137 activity concentration in muscle tissue varied from 0.26 kBq kg^{-1} ww in roach to 1.54 kBq kg^{-1} ww in perch (Kudelsky, et al., 2005). In 2004, the value of pH, K^+, NH_4^+ and organic carbon in the water were 7.18, 1.25 mg l^{-1}, 0.20 mg l^{-1}, and 9.44 mgC l^{-1} (**Table 1.5**).

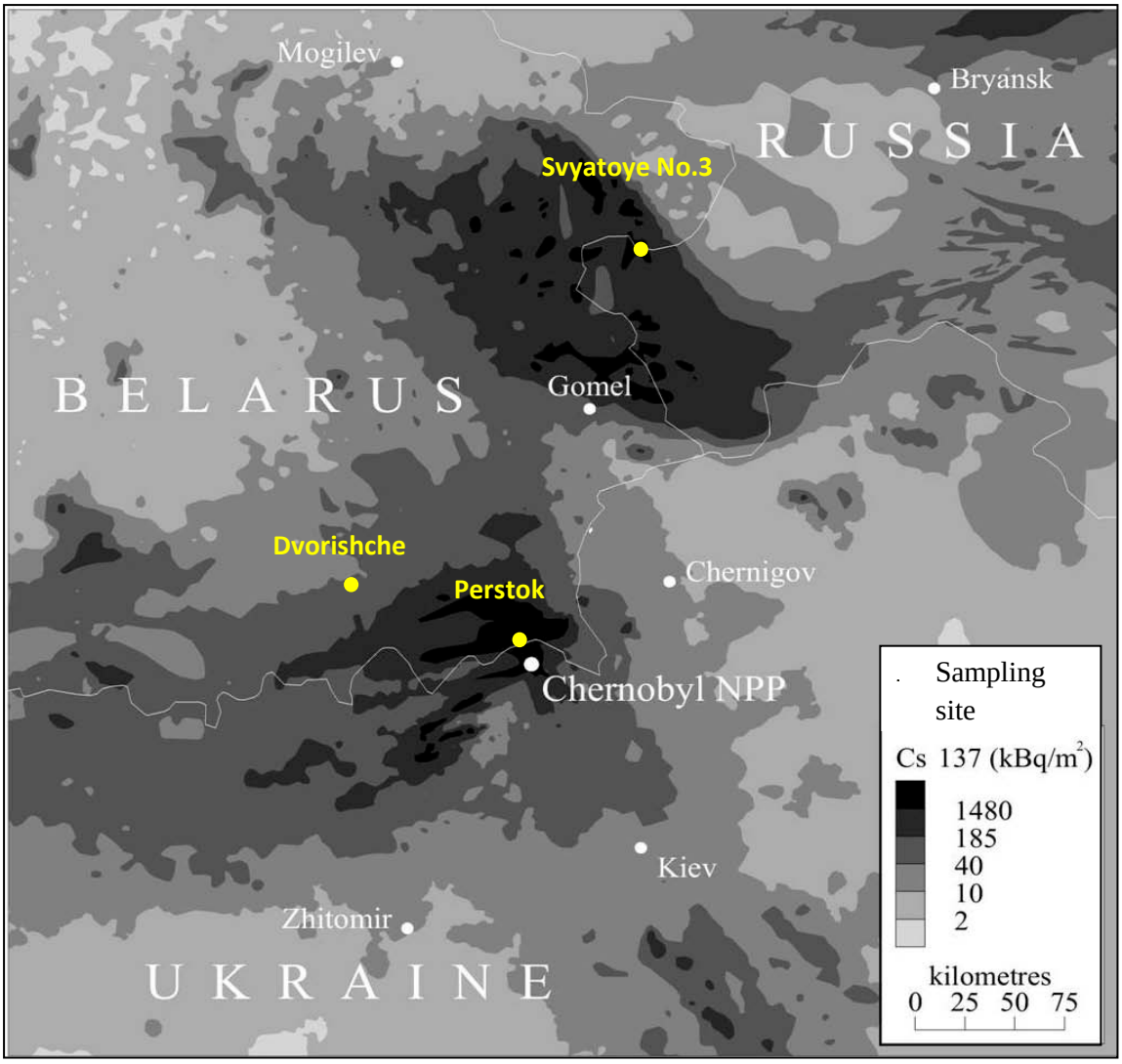

Figure 1.9 Illustration of the sampling lakes containing varying degrees of the Cs-137 contamination in Ukraine, Belarus, and Russia.

Figure 1.10 Photographs of Svyatoye No.3 and its surrounding area in Belarus (Taken by the author during field visit, 3-10 June 2007).

Figure 1.11 Photographs of the Perstok lake and its surrounding area in Belarus (Taken by the author during field visit, 3-10 June 2007).

Figure 1.12 Photographs of the Dvorishche lake and its surrounding area in Belarus (Taken by the author during field visit, 6-13 July 2008).

Table 1.4 General description of study lakes in Belarus (Data from Kudelsky, et al.(2005))

No.	Lake	Water Surface area, km^2	Depth (max), m	Water mass, m^3	Watershed area, km^2	Distance from the ChNPP, km	Cs-137 contamination density in watershed area, * 10^6 kBq km^{-2}	Cs-137 inventory in watershed area, * 10^7 kBq
3	Svyatoye	0.25	5.1	717,950	1.02	225	1368.1	138.8
15	Perstok	0.176	2.0	257,800	1.41	13	3700.0	521.7
17	Dvorishche	0.128	3.5	256,000	NA	95	To 185.0	NA

* as of 01.01.1997, NA = data not available

Table 1.5 Chemical composition and Cs-137 activity of the lake water (Data from Kudelsky, et al. (2005))

Lake	Date of sampling	Depth of sampling, m	NH_4^+	K^+	Na^+	Ca^{2+}	Mg^{2+}	Cl^-	HCO_3^-	SO_4^{2-}	NO_3^-	Ion sum	pH	Organic Carbon, mgC l^{-1}	Cs-137	Sr-90
			Numerator – mg l^{-1}; denominator - meq												Bq l^{-1}	
Svyatoye#3	19.08.02	0.2	0.1 0.01	7.00 0.18	2.30 0.1	16.03 0.8	2.43 0.2	11.7 0.33	55.53 0.91	2.88 0.06	0.25	98.22 2.1	7.51	4.32	10.74	NA
Perstok#15	24.08.02	0.2	0.18 0.01	6.1 0.16	6.35 0.28	26.45 1.32	3.04 0.25	12.05 0.34	68.95 1.13	17.77 0.37	- -	140.89 3.86	7.75	12.6	14.09	22.0*
Dvorishche#17	05.06.04	0.2	0.20 0.01	1.25 0.03	3.43 0.15	15.03 0.75	4.86 0.40	8.15 0.23	54.31 0.89	4.80 0.10	1.19 0.02	93.22 2.58	7.18	9.44	5.02	NA

* near bottom water A Sr-90 = 61 Bq l^{-1} (depth 2m)

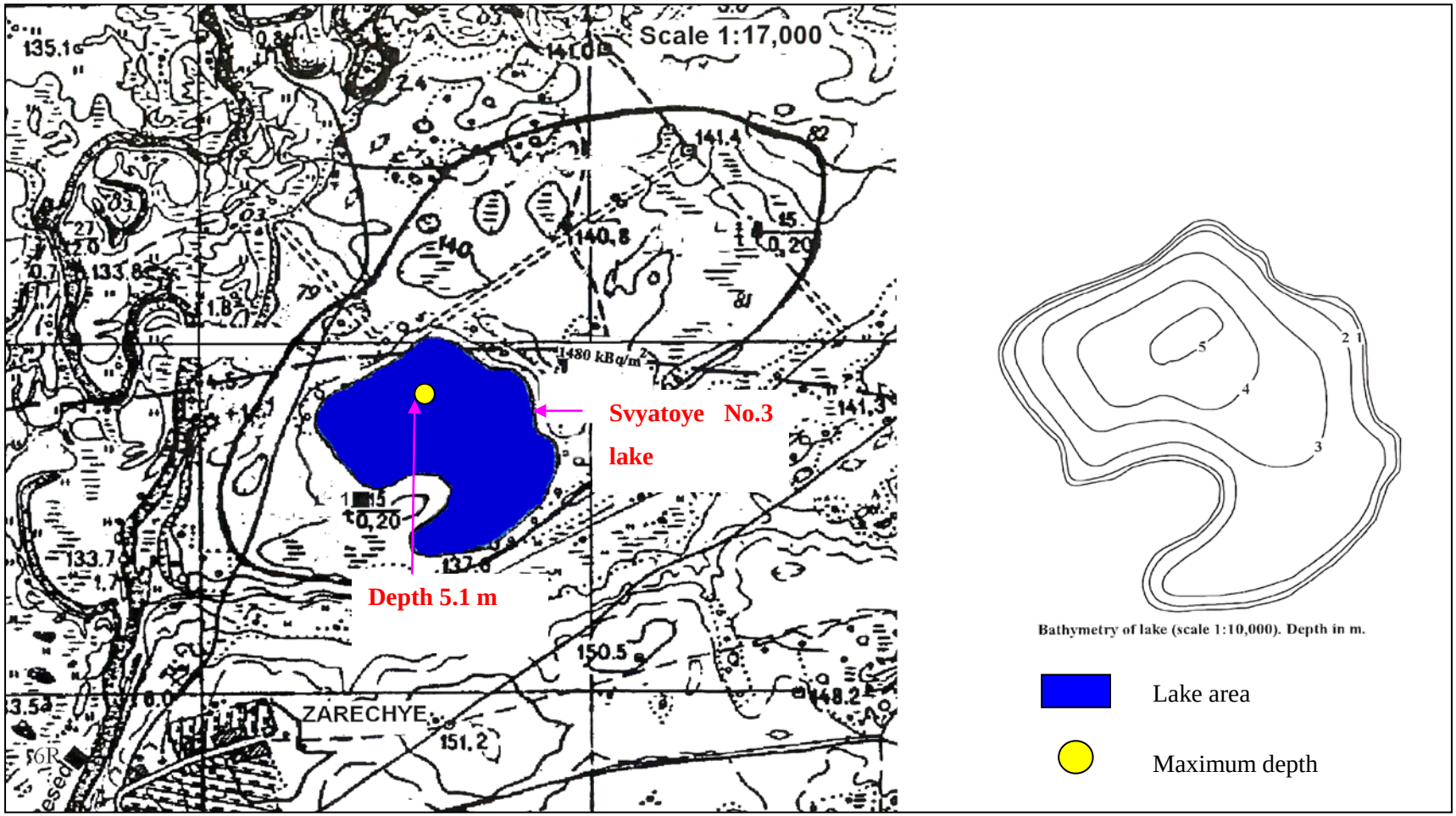

Figure 1.13 Sketch map showing the location of the Svyatoye No.3 near the village of Zarechye in the Kostyukovichy district and bathymetry of the lake (Tumnoi, 2006).

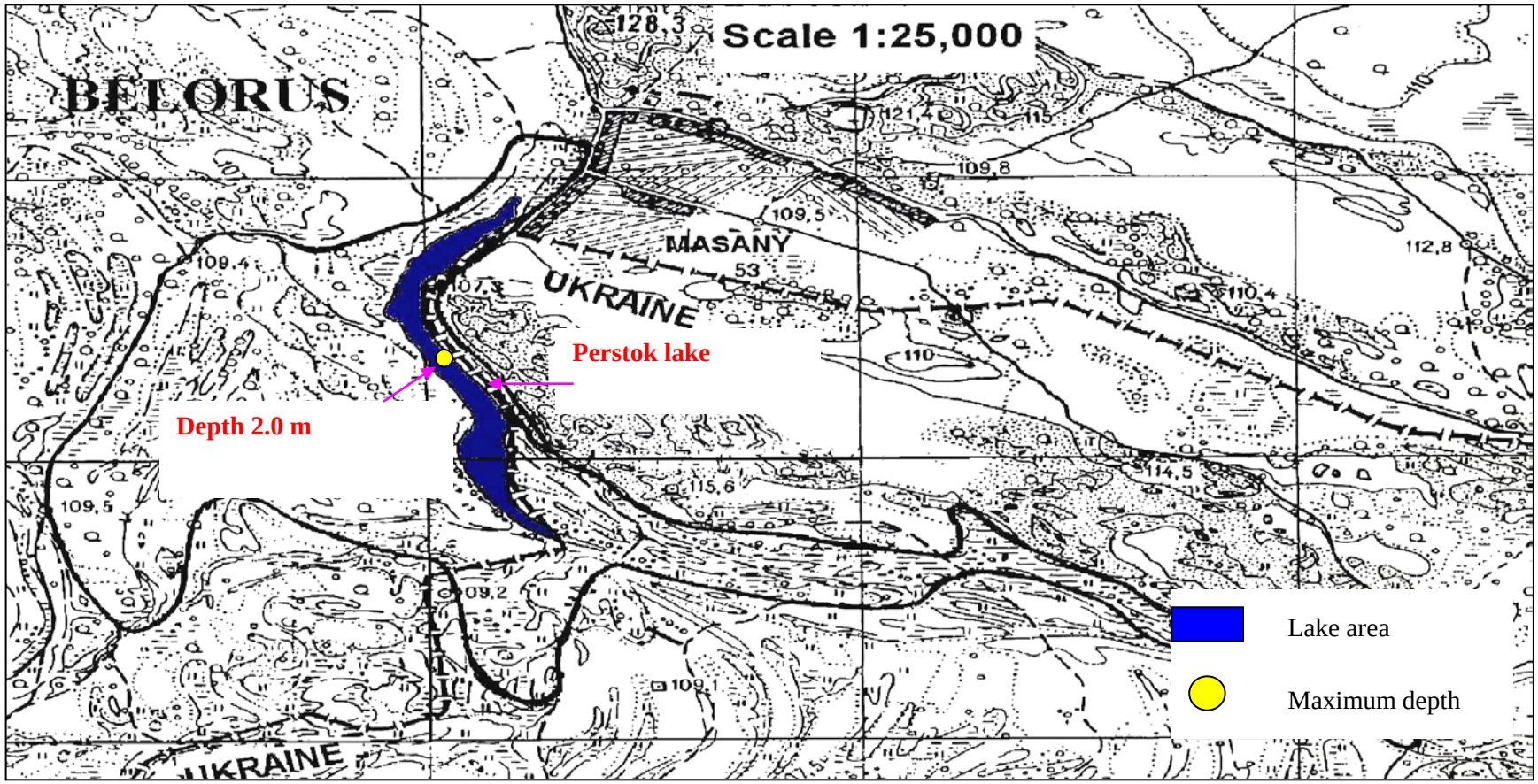

Figure 1.14 Sketch map showing the location of the Perstok lake near the village of Masany in the Khoiniki district and bathymetry of the lake (Tumnoi, 2006).

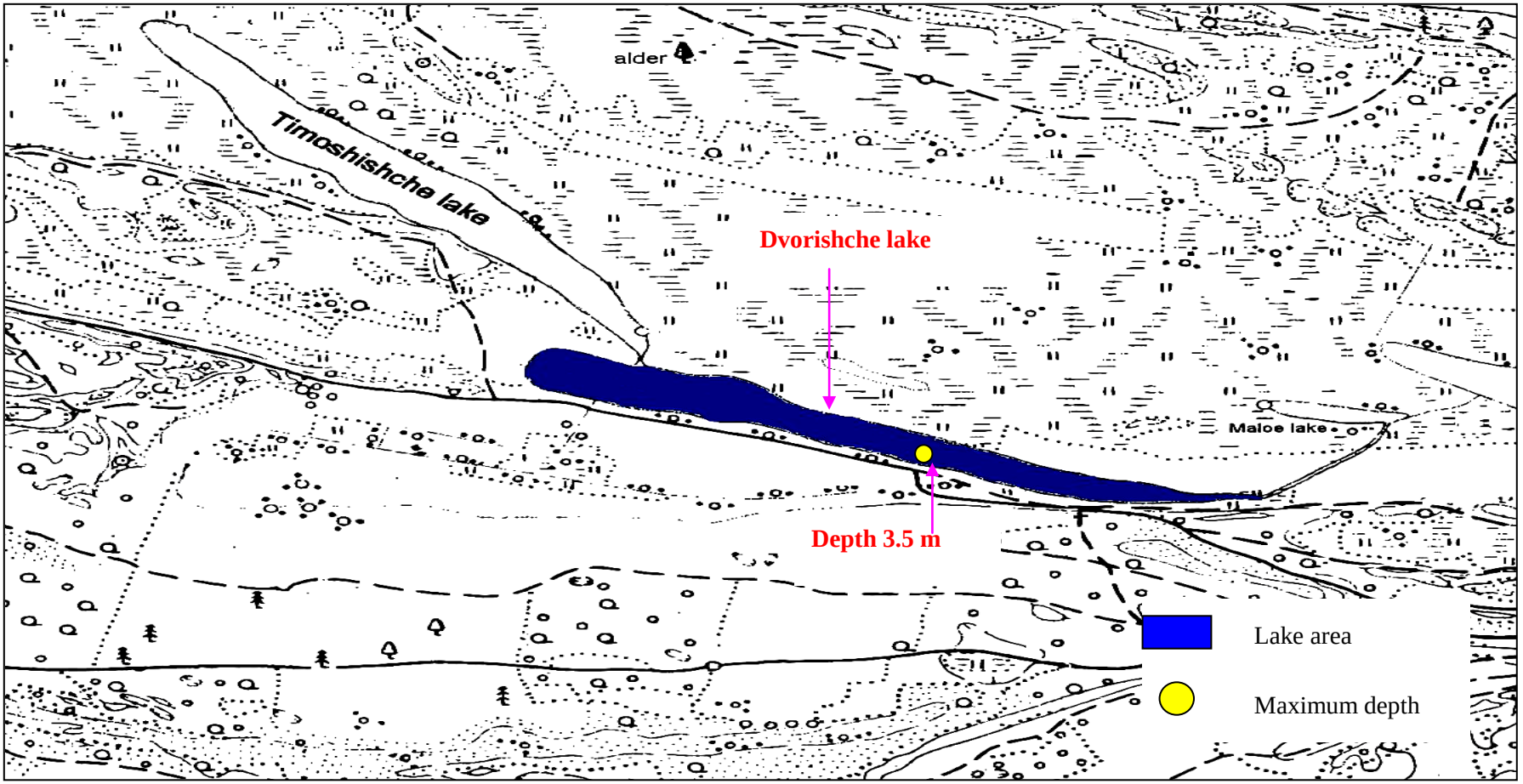

Figure 1.15 Illustration of the sketch map showing the location of the Dvorishche lake near the village of Shareiki in the Kalinovichi district (Tumnoi, 2006).

1.7 Previous studies of radiation doses in contaminated environments

TLDs studies

In the two decades following the Chernobyl accident, scientists have conducted numerous studies of the effect of the contamination and exposure on the biota that resides in the contaminated zones. A number of models have been developed to measure the behaviour of the isotopes, the external and internal radiation exposure of organisms and biological effects. Moreover, a few experiments have been carried out of in-situ measurement of doses of sub surface or sediment/water interface by using TLDs.

One of the first measurements of in-situ dose to biota before the ChNPP accident was made by Woodhead in 1973. Here, measurements of radiation dose to Plaice in the Irish Sea off Sellafield were made by tagging the fish with TLDs which were then released and recaptured. The work was able to estimate the dose rates to their gonads to be a maximum of 18μGy hr^{-1} (Woodhead, 1973). After the ChNPP accident, there have been several studies of in-situ measurement to biota dose. The first in situ measurements of the sub-surface gamma dose rate for Cs-137 contaminated land that quantified variation in dose rate with depth (by using TLDs to determine external gamma dose) was reported in 2005. Two different soil types (mineral and organic) were observed. The different soil type caused to different Cs-137 mobility and led to the variation in the gamma dose rate with soil type. The vertical migration rate of mineral soil was slower than organic soil. The gamma dose rate from Cs-137 was found to be significant in below or above contaminated areas. The dose rate at both sides did not reach background levels until 40 cm depth. This method was limited in that only the dose arising from gamma radiation was recorded. It could not measure beta radiation (D. N. Timms, Smith, Coe, Kudelsky, & Yankov, 2005). In 2004, TLDs were used to measure radiation dose at the sediment/water interface of the Chernobyl cooling pond**.** A number of TLDs were placed in a sealed plastic tube before being driven into the lake sediment. Sediment core samples were later taken alongside the TLDs to determine the Cs-137 depth profile. The maximum dose was at approximately 5 cm below the layer of sediment/water interface because Cs-137 deposited from the surface water to the sediment and then migrated to the sediment (D.N. Timms, 2006).

Model studies

A study by Beresford et al. (Beresford, Gaschak, et al., 2008) estimated the exposure of 3 species of small mammals in three forest sites (low, medium and high soil activity concentrations) within the Chernobyl exclusion zone. Whole-body activity of Sr-90 and Cs-137 was determined and compared with the activity predicted by the ERICA model. The activity concentration of Sr-90 and Cs-137 from the model prediction and the measurement were within an order of magnitude of the observed data means. Also, Therrnoluminescent dosimeters (TLDs) were used to estimate external dose rate by mounting them on the collars of the mammals. These measurements were also compared with the prediction from the ERICA model. The agreement of external dose rate from the measurement of TLDs and the prediction of the model was acceptable when the uncertainties of a study such as the differences in soil types have been taken into account.

A model-model comparison exercises reported by Beresford et al. (Beresford, Balonov, et al., 2008). In 2007, Vivies i Batlle et al. carried out an international comparison of models to estimate unweighted absorbed dose rates to non-human biota (Vives i Batlle, et al., 2007). 11 models and 7 radionuclides (H-3, C-14, Co-60, Sr-90, Cs-137, U-238 and Am-241) were used to estimate internal and external unweighted absorbed dose rates. A nominal activity concentration of 1 Bq kg^{-1} in an organism and surrounding media were used as the input to each model. The estimated internal dose rates were not so different between the models (coefficient of variation <25%). In the FASSET model, however, estimated the internal dose conversion coefficient (DCC) for aquatic organisms to be twice as high as in the other models because it included U-234 which is a daughter product of U-238 in the estimation. The external dose rates from the different models were more variable than the internal dose rates with coefficient of variation 120%. The external dose rates of terrestrial organisms for Sr-90 estimated by ERICA were lower than the other models because this model had taken into account fur/feathers shielding. Beresford et al. 2008 (Beresford, Barnett, et al., 2008) compare the activity concentration of terrestrial and freshwater organisms predicted by 8 models (RESRAD-BIOTA, R&D128, FASSET, ERICA, ECOMOD, AEC, LIETDOS-BIO and DosDiMEco). An activity concentration of 1 Bq kg^{-1} in surrounding media was used to be input of each model. There was a significant variation of the prediction in different models. The reasons of the variability are linkages between databases used, user

interpretation, data source, data availability and food chain versus CR approaches. The variability of the comparison of the prediction of activity concentration is higher than the comparison of exposure doses. The parameter of the models transfer components is the most important for the variability of the model predictions. For a model-data comparison, the comparison between the measured and predicted activity concentration was performed in the terrestrial wildlife in the Chernobyl exclusion zone (Beresford, et al., 2010) and in Perch Lake, Canada (Yankovich, et al., 2010).

1.8 Project objectives

The purpose of the present study is to further compare and test models for estimating radiation doses to biota in the natural environment.

In addition to carrying out further model intercomparison and testing against empirical data, this research will also support previous work on the effects of radiation on aquatic biota (e.g. (Cailes, 2006) and (Tumnoi, 2006)) by accurately measuring the dose in the littoral zone of the lakes. These workers have assessed the diversity of aquatic invertebrates in lakes situated in and around the most contaminated areas of Ukraine and Belarus. They also studied the genetic diversity and fluctuating asymmetry of populations of red-eyed damselfly, *Erythromma najas* and roach. However, in order to evaluate the results of these effects studies, it is important to accurately estimate doses to the organisms studied.

The main objectives of this work are therefore:

1. Development of a suitable thermoluminescent dosimetry system for measuring external radiation doses in aquatic environments. This project will investigate the feasibility of performing new in situ measurements of beta dose by using a combination of filters and analysis of the TLD glow curve. No such in situ beta measurements are reported in the current literature.

2. New field visits to the Chernobyl contaminated regions of Belarus to undertake in-situ measurements of external beta and gamma dose for chosen aquatic environments.

3. The verification and critical analysis of various models used for estimating radiation exposure of biota.

4. The testing of model calculations of radiation exposure to aquatic organisms by comparison with the measurements of vertical profiles of radiation dose above and below the sediment-water interface.

1.9 References

Anspaugh, L. R., Catlin, R. J., & Goldman, M. (1988). Global impact of the Chernobyl reactor accident. *Journal Name: Science (Washington, D.C.); (United States); Journal Volume: 242:4885*, Medium: X; Size: Pages: 1513-1519.

Attix, F. H., Roesch, W. C., & Tochilin, E. (1968). *Radiation Dosimetry Vol. 1* (2 nd ed.). London: Academic Press, INC.

Belarus Maps. (2008). Retrieved 1 February, 2010, from http://www.lib.utexas.edu/maps/commonwealth/chornobyl_radiation96.jpg

Beresford, N. A., Balonov, M., Beaugelin-Seiller, K., Brown, J., Copplestone, D., Hingston, J. L., et al. (2008). An international comparison of models and approaches for the estimation of the radiological exposure of non-human biota. *Applied Radiation and Isotopes, 66*(11), 1745-1749.

Beresford, N. A., Barnett, C., Brown, J., Cheng, J., Copplestone, D., Filistovic, V., et al. (2008). Inter-comparison of models to estimate radionuclide activity concentrations in non-human biota. *Radiation and Environmental Biophysics, 47*(4), 491-514.

Beresford, N. A., Barnett, C. L., Brown, J. E., Cheng, J. J., Copplestone, D., Gaschak, S., et al. (2010). Predicting the radiation exposure of terrestrial wildlife in the Chernobyl exclusion zone: an international comparison of approaches. *Journal of Radiological Protection, 30*(2), 341.

Beresford, N. A., Gaschak, S., Barnett, C. L., Howard, B. J., Chizhevsky, I., Strømman, G., et al. (2008). Estimating the exposure of small mammals at three sites within the Chernobyl exclusion zone - a test application of the ERICA Tool. *Journal of Environmental Radioactivity, 99*(9), 1496-1502.

Boice, J. D. (2010). Risk factors. Retrieved 1 February, 2010, from http://rex.nci.nih.gov/NCI_Pub_Interface/raterisk/risks90.html

Cailes, C. R. (2006). *Phenotypic and genetic effects of Chernobyl-derived radionuclide contamination on the red-eyed damselfly Erythromma Najas (Odonata, Coenagrionidae).* University of Plymouth, Plymouth.

Chambers, D. B., Osborne, R. V., & Garva, A. L. (2006). Choosing an alpha radiation weighting factor for doses to non-human biota. *Journal of Environmental Radioactivity, 87*(1), 1-14.

Copplestone, D., Andersson, P., Beresford, N., Brown, J., Dysvik, S., Garnier-Laplace, J., et al. (2009). Protection of the environment from ionising radiation in a regulatory context (PROTECT): Review of current regulatory approaches to both chemicals and radioactive substances. *Radioprotection, 44*(5), 881-886.

Copplestone, D., & et al. (2010). Considerations for the integration of human and wildlife radiological assessments. *Journal of Radiological Protection, 30*(2), 283.

Delistraty, D. (2008). Radioprotection of nonhuman biota. *Journal of Environmental Radioactivity, 99*(12), 1863-1869.

EuropianCommission. (2009). *Health effect of exposure to EMF*. Brussels: Europian Commission.

Fairlie, I., & Sumner, D. (2006). *The Other Report on Chernobyl (TORCH)*. Berlin, Brussels, Kiev: The Greens/EFA in the European Parliament.

Furetta, C. (2003). Handbook of Thermoluminescence Available from http://site.ebrary.com/lib/portsmouth/Doc?id=10085582&ppg=124

Furetta, C., Prokic, M., Salamon, R., Prokic, V., & Kitis, G. (2001). Dosimetric characteristics of tissue equivalent thermoluminescent solid TL detectors based on lithium borate. *Nuclear Instruments and Methods in Physics Research Section A: Accelerators, Spectrometers, Detectors and Associated Equipment, 456*(3), 411-417.

Greening, J. R. (1985). *Fundamentals of radiation dosimetry* (2 nd ed.). Great Britain: Page Bros (Norwich) Ltd.

Holm, L. E. (2004). A common approach for radiological protection of humans and the environment. *Journal of Environmental Radioactivity, 72*(1-2), 57-63.

IAEA. (1992). *Effects of ionising radiation on plants and animals at levels implied by current radiation protection standards*. Vienna: IAEA.

IAEA. (2003). *Protection of the Environment from Ionizing Radiation: The Development and Application of a System of Radiation Protection for the Environment*. Vienna: IAEA.

IAEA. (2006a). *Chernobyl's Legacy: Health, Environmental and Socio-Economic Impacts and Recommendations to the Governments of Belarus, the Russian Federation and Ukraine*. Vienna: IAEA.

IAEA. (2006b). *Environmental Consequences of the Chernobyl Accident and Their Remediation: Twenty years of Experience (Report of the Chernobyl Forum Expert Group 'Environment')*. Vienna: IAEA.

IAEA, & ANSTO. (2004a). Method of Radiation Detection *Radiation Protection Distance Learning Project*.

IAEA, & ANSTO. (2004b). Radiation Protection Distance Learning Project.

ICRP. (1977). *Recommendations of the International Commission on Radiological Protection. ICRP Publication 26*. Oxford: ICRP.

ICRP. (1991). *Recommendations of the International Commission on Radiological Protection. ICRP publication 60*. Oxford: ICRP.

KAERI. (2000). Table of Nuclides. Retrieved 10 October, 2010, from http://atom.kaeri.re.kr/

Knoll, G. F. (1989). *Radiation detection and measurement* (2nd ed.). Singapore: John Wiley & Sons, Inc.

Kocher, D. C., & Trabalka, J. R. (2000). On the Application of A Radiation Weighting Factor for Alpha Particles in Protection of Non-Human Biota. *Health Physics, 79*(4), 407-411.

Kudelsky, A. V., Pashkevich, V. I., Yankov, A. I., Samodurov, V. P., Savchik, S. F., & Rudemok, A. A. (2005). *Radio-ecological study of the Chernobyl Cooling Pond and options for remediation*. Minsk: National Academy of Science of Belarus.

Lawson, R. (1999). An Introduction to Radioactivity. Retrieved from http://www.e-radiography.net/articles/Introduction%20to%20Radioactivity.pdf

McKinlay, A. F. (1981). *Thermoluminescence dosimetry*. Bristol: Adam Hilger Ltd.

NPL. (2010). Ionising Radiation Quantities & Units. Retrieved 1 February, 2010, from http://www.npl.co.uk/ionising-radiation/ionising-radiation-quantities-and-units

OECD/NEA. (2002). *Chernobyl Assessment of Radiological and Health Impacts*. Paris: OECD.

Pentreath, R. J. (1998). Radiological Protection Criteria for the Natural Environment. *Radiation Protection Dosimetry, 75*(1-4), 175-179.

Pentreath, R. J. (2002). Radiation protection of people and the environment: developing a common approach. *Journal of Radiological Protection, 22*(1), 45.

Pentreath, R. J., & Woodhead, D. S. (2001). A system for protecting the environment from ionising radiation: selecting reference fauna and flora, and the possible dose models and environmental geometries that could be applied to them. *The Science of The Total Environment, 277*(1-3), 33-43.

Ranogajec-Komor, M. (2003). Thermoluminescence Dosimetry - Application in Environmental Monitoring. *Radiation Safety Management, 2*(1), 2-16.

Smith, J. T. (2005). The case against protecting the environment from ionising radiation. *Radioprotection, 40*(Suppl. 1), S967-S972.

Smith, J. T., & Beresford, N. A. (2005). Introduction. In J. T. Smith & N. A. Beresford (Eds.), *Chernobyl-Catastrophe and Consequences* (pp. 1-34). Berlin: Praxis Publishing Ltd.

Smith, J. T., Kudelsky, A. V., Ryabov, I. N., Hadderingh, R. H., & Bulgakov, A. A. (2003). Application of potassium chloride to a Chernobyl-contaminated lake: modelling the dynamics of radiocaesium in an aquatic ecosystem and decontamination of fish. *The Science of The Total Environment, 305*(1-3), 217-227.

Smith, J. T., Voitsekhovitch, O. V., Konoplev, A. V., & Kudelsky, A. V. (2005). Radioactivity in aquatic systems. In J. T. Smith & N. A. Beresford (Eds.), *Chernobyl-Catastrophe and Consequences* (pp. 139-189). Berlin: Praxis Publishing Ltd.

Stabin, M. G. (2008). *Radiation Protection and Dosimetry: An Introduction ot Health Physics*. New York: Springer Science+Business Media, LLC.

Timms, D. N. (2006). The measurement of radiation dose at the sediment/water interface of the Chernobyl cooling pond. . University of Portsmouth.

Timms, D. N., Smith, J. T., Coe, E., Kudelsky, A. V., & Yankov, A. I. (2005). In situ measurements of the sub-surface gamma dose from Chernobyl fallout. *Applied Radiation and Isotopes, 62*(6), 923-930.

Tumnoi, Y. (2006). *The effects of chronic radiation dose on the fitness and genetic diversity of Roach (Rutilus rutilus L.) in the Chernobyl region.* University of Portsmouth.

U.S.EPA. (2009a). Alpha Particles. Retrieved 1 February, 2010, from http://www.epa.gov/rpdweb00/understand/alpha.html

U.S.EPA. (2009b). Ionizing & Non-Ionizing Radiation. Retrieved 1 February, 2010, from http://www.epa.gov/radiation/understand/ionize_nonionize.html

UNSCEAR. (1996). *Sources and effects of ionising radiation*. New York: United Nations.

UNSCEAR. (2000). *Sources and effects of ionising radiation. Volume II: Effect*. New York: United Nations.

Vives i Batlle, J., Balonov, M., Beaugelin-Seiller, K., Beresford, N., Brown, J., Cheng, J. J., et al. (2007). Inter-comparison of absorbed dose rates for non-human biota. *Radiation and Environmental Biophysics, 46*(4), 349-373.

Woodhead, D. S. (1973). The radiation dose received by plaice (Pleuronectes platessa) from the waste discharged into the north-east Irish Sea from the fuel reprocessing plant at Windscale. *Health Physics, 25*(2), 115-121.

Yankovich, T. L., Batlle, J. V. i., Vives-Lynch, S., Beresford, N. A., Barnett, C. L., Beaugelin-Seiller, K., et al. (2010). An international model validation exercise on radionuclide transfer and doses to freshwater biota. *Journal of Radiological Protection, 30*(2), 299.

Chapter 2

Methods

2.1 Introduction

Currently, there are many modelling approaches for estimating radiation doses to biota. Some of the available models are country-specific research models (for example RESRAD-BIOTA and R&D128), but there are also models which are effective for the prediction of the radiation doses in biota at any given site (for example FASSET, ERICA and D-MAX model).

The assessment of radiation doses can be divided into two categories: internal and external doses. Model calculation is, of course, an effective method to determine both internal and external doses. In this chapter, the five models (RESRAD, FASSET, ERICA, R&D128 and the D-Max model) used in this thesis for estimating both internal and external doses are described.

External radiation dose can also be determined by in situ measurement: such measurements are important for model validation purposes, and to give a direct assessment of doses to organisms at particular contaminated sites. From a review of the literature, it was found that there have been some experiments using thermoluminescent dosimeter (TLD) for determination of external dose from gamma radiation (Abraham, Whicker et al. 2000; Timms, Smith et al. 2005) but none have attempted to use TLDs to determine external dose form beta radiation.

A new in situ measurement for the prediction of external gamma and beta radiation by using TLDs will be described. TLD is chosen for in situ measurement because it is passive dosimeter (it keeps a cumulative record until the evaluation), suitable for the selected environment (water and sediment), small and reliable (Timms, Smith et al. 2005). For comparing model predicted external doses with measured values, measurements will be presented of radionuclides in sediments of the study lakes. Gamma spectrometry using a germanium semiconductor detector was also used to measure the activity concentration of Cs-137 in environmental media samples (sediment, water and tissue concentration) in Svyatoye, Perstok and Dvorishche lakes. For Sr-90, the activity concentrations in environmental media samples were measured

by using alpha/beta gas flow detector. Because of the difficulty of transporting samples to the UK, the radioactivity concentration measurements had to be made by collaborators at the Belarussian State University, Minsk. However, the sample methods used will be presented here.

2.2 External dosimetry measurements

2.2.1 Design of the thermoluminescent dosimeter array

This study used thermoluminescent dosimeters (TLDs) to measure in situ gamma and beta doses in the lake sediments and water. In order to differentiate between beta and gamma radiation, both shielded and unshielded TLDs were used. TLDs shielded by acrylic plastic plates gave the gamma dose and the unshielded TLDs gave the combined beta and gamma dose. The required thickness of shielding was determined from the range in beta radiation. Beta radiation in the lake mostly comes from strontium-90 (Sr-90), Caesium-137 (Cs-137) and Potassium-40 (K-40).

Sr-90 is still radiologically significant in areas close to the Chernobyl nuclear power plant (Mück, Pröhl et al. 2002) such as Perstok lake. Sr-90 undergoes beta decay (0.546 MeV) to Yttrium-90 (Y-90) which undergoes beta decay energy 2.280 MeV to Zr-90 (Zirconium) which is a stable isotope (KAERI 2000). The beta energy spectra of Sr-90, Y-90 and Sr-90/Y-90 are shown in **Figure 2.1.** There are two beta energies emitted from Cs-137; (1) 0.514 MeV maximum energy (94.4% yield) and (2) 1.176 MeV maximum energy (5.6% yield) (KAERI 2000). The decay scheme of the nuclide was already presented in **Figure 1.7** in Chapter 1. There are three isotopes of Potassium: naturally occurring: K-39 (93.3%), K-40 (0.012%) and K-41 (6.7%) (Audi, Bersillon et al. 1997). K-39 and K-41 are stable isotopes whilst K-40 is Naturally Occurring Radioactive Material (NORM). K-40 decays with a 1.26×10^9 year half-life. The decay of K-40 produces 89% of beta particles with a maximum energy 1.314 MeV to the stable nuclide Calcium-40 (Ca-40) and the remainder (11%) decaying via the electron capture and then disintegrates gamma rays 1.460 MeV to the stable nuclide Argon-40 (Ar-40) (Knoll 1989). The decay scheme of the nuclide is presented in **Figure 2.2**

The maximum beta energy of Sr-90 shows the highest value (2.280 MeV) comparing between Sr-90, Cs-137 and K-40. So, the thickness of beta shielding was determined

from the maximum beta energy of Sr-90. Cs-137 and K-40 give the lower maximum beta energy (1.176 and 1.314 MeV) respectively.

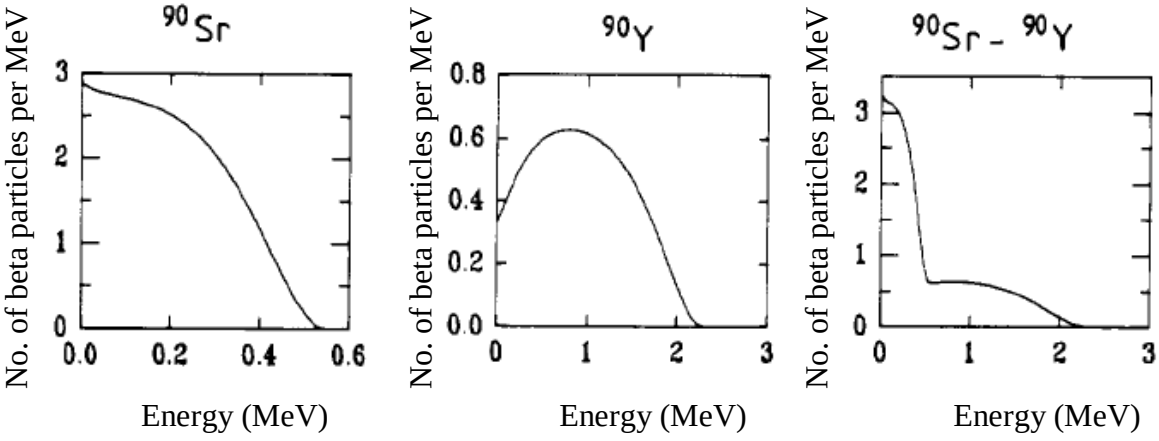

Figure 2.1 Beta energy spectrums (a) Sr-90 (b) Y-90 (c) Sr-90/Y-90 (Cross, Ing et al. 1983).

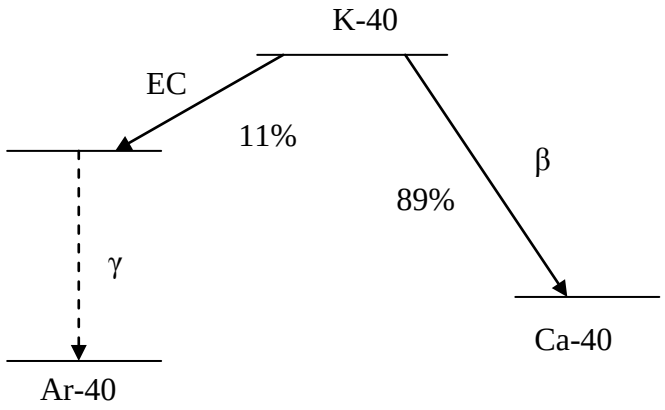

Figure 2.2 Decay scheme of Potassium-40 (Knoll 1989).

Unlike alpha particles and gamma rays, which are emitted in discrete energy bands, beta particles are emitted in a continuous energy spectrum (energy ranging from zero to the maximum energy) (Stabin 2008). The average energy can be estimated to be about one-third of maximum energy (Lilley 2009). For Sr-90/Y-90 decay, the maximum energy and average energy can be used from Y-90 decay which is 2.280 MeV and 0.76 MeV respectively.

The range of beta particles can be calculated from Equation 2.1 (Stabin 2008) where R is the range of beta particles in mg cm^{-2} travelling in low atomic number materials and E is kinetic energy in the range 0.01<E<2.5 MeV.

$$R = 412E^{1.265-0.0954\ln E} \quad (2.1)$$

From Equation 2.1, the maximum range of beta particles from Sr-90 can be calculated from the maximum energy (2.280 MeV) which is around 1.1 g cm^{-2}. The density of the acrylic plastic which is use to make a TLD array is 1.2 g cm^{-3}. So, the maximum range of beta from Sr-90 in plastic is around 0.92 cm. A thickness of plastic plate greater than 0.92 cm was therefore used for shielding the TLDs from Sr-90 (also Cs-137 and K-40) beta radiation. For the unshielded dosimeters (to measure the sum of beta and gamma radiation), eleven holes were made in both front and back plastic plate at 5 cm intervals. As can be seen in **Figure 2.3**, the instrument is separated into 2 columns. Column A is designed for measuring gamma radiation which has 1.0 cm plastic for beta radiation shielding. Column B is design for measuring both beta and gamma radiation because it has no plastic shielding. Beta radiation can be determined by subtracting the dose from TLDs in column A by those from column B.

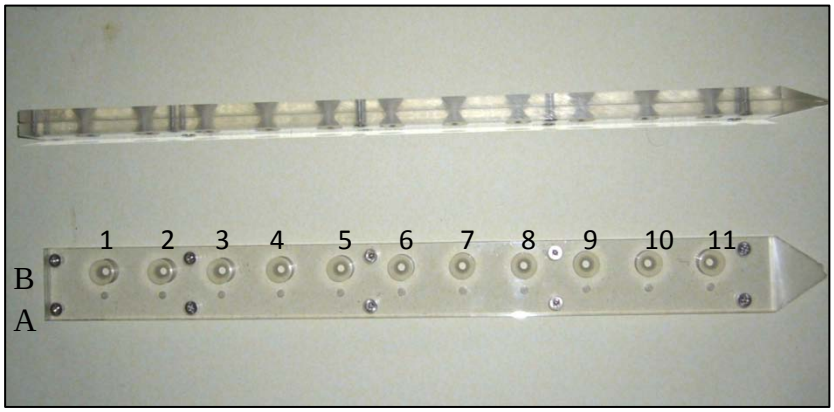

Figure 2.3 The instrument for measuring radiation doses in the lake sediments and water.

The TLDs used in this study were Harshaw TLD-100 that consist of lithium fluoride doped with magnesium and titanium (LiF:Mg,Ti). The dimensions of each TLD are 3.2 mm x 3.2 mm x 0.9 mm. Before using, the annealing process of 1 h 400 °C followed by 24 h 80 °C was used to ensure that the sensitivity and background of each TLD is standardised. The TLD-100 is calibrated using Cs-137 photons in a UKAS accredited facility at the Defence Science and Technology Laboratory (DSTL), Alverstoke. The

TLD-100 fading is lower than 5% per month at 25 °C. The higher temperatures and humidity will increase the fading rate. However, the effect of humidity can minimised by using heat sealed protective plastic sachet. A protective plastic film which has a wall thickness of 75 μm was used to seal each TLD chip: this was heat-sealed making it both light protective and waterproof.

The TLD chips sealed with plastic film were placed in each hole so that a total of 22 TLD chips were placed in each TLD array. For the estimation of the absorbed dose rate of the water in each level, TLD chips number 1,2,3,4 and 5 represent absorbed dose rate at level 25, 20, 15, 10 and 5 cm above sediment surface respectively. TLD chips number 6 represent absorbed dose rate at the sediment surface. For the absorbed dose in the sediment, TLD chips number 7, 8, 9, 10 and 11 represent absorbed dose rate at level 5, 10, 15, 20 and 25 cm underneath the sediment surface respectively. The relationship of each TLD chip to the absorbed dose rate in each level was illustrated in **Figure 2.4**.

Three TLD arrays were then placed in each of the three study lakes (Svyatoye, Perstok and Dvorishche lake) at marked positions for measuring both gamma and beta doses. The sampling points in each lake were chosen near the lake bank (lake littoral zone) because this thesis is concerned with the radiation dose received by biota: the organisms in the littoral zone are more diverse than in the deeper areas of the lake. The experimental sites were the same as those previously used for invertebrate studies in these lakes (Cailes 2006) allowing direct estimation of external dose rates to these organisms. In summer 2007, a pilot study was performed, but the results of this indicated the potential “smearing” of contaminated sediment down the core tube. In the second field campaign (2008), a stainless steel sleeve was used to protect the sediment in each section as the TLD was driven into the sediment. TLD arrays number 1, 2 and 3 were placed in Svyatoye lake for 3 months from 9 July 2008 to 8 October 2008 in positions shown in **Figure 2.5.** TLD arrays number 4, 5 and 6 were placed in Perstok lake for 3 months from 11 July 2008 to 10 October 2008 in positions shown in **Figure 2.6**. TLD arrays number 7, 8 and 9 were placed in Dvorishche lake for 3 months from 11 July 2008 to 10 October 2008 in positions shown in **Figure 2.7**. The results of these experiments will be described in Chapter 5.

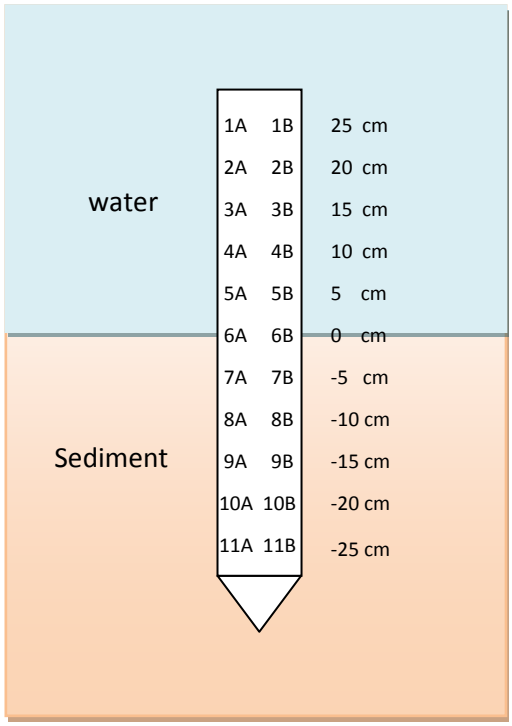

Figure 2.4 The representative TLD chips in each level of water and sediment.

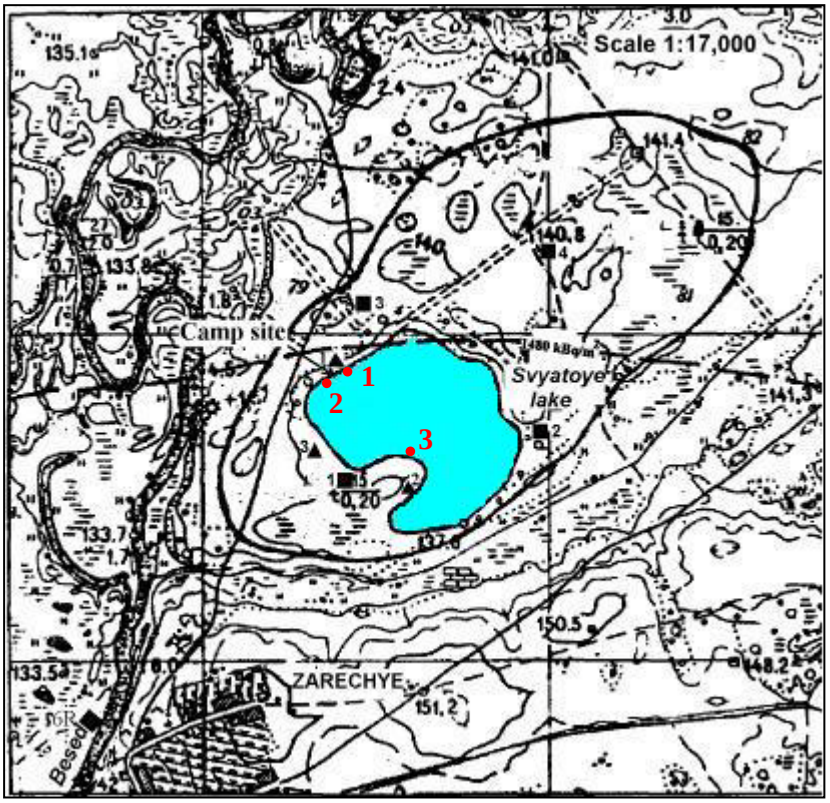

Figure 2.5 The locations of three TLD arrays that were positioned at Svyatoye lake.

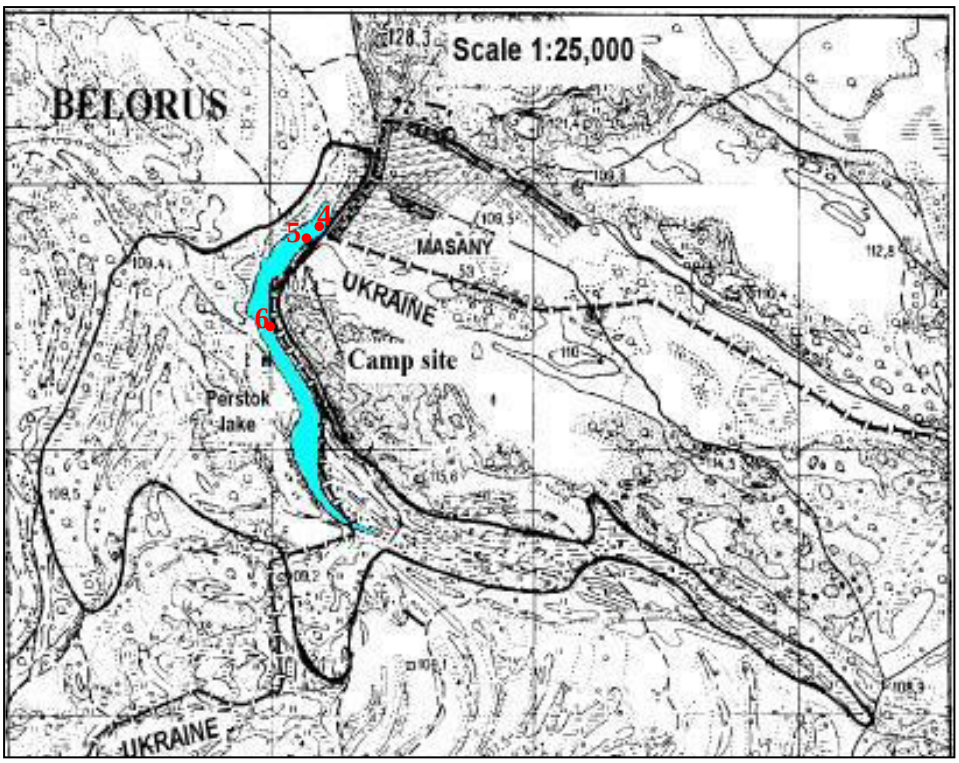

Figure 2.6 The locations of three TLD arrays that were positioned at Perstok lake.

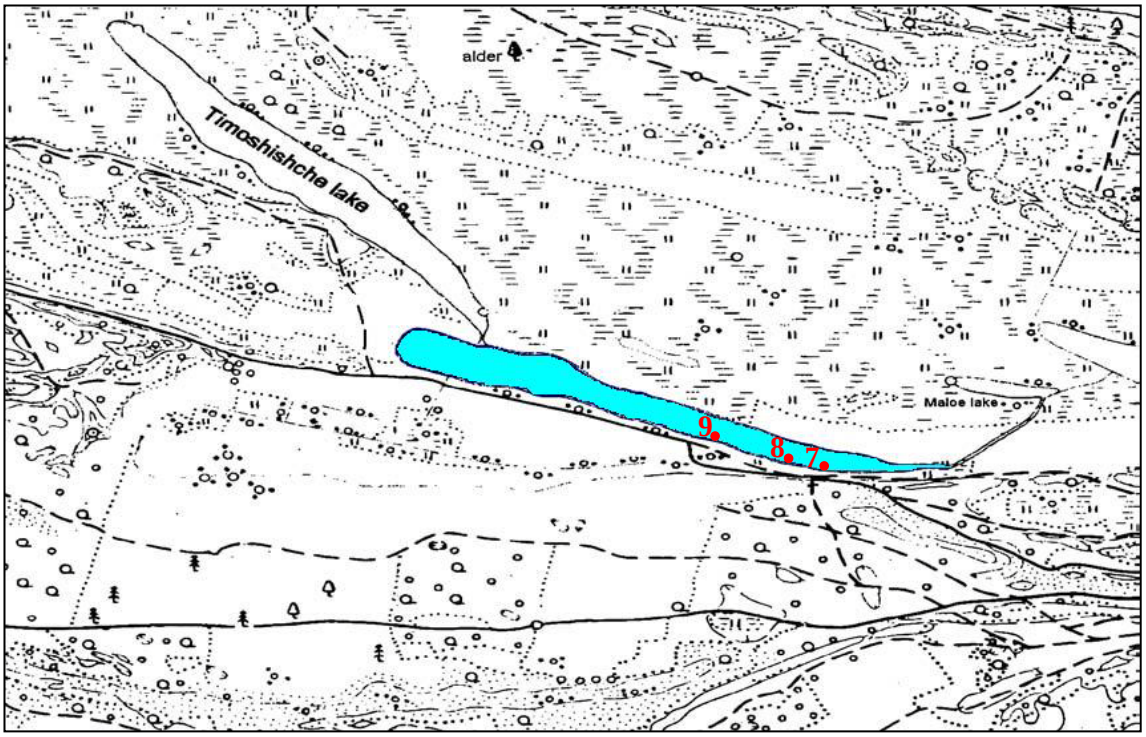

Figure 2.7 The locations of three TLD arrays that were positioned at Dvorishche lake.

After the period of exposure time, the TLDs were returned to Defence Science and Technology Laboratory (DSTL) for reading. TLDs were assessed by using a Toledo Model 654 TLD Reader. The heating cycle consisted of a 16 second pre-anneal at 135 °C followed by 16 second read-out at 240 °C and 16 second post-anneal at 240 °C.

2.2.2 Sediment sampling

Three sediment sampling points were taken in each lake (Svyatoye, Perstok and Dvorishche lake) by workers at the Institute of Geochemistry and Geophysics in Belarus. Sediment samples were collected on 8 October 2008 for Svyatoye lake, 10 October 2008 for Perstok lake and 10 October 2008 for Dvorishche lake. The sampling points were taken close to the positioned-TLD array near the lake bank. The sediment sampling equipment illustrated in **Figure 2.8** was designed and made by Belarusian scientists. The sediment water samples were collected in each 5 cm vertical depth profile from the sediment surface until 25 cm depth.

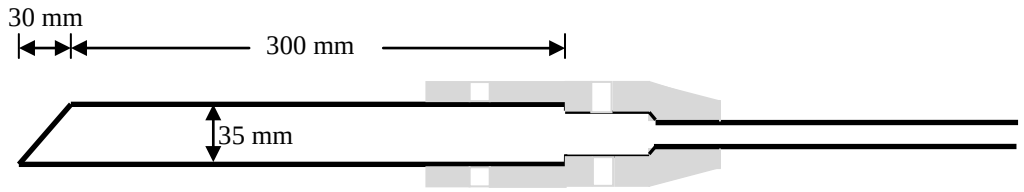

Figure 2.8 Sediment sampling equipment.

It was impossible to carry out the sediment samples from the site to analyse outside of Belarus. So, the sample analysis was carried out by Belarusian scientists according to an agreed protocol described below.

2.2.3 The determination of Cs-137

The sediment sample preparation was performed before sample analysis by drying the samples at 293-298 °K and then homogenising the samples by grinding them using a pestle and mortar. The Canberra gamma-spectrometry system consisted of a coaxial high-purity germanium detector with carbon window composition, multichannel analyser DSA 1000 and lead shielding was used for determining activity concentration of Cs-137 in sediment samples. The germanium detector has 50% relative efficiency

and has an energy range from 20 keV to 2 MeV. The lead shielding (model 747E) covered with cadmium-copper sheet inside the chamber was used for reducing the level of background radiation.

2.2.4 The determination of Sr-90

The sediment sample preparation for determination of Sr-90 activity concentration used the same method as the sample preparation for determination of Cs-137 described above. In addition, the incineration of the sediment sample for destruction of organic substances was carried out. The sediment sample was placed and incinerated at 823-873 °K for 6-8 hours. Radiochemical analysis was performed by using the guidance of Inter-departmental commission of radiation control of the environment in 1989 and "Measurement of Radionuclides in Food and the Environment"- Technical report series No.295, 1989 (IAEA 1989). The Canberra alpha-beta gas flow counter (Model LB4100) and atomic-absorption spectrophotometer (SOLAAR S2) were used to determine Sr-90 activity concentration.

2.3 Gamma-ray spectroscopy

Gamma spectrometry was used in this experiment for evaluating gamma-emitting radionuclides in water and sediment samples. The sample preparation before gamma measurement was described above. In this experiment, gamma spectrometry was performed for measuring activity of Cs-137 in water and sediment samples.

2.3.1 Gamma-ray spectroscopy system

The basic electronics system for a gamma-ray spectroscopy system consists of a detector, high voltage power supply, preamplifier, amplifier, analog to digital convertors (ADC), discriminator, multichannel analyser (MCA) and data storage.

Gamma-ray detector

Currently, there are only two main detector types for measuring gamma-ray energies above several hundred keV: sodium iodide scintillation detector (NaI) and germanium semiconductor detectors (Knoll 1989).

Sodium iodide scintillation detector (NaI) is one type of scintillation detectors comprising an inorganic scintillator. The scintillation mechanism can be described in

terms of the crystal lattice structure of the material. There are two electron bands in the lattice of material: the valence band (lower band) and conduction band (higher band). In the normal situation, electrons are filled in the valence band. When gamma-ray photons come through the lattice, they transfer their energy to the electrons in the valence band. The electrons in valence band then have enough energy to move across the band gap to the conduction band by the excitation process. However, the electrons can't remain in the conduction band, so they drop again to the valence band. The light released when the electrons move from the conduction band to the valence band is converted to an electrical signal by a system of electronic amplification. The size of the electrical signal depends on the number of moving electrons and the amount of radiation that is incident on the detector (McKinlay 1981; Knoll 1989).

The germanium semiconductor detector is another type of solid state conductivity detector which uses germanium as a crystal for measuring the radiation. This solid state detector consists of N-type and P-type semiconductors joined together (IAEA and ANSTO 2004). The N-type of semiconductor contains donor impurity elements with five valence electrons such as phosphorus, arsenic and antimony (Debertin and Helmer 1988). The P-type of semiconductor is an acceptor which contains impurity with three valence electrons such as boron, aluminium, gallium or indium (Debertin and Helmer 1988). A reverse bias voltage (positive voltage for n-type and negative voltage for P-type) is applied across the junction which makes electron and "holes" move away from the junction. The area between the junction which is free from electrons and holes is called the depletion layer (Knoll 1989; IAEA and ANSTO 2004). The electrons and holes are produced when ionising radiations pass through the depletion layer. These electrons and holes are converted to an electrical signal by the electronic amplification system.

There are two main factors for consideration in gamma spectrometry: counting efficiency and energy resolution. The counting efficiency of the NaI detector is higher than the germanium semiconductor detector because the NaI detector has a large size and high density of material which results in high interaction probabilities for gamma rays (Knoll 1989). However, the energy resolution of NaI is poor if compared with the germanium semiconductor detector. The germanium semiconductor detector is widely used to analyse complex gamma-ray spectrum which have many peaks. However, the germanium semiconductor detector must be cooled to reduce the leakage current (Knoll

1989). This condition makes the germanium semiconductor detector less portable than the NaI detector.

The energy resolution of detector is the potentiality of the detector to separate the close energy peak. The energy resolution can determined from the width of the peak (Stabin 2008). If the peak is wider, the energy resolution is poorer. The energy resolution of detector can defined from the Full With at Half Maximum (FWHM) divided by the location of the peak centroid (H_0) (Knoll 1989) as show in **Figure 2.9**.

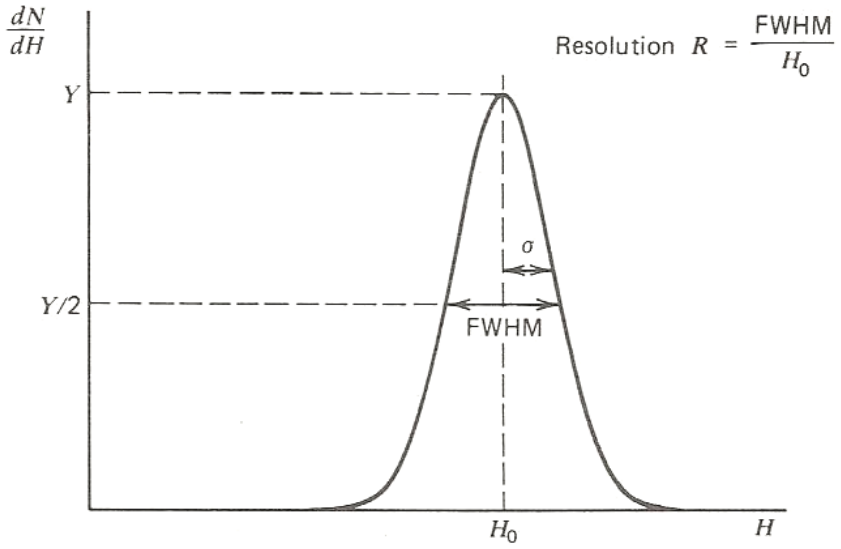

Figure 2.9 The definition of FWHM (Knoll 1989).

Electrical system and amplification.

A high voltage power supply (HV) is necessary for the detector to supply operating potential (IAEA and ANSTO 2004). The level of HV depends on type of detector from hundreds volts for a small detector to over 4000 volts for a large detector (Debertin and Helmer 1988). The preamplifier is important for the detector because the signal from the detector is so small. The preamplifier is situated close to the detector to prevent the loss of the signal. The main function of amplifier is to gain the signal from the detector from very low current to current which can be measured by ammeter (IAEA and ANSTO 2004). The stability of the amplifier is really important to the detector because if the amplifier changes, the peak channel also will change.

The signal which comes from the amplifier is analog output but a digital signal output is necessary for the processing. ADC is needed for changing the analog output to digital output.

Some output signals are too high and some of them are too low. Discriminator is applied to use for eliminating both too high and too low signal from the system. Lower Level Discriminator (LLD) can set to eliminate the unwanted noise from the system. The standard size of pulse is provided by the discriminator for counting system when the pulse is into the discriminator range (IAEA and ANSTO 2004).

The MCA is used to separate the pulses into different memory channel which depends on their height. The energy spectrum of radiation can be defined from the number of pulses accumulated in each channel.

2.3.2 Spectrum analysis

The main purpose of gamma spectrometry is the determination of the amount and energy of photons emitted by a radiation source (Debertin and Helmer 1988). The information from a gamma spectrum can identify the radionuclide in the source and also can determine the activity of each radionuclide that is present. The radionuclide can be identified by using the distinction between the emission energy of each radionuclide. For example, the result of an analysis of unknown source shows energy peaks at 661.11, 1173 and 1332 keV. The radionuclide in the sample as analysed by gamma spectrometry will be Cs-137 and Co-60 because of the known emission energies of their gamma photons. The activity of radionuclide can be determined from the area under the peak (count rate of the peak) by comparing with a standard radiation source.

The peak shapes of NaI scintillation detector and Ge(Li) detector semiconductor detector are shown in **Figure 2.10**.

Energy calibration

Energy calibration is necessary for gamma spectrometry to identify the energy of the peak. Before the energy calibration process, the spectrum of energy is only known as a scale between the pulse height and channel number. The channel number must be calibrated with a standard source to determine the relationship between the channel number and the energy. The standard source is a radiation source which consists of

radionuclides of known energy. After the energy calibration process, the energy spectrum will show on a scale of the pulse height against energy.

Efficiency calibration

Efficiency can be defined as the ratio between the instrument response (scale reading, current, count rate, etc.) and the measurement value of a physical quantity (Debertin and Helmer 1988). For gamma spectrometry, the instrument response is the count rate of the peak, and the measurement value of the physical quantity is the emission rate of gamma rays. Then, the efficiency calibration is the calibration relating the emission rate of gamma rays to the count rate of the peak. By using efficiency calibration, the count rate of the peak can be converted to the activity of radionuclide.

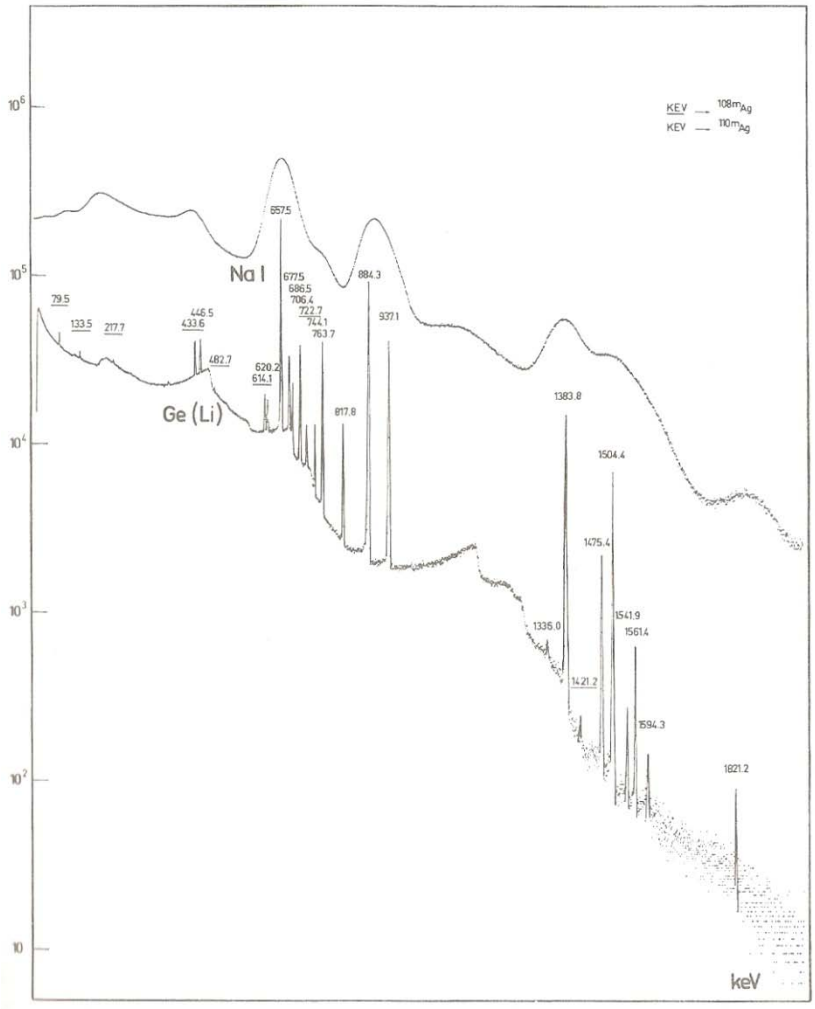

Figure 2.10 The peak shape of energy calibrated NaI and Ge(Li) detectors (Knoll 1989).

2.4 The description of the models used in this study

Over the past decade, the international organisations for radiation protection (IAEA, ICRP) have addressed the protection of the environment from ionising radiation (Vives i Batlle, Balonov et al. 2007; Beresford, Balonov et al. 2008; Beresford and et al. 2010). Some countries such as the United Stated of America (USA), England and Wales and Canada already have requirements and guidelines for the protection of non-human biota (Beresford, Balonov et al. 2008).

In response to these requirements, many models and approaches are currently being used for estimating radiation exposure to non-human biota (Beresford, Balonov et al. 2005; Vives i Batlle, Balonov et al. 2007; Beresford, Balonov et al. 2008; Beresford and et al. 2010). The generic structure of the models for evaluating the environmental impact of ionising radiation is shown in **Figure 2.11**. For such assessments, the ecosystem (freshwater, terrestrial and marine), type of organisms and type of radionuclides need to be considered. By using media activity concentration data (water, sediment/soil or air concentration) as input data, the internal and external dose rates for each organism can be estimated. However, parameters such as physical dimensions (geometry), residence time (time spent in a particular site), habitat (time spent in different areas of the site) and trophic transfer of radionuclides for each organism can vary considerably, leading to uncertainties in model assessments (Wood 2010). From **Figure 2.11**, the external dose rates can be predicted by using media concentration data and the parameters, whilst the internal dose rate uses the media activity concentration to predict tissue activity concentration/ or use tissue activity concentration from the measurement to predict the dose rate. The predicted dose rates are compared with the guidelines and/or radiation effects to determine impacts of the radiation and then formulated the decision.

There are five models (FASSET, ERICA, RESRAD-BIOTA, R&D128 and D-MAX model) described and used in this thesis because of open sources.

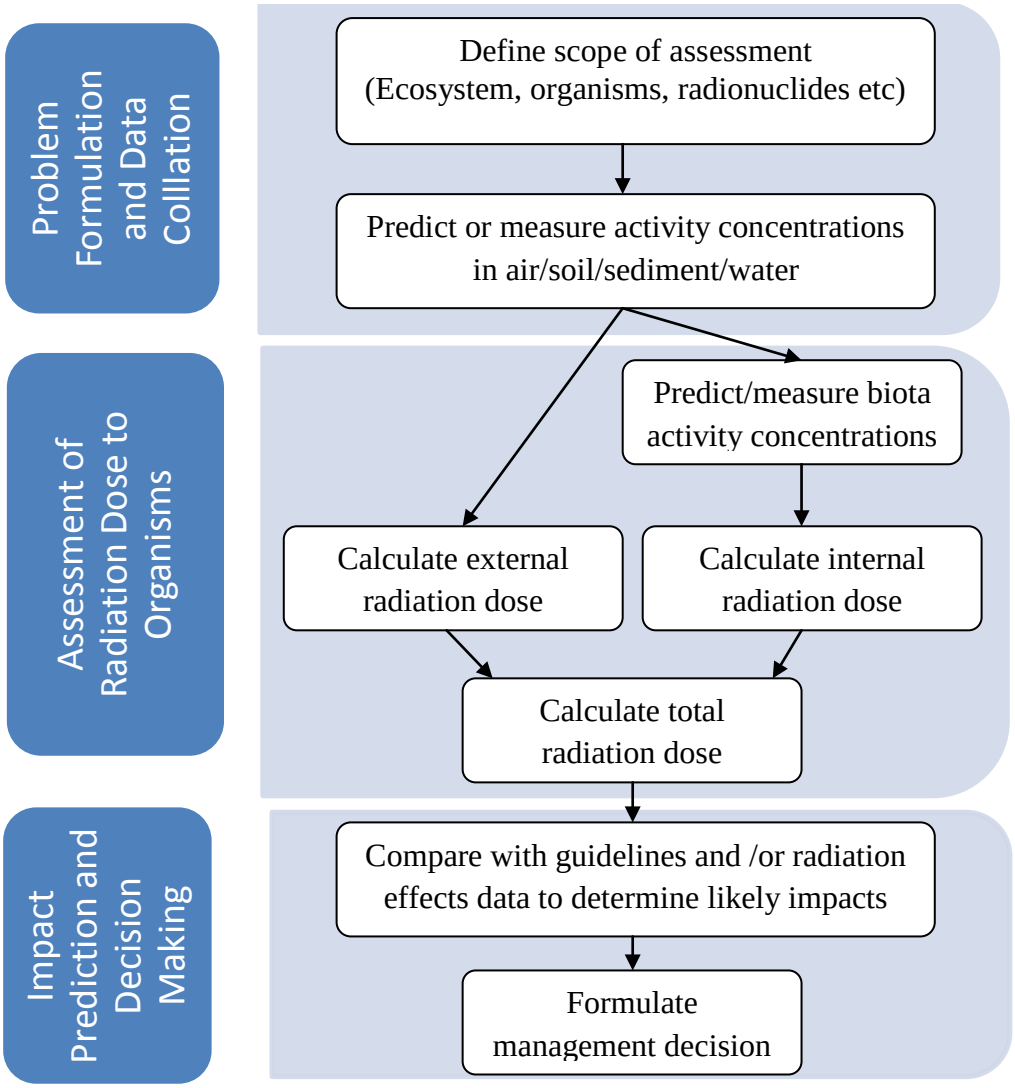

Figure 2.11 The generic structure of the models for evaluating the environmental impact of ionising radiation (Wood 2010).

2.4.1 FASSET model

The FASSET project is the 5th European Commission (EC) framework programme that was launched on November 2000 and finished on October 2003 for assessing the environmental impact of ionising radiation in European countries. There were 15 organisations and 7 European Countries involved in this project (Larsson 2004). The FASSET model is a complex Monte Carlo programme which is presented as look-up table for assessing radiation exposures to biota. This dosimetric model enables the assessment of exposures to a broad range of target organisms due to both internal and external exposure. Seven ecosystems (forest, semi-natural, agricultural, wetlands, freshwater, marine and brackish water) and radioisotopes of 20 elements (H, C, K, Cl,

Ni, Sr, Nb, Tc, Ru, I, Cs, Po, Pb, Ra, Th, U, Pu, Am, Np, Cm) are taken into account (FASSET 2003). Concentration ratios (CRs) from the literature and activity concentrations in contaminated media such as soil, water or sediments are used to estimate activity concentration in biota (Beresford, Barnett et al. 2008). Nuclide-specific dose conversion coefficients (DCCs) are derived taking into account habitat, target size and exposure route.

Ecosystems

Europe has wide range ecosystems from Mediterranean to polar desert. The FASSET project has considered the exposure of biota in every ecosystem, although it should be noted that empirical data are better available for some ecosystems than others (FASSET 2001). Even though seven ecosystems had been taken into account, there were only two groups of reference organism: these are Terrestrial (forest, semi-natural, agricultural and wetlands) and Aquatic (freshwater, marine and brackish water). Two main categories of ecosystem have been defined for The FASSET model: terrestrial (on soil and in soil) and aquatic (coastal and fresh water) ecosystems.

Radionuclides

There are many man-made and natural radionuclides that need to be considered for assessing radiation exposure to biota, but it is impossible to include all of them in the approach. The FASSET model selected 20 radionuclides (37 radioisotopes) that are normally used in the assessment of releases of wastes from various facilities as well as accidental releases. Radionuclides and their radioisotope that selected by FASSET model are shown in **Table 2.1**.

Reference organisms

As in the case of radionuclides, it is not possible to select all organisms for assessing radiation exposure. The reference organism species selected in the FASSET approach are chosen to be representative of a wide range of ecosystems. The reference organisms for terrestrial and aquatic ecosystems for the FASSET model are shown in **Table 2.2**.

Table 2.1 Radionuclides chosen for inclusion in the FASSET model (FASSET 2001)

Radionuclide	Radioisotope
H	H-3
C	C-14
K	K-40
Cl	Cl-36
Ni	Ni-63, Ni-59
Sr	Sr-89, Sr-90
Nb	Nb-94
Tc	Tc-99
Ru	Ru-106
I	I-129, I-131
Cs	Cs-134, Cs-135,Cs-137
Po	Po-210
Pb	Pb-210
Ra	Ra-226
Th	Th-227, Th-228, Th-230, Th-231, Th-232, Th-234
U	U-234, U-235, U-238
Pu	Pu-239, Pu-240, Pu-241
Am	Am-241
Np	Np-237
Cm	Cm-242, Cm-243, Cm-244

Table 2.2 Reference organisms for terrestrial and aquatic ecosystems (FASSET 2003).

Ecosystems	Organisms
Terrestrial	microorganism, fungi, lichen/bryophyte, grass/herb/crop, plant, shrub, tree, worm, canopy invertebrate, detritivorous insect, herbivorous mammal, burrowing mammal, carnivorous mammal, bird egg
Aquatic	Bacteria, phytoplankton, macroalgae, vascular plant, worm, bivalve mollusc, insect larvae, zooplankton, crustacean, benthic fish, pelagic fish, amphibian, wading bird, mammal

Assessment methodology

For the FASSET approach, the absorbed dose rate (in units of µGy per hour) received by an organism can be calculated from the activity concentration of radionuclides in the media (soil, water or air) of their habitat using Dose Conversion Factors (DCC). DCC is a factor provided in a look-up table.

Any organism can be exposed to the sum of external and internal exposure from ionising radiation from radionuclides in media. The total absorbed dose rate can be derived in terms of the internal dose rate and the external dose rate that show in equation 2.2 (FASSET 2003).

$$D_{total} = D_{int} + D_{ext} \quad (2.2)$$

Where D_{total} is the total absorbed dose rate received by the biota (µGy hr^{-1}),

D_{int} is the internal absorbed dose rate received by the biota (µGy hr^{-1}) and

D_{ext} is the external absorbed dose rate received by the biota (µGy hr^{-1})

Assessment of the external exposure

The FASSET Model has used Monte Carlo calculations to calculate the energy range of monoenergetic photons and electrons in soil. DCC can be given by the value of the absorbed dose rate normalised per starting photon and surface unit (FASSET 2003).

$$C_{surf} = \frac{D}{j} = \frac{D}{n} \times A_{surf} = D \times A_{surf} \quad (2.3)$$

Where C_{surf} is dose rate conversion coefficient (Gy s^{-1})/(photon s^{-1} m^{-2}),

D is absorbed dose rate in target (Gy s^{-1}),

j is flow rate of source photons (photon s^{-1} m^{-2}),

n is number of source photon emitted in unit time (photon s^{-1}),

A_{surf} is surface area of the source (m^2) and

D is absorbed dose normalised per starting photon (Gy)

The estimation of the external exposure for the terrestrial environment is more complicated than the aquatic environment because of the differentiation of the composition and density of soil, air and organic matter and cannot be appropriately taken into account by analytical solutions (FASSET 2003). Therefore, Monte Carlo Method provides several advantages, for example, the composition and density of

material can be considered, complex geometries of sources and targets can be simulated, self shielding is considered and the uncertainty of the simulation is very low (FASSET 2003). In order to estimate the external dose when the reference organism deposited at some depth into the soil, the important factors are the energy of emitted radiation and the distribution of radionuclide concentration in the soil. Monte Carlo Technique is used to calculate the absorbed dose for considering the effect of depth distribution assuming monoenergetic gamma emitters uniformly distributed on a plane at different depths (FASSET 2003).

The external dose rate for aquatic and terrestrial organisms are calculated in a slightly different ways. The equation in each environment is given as the following (FASSET 2003);

Terrestrial ecosystems:

$$D_{ext} = \sum v \sum C^{*}DCC_{ext} \quad (2.4)$$

Where C is the average concentration of the radionuclide in the reference media (Bq kg^{-1} dry weight),

DCC_{ext} is the dose conversion coefficient for external exposure (μGy hr^{-1} per Bq kg^{-1}) and

v is the fraction of the time that the organism expends in the habitat

Aquatic ecosystems:

$$D_{ext} = \sum DCC_{ext} * [v_{water}+0.5v_{watsurf}+0.5v_{sedsurf}).C_{water} + (0.5v_{sedsurf}+v_{sed}).C_{sed}] \quad (2.5)$$

Where C_{water} is the average concentration of the radionuclide in water (Bq l^{-1}, dissolved phase),

C_{sed} is the average concentration of the radionuclide in sediment (Bq kg^{-1}, fresh weight),

DCC_{ext} is the dose conversion coefficient for external exposure (μGy hr^{-1} per Bq kg^{-1}) and

V_{water}, $V_{watsurf}$, $V_{sedsurf}$ and V_{sed} are the fraction of time that the organism spends in the water column, at the air-water interface, at the sediment surface and buried in the sediment respectively.

Assessment of the internal exposure

In the same way as external exposure, the DCC of internal dose rate can be defined as the ratio between the absorbed dose in the target and the mass activity concentration in contaminated tissue (FASSET 2003).

$$C_{int} = \frac{D}{Sm} = \frac{D}{n} \times m = D \times m \quad (2.6)$$

Where C_{int} is dose rate conversion coefficient for organism (Gy s^{-1})/(photon s^{-1} kg^{-1}),

D is absorbed dose rate in target (Gy s^{-1}),

S_m is number of source photon emitted per unit mass per unit time (photon s^{-1} kg^{-1}),

n is number of source photon emitted per unit time (photon s^{-1}), m is target mass (kg) and

D is absorbed dose normalised per starting photon (Gy)

The internal dose rate for terrestrial and aquatic biota can be calculated from the activity concentration of organism and DCC using the following equation.

$$D_{int} = \sum C * DCC_{int} \quad (2.7)$$

Where C is the average concentration of radionuclide in the reference organism (Bq kg^{-1} fresh weight) and

DCC_{int} is the dose conversion coefficient for internal exposure (µGy hr^{-1} per Bq kg^{-1})

The activity concentration of radionuclide in reference biota can be estimated from concentration ratios (CRs) and media activity concentration. The CRs are defined as:

For terrestrial ecosystems,

$$CR = C_b / C_{soil} \quad (2.8)$$

Where CR is the concentration ratio for reference organism,

C_b is the activity concentration of radionuclide in biota (Bq kg^{-1} fresh weight) and

C_{soil} is the activity concentration of radionuclide in soil (Bq kg^{-1} dry weight)

For aquatic ecosystems,

$$CR = C_b/C_{aq} \quad (2.9)$$

Where CR is the concentration ration for reference organism,

C_b is the activity concentration of radionuclide in biota (Bq kg^{-1} fresh weight) and

C_{aq} is the activity concentration of radionuclide in aqueous phase (Bq l^{-1})

The CRs from the FASSET model were inferred from the recommendation from IAEA, atmospheric deposition soil-plant model and the England and Wales Environment Agency approach (Beresford, Barnett et al. 2008).

2.4.2 ERICA Model

ERICA project co-funded by European Commission under the Euratom Research and Training Programme on Nuclear Energy within Sixth Framework Programme (2002-2006). ERICA is a development of FASSET model, so there are many similarities between ERICA and FASSET model. ERICA model is a computer software programme which based on and adapted from the FASSET Model.

Radionuclides

The ERICA model has used the radionuclide database from the FASSET model. There are some more radionuclides added into the database, increasing it from 20 radionuclides (37 radioisotopes) in FASSET model to 31 radionuclides (63 radioisotopes) in the ERICA model. List of radionuclides in ERICA model is shown in **Table 2.3**.

Table 2.3 Radionuclides chosen for ERICA Tool (ERICA 2007).

Radionuclide	Radioisotope
Ag	Ag-110m
Am	Am-241
C	C-14
Cd	Cd-109
Ce	Ce-141, Ce-144
Cl	Cl-36
Cm	Cm-242, Cm-243, Cm-244
Co	Co-57, Co-58, Co-60

Radionuclide	Radioisotope
Cs	Cs-134, Cs-135, Cs-136, Cs-137
Eu	Eu-152, Eu-154
H	H-3
I	I-125, I-129, I-131, I-132, I-133
Mn	Mn-54
Nb	Nb-94, Nb-95
Ni	Ni-59, Ni-65
Np	Np-237
P	P-32, P-33
Pb	Pb-210
Po	Po-210
Pu	Pu-238, Pu-239, Pu-240, Pu-241
Ra	Ra-226, Ra-228
Ru	Ru-103, Ru-106
S	S-35
Sb	Sb-124, Sb-125
Se	Se-75, Se-79
Sr	Sr-89, Sr-90
Tc	Tc-99
Te	Te-129m, Te-132
Th	Th-227, Th-228, Th-230, Th-231, Th-232, Th-234
U	U-234, U-235, U-238
Zr	Zr-95

Reference organisms

The concept of reference organisms in the ERICA tool and the Reference Animals and Plants (RAP) approach of ICRP is similar but the ERICA uses some reference organisms proposed by ICRP (ERICA 2007). According to varieties of a species of an organism, it is not possible to develop the species-specific assessment system. The definition of reference organisms of ERICA (originally formulated in the FASSET project) stated that “Reference Organisms: a series of entities that provide a basis for the estimation of radiation dose rate to a range of organisms that are typical, or representative, of a contaminated environment. These estimates, in turn, would provide a basis for assessing the likelihood and degree of radiation effects.” (Forsberg and Oughton 2006). The reference organisms in each ecosystem selected in the ERICA Tool

is shown in **Table 2.4**. These reference organisms were designed to be representative of all species found in Europe.

Assessment methodology

The ERICA approach is a computer software programme designed to help the user to estimate radiation dose rate to selected organisms, and it can help the user to make the decision whether the effects to biota are likely to be low or negligible. The assessment tool has a function to help the user to estimate environmental media activity concentration (soil/sediment/water), biota activity concentration and biota dose rate. The ERICA tool has 3 separate tiers that are suitable for the purpose of the user.

Table 2.4 Reference organisms in each ecosystem in ERICA Tool (ERICA 2007).

Ecosystems	Organisms
Terrestrial	amphibian (frog), bird (duck), bird egg (duck egg), detritivorous invertebrate, flying insects (bee), gastropod, grasses and herbs (wild grass), lichen and bryophyte, mammal (rat, deer), reptile, shrub, soil invertebrate (earthworm), tree (pine tree)
Freshwater	amphibian (frog), benthic fish, bird (duck), bivalve mollusc, crustacean, gastropod, insect larvae, mammal, pelagic fish (salmon, trout), phytoplankton, vascular plant, zooplankton
Marine	(wading) bird (duck), benthic fish (flat fish), bivalve mollusc, crustacean (crab), macro algae (brown seaweed), mammal, pelagic fish, phytoplankton, polychaete worm, reptile, Sea anemones/true corals, vascular plant, zooplankton

Tier 1 assessment: screening assessment

Tier 1 assessment is a simple tool for screening the risk of radiation effect to biota. This tier requires a few inputs (radioisotope, ecosystem and activity concentration of media) for the assessment. The default dose rate screening value 10 μGy hr^{-1} is used for all ecosystems and organisms. However, the user can change the default dose rate

screening value to a custom level. The ERICA dose rate screening value was obtained from a species sensitivity distribution analysis on chronic exposure data in the FREDERICA database (ERICA 2007). If the result of the dose rate is above the screening value, the tool will recommend the user to continue to the next tier.

Tier 2 assessment: the generic assessment

Tier 2 assessment is more complex than Tier 1. The tool allows the user to change the default parameter or add new parameters. This tier requires the selection of radioisotope, organism, dose rate screening value and uncertainty factor. The user can run this tier with the default reference organisms or make the model more site-specific by using the function “create organism” wizard. This function allows the user to change the dimensions of the organism to their site-specific values. The user has to input activity concentration of media and organism parameter for assessing the data. The output gives the external dose rate, the internal dose rate, the total dose rate, the activity concentration in organism and media, risk quotient and total dose rate per organism.

Tier 3 assessment: the detailed assessment

Tier 3 assessment is similar to, but more complex than, Tier 2. Tier 3 has no simple yes/no question and screening dose rate. Tier 3 has probabilistic capability to allow the input of probability distribution function for activity concentration data and transfer parameters. The results can be shown both assessment data of deterministic value and probabilistic data.

The estimation of exposure

The absorbed dose rate (μGy hr^{-1}) can be determined by using DCC, media activity concentration, and organism activity concentration. For the internal absorbed dose rate, if the organism activity concentration is not known, the ERICA tool can predict this from the media concentration activity by using concentration ratio (CR). For the aquatic environment, the distribution coefficient (Kd) is used for determining the activity concentration of sediment using the water activity concentration. Concentration ratios and distribution coefficients for ERICA are defined in the following equations (ERICA 2007).

Terrestrial ecosystem:

$$CR = \frac{\text{Activity concentration in biota whole body (Bq/kg fresh weight)}}{\text{Activity concentration in soil (Bq/kg dry weight)}} \quad (2.10)$$

For chronic atmospheric releases of H-3, C-14, P-32, P-33 and S-35 where:

$$CR\ (m^3 kg^{-1}) = \frac{\text{Activity concentration in biota whole body (Bq } kg^{-1} \text{ fresh weight)}}{\text{Activity concentration in air (Bq } m^{-3})} \quad (2.11)$$

Aquatic ecosystems:

$$CR\ (l\ kg^{-1}) = \frac{\text{Activity concentration in biota whole body (Bq } kg^{-1} \text{ fresh weight)}}{\text{Activity concentration of filtered water (Bq } l^{-1})} \quad (2.12)$$

$$Kd\ (l\ kg^{-1}) = \frac{\text{Activity concentration in sediment (Bq } kg^{-1} \text{ dry weight)}}{\text{Activity concentration of filtered water (Bq } l^{-1})} \quad (2.13)$$

The method to calculate the DCC value in ERICA tool is the same method as in the previous FASSET model described above.

2.4.3 RESRAD-BIOTA model

The RESRAD-BIOTA model is a computer code which was sponsored and developed by the U.S. Department of Energy (DOE), with support from the U.S. Environmental Protection Agency (EPA) and the U.S. Nuclear Regulatory Commission (NRC) (U.S.DOE 2002; U.S.DOE 2004; U.S.DOE 2009). This model was developed as a tool for implementing screening and analysis methods for evaluating radiation doses to aquatic and terrestrial biota. The model can calculate both internal and external radiation of exposure of living organisms from various input parameters: water concentration, sediment concentration, tissue concentration, specific nuclide, size and type of organisms.

Ecosystem

For RESRAD-BIOTA, two main ecosystems, terrestrial and aquatic, are modelled. There are 4 main organism types which are included in the model: terrestrial plant and terrestrial animal for the terrestrial ecosystem and aquatic and riparian animal for the aquatic ecosystem.

Radionuclides

In RESRAD-BIOTA, there are 29 radionuclides (46 radioisotopes) that the user can select from the list of potential contaminants. List of radionuclides and radioisotopes selected for RESRAD-BIOTA is shown in **Table 2.5**.

Table 2.5 Radionuclides selected for RESRAD-BIOTA (U.S.DOE 2002).

Radionuclide	Radioisotope
Am	Am-241
Ba	Ba-140
C	C-14
Ce	Ce-141, Ce-144
Cf	Cf-252
Cl	Cl-36
Cm	Cm-242, Cm-244
Co	Co-58, Co-60
Cr	Cr-51
Cs	Cs-134, Cs-135, Cs-137
Eu	Eu-152, Eu-154, Eu-155
H	H-3
I	I-129, I-131
Ir	Ir-192
K	K-40
Np	Np-237
Pa	Pa-231
Pb	Pb-210
Po	Po-210
Pu	Pu-238, Pu-239
Ra	Ra-226, Ra-228
Sb	Sb-125
Se	Se-75
Sr	Sr-90
Tc	Tc-99
Th	Th-228, Th-229, Th-230, Th-232, Th-234
U	U-233, U-234, U-235, U-238
Zn	Zn-65
Zr	Zr-95

Reference organisms

There are only four default organisms in this approach: aquatic animal, riparian animal, terrestrial animal and terrestrial plant (USDOE 2004). However, the user can add new organisms or edit the default organisms in Level 3 of this approach for which 8 different organism sizes (0.00001, 0.001, 0.01, 1, 10, 100, 500, 1000 kg) can be selected. The representative organism in each size category and dimension of organism is shown in **Table 2.6.**

Table 2.6 Selected geometry for each reference organism for RESRAD-BIOTA (U.S.DOE 2002).

Mass (kg)	Example Receptors	Dimension(cm)
0.00001	Fish egg, fish (larvae), Plant root (meristem), Plant seed, Plant shoot (meristem)	0.2x0.2x0.2
0.001	Fish (young-of-years, Molluscs, Plant seeding, Tadpoles	2.5x1.2x0.62
0.01	Fathead minnow, Frogs, Hispid cotton rat, Sculpins, Shrews, Voles, White-footed mouse	10x2x2
1	Black bass, Large fish, Suckers	45x8.7x4.9
10	Beaver, Carp, Catfish (channel and B coyote, Fox (red or grey), Raccoon, Striped bass	50x26x13
100	Mule deer, White-tailed deer	100x42x33
500	Elk	270x66x48
1000	Grizzly bear	220x100x100

Assessment methodology

There are three levels of assessment: screening, analysis and dose assessment. Level 1 is a conservative, screening, level which requires as input only a two parameters (nuclide and media concentration) to assess whether the environment media would exceed the biota concentration guide level (BCG). The Level 2 analysis can calculate the absorbed dose rate using inputs of nuclide and media concentration. In the Level 3 dose assessment the user can calculate absorbed dose rate as well as being able to edit size

parameters of the selected organism, add a new organism through a new organism wizard and remove any created organisms (USDOE 2004).

RASRAD-BIOTA calculates absorbed dose rate for both external and internal exposure. For external exposure, the habitat of organism (the time that the organism spends in contaminated media) is taken into account for this approach. The external exposure can be calculated by using External Dose Conversion Factor (DCF) and media concentration. For internal exposure, the intake of radionuclide (inhalation of dust particles and ingestion contaminated water, soil, sediment and foodstuffs) is taken into account. The internal exposure can be calculated by using Internal DCF and tissue concentration of organism. If the tissue concentration is not known, this can be calculated from the media concentration and Bioaccumulation factor (BIV). This approach also has a kinetic-allometric approach to estimate the transfer of some radionuclides (Am, Co, Cs, Eu, I, H, Pu, Ra, Sb, Sr, Tc, Th, U, Zn and Zr) from media to tissue concentration of organism (Beresford, Balonov et al. 2008; Beresford, Barnett et al. 2008).

The tissue concentration of organism for riparian animal and terrestrial animal and any organisms which are derived from these two reference organisms are calculated by using allometric option (USDOE 2004). The “allometric” tab in the allometric function of RESRAD is divided into three subtabs: Metabolism, Equations/Parameters and Intake Rates (USDOE 2004). Those three functions are used for calculating food intake rate of an organism by choosing appropriate input functions such as radionuclide, fraction of intake assimilated into the body, body mass and caloric value of food. The calculated food intake rate can be used instead of BIV to calculate tissue concentration of the organism. BIV values from literature were used for the freshwater reference organism (Beresford, Barnett et al. 2008).

2.4.4 R&D publication 128 model

The Environment Agency R&D Publication 128: “Impact assessment of ionising radiation in wildlife” was produced in June 2001, under R&D Project P3-085. This model was developed to assess radiation exposure of biota receiving radioactive discharges in England and Wales (Beresford, Barnett et al. 2008). R&D 128 and the ERICA model use a similar basic approach, however the ERICA model gives results for a wider range of radionuclides and organisms (Copplestone, Bielby et al. 2001). This

model has been programmed into three EXCEL spreadsheets (coastal aquatic ecosystem, fresh water ecosystem and terrestrial ecosystem). The spreadsheets can be used to calculate both external and internal doses to wildlife of different species and radionuclides using input water concentration, sediment concentration, soil concentration and tissue concentration.

Ecosystem

R&D128 mainly considers the release of radionuclides into ecosystems typically found in England and Wales. There are three ecosystems (freshwater, estuarine/marine and terrestrial ecosystems) in this approach.

Table 2.7 Radionuclides selected for R&D128 model (Copplestone, Wood et al. 2003)

Radionuclide	Radioisotope	Radionuclide	Radioisotope
Coastal and Fresh water ecosystems		Terrestrial ecosystem	
H	H-3	H	H-3
C	C-14	C	C-14
Tc	Tc-99	S	S-35
Sr	Sr-90	Sr	Sr-90
Cs	Cs-137	Cs	Cs-137
Pu	Pu-239+240	Pu	Pu-239+240
U	U-238	U	U-238
I	I-129, I-131	I	I-129, I-131
Co	Co-60	Po	Po-210
Ru	Ru-106	Ar	Ar-41
Th	Th-234	Co	Co-60
Pa	Pa-234m	Ru	Ru-106
Am	Am-241	Th	Th-234
P	P-32	Pa	Pa-234m
Po	Po-210	Am	Am-241
		P	P-32
		Kr	Kr-85

Radionuclides

The selected radionuclides in this approach depend on their presence and importancet in regulated nuclear discharges in England and Wales (Copplestone, Bielby et al. 2001). The selection of radionuclides for R&D 128 model shows in **Table 2.7**.

Reference Organisms

The selection of reference organisms in this approach uses the same reference organism concept of organism as the FASSET and ERICA models discussed above (Copplestone, Bielby et al. 2001). The selected reference organism is based on considerations of ecological sensitivity and radiological sensitivity. The selection of organism in each ecosystem for R&D 128 is shown in **Table 2.8**.

Table 2.8 Selected organisms in each ecosystem from R&D128 (Copplestone, Wood et al. 2003)

Ecosystems	Organisms
Terrestrial	Bacteria, Lichen, Tree, Shrub, Herb, Seed, Fungus, Caterpillar, Ant, Bee, Woodlouse, Earthworm, Herbivorous, mammal, Carnivorous mammal, Rodent, Bird, Bird egg
Freshwater	Bacteria, Macrophyte, Phytoplankton, Zooplankton, Benthic Mollusc, Small Benthic crustacean, Large Benthic crustacean, Pelagic fish, Benthic fish, Amphibian, Duck, Aquatic mammal
Marine	Bacteria, Macrophyte, Phytoplankton, Zooplankton, Benthic Mollusc, Small Benthic crustacean, Large Benthic crustacean, Pelagic fish, Benthic fish, Fish egg Seabird, Seal, Whale

Assessment methodology

As for the other approaches, the R&D 128 model can calculate both external and internal dose rate of aquatic and terrestrial organisms. The method of dose calculation for aquatic and terrestrial organisms is similar.

Aquatic ecosystems

The equations for aquatic ecosystems (freshwater and coastal ecosystems) are defined in the following (Copplestone, Wood et al. 2003);

$$C_s = C_w \times CF_s \times (\text{Solid fraction}) \quad (2.14)$$

$$D_{int} = C_w \times CF \times DPUC_{int} \quad (2.15)$$

$$D_{ext} = DPUC_{ext} \times \left[(C_s \; xt(f_{sed} + f_{sedsur}/2)) + (f_w \; 2)C_w/1000)\right] \quad (2.16)$$

Where C_s is sediment concentrations (Bq kg^{-1}) dry weight,

C_w is water concentrations (Bq m^{-3}) in the dissolved phase,

CF_s is concentration factors of soil (m^3 kg^{-1}), solids fraction is the fractional dry solids content of fresh soil,

D_{int} is internal dose rate (µGy hr^{-1}),

CF is concentration factors (m^3 kg^{-1}),

$DPUC_{int}$ is internal dose per unit concentration factor (µGy hr^{-1} per Bq kg^{-1}) fresh weight,

D_{ext} is external dose rate (µGy hr^{-1}),

$DPUC_{ext}$ is external dose per unit concentration factor (µGy hr^{-1} per Bq kg^{-1}) fresh weight,

f_{sed} is the fraction of time the organism spends buried in sediment,

f_{sedsur} is the fraction of time the organism spends at the sediment/water interface and

f_w is the fraction of time the organism spends in the water column.

Terrestrial ecosystem

The equations for terrestrial ecosystem are defined as the following (Copplestone, Wood et al. 2003).

$$C_s = C_{air} \times CF_s \quad (\text{for } H^3, C^{14}, P^{32}, S^{35}) \quad (2.17)$$

Where C_s is soil concentrations (Bq kg^{-1}) dry weight,

C_{air} is air concentrations for H^3, C^{14}, P^{32}, S^{35} (Bq m^{-3}),

CF_s is concentration factors of soil (m^3 kg^{-1})

$$C_s = C_{s(dry)} \times \text{(Solid fraction)} \quad \text{(for other nuclides)} \quad (2.18)$$

Where $C_{s(dry)}$ is the input of soil concentration for other nuclides (Bq kg^{-1}) dry weight, solids fraction is the fractional dry solids content of fresh soil

$$D_{int} = C_{air} \times CF \times DPUC_{int} \quad \text{(for } H^3, C^{14}, P^{32}, S^{35}\text{)} \quad (2.19)$$

Where D_{int} is internal dose rate (µGy hr^{-1}),

CF is concentration factors (m^3 kg^{-1}),

CF for H^3, C^{14}, P^{32}, S^{35} is concentration factors of soil (m^3 kg^{-1}) fresh weight or organism per Bq m^{-3} in air,

$DPUC_{int}$ is internal dose per unit concentration factor (µGy hr^{-1} per Bq kg^{-1}) fresh weight

$$D_{int} = C_s \times CF \times DPUC_{int} \quad \text{(for other nuclides)} \quad (2.20)$$

Where CF for other nuclides is concentration factor of organism per Bq kg^{-1} (dry weight) of soil

$$D_{ext} = DPUC_{ext} \times \left[C_s \times ((f_{soil} + f_{soilsur}/2) + (f_{air} \times \text{reduction factor}_{\text{radiation type}}))\right] \quad (2.21)$$

Where D_{ext} is external dose rate (µGy hr^{-1}),

$DPUC_{ext}$ is external dose per unit concentration factor (µGy hr^{-1} per Bq kg^{-1}) fresh weight,

f_{soil} is the fraction of time the organism spends buried in or burrowing into soil,

$f_{soilsur}$ is the fraction of time the organism spends on the ground surface,

f_{air} is the fraction of time the organism spends above the ground surface, flying or roosting etc.,

reduction factor is a factor, dependent on radiation type, by which the radiation dose rate above the ground surface is lower than that within the soil itself. The default vales set for this factor are zero for alpha and low energy beta and 0.25 for high energy beta and gamma.

2.4.5 D-MAX model

Smith (2005) gives details of a screening model for calculation of the exposure of an organism that is situated in an infinite extended medium of uniform contamination density. This model is similar to the other models that stated above but it considers a general scenario (it does not focus on any particular organism and environmental medium). Minimum concentration in organism, tissue or environmental medium which would lead to a guideline dose rate can be estimated by this approach. The approach assumes that the maximum allowable dose rate to organism is 1 mGy d^{-1} recommended by IAEA (IAEA 1992), though other reference levels could be used.

For the case of uniform contamination of an infinitely extended medium, the dose rate can be calculated using the following equation (Smith 2005).

$$E = C \times 1.6 \times 10^{-19} \sum_i \varepsilon_i \qquad (2.22)$$

Where E is the rate of energy deposition (dose rate) (Gy s^{-1}), C is concentration of radionuclides in an organism, tissue or environmental medium (Bq kg^{-1}) wet weight and ε_i is the mean energy in electron volts (1ev = 1.6 x 10^{-19} J), of i th radiation emitted (weighted by intensity) when the radionuclide undergoes decay.

Form the above equation, the minimum concentration, C_{min} (Bq kg^{-1} wet weight), can be defined as the following equation (Smith 2005).

$$C_{min} = \frac{1}{60\times60\times24\times1000} \times \frac{1}{1.6\times10^{-19} \sum_i \varepsilon_i} = \frac{1}{1.38\times10^{-11} \sum_i \varepsilon_i} \qquad (2.23)$$

The C_{min} values for alpha emitting radionuclides and beta and gamma emitting radionuclides are given in **Table 2.9** and **2.10** respectively.

For external exposure, absorbed dose rate can be calculated by using the dose rate conversion factor (mGy d^{-1} per Bq kg^{-1}) stated above and environmental medium concentration (water, sediment and soil). Similarly for internal exposure, absorbed dose rate can be calculated by using dose rate conversion factor and tissue concentration of biota.

Table 2.9 Minimum concentration, C_{min} (wet weight) of alpha emitting radionuclide in an organism or tissue (Smith 2005).

Radionuclides	Mean ∑ε per disintegration (MeV)	Dose rate (mGy d^{-1} per Bq kg^{-1})	Minimum concentration (Bq kg^{-1})
U-234	4.77	6.6×10^{-5}	15200
U-235	4.58	6.3×10^{-5}	15800
U-238	4.18	5.8×10^{-5}	17300
Pu-238	5.48	7.6×10^{-5}	13200
Pu-239	5.14	7.1×10^{-5}	14100
Pu-240	5.12	7.1×10^{-5}	14000
Am-241	5.45	7.5×10^{-5}	13300

Table 2.10 Minimum concentration, C_{min} (wet weight) of beta and gamma emitting radionuclide in an organism, tissue or environmental medium (Smith 2005).

Radionuclides	Mean ∑ε per disintegration (MeV)	Dose rate (mGy d^{-1} per Bq kg^{-1})	Minimum concentration (Bq kg^{-1})
H-3	0.0059	8.17×10^{-8}	12300000
C-14	0.051	7.05×10^{-7}	1420000
P-32	0.696	9.6×10^{-6}	104000
Co-60	2.60	3.59×10^{-5}	27900
Sr-90/Y-90	1.13	1.56×10^{-5}	64000
Tc-99	0.085	1.2×10^{-6}	854000
I-131	0.55	7.6×10^{-6}	131500
Cs-134	1.7	2.35×10^{-5}	42600
Cs-137/^{m}Ba-137	0.81	1.12×10^{-5}	90000

However, in the case of the prediction of internal exposure of radionuclides in fish, the user can predict Concentration Ratio (CR). For example, for radiocaesium, the approach uses potassium concentration in water, as shown in the following equations (Smith, Kudelsky et al. 2000).

For predatory/omnivorous fish,

$$\mathrm{CR\ (predatory)} = \frac{4880}{[K^+]} \tag{2.24}$$

And non-predatory fish

$$\mathrm{CR\ (non\text{-}predatory)} = \frac{2390}{[K^+]} \tag{2.25}$$

For the best estimation value, the uncertainty range is estimated to be 0.5-2 times. For the estimation of internal exposure of Sr-90 in fish, the user can predict CR by using calcium concentration in water as the following equation (Smith, Sasina et al. 2009).

$$\mathrm{CR\ (muscle)} = \frac{181}{[Ca]^{1.2}} \tag{2.26}$$

$$\mathrm{CR\ (bone)} = \frac{16317}{[Ca]^{1.2}} \tag{2.27}$$

Assuming wet weigh of bony parts of fish is 23% that gives a whole fish CR as the following equation (Smith, Sasina et al. 2009).

$$\mathrm{CR\ (whole\ fish)} = \frac{3850}{[Ca]^{1.2}} \tag{2.28}$$

For the best estimation value, the uncertainty range should be 0.33-3 times. For the case of a non uniform contamination, such as typically observed in sediments and soils, where contamination changes with depth, this model can be used to give the maximum exposure by using the peak contamination value.

2.5 References

Abraham, J. P., Whicker, F. W., Hinton, T. G., & Rowan, D. J. (2000). Inventory and spatial pattern of 137Cs in a pond: a comparison of two survey methods. *Journal of Environmental Radioactivity, 51*(2), 157-171.

Audi, G., Bersillon, O., Blachot, J., & Wapstra, A. H. (1997). The N evaluation of nuclear and decay properties. *Nuclear Physics A, 624*(1), 1-124.

Beresford, N. A., Balonov, M., Beaugelin-Seiller, K., Børretzen, P., Brown, J., Cheng, J.-J., et al. (2005). *Models and approaches available to estimate the exposure of non-human biota: An international comparison of predictions.* Østerås: Norwegian Radiation Protection Authority.

Beresford, N. A., Balonov, M., Beaugelin-Seiller, K., Brown, J., Copplestone, D., Hingston, J. L., et al. (2008). An international comparison of models and approaches for the estimation of the radiological exposure of non-human biota. *Applied Radiation and Isotopes, 66*(11), 1745-1749.

Beresford, N. A., Barnett, C., Brown, J., Cheng, J., Copplestone, D., Filistovic, V., et al. (2008). Inter-comparison of models to estimate radionuclide activity concentrations in non-human biota. *Radiation and Environmental Biophysics, 47*(4), 491-514.

Beresford, N. A., Barnett, C. L., Brown, J. E., Cheng, J. J., Copplestone, D., Gaschak, S., et al. (2010). Predicting the radiation exposure of terrestrial wildlife in the Chernobyl exclusion zone: an international comparison of approaches. *Journal of Radiological Protection, 30*(2), 341.

Cailes, C. R. (2006). *Phenotypic and genetic effects of Chernobyl-derived radionuclide contamination on the red-eyed damselfly Erythromma Najas (Odonata, Coenagrionidae).* University of Plymouth, Plymouth.

Copplestone, D., Bielby, S., Jones, S. R., Patton, D., Daniel, P., & Gize, I. (2001). *Impact Assessment of Ionising Raditaiton on Wildlife: R&D Publication 128*. Bristol: Environmental Agency.

Copplestone, D., Wood, M. D., Bielby, S., Jones, S. R., Vives, J., & Beresford, N. A. (2003). *Habitats regulations for Stage 3 assessments: radioactive substances authorisations*. Bristol: Environment Agency.

Cross, W. G., Ing, H., & Freedman, N. (1983). A short atlas of beta-ray spectra. *Physics in Medicine and Biology, 28*(11), 1251-1260.

Debertin, K., & Helmer, R. G. (1988). *Gamma- and X-ray Spectrometry with Semiconductor Detectors*. Amsterdam: Elsevier Science Pubishers B.V.

ERICA. (2007a). *Application of ERICA Integrated Approach at case study sites: Deliverable D10*: Swedish Radiation Protection Authority.

ERICA. (2007b). *D-ERICA: An INTEGRATED APPROACH to the assessment and management of environmental risks from ionising radiation*: Swedish Radiation Protection Authority.

FASSET. (2001). *Identification of candidate reference organisms from a radiation exposure pathways perspective. Deliverable 1*. Stockholm: Swedish Radiation Protection Authority.

FASSET. (2003a). *Dosimetric models and data for assessing radiation exposures to biota. Deliverable 3*. Stockholm: Norwegian Radiation Protection Authority.

FASSET. (2003b). *Handbook for Assessment of the Exposure of Biota to Ionising Radiation from Radionuclides in the Environment. Deliverable 5*. Stockholm: Swedish Radiation Protection Authority.

Forsberg, E.-M., & Oughton, D. (2006). *The ERICA Consensus Seminar: Deliverable D7f*: Swedish Radiation Protection Authority.

IAEA. (1989). *Measurements of radionuclides in food and the environment. A Guidebook (Technical Report Series No. 295)*

Vienna: IAEA.

IAEA. (1992). *Effects of ionisng radiation on plants and animals at levels implied by current radiation standards*. Vienna: IAEA.

IAEA, & ANSTO. (2004). Method of Radiation Detection *Radiation Protection Distance Learning Project*.

KAERI. (2000). Table of Nuclides. Retrieved 10 October, 2010, from http://atom.kaeri.re.kr/

Knoll, G. F. (1989). *Radiation detection and measurement* (2nd ed.). Singapore: John Wiley & Sons, Inc.

Larsson, C. M. (2004). The FASSET Framework for assessment of environmental impact of ionising radiation in European ecosystems - an overview. *Journal of Radiological Protection, 24*(4A), A1-A12.

Lilley, J. S. (2009). *Nuclear Physics Principles and Applications*. Chichester: John Wiley & Sons, Ltd.

McKinlay, A. F. (1981). *Thermoluminescence dosimetry*. Bristol: Adam Hilger Ltd.

Mück, K., Pröhl, G., Likhtarev, I., Kovgan, L., Meckbach, R., & Golikov, V. (2002). A Consistent Radionuclide Vector After the Chernobyl Accident. *Health Physics, 82*(2), 141-156.

Smith, J. (2005). Effects of ionising radiation on biota: do we need more regulation? *Journal of Environmental Radioactivity, 82*(1), 105-122.

Smith, J. T., Kudelsky, A. V., Ryabov, I. N., & Hadderingh, R. H. (2000). Radiocaesium concentration factors of Chernobyl-contaminated fish: a study of the influence of potassium, and "blind" testing of a previously developed model. *Journal of Environmental Radioactivity, 48*(3), 359-369.

Smith, J. T., Sasina, N. V., Kryshev, A. I., Belova, N. V., & Kudelsky, A. V. (2009). A review and test of predictive models for the bioaccumulation of radiostrontium in fish. *Journal of Environmental Radioactivity, 100*(11), 950-954.

Stabin, M. G. (2008). *Radiation Protection and Dosimetry: An Introduction ot Health Physics*. New York: Springer Science+Business Media, LLC.

Timms, D. N., Smith, J. T., Coe, E., Kudelsky, A. V., & Yankov, A. I. (2005). In situ measurements of the sub-surface gamma dose from Chernobyl fallout. *Applied Radiation and Isotopes, 62*(6), 923-930.

U.S.DOE. (2002). *A Graded Approach for Evaluating Radiation Doses to Aquatic and Terrestrial Biota Module 1: Principles and Application*: U.S.DOE.

U.S.DOE. (2004). *RESRAD-BIOTA: A Tool for Implementing a Graded Approach to Biota Dose Evaluation*. Washington D.C.

U.S.DOE. (2009). RESRAD-BIOTA for Windows (Version 1.5): U.S. Department of Energy.

USDOE. (2004). *RESRAD-BIOTA: A Tool for Implementing a Graded Approach to Biota Dose Evaluation*. Washington D.C.

Vives i Batlle, J., Balonov, M., Beaugelin-Seiller, K., Beresford, N., Brown, J., Cheng, J. J., et al. (2007). Inter-comparison of absorbed dose rates for non-human biota. *Radiation and Environmental Biophysics, 46*(4), 349-373.

Wood, M. D. (2010). *Assessing the impact of ionising radiation in temperate coastal sand dune ecosystems: measurement and modelling.* University of Liverpool, Liverpool.

Chapter 3

The comparison and critical analysis of the models

3.1 Introduction

The radiation exposure of organisms can be estimated by a combination of in-situ measurement and/or model prediction. In some cases, it is difficult, or expensive, to directly measure radiation exposures by in-situ measurement. Models are therefore an important method to predict the radiation doses to biota.

Currently, there are many models and approach for estimating radiation doses to non-human biota but the validation and the comparison of the outputs of the different models have been limited (Beresford, Balonov et al. 2005; Beresford, Balonov et al. 2008; Beresford, Barnett et al. 2008). To fill this gap, the International Atomic Energy Agency (IAEA) established the Biota Working Group (BWG; http//www-ns.iaea.org/projects/emras/emras-biota-wg.htm) as a part of the EMRAS (Environmental Modelling for Radiation Safety) programme to compare and improve both already developed models and those under development (Beresford, Balonov et al. 2005; Vives i Batlle, Balonov et al. 2007; Beresford, Balonov et al. 2008; Beresford, Barnett et al. 2008) . This research has compared models for radiation doses at the Perch Lake site in Canada (Yankovich and et al. 2010) and to terrestrial organisms at Chernobyl (Beresford and et al. 2010).

This chapter will carry out a further analysis of some of these models by presenting predictions of internal and external radiation doses in selected aquatic and terrestrial biota for Cs-137 and Sr-90 from five different models (RESRAD, The FASSET, ERICA (an improve version of FASSET), R&D128 and the D-Max model) against biota size (weight). This will lead to a better understanding of the prediction of internal and external dose by the models and of the influence of organism size and shape on dose. The details of the five different models were discussed in chapter 2.

3.2 Methods

The five models; RESRAD, FASSET, ERICA, R&D128 and the D-Max model were used to estimate the internal and external radiation doses by using an example scenario which assumes the water concentration to be 1 Bq l^{-1} (1000 Bq m^{-3}), sediment and soil concentration to be 1 Bq kg^{-1} (dry weight) and tissue concentration to be 1 Bq kg^{-1}(fresh weight). Two radionuclides (Cs-137 and Sr-90) were chosen. A selection of aquatic, terrestrial and riparian animals was studied based on the default organisms in each model (Copplestone, Bielby et al. 2001; FASSET 2003; USDOE 2004; ERICA 2007) as described in Chapter 2.

3.2.1 Assumed weights of the selected aquatic animals

For aquatic animals, eight different biota weights for the RESRAD model, six different organisms for FASSET model, twelve different organisms for ERICA model, and eight different organisms for R&D Model were chosen for the dose calculations. The D-Max model is independent of organism size and so nominally we have used biota of $1x10^{-5}$ and $1x10^{4}$ kg to calculate the doses. The summary of organism weights in each model for aquatic animals is shown in **Table 3.1**.

3.2.2 Assumed weights of selected terrestrial animals

For terrestrial environment, eight different biota weights for the RESRAD model, ten different organisms for the FASSET model, fourteen different organisms for the ERICA model and sixteen different organisms for the R&D128 model were chosen to calculate the doses. The D-Max model again used $1x10^{-5}$ and $1x10^{4}$ kg biota to calculate the doses. The summary of organism weights in each model for terrestrial animals is shown in **Table 3.2.**

3.2.3 Weight data of selected riparian animals

For riparian animals, there are two representative animals from FASSET Model which are muskrat and ringed seal (1.3 and $8x10^{1}$ kg respectively) used for this calculation. The other models have no reference organism for riparian animals.

Table 3.1 Summary of organism weights in each model for aquatic animals.

Model	Weights (kg)
ResRad	$1x10^{-5}$ (Fish egg and Fish (larvae), $1x10^{-3}$ (Fish (young-of-year), Molluscs and Tadpoles), $1x10^{-2}$ (Fathead minnow and Sculpins), 1 (Black bass, Large fish and Suckers), $1x10^{1}$ (Carp, Catfish and Striped bass), $1x10^{2}$ (large fish), $5x10^{2}$ (Mammal), $1x10^{3}$ (Mammal)
FASSET	$1.90x10^{-9}$ (Phytoplankton), $1.5x10^{-5}$ (Crustacean), $2x10^{-5}$ (Insect larvae), $3.5x10^{-1}$ (Pelagic fish), $4x10^{-1}$ (Bird), 1.5 (Benthic fish)
ERICA	$2.05x10^{-12}$ (Phytoplankton), $2.35x10^{-6}$ (Zooplankton), $1.57x10^{-5}$ (Crustacean), $1.77x10^{-5}$ (Insect larvae), $1.05x10^{-3}$ (Vascular plant), $3.53x10^{-3}$ (Gastropod), $3.14x10^{-2}$ (Amphibian), $7.07x10^{-2}$ (Bivalve mollusc), 1.26 (Bird), 1.26 (Pelagic fish), 1.47 (Benthic fish), 3.90 (Mammal)
R&D128	$6.5x10^{-11}$ (Phytoplankton), $1.6x10^{-5}$ (Zooplankton), $1.6x10^{-5}$ (Small benthic crustacean), $2.1x10^{-4}$ (Macrophyte), $1x10^{-3}$ (Benthic mollusc), $2x10^{-3}$ (large benthic crustacean), 1 (Pelagic fish), 1 (Benthic fish)
D-MAX	$1x10^{-5}$, $1x10^{4}$ (nominal values)

Table 3.2 Summary of organism weights in each model for terrestrial animals.

Model	Weights (kg)
ResRad	$1x10^{-5}$ (Plant root (meristem), Plant seed and Plant shoot (meristem)), $1x10^{-3}$ (Plant seedling), $1x10^{-2}$ (frogs, Hispid cotton rat, Shrews, Voles and White-footed Mouse), 1, $1x10^{1}$ (Beaver, Coyote, Fox (red or grey) and Raccoon), $1x10^{2}$ (Mule deer and White-tailed deer) , $5x10^{2}$ (Elk), $1x10^{3}$ (Grizzly bear)
FASSET	$1.7x10^{-4}$ (Wood-louse), $6x10^{-3}$ (earth-worm), $3.5x10^{-2}$ (mouse), $9.7x10^{-2}$ (mole), $9.9x10^{-2}$ (weasel), $7.4x10^{-1}$ (snake), 2 (rabbit), 6.6 (red fox), $2.4x10^{1}$ (roe deer) and $5.5x10^{2}$ (cattle)
ERICA	$1.1x10^{-4}$ (Lichen & bryophytes), $1.7x10^{-4}$ (Detritivorous invertebrate), $5.89x10^{-4}$ (Flying insect), $1.4x10^{-3}$ (Gastropod), $2.62x10^{-3}$ (Grasses & Herbs), $2.62x10^{-3}$ (Shrub), $5.24x10^{-3}$ (Soil invertebrate), $3.14x10^{-2}$ (Amphibian), $5.03x10^{-2}$ (Bird egg), $3.14x10^{-1}$ (Rat), $7.44x10^{-1}$ (Reptile), 1.26 (Bird), $2.45x10^{2}$ (Deer) and $4.71x10^{2}$ (Tree)
R&D128	$1.8x10^{-6}$ (Germinating seed), $2x10^{-5}$ (Ant), $2.1x10^{-4}$ (Tree (root)), $2.1x10^{-4}$ (Shrub (root)), $2.1x10^{-4}$ (Herb (root)), $7.7x10^{-4}$ (Caterpillar), $1x10^{-3}$ (Woodlouse), $1.3x10^{-3}$ (Bird egg), $2x10^{-3}$ (Bee), $2.63x10^{-3}$ (Fungal fruiting body), $3.5x10^{-3}$ (Earthworm), $2x10^{-2}$ (Rodent), $8x10^{-1}$ (herbivorous mammal), 1.5 (Woodland bird), 2.26 (reptile) and 5.5 (carnivorous mammal)
D-MAX	$1x10^{-5}$, $1x10^{4}$ (nominal values)

3.2.4 Prediction of internal dose rate

The internal dose rates of the organism are predicted by assuming that the activity concentration of each organism is 1 Bq kg^{-1} (fresh weight). The 5 different models are used for the prediction of internal dose rates of Cs-137 and Sr-90, these being, at the present time, the dominant radionuclides in the Chernobyl affected regions.

The RESRAD Model was used to calculate the internal dose rate using a Level 3 assessment for a tissue concentration of 1 Bq kg^{-1}. The prediction of the internal dose from the FASSET Model was calculated using dose conversion coefficients (DCCs) for internal exposure which were provided in the look-up table in the model documentation. For the ERICA Model, a Tier 3 assessment was used for the prediction of the internal doses with occupancy factors and the radiation weighting factor set to their default value. For ERICA, uncertainty estimation is possible: for this, the number of simulations (1000) was selected. For the R&D128 Model, the EXCEL spread sheet of freshwater or terrestrial ecosystem was used for the prediction. The D-MAX Model can give the maximum exposure by using DCCs to convert 1 Bq kg^{-1} of activity concentration of biota to internal dose rate. For this model, the DCC of Cs-137 and Sr-90 are $1.12x10^{-5}$ and $1.56x10^{-5}$ mGy d^{-1} per Bq kg^{-1} respectively (Smith 2005).

3.2.5 The prediction of external dose rate

The external dose rates of the organism are predicted by again assuming the activity concentration the water concentration to be 1 Bq l^{-1} or 1000 Bq m^{-3}, sediment and soil concentration are 1 Bq kg^{-1} (dry weight).

The RESRAD Model was used to calculate the external dose rate by setting the parameters to the following: ecosystem (terrestrial or aquatic, as required for the particular organism), Level 3, SI unit, nuclide contaminants (Cs-137 and Sr-90), type of organisms (listed in Section 3.2.1 and 3.2.2), sediment and soil concentration 1 Bq kg^{-1} and water concentration 1000 Bq cm^{-3}.

The prediction of the external dose from the FASSET Model was calculated by using water concentration, sediment concentration and soil concentration (1 Bq l^{-1} or 1 Bq kg^{-1}) and dose conversion coefficients (DCCs) for external exposure which were provided in the look-up table in the model documentation (FASSET 2003). The external exposure of pelagic and benthic fish must be calculated in different ways because of

their different habitats. In the FASSET model, pelagic fish are assumed to be living permanently in the water column, whilst benthic fish are assumed to be living permanently on the sediment surface. For pelagic fish, the external exposure is calculated from the water activity concentration multiplied by the DCCs of the radionuclide. In the case of benthic fish, the external exposure was calculated as the summation of half of water concentration and half of sediment concentration multiplied by the DCCs of each radionuclide. The external exposure for pelagic fish and benthic fish are shown in Equations 3.1 and 3.2 (FASSET 2003).

$$D_{ext} = \sum DCC_{ext} * C_{water} \quad (3.1)$$

$$D_{ext} = \sum DCC_{ext} * [0.5\ C_{water} + 0.5\ C_{sed}] \quad (3.2)$$

Where C_{water} is the average concentration of the radionuclide in water (Bq/l, dissolved phase),
C_{sed} is the average concentration of the radionuclide in sediment (Bq/kg, fresh weight),
DCC_{ext} is the dose conversion coefficient for external exposure (μGy/hr per Bq/kg)

For the ERICA Model, a Tier 3 assessment was used for the prediction of the external doses and parameters were set to their default values. For the R&D128 Model, The habitat factors were set the same as in the ERICA Model (the ERICA and R&D128 Models allow the user to change the habitat occupancy factors of the organism). The default habitat factor of the R&D128 Model is different from the ERICA Model. The summaries of the habitats of aquatic and terrestrial animals are shown in **Tables 3.3** and **3.4** respectively.

As for the internal dose, the D-MAX Model can give the maximum exposure to organisms by using DCCs to convert 1 Bq kg^{-1} or Bq l^{-1} of activity concentration of media to external dose rate. The DCC of Cs-137 and Sr-90 are $1.12x10^{-5}$ and $1.56x10^{-5}$ mGy d^{-1} per Bq kg^{-1} respectively (Smith 2005).

Table 3.3 shows a summary of the habitat of aquatic animals in all models.

Habitat	Organism
Sediment surface	Benthic fish, crustacean, bivalve mollusc, gastropod and vascular plant
Sediment	insect larvae
Water	Pelagic fish, zooplankton, amphibian, bird, mammal, macrophyte and phytoplankton

Table 3.4 shows a summary of the habitat of terrestrial animals in all models.

Habitat	Organism
On soil	amphibian, bird, gastropod, bird egg, flying insects, grasses & herbs, lichen & bryophytes, deer, reptile, seed, fungi, caterpillar, ant, woodlouse, herbivorous mammal, carnivorous mammal, shrub and tree
In soil	Detritivorous invertebrate, rat, rodent and soil invertebrate

3.2.6 The prediction of total internal and external dose rate

The estimation of total internal and external dose was calculated by the total of the internal and the external dose rates. In some models, for example RESRAD, ERICA and R&D128, the total dose was calculated by using a function within the model. For the FASSET model, the total dose was calculated by using the summation of the internal and the external dose rate determined from the DCC values. The dose that calculated by the D-MAX model is the total dose rate from both pathways.

3.2.7 Statistical analysis

Student's t-test use to compare the data between two sample groups. In this case, student's t-test was used to test the correlation between the dose rates from the model predicted and the dose rate from the equation predicted. The null hypothesis was set to test the hypothesis. The null hypothesis was "no difference in the dose rates between the model and the equation predicted". The null hypothesis is rejected, and another hypothesis is accepted when calculated t-value exceeds the critical t-value (two-tailed)

or P-value is less than the level of statistical significance (α) (Smithson 2000; Mendenhall and Sincich 2006). For this study, α = 0.05 was chosen for the criteria.

- P-value > 0.05 indicates no evidence accepted the null hypothesis (no difference in the dose rates between the model and the equation predicted); and

- P-value < 0.05 indicates no evidence rejected the null hypothesis (significant difference in the dose rates between the model and the equation predicted).

3.3 Results

3.3.1 The prediction of the internal dose rate of Cs-137

The predictions of the internal dose rate from the 5 models for Cs-137 are illustrated in **Figure 3.1** which plots the predicted internal dose rate (μGy hr^{-1}) against the weight (kg) of organism. The internal dose rate increases gradually as weight increases up to 0.8 kg; after that, there is a steeper rise.

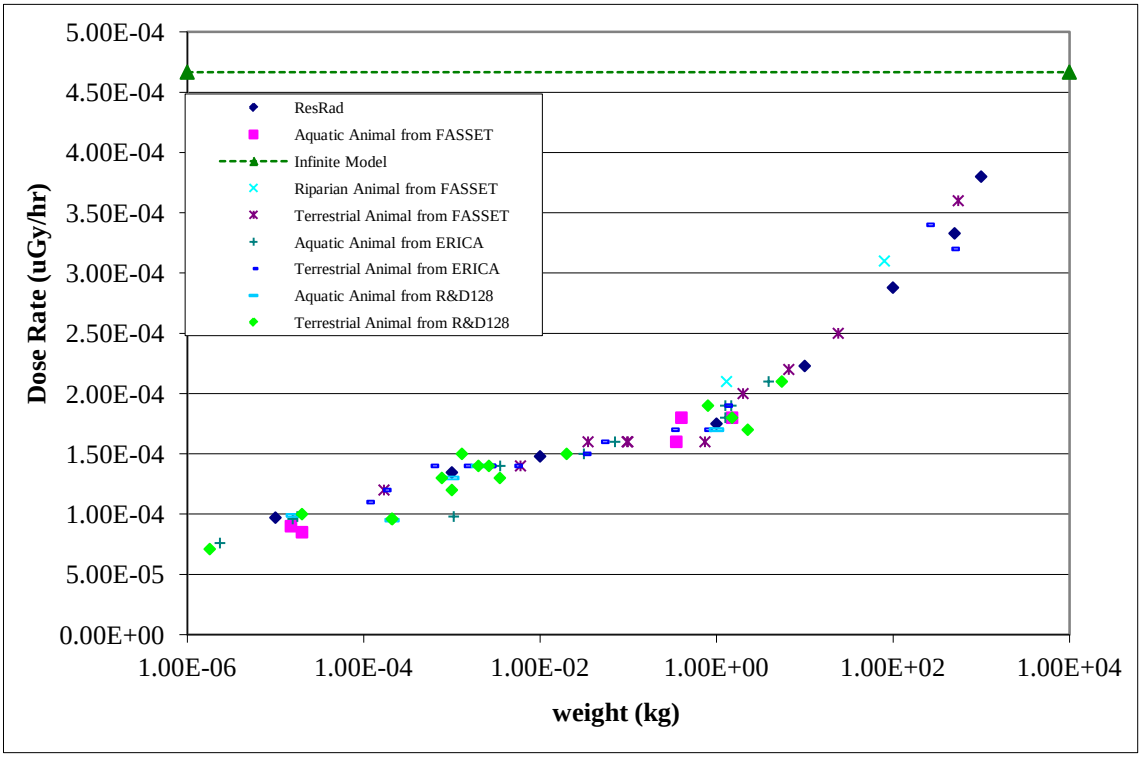

Figure 3.1 Predicted dose rate using 5 models for Cs-137 internal dose rate.

Even though various functions (exponential, logarithmic, polynomial in any degree and power) were tried to fit the data but they were not as good as the split linear equations.

The above relationship between predicted dose rate and organism mass can be separated into two sections. The first section is from $1x10^{-6}$ kg to $8x10^{-1}$ kg mass and the second section is from $8x10^{-1}$ kg to $1x10^{4}$ kg mass. Trend lines were fitted to determine relationships for each section of the graph individually, as illustrated in **Figure 3.2**. The equation of the first section is

$D = 7.79E\text{-}6\ Ln(m) + 1.80E\text{-}4$ ($1x10^{-6}$ kg to $8x10^{-1}$ kg) (3.3)

$R^2 = 0.884$, $P = 0.9965$

and the equation of the second section is

$D = 2.89E\text{-}5\ Ln(m) + 1.71E\text{-}4.$ ($8x10^{-1}$ kg to $1x10^{4}$ kg) (3.4)

$R^2 = 0.967$, $P = 0.9069$

Where D is Dose rate in $\mu Gy\ hr^{-1}$

m is weight of organism in kg

The residual can be calculated as the difference between the trend line and the model predicted internal dose rates, as shown in **Figure 3.3**. The percent deviation can be calculated from the internal dose rate of the prediction of the model and the above equation as shown in **Figure 3.4**. The histogram of % deviation is shown in **Figure 3.5**.

There were 86 percent (64 out of 74 data) of model fitted values which were within ± 10 percent deviation and 99 percent (73 out of 74 data) where the deviation was within ± 20 percent deviation. Only one data (-23%) from vascular plant from the ERICA Model was over ± 20 percent deviation. There were no significant differences in Cs-137 internal dose rate between trend line and the model predicted at P=0.9965 in first section and at P=0.9069 in second section. All of figures show the relatively good fit of the equation to the model predicted internal dose rates from Cs-137 for various reference organisms, implying relatively little influence of organism geometry on dose rate.

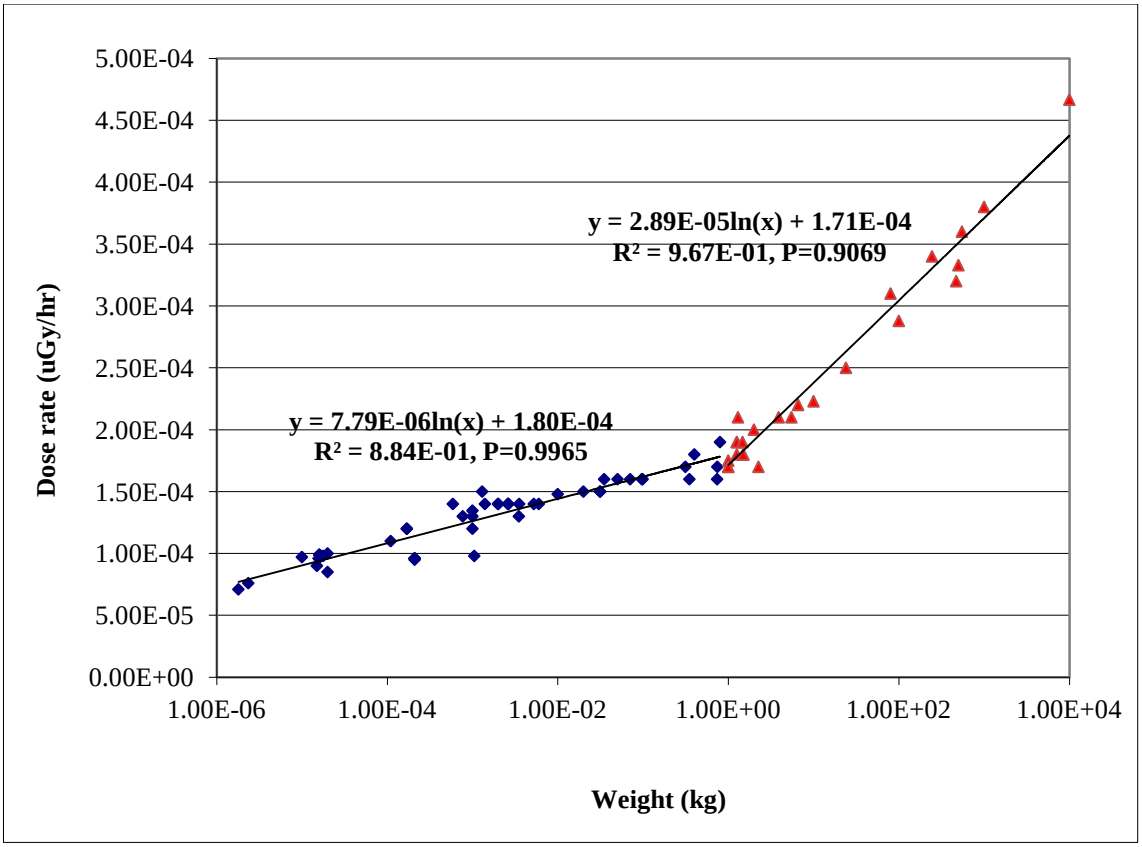

Figure 3.2 Fitted equations to model predictions for Cs-137 internal dose rate.

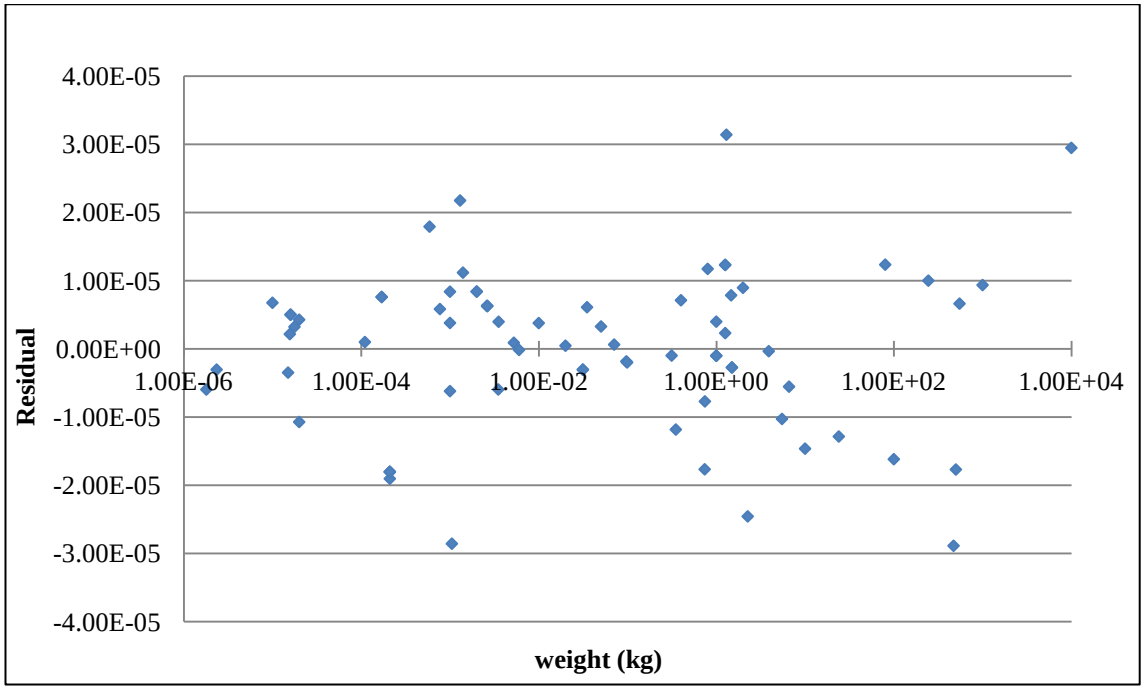

Figure 3.3 Residuals of the fit of the trendlines to the model predictions for Cs-137 internal dose.

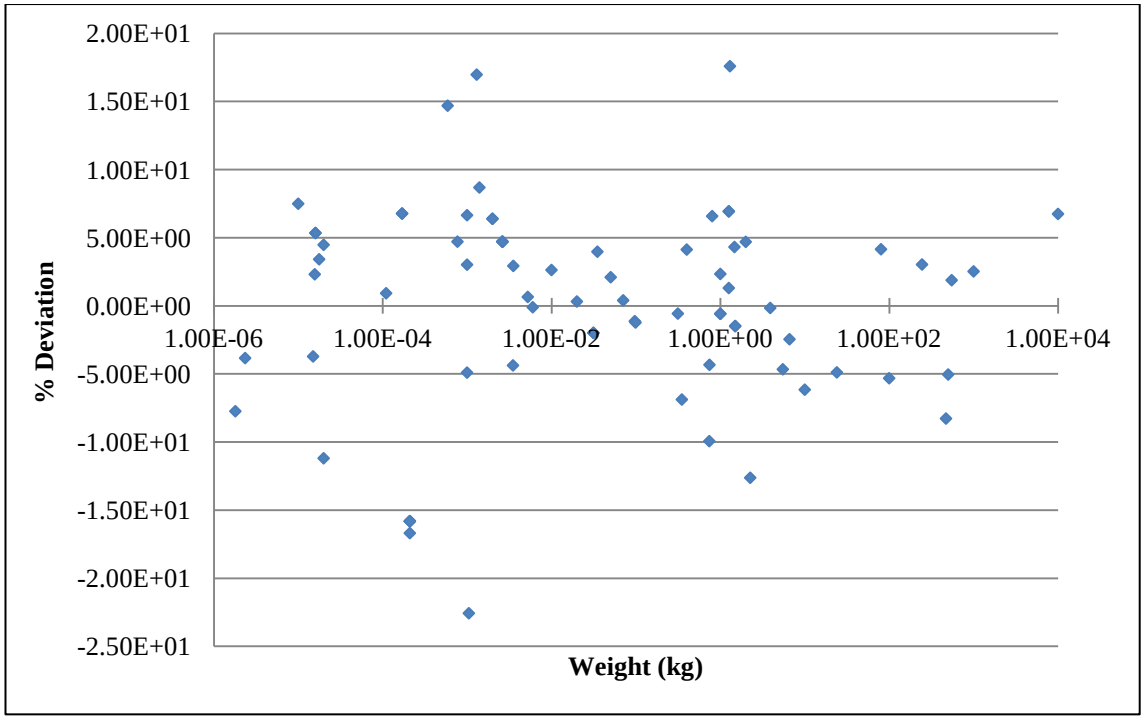

Figure 3.4 The % deviation of the trendline from Cs-137 internal dose predicted by the models.

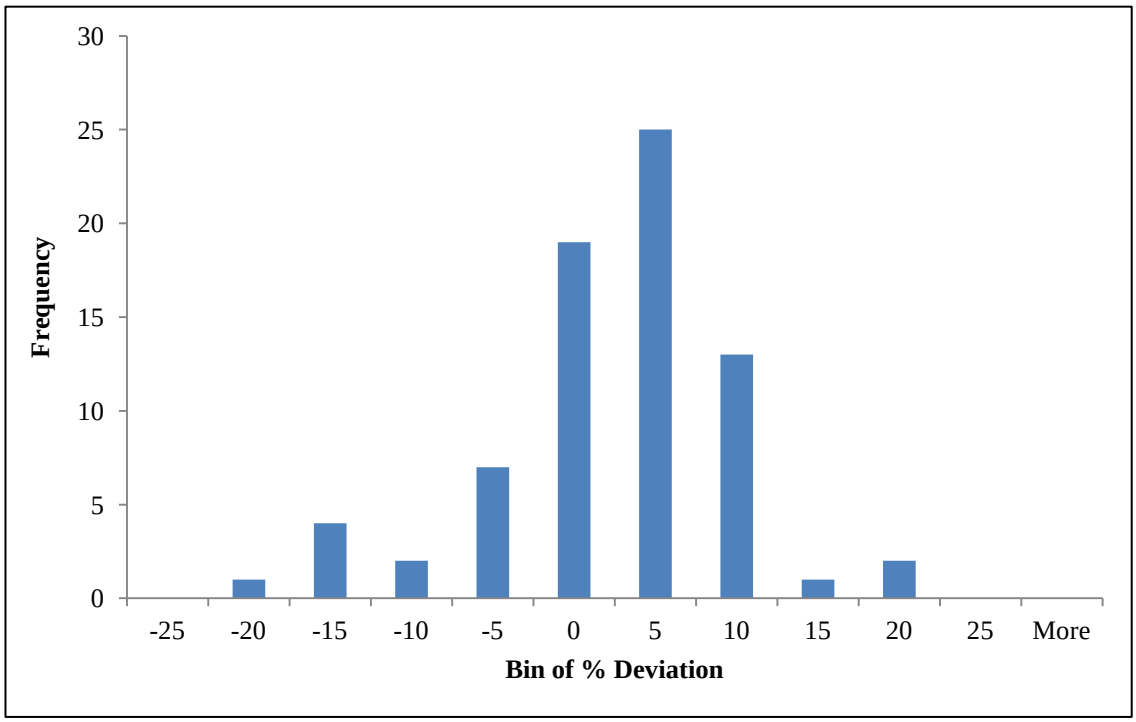

Figure 3.5 The histogram of % deviation for predicted Cs-137 internal dose to various organism compared with a logarithmic regression fit.

3.3.2 The prediction of internal dose rate of Sr-90

The results of the predictions of 5 models for Sr-90 are illustrated in **Figure 3.6**, which plots the internal doses rate (μGy hr^{-1}) against the weight (kg) of organisms. The internal dose rate increases steeply up to a weight of approximately $1x10^{-2}$ following which there is a more gradual rise up to around $2.4x10^{1}$. The internal dose rate for organisms of weight between $2.4x10^{1}$ kg to $1x10^{4}$ kg is approximately constant at $6.5x10^{-4}$ μGy hr^{-1} which is the same as the D-MAX Model prediction of the maximum possible value.

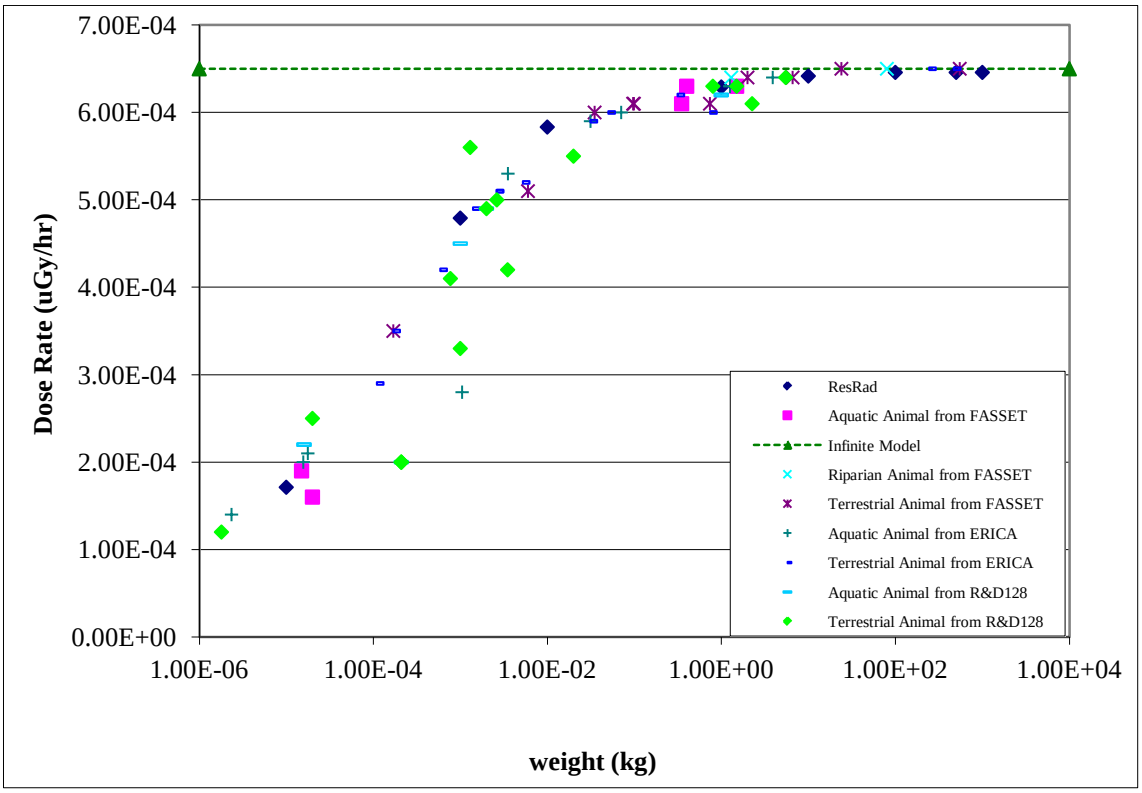

Figure 3.6 Predicted dose rate using 5 models for Sr-90 internal dose rate.

The above relationship between predicted dose rate and organism mass can be fitted by regression to data separated into three mass ranges. The first section is from $2x10^{-6}$ kg to $1x10^{-2}$ kg, the second section is from $1x10^{-2}$ kg to $2.4x10^{1}$ kg weight and the third section is above $2.4x10^{1}$ kg. **Figure 3.7** illustrates the equations of each section of the graph. The equation of the first section is

$$D = 5.46\text{-}5\ \mathrm{Ln}(m) + 7.95E\text{-}4 \qquad (2x10^{-6}\ \text{kg to}\ 1x10^{-2}\ \text{kg}) \qquad (3.5)$$

$R^2 = 0.796$, $P = 0.8982$

and the equation of the second section is

$D = 9.68E\text{-}6\ Ln(m) + 6.24E\text{-}4$ ($1x10^{-2}$ kg to $2.4x10^{1}$ kg) (3.6)

$R^2 = 0.762$, $P = 0.9446$

Where D is Dose rate in μGy/hr

m is weight of organism in kg

The residual was calculated as the difference between the internal dose rate given by the above equation and the predictions of the models, as shown in **Figure 3.8**. The % deviation can be calculated from the internal dose rate predicted by the model and the above equation, as shown in **Figure 3.9**. The histogram of % deviation is shown in **Figure 3.10**.

75 percent (49 out of 65 points) had percent deviation within ± 10 % and 83 percent (54 out of 65 points) had a percent deviation within ± 20 %. Almost all of model predicted values are within 40% deviation of fitted lines with the fit improving for heavy weights. At weight greater than 0.01 kg, all energy from the beta particle which is emitted from Sr-90 is absorbed by a large medium. Only two of the reference organisms (seed from terrestrial R&D128 model and zooplankton from the aquatic ERICA model) were more than 40% above the fitted lines, these being in the lowest weight category. There were no significant differences in Sr-90 internal dose rate between trend line and the model predicted at P=0.8982 in first section and at P=0.9446 in second section. All of figures show the relatively good fit of the equation to the model predicted internal dose rates from Sr-90 for various reference organisms. In heavy weight organisms, the internal dose rate seems to be constant at the 14.73 kg weight organism.

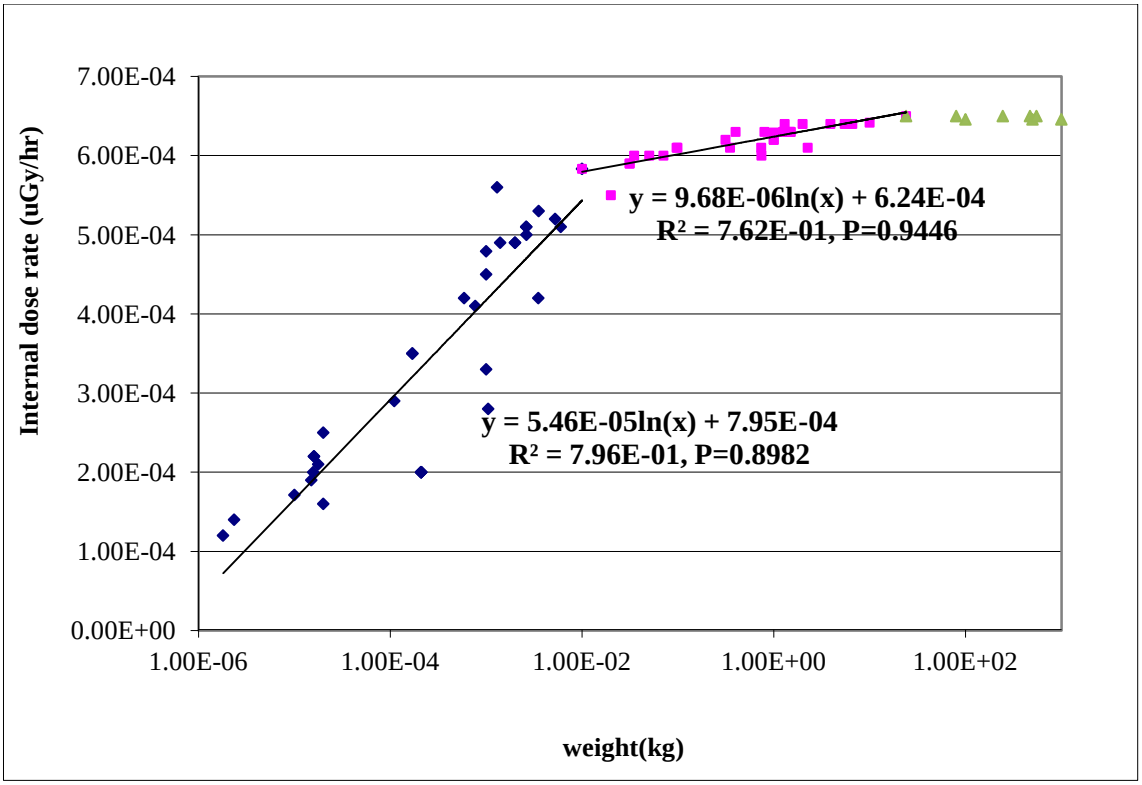

Figure 3.7 Fitted equations to model predictions for Sr-90 internal dose rate.

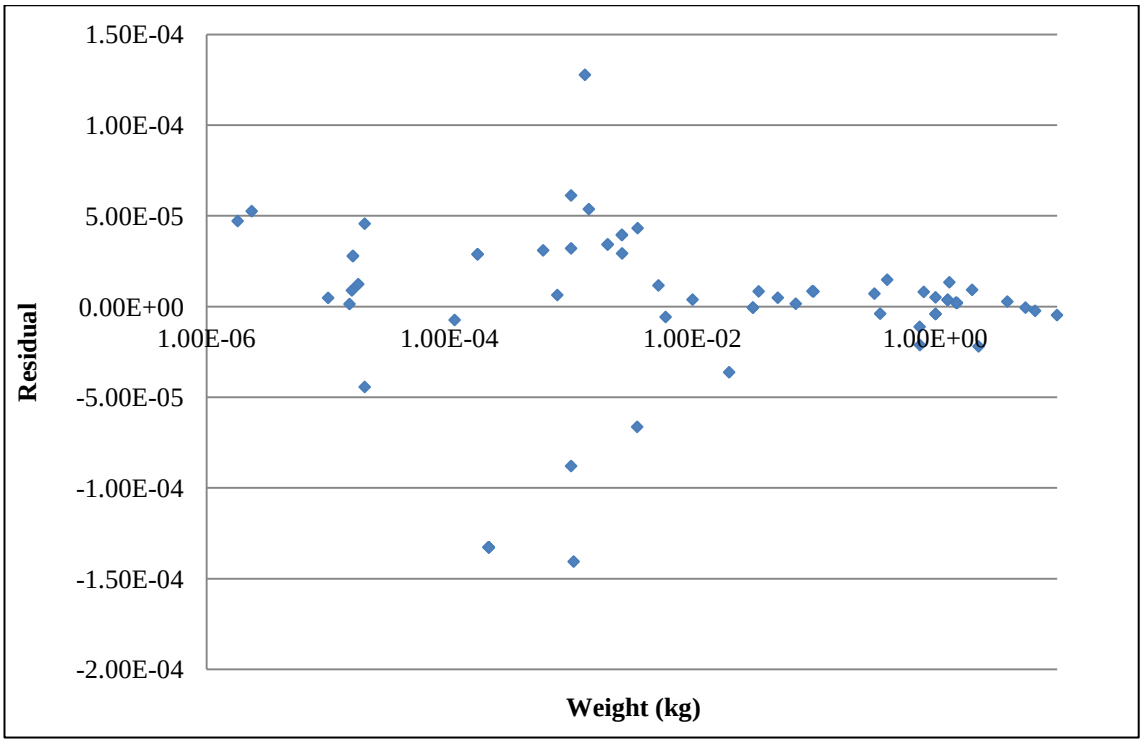

Figure 3.8 Residuals of the fit of the trend lines to the model predictions for Sr-90 internal dose.

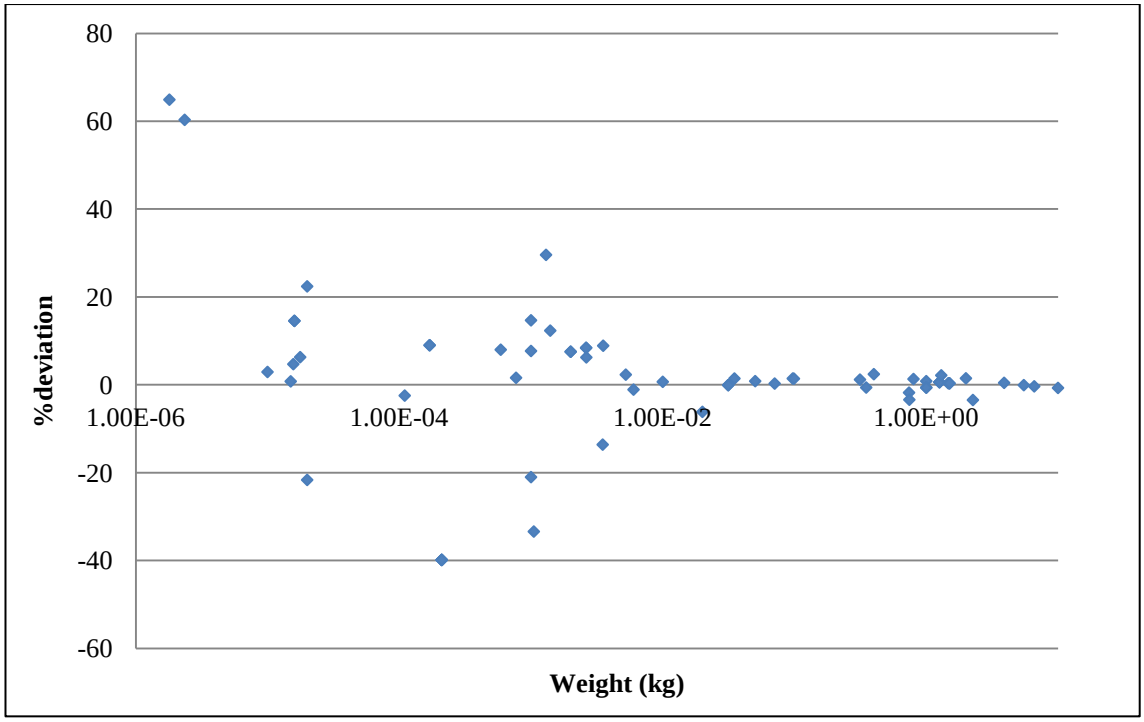

Figure 3.9 The percent deviation of the trend line from Sr-90 internal dose rate predicted by the models.

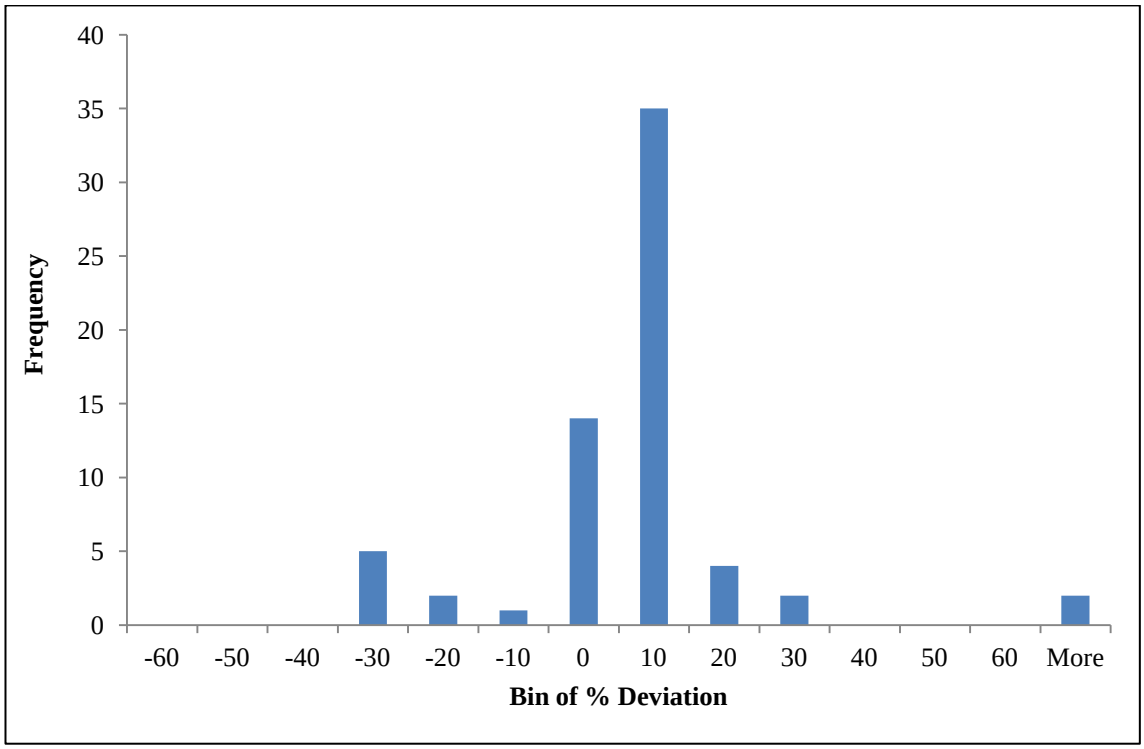

Figure 3.10 The histogram of % deviation for predicted Sr-90 internal dose to various organism compared with a logarithmic regression fit.

3.3.3 The prediction of the external dose rate of Cs-137

The predictions for the external dose rate of 5 models for Cs-137 are illustrated in **Figure 3.11** which plots the predicted external dose rate (μGy hr^{-1}) against the weight (kg) of organism. There are two plots within the same figure. One is significantly higher than the other and represents aquatic organisms and those terrestrial organisms which live within the soil. The lower line represents those terrestrial organisms which live on or above the soil surface. Both lines can be separated into two sections. For the higher line, the external dose rate remains approximately constant for the low weight organism until up to approximately $1.9x10^{-9}$ kg. Above this weight, there is steep decrease in predicted external dose rate as weight increases up to 1 kg followed by a dramatic fall from 1 to approximately 1000 kg. For the lower line (terrestrial organisms living on the soil surface), the external dose rate decreases gradually as weight increases up to 1 kg; after which, there is a steeper fall.

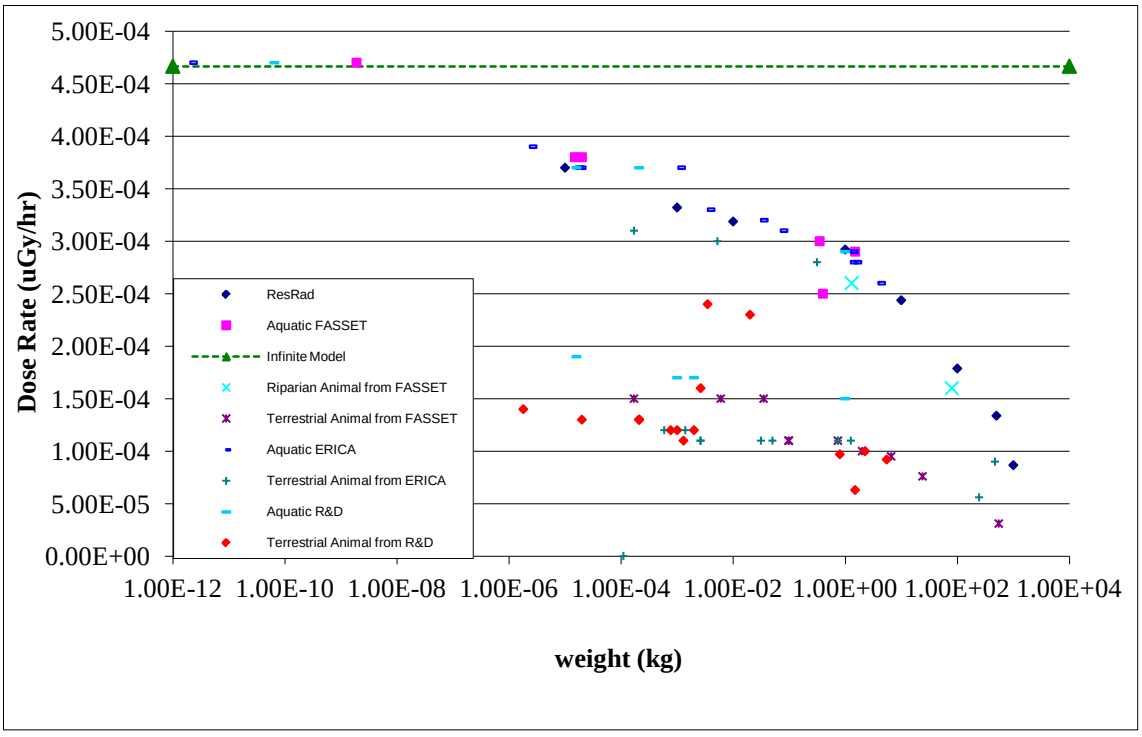

Figure 3.11 Predicted dose rate using 5 models for Cs-137 external dose rate

The above relationship between predicted dose rate and organism mass can be separated into three sections for the higher line (aquatic and in-soil terrestrial organisms) and two sections for the lower line (on-soil terrestrial.). For the higher line, the dose rate of the first section is constant at around $4.7x10^{-12}$ μGy/hr (D-MAX model = $4.667x10^{-12}$) until the organism weight is approximately 1.9 $x10^{-9}$ kg (phytoplankton from aquatic

FASSET model). The second section is from about 1.9 $x10^{-9}$ kg to 1 kg weight, the third section is from 1 kg to 1000 kg (RESRAD model) weight of organism. For the lower line, the first section is from 1.8$x10^{-6}$ kg (seed from terrestrial R&D128) to 1 kg weight of organism which is the same point as the higher line. The second section is from 1 kg to 550 kg (cattle from terrestrial FASSET model) weight of organism. **Figure 3.12** illustrates the equations of each section of the line. For the above line, the equation of the second section is

$D = -1.01E-05 \ln(m) + 2.59E-4$ (1.9 $x10^{-9}$ kg to 1 kg) (3.7)

$R^2 = 0.633$, $P = 0.9461$

and the equation of the third section is

$D = -2.81E-5 \ln(m) + 2.89E-4$ (1 kg to 1000 kg) (3.8)

$R^2 = 0.960$, $P = 0.9041$

For the lower graph, the equation of the first section is

$D = -2.86E-6 \ln(m) + 1.13E-4$ (1.8$x10^{-6}$ kg to 1 kg) (3.9)

$R^2 = 0.263$, $P = 0.9220$

and the equation of the second section is

$D = -1.17E-5 \ln(m) + 1.12E-4$ (1 kg to 550 kg) (3.10)

$R^2 = 0.633$, $P = 0.9446$

Wher D is Dose rate in μGy/hr
m is weight of organism in kg

The residuals can be calculated as the difference between the external dose rate given by the above equation and the predictions of the models, as shown in **Figure 3.13**. The percentage deviation can be calculated from the external dose rate predicted by the model and equation 3.7 to 3.10, as shown in **Figure 3.14**. The histogram of % deviation is shown in **Figure 3.15**.

67.12 percent (49 out of 73 data points) within ± 10 % deviation and 86.30 percent (63 out of 73 data points) within ± 20% deviation. Almost all (70 out of 73) of the external dose rates were predicted to within 30% deviation. The three organisms with greater than 30% deviation were small benthic crustaceans (R&D128 model) at 29.08%, benthic fish (R&D128 model) at 33.93% and birds (terrestrial R&D128 model) at -41.26%. In light weight organisms, the external dose rate seems to be constant up to 1.35×10^{-10} kg. The estimation of that point can be calculated by an equation describing the second section. There were no significant differences in Cs-137 external dose rate between trend line and the model predicted at P=0.9461 in above line in first section, at P=0.9041 in above line in second section, at P=0.9220 in lower line in first section and at P=0.9446 in lower line in second section.

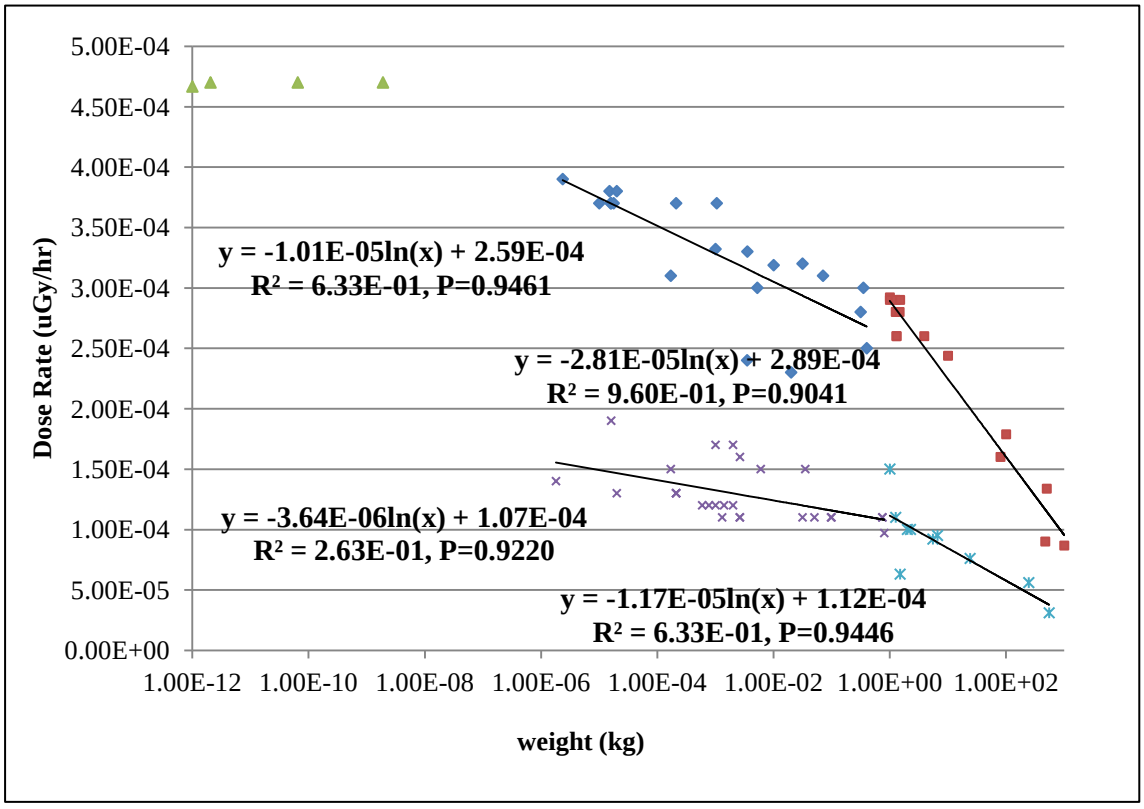

Figure 3.12 Fitted equations to model predictions for Cs-137 external dose rate.

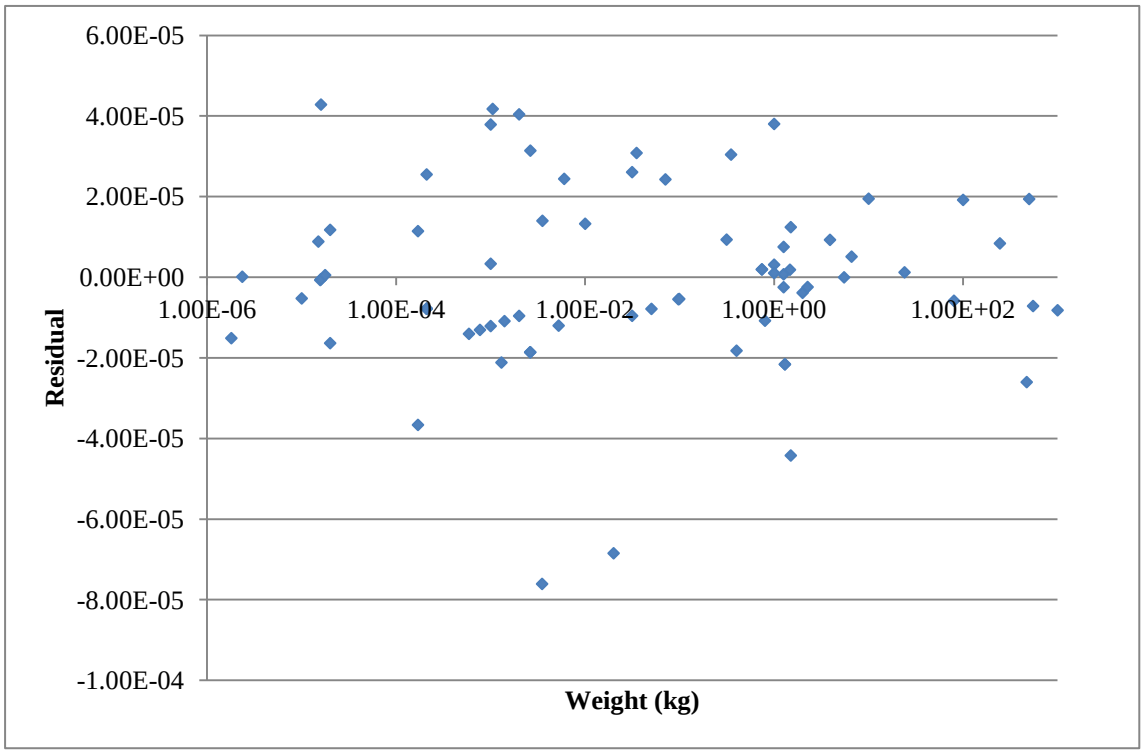

Figure 3.13 Residuals of the fit of the trend lines to the model predictions for Cs-137 external dose.

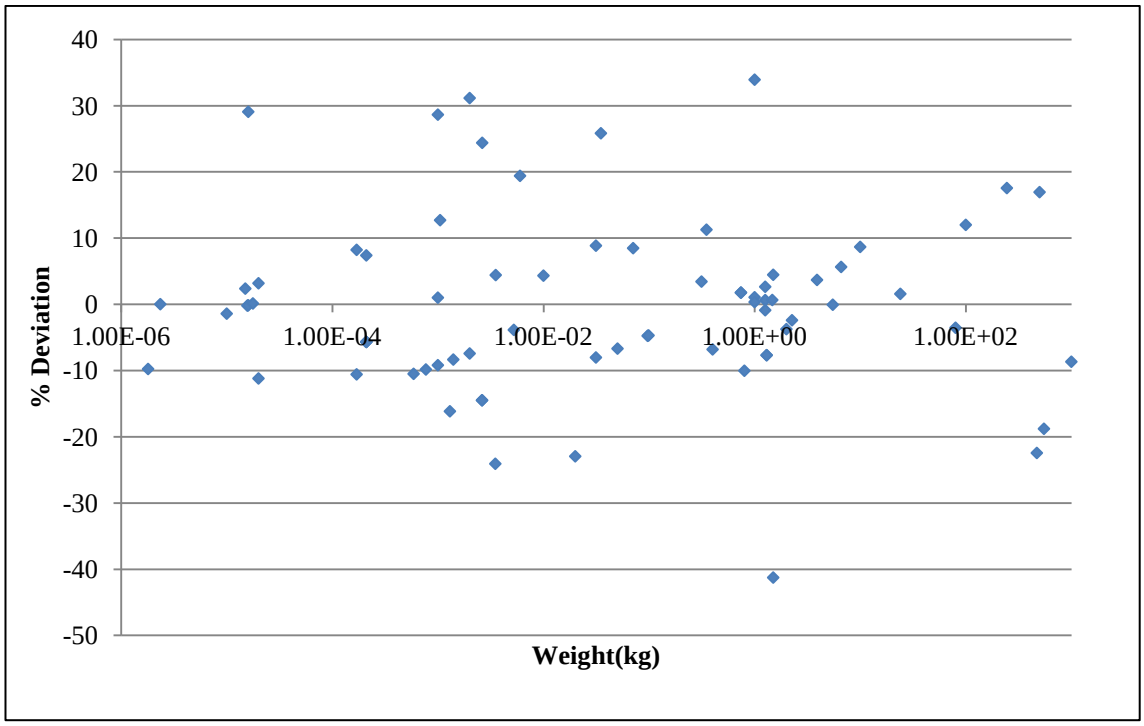

Figure 3.14 The percent deviation of the trend line from Cs-137 external dose rate predicted by the models.

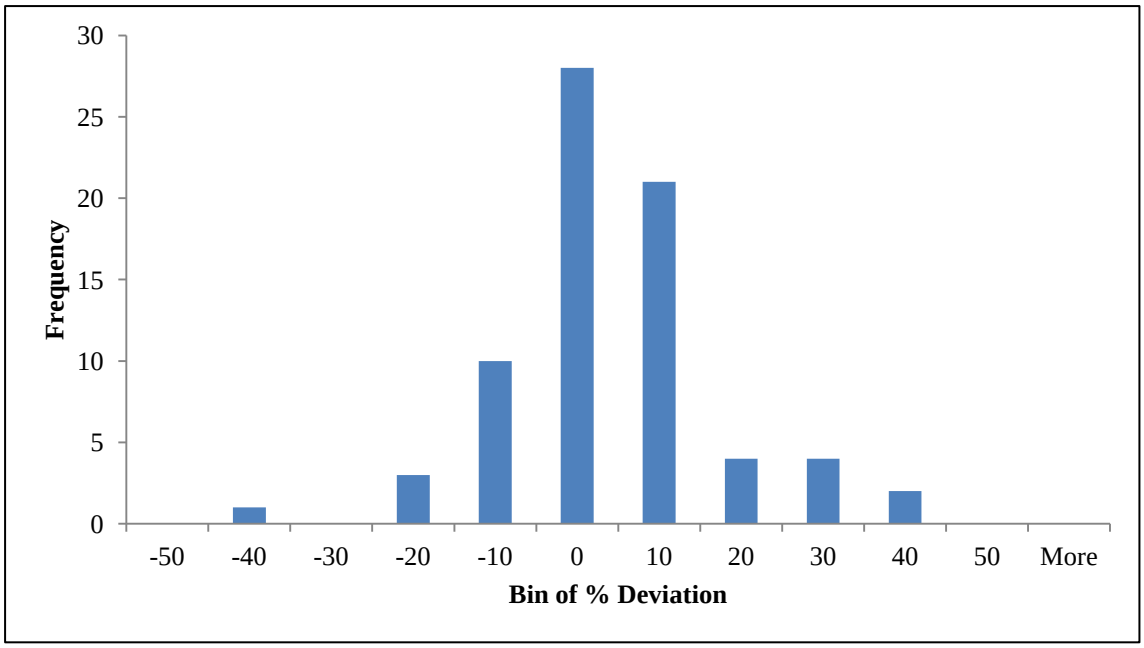

Figure 3.15 The histogram of % deviation for predicted Cs-137 external dose to various organism compared with a logarithmic regression fit.

3.3.4 The prediction of the external dose rate of Sr-90

The predictions of the external dose rate from Sr-90 for the 5 models are illustrated in **Figure 3.16** which plots the predicted external dose rate (μGy hr^{-1}) against the weight (kg) of organism. There are two lines within this Figure. The first upper line represents aquatic organisms and those terrestrial organisms living within the soil. The lower graph represents to the terrestrial organisms living above the soil surface. Both lines can be separated into two sections. For the aquatic and soil-dwelling organisms, the external dose rate remains constant for light weight organisms until up to approximately $1.9x10^{-9}$ kg, after which there is a dramatic decrease as weight increases up to 0.01 kg. There is then a gradual decline from 0.01 to around 1000 kg. For the lower line, the external dose rate decreases steeply as weight increases up to 0.01 kg; after that, there is a gradual fall.

For the external dose from Sr-90, the prediction of the external dose of all the terrestrial biota from the FASSET and ERICA models are of a different order to the other models (the dose rate predictions for terrestrial biota from the FASSET and ERICA models are in the range 10^{-9} to 10^{-16} μGy hr^{-1}, whilst the others are in the range 10^{-4} to 10^{-6} μGy hr^{-1}). A plot of the predictions of external dose of terrestrial biota from the FASSET and

ERICA models are shown in **Figure 3.17**. This study will not use these predictions from FASSET and ERICA to fit the equation: this will be discussed further in Section below.

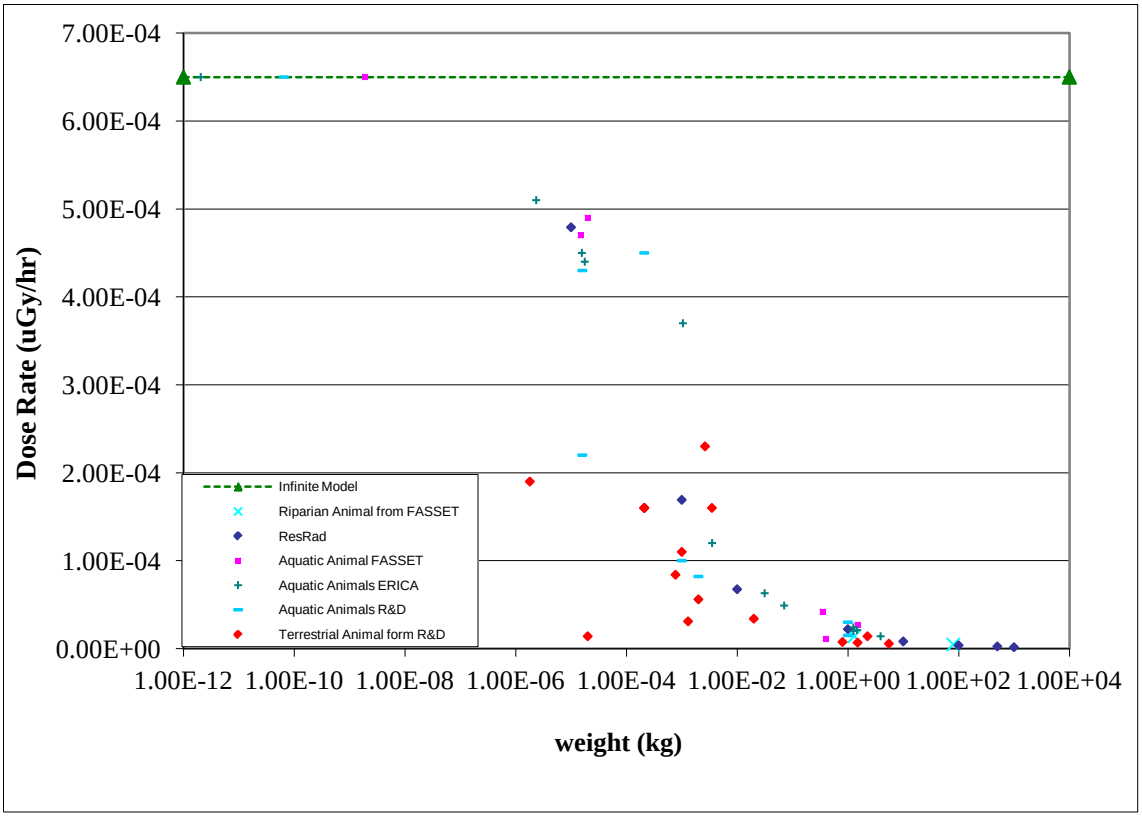

Figure 3.16 Predicted dose rate using 5 models for Sr-90 external dose rate.

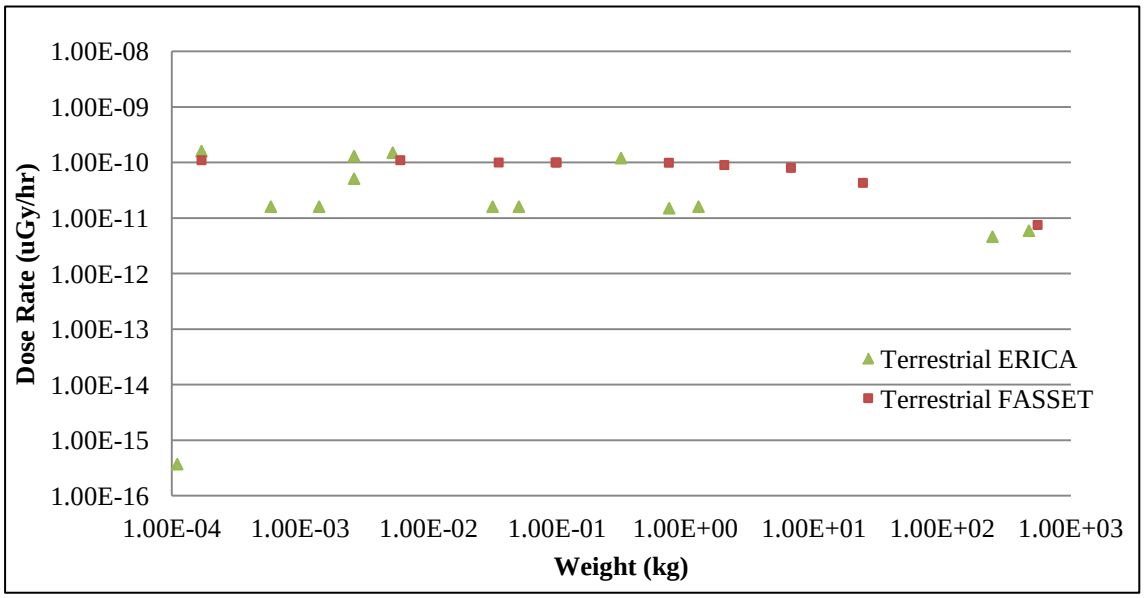

Figure 3.17 Predicted Sr-90 external dose rate of terrestrial biota from FASSET and ERICA models

The above relationship between predicted dose rate and organism mass can be separated into three sections in the upper line and two sections in the lower line in the same way as for the external dose rate from Cs-137. For the upper line, the dose rate of the first section is stable at around $6.5x10^{-4}$ μGy/hr (D-MAX model = $6.5x10^{-4}$) until the organism weight around 1.9 $x10^{-9}$ kg (phytoplankton from aquatic FASSET model). The second section is from about 1.9 $x10^{-9}$ kg to 0.01 kg weight of organism, the third section is from 0.01 kg to 1000 kg (RESRAD model) weight of organism. For the lower line, the first section is from $1.8x10^{-6}$ kg (seed from terrestrial R&D128) to 0.01 kg weight of organism which is the same point as the higher graph. The second section is from 0.01 kg to 5.5 kg (carnivorous mammal from terrestrial R&D128 model) weight of organism. **Figure 3.18** illustrates the equations of each section of the line. For the above line, the equation of the second section is

$$D = -5.31E\text{-}5 \ln(m) - 1.26E\text{-}4 \qquad (1.9 \times 10^{-9} \text{ kg to } 0.01 \text{ kg}) \qquad (3.11)$$

$R^2 = 0.840$, $P = 0.8267$

and the equation of the third section is

$$D = -6.31E\text{-}6 \ln(m) + 3.18E\text{-}5 \qquad (3.12)$$

$R^2 = 0.863$, $P = 0.2189$

For the lower graph, the equation of the first section is

$$D = -2.06E\text{-}5 \ln(m) - 4.82E\text{-}5 \qquad (3.13)$$

$R^2 = 0.662$, $P = 0.9998$

and the equation of the second section is

$$D = -1.43E\text{-}6 \ln(m) + 1.04E\text{-}5 \qquad (3.14)$$

$R^2 = 0.108$, $P = 0.9955$

Where D is Dose rate in μGy/hr

m is weight of organism in kg

The residuals calculated as the difference between the external dose rate given by Equations 3.11 to 3.14 and the predictions of the models, are shown in **Figure 3.19**. The % deviations are shown in **Figure 3.20** and a histogram of % deviation is shown in **Figure 3.21**.

76.09 percent (35 out of 46) of dose rate estimates have deviation within ± 30 % of the fitted line, 86.95 percent (40 out of 46) with deviation within ± 50 % deviation and 93.48 percent (43 out of 46) with deviation within ± 100 % deviation. Three of the reference organisms were more than 100% different to the trend line: the 100 kg biota from RESRAD model (at -141.15%), the 500 kg biota from the RESRAD model (at -111.06%) and the 1000 kg biota from the RESRAD model (at -105.55%). All models and reference organisms give external dose rates relatively close to the trend line except the terrestrial biota from the FASSET and ERICA models which give much lower predicted dose rates than the other models. In light weight organisms, the external dose rate seems to be constant up to 4.5×10^{-7} kg. There were no significantly different in Sr-90 external dose rate between trend line and the model predicted at P=0.8267 in above line in first section, at P=0.2189 in above line in second section, at P=0.9998 in lower line in first section and at P=0.9955 in lower line in second section.

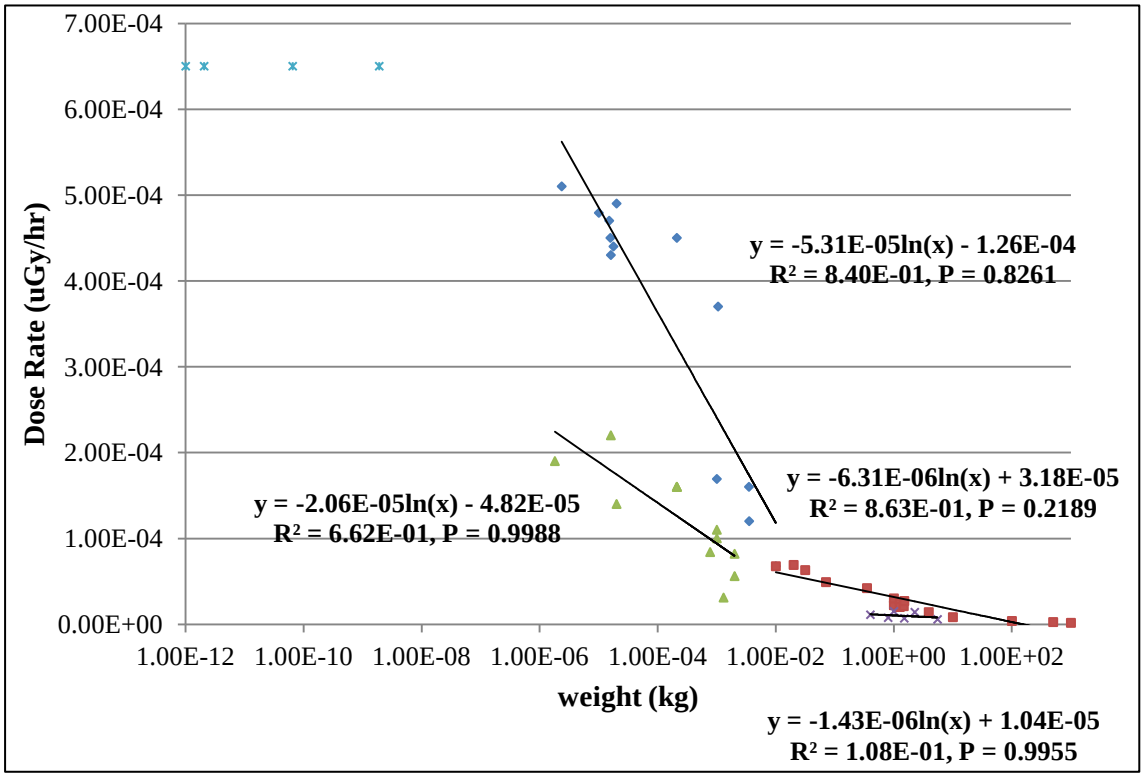

Figure 3.18 Fitted equations to model predictions for Sr-90.

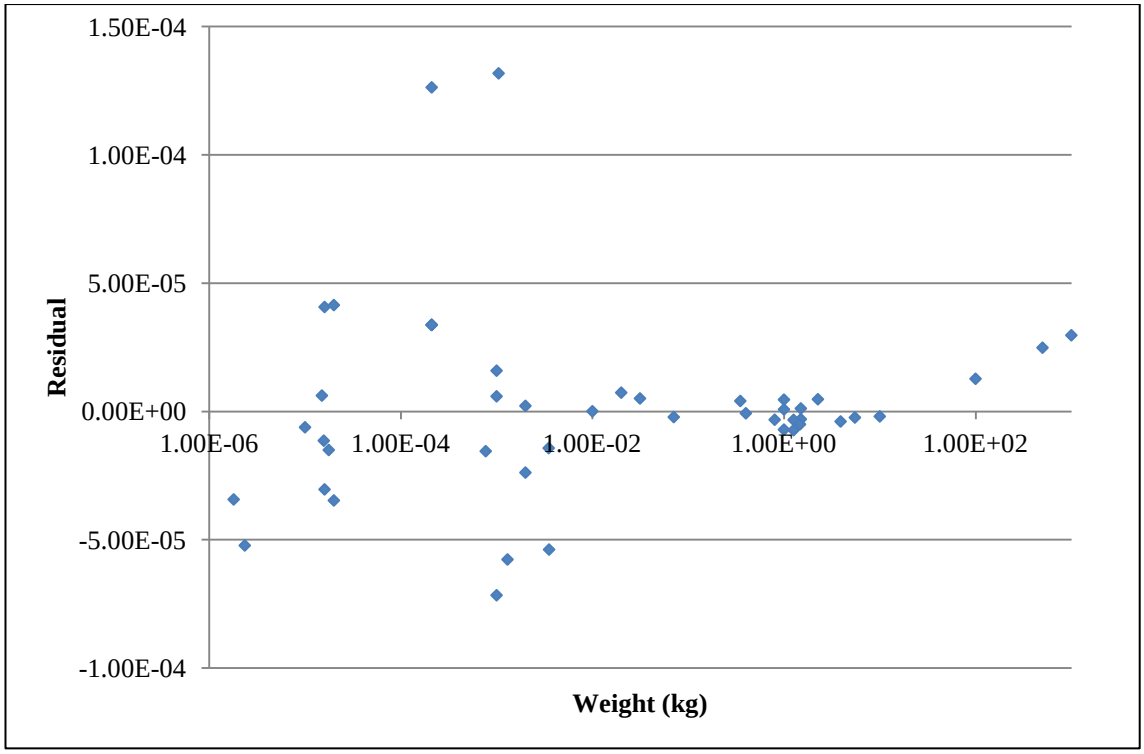

Figure 3.19 Residuals of the fit of the trend lines to the model predictions for Sr-90.

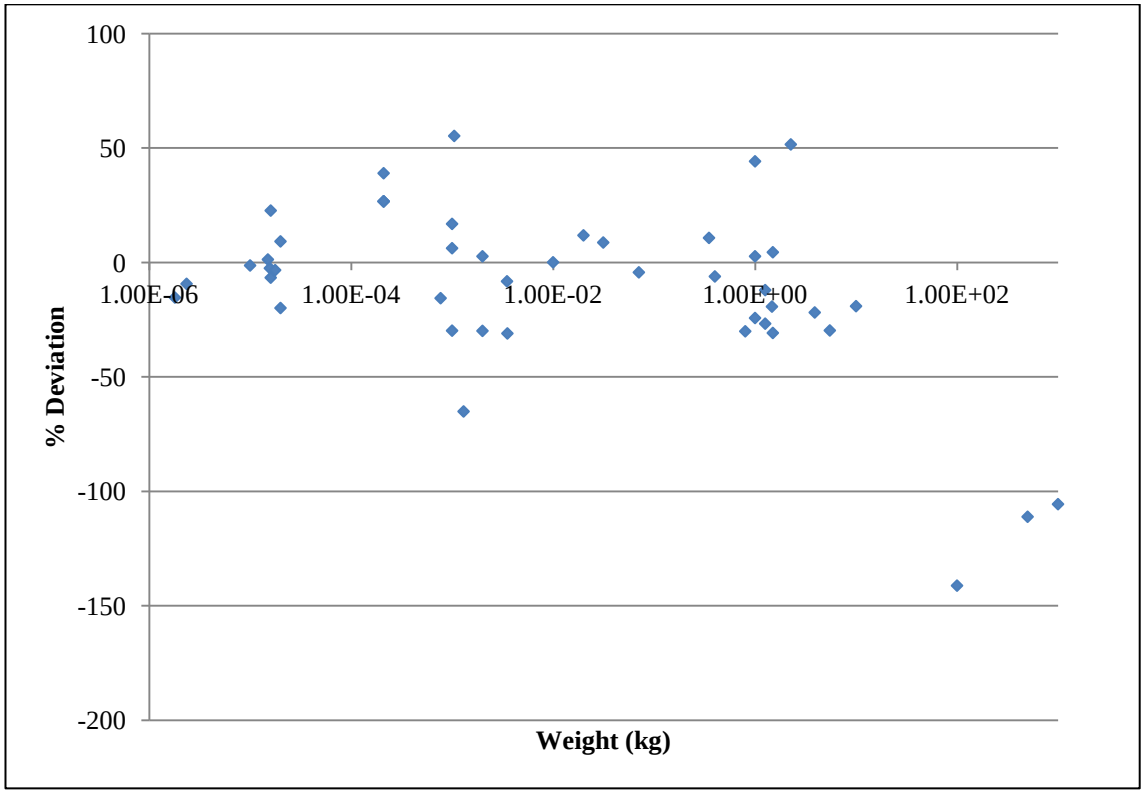

Figure 3.20 The percent deviation of the trend line from the external dose rate predicted by the models.

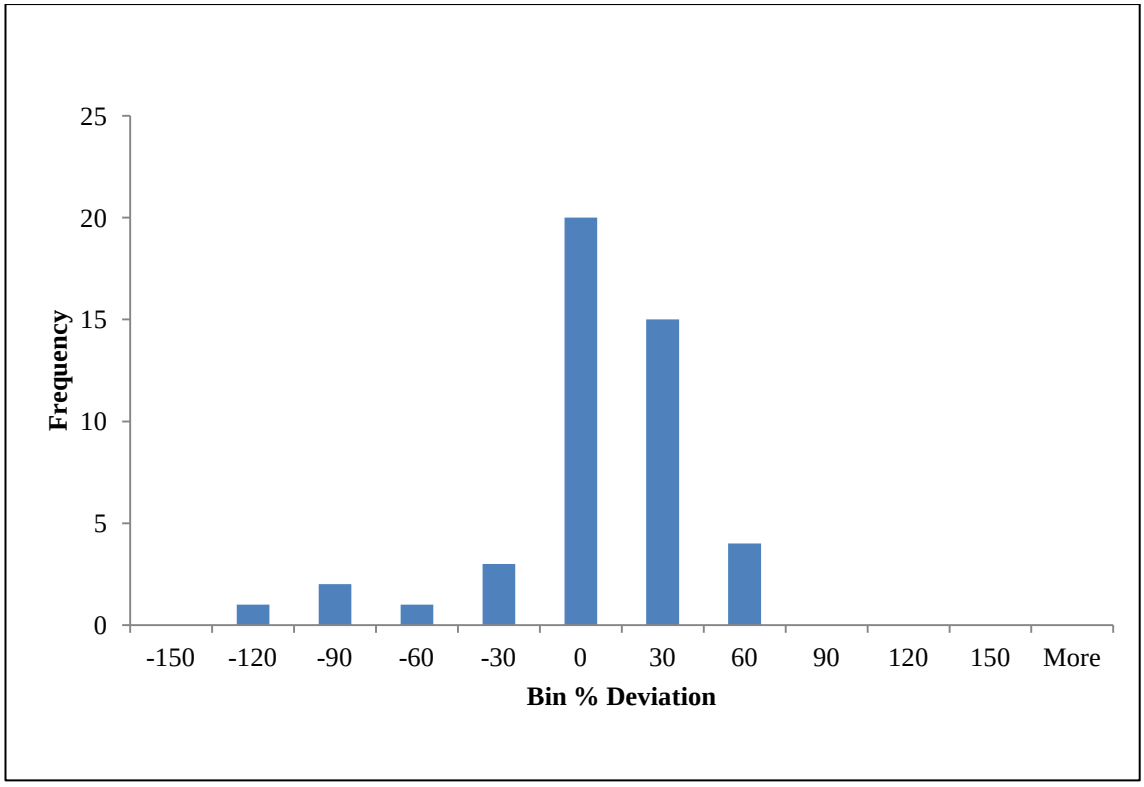

Figure 3.21 The histogram of % deviation for predicted Sr-90 external dose to various organisms compared with a logarithmic regression fit.

3.3.5 The prediction of the total dose rate of Cs-137

The predictions of the total dose rate of the five models for Cs-137 are illustrated in **Figure 3.22**. This plots the predicted total dose rate (μGy hr^{-1}) as a function of the weight (kg) of organism. The estimation of total internal and external dose rate from Cs-137 of aquatic biota (especially pelagic organisms) and in soil terrestrial biota of the RESRAD, FASSET, ERICA and R&D128 models is quite close to the estimation of the maximum possible dose of the D-MAX model. However, the estimation of total dose rate of benthic biota from R&D128 model and on-soil terrestrial biota from FASSET, ERICA and R&D128 models are significantly lower.

The percent deviations of the total dose in each model from the D-MAX model are illustrated in **Figure 3.23** which plots percent deviation against the weight (kg) of organism. The deviations of the aquatic and riparian biota are almost within ±10 % except benthic biota which are within -30 to -40% whilst, the deviation of on soil terrestrial biota are almost within -30 to -60%.

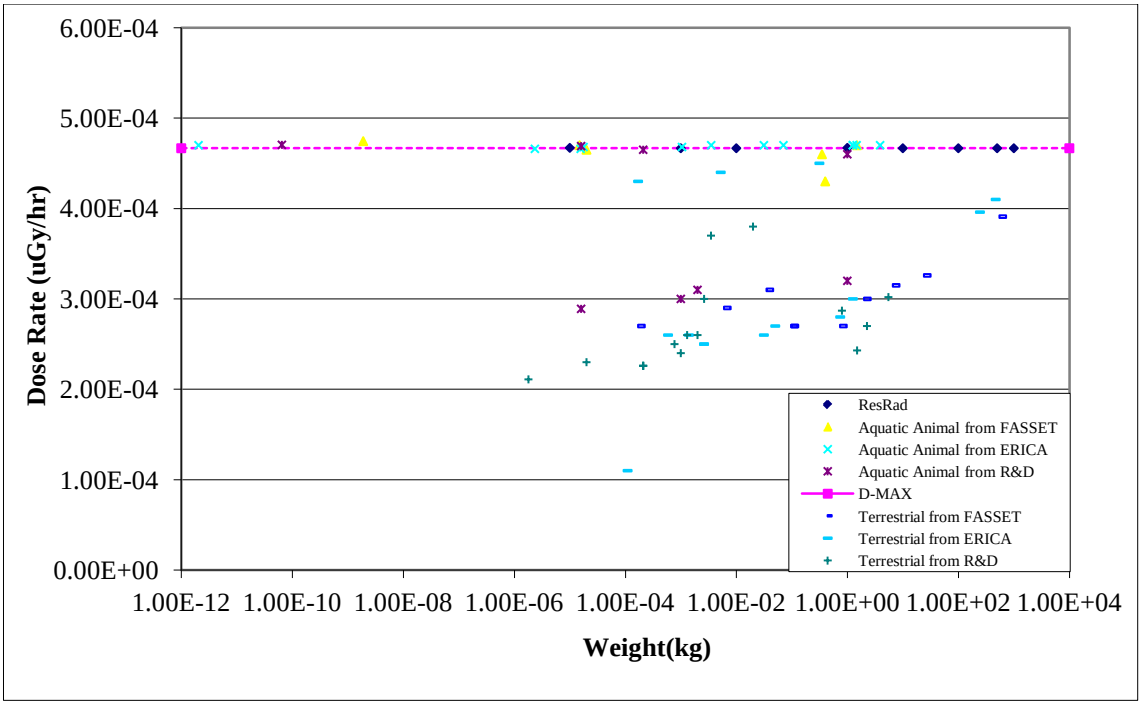

Figure 3.22 Predicted dose rate using 5 models for the total dose Cs-137.

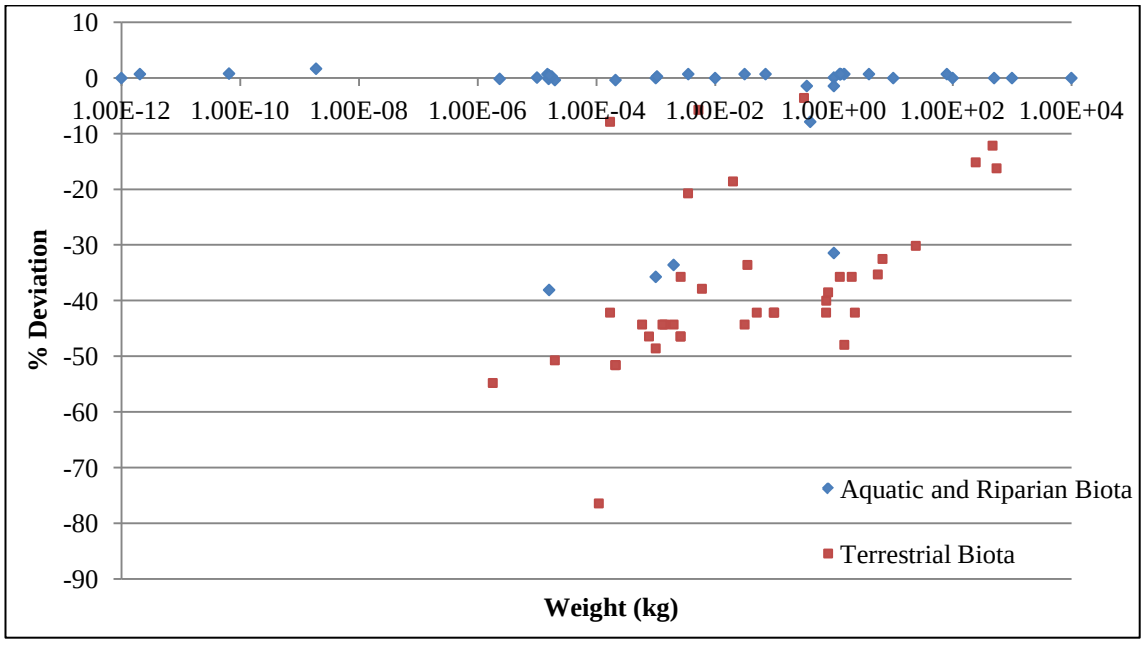

Figure 3.23 The percent deviation of the total dose in each model from the D-MAX model for equal concentration in organism and medium for Cs-137.

3.3.6 The prediction of the total dose rate of Sr-90

The predictions of the total dose rate of 5 models for Sr-90 are illustrated in **Figure 3.24** which plots the predicted total dose rate (μGy hr^{-1}) against the weight (kg) of organism. As for the estimation of the total dose rate of Cs-137, the estimation of the total dose

rate of Sr-90 of aquatic biota and in-soil terrestrial biota of the RESRAD, FASSET, ERICA and R&D128 models is quite close to the estimation of the D-MAX model whilst, the estimation of the total dose rate of benthic biota from R&D128 and on soil terrestrial biota from FASSET, ERICA and R&D128 are significantly lower.

The percent deviations of the total dose in each model from the D-MAX model are illustrated in **Figure 3.25**. The deviations of the aquatic, riparian and in soil terrestrial biota are quite close to 0% except benthic biota from R&D model which are within -10 to -40% whilst, the deviation of on-soil terrestrial biota are almost within -30 to -60%. As can see from **Figure 3.25**, the deviation of the total dose rate of Sr-90 is low when the biota weight is heavy. The shape of the total dose rate graph of the terrestrial biota of FASSET and ERICA is similar to the internal dose rate because the prediction of the external dose rate from those biota is quite low when compared with the internal dose. In this case, the total dose rates therefore mainly depend on the internal dose rate. When a beta source is inside an organism, almost all of the beta radiation energy is transferred to the tissue of the organism. On the other hand, if the beta source is external, only a small fraction of the beta radiation energy is transferred to the organism because it is a low penetrating radiation, particularly for organisms > a few mm in size. Therefore, the internal dose rate is more important than the external dose rate for beta radiation.

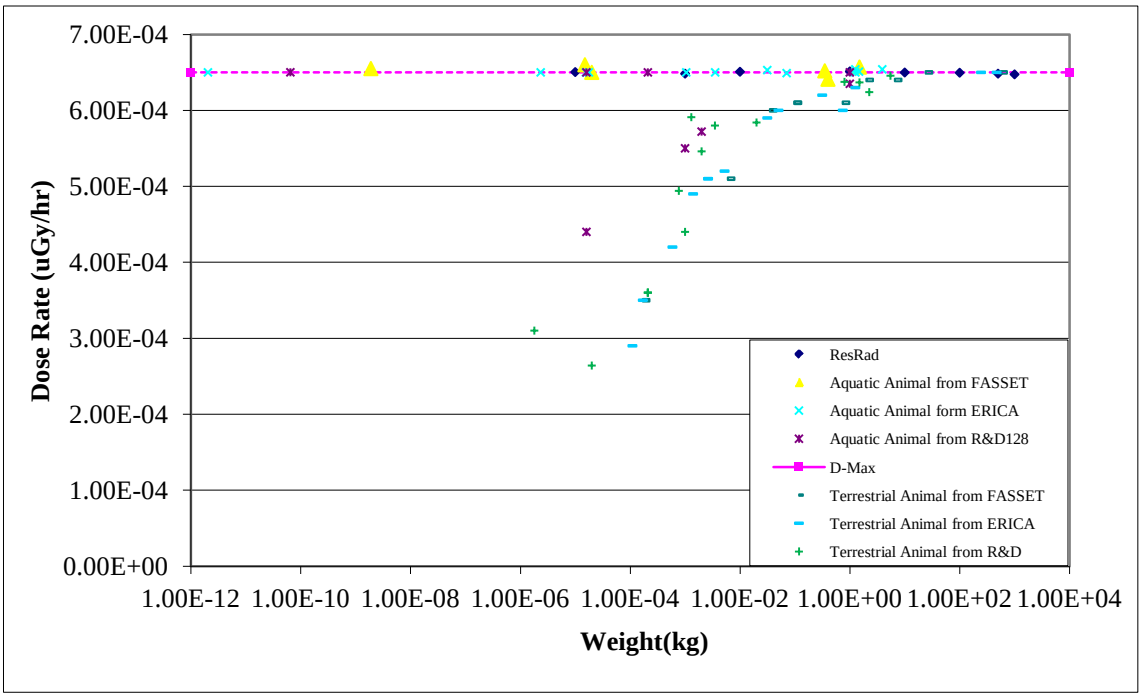

Figure 3.24 Predicted dose rate using 5 models for the total dose Sr-90.

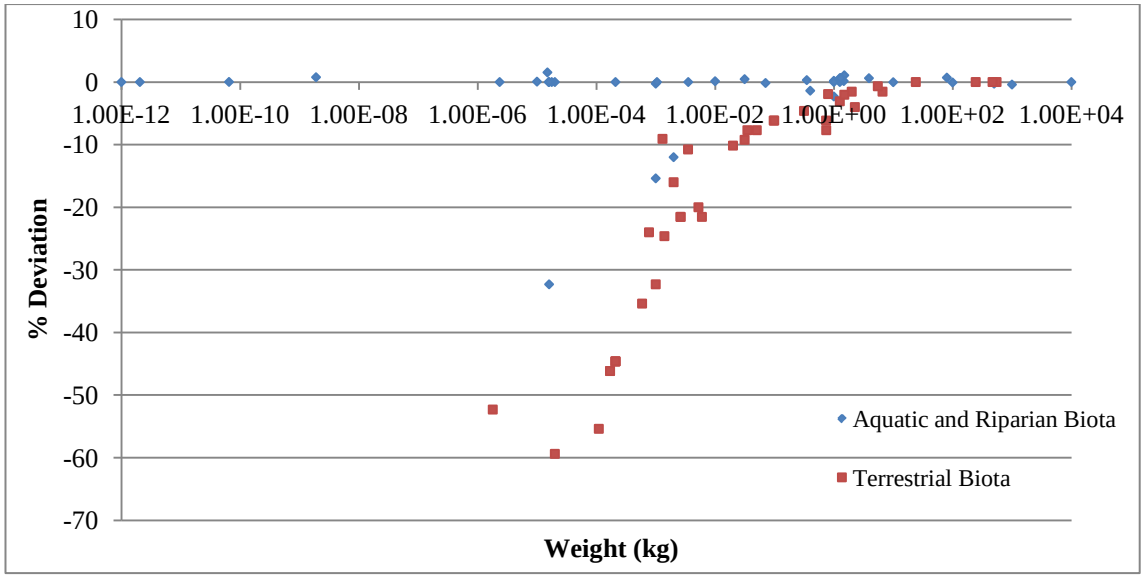

Figure 3.25 The percent deviation of the total dose in each model from the D-MAX model for equal concentration in organism and medium for Sr-90.

3.4 Discussion

Currently, a model-model comparison exercise for the estimation of the radiation exposure of non-human biota has been reported in several previous studies: unweight absorbed dose rates (Vives i Batlle, Balonov et al. 2007) and Whole-body radionuclide activity concentration (Beresford, Barnett et al. 2008). Those exercises, however, was not aimed to determine whether the predictions of the different models were correct or not (Vives i Batlle, Balonov et al. 2007; Beresford, Barnett et al. 2008). In this study, the internal and external absorbed dose rates predicted by the different models were estimated. The outputs of the results were shown in the relationship between absorbed dose rate (μGy hr^{-1}) and mass of different organisms. The absorbed dose rate was calculated by assuming both biota activity concentration and medium concentration to be 1 Bq kg^{-1} to make comparisons more clear. Therefore, the calculated absorbed dose rate was absorbed dose rate (μGy hr^{-1}) per Bq $kg^{-}1$ or Dose Conversion Coefficient (DCC). The developed relationships for DCC can be applied to give approximate values of absorbed dose rate as a function of biota mass, and to compare the model predictions for different organism types. The difference between the previous work and this work is the previous work has just compared models with the different calculated absorbed dose rates or whole-body radionuclide activity concentration, but this work compared the absorbed dose rate with mass of different organisms using the 5 different models. This work gives the simple DCC as a function of biota mass to calculate both internal and

external dose for Cs-137 and Sr-90. For the internal dose, DCC depends on the biota mass. The internal dose rate increases as weight increases. The equation 3.3 and 3.4 for Cs-137 and the equation 3.5 and 3.6 for Sr-90 can be used to predict the internal dose rate as a function of biota mass. For the external dose, DCC depends on biota mass and occupancy factor. The external dose decreases as weight increases and on-soil terrestrial animals get lower dose than the aquatic and in-soil terrestrial animals. The equation 3.7 and 3.8 can be used to predict the Cs-137 external dose rate for in-soil terrestrial biota, whilst the equation 3.9 and 3.10 can be used to predict the Cs-137 external dose for on-soil terrestrial and aquatic biota. The equation 3.11 and 3.12 can be used to predict the Sr-90 external dose rate for in-soil terrestrial biota, whilst the equation 3.13 and 3.14 can be used to predict the Sr-90 external dose for on-soil terrestrial and aquatic biota.

The finding that the inclusion of water chemistry data to improve CR estimates for fish agrees with the conclusion of the Perch Lake study (Yankovich and et al. 2010) who came to a similar conclusion. The importance of the CR in causing variability in model predictions, an important conclusion of this thesis, supports the previous work (Beresford et al. 2010; Vives i Batlle, et al., 2007) which found that variability in CR predictions was much greater than variability in DCC estimates.

It is important to note that the concept of the dose for biota is usually different to that in humans, particularly when applied for regulating environmental releases. The dosimetry in humans focuses on stochastic effects, whilst the dosimetry in biota focuses on deterministic effects (morbidity, mortality, reduced reproductive success and mutation) (Larsson 2004). For human dosimetry, there is a system of determining effective whole-body doses from doses to particular organs. For biota, there is no such system, so doses are calculated as average whole-body doses. For Cs-137 internal dose, this is a good approximation because the isotope is distributed quite evenly through the body (Coughtrey and Thorne 1983), but for larger organisms, the Sr-90 internal dose may be mainly to bony tissues or to organs close to those tissues where the isotope is concentrated (Coughtrey and Thorne 1983). External dose, also in larger organisms, for primarily beta-emitting radionuclides, is also mainly to the outer tissues. However, as a simplification, all models assume a whole-body average dose. This also makes comparison between models simpler.

The predictions of the models also depend on assumptions about the variability of shapes, size, habitats and source-target relationships (Ulanovsky, Pröhl et al. 2008). The shape of the biota is categorised in a simple shapes as spheres, ellipsoids and cylinders to simplify the various shapes of different life forms (Ulanovsky, Pröhl et al. 2008). For the organism dimensions, the radiation dose in aquatic biota represents the simplest case because of the uniform distribution of activity thought out its body. If the organism dimensions are much larger than the radiation range in the medium, the internal dose is close to $D_{\infty,}$ whilst the external dose will be effectively zero (assuming the same activity concentration in organism and medium). On the contrary, if the biota sizes are much smaller than the radiation range in the medium, the internal dose will approach zero because the radiation escapes from the body, whilst the external dose approaches $D_{\infty.}$ $D_{\infty}(E) = 5.76x10^{-4}$ E where E is the energy (MeV) of a mono-energetic source (Ulanovsky, Pröhl et al. 2008).

For the results for the study of the internal dose rate, all of the simple model fits give reasonably good estimates of the dose to the different reference organisms used in the models. These are within 20% deviation for Cs-137 (a beta and gamma emitter) and 40% deviation for Sr-90 (beta emitter) is similar to the estimation of differences in internal dose rates in an international comparison of models (Beresford, Balonov et al. 2008) which observed a coefficient of variation of 25%. As also found in the previous study of Vives i Batlle et al. (Vives i Batlle, Balonov et al. 2007), the estimates of the internal dose rate compare well between the different models. The deviation of the internal dose of Cs-137 seems to be uniform as a function of weight, even for low weight organisms, whilst the deviation of the internal dose of Sr-90 is high in low weight organisms but quite low in high weight organisms.

The different shape of the predicted dose rate using 5 models for Cs-137 (Figure 3.1) and Sr-90 (Figure 3.6) internal dose rate is observed. For Cs-137 internal dose rate, gamma radiation from Cs-137 can escape from an organism when the size (or weight) of an organism is small because the range of gamma radiation is high. The increasing of the amount of gamma radiation from Cs-137 is absorbed in an organism, when the size of an organism is increasing. Therefore, for the Cs-137, the internal dose rate increases gradually when the size of an organism is small and then there is steeper rise when the size of an organism is bigger. For Sr-90 internal dose rate, beta radiation from Sr-90 which is short range is almost stop within an organism when an organism is around 1

kg. Therefore, for the Sr-90, the internal dose rate increases dramatically up to 1 kg and then remains constant at the same level as the D-MAX model prediction of the maximum possible value.

For internal dose rate prediction, the phytoplankton in the FASSET, ERICA and R&D ($1.9x10^{-9}$, $2.05x10^{-12}$ and $6.5x10^{-11}$ kg respectively) were therefore eliminated from the estimation because of very low weight organism. The models do not seem to give consistent estimates for the low weight biota, though this is generally not an important issue because of the low internal component of dose in these very low weight organisms.

The results of the comparison of the external dose rate are more variable than the internal dose rate (Vives i Batlle, Balonov et al. 2007). The most important factor determining the external dose for biota predicted by the models appears to be occupancy factor. As can be seen from the prediction of the external dose in **Figure 3.12** (fitted equations to model predictions for Cs-137) and 3.18 (fitted equations to model predictions for Sr-90), the plot shows two clearly different trend lines. The upper line represents the external dose to aquatic animals and in-soil terrestrial animals. Both groups of animals are assumed to receive 100% of the external dose from the medium. The lower line represents the external dose from on-soil terrestrial animals. These animals get only the external dose form soil, but not from the air, since air activity concentrations are low. So, the external dose of on-soil terrestrial animals is lower than the aquatic and in-soil terrestrial animals by the factor of two. The discussion of the different assumed occupancy factors in different models of Beresford, et al., 2010 shows that different models use the different occupancy factors (Beresford and et al. 2010). For example, for bird in the R&D128, the fraction of in air:on soil occupancy fac tor is 0.5:0.5, whilst the ERICA model is 0.2:0.8. Therefore, for bird, the external dose from the ERICA is higher than the R&D128. Some models, for example ERICA and R&D128, have a function to allow the user to change the habitat of the organism. In this study, this function has been set to the same value in both models because if the occupancy of the organism is not the same, the external dose rate of organism will not be comparable.

All models give predictions which are within 30% deviation (for the Cs-137) and almost 50% deviation (for Sr-90) from the trend lines. The deviation of the external dose of Cs-137 and Sr-90 seems to be uniform in low and heavy weight organism. For external

dose rate predictions for Sr-90, the terrestrial animals from the FASSET and ERICA models were eliminated from the fitted equation because the external dose rate from the these models is quite low when compared with the other models. This is a result of the consideration of a shielding skin/fur layer in ERICA and FASSET model (only for the terrestrial but not for aquatic biota) (Vives i Batlle, Balonov et al. 2007).

3.5 Summary

The results of this study confirm the conclusion of Vives i Battle, et al., 2007 that there are no major differences in the external and internal dose predictions of the different models (Vives i Batlle, Balonov et al. 2007). The comparison of model predictions for different weights of organisms has additionally shown that (for the reference organisms used in the models) there are no big differences in predicted doses as a result of different organism body shape assumptions. An important result of this model comparison is that the influence of assumptions about organism occupancy factor and shielding by skin or fur seem to have a more important effect on predicted dose than body shape. It should also be noted that organism size at different life stages will have a large influence on dose (as shown by the change in dose as a function of body mass). These life-cycle changes are not included in current models. This issue will be discussed further in Chapter 6.

3.6 References

Beresford, N. A., Balonov, M., Beaugelin-Seiller, K., Børretzen, P., Brown, J., Cheng, J.-J., et al. (2005). *Models and approaches available to estimate the exposure of non-human biota: An international comparison of predictions.* Østerås: Norwegian Radiation Protection Authority.

Beresford, N. A., Balonov, M., Beaugelin-Seiller, K., Brown, J., Copplestone, D., Hingston, J. L., et al. (2008). An international comparison of models and approaches for the estimation of the radiological exposure of non-human biota. *Applied Radiation and Isotopes, 66*(11), 1745-1749.

Beresford, N. A., Barnett, C., Brown, J., Cheng, J., Copplestone, D., Filistovic, V., et al. (2008). Inter-comparison of models to estimate radionuclide activity concentrations in non-human biota. *Radiation and Environmental Biophysics, 47*(4), 491-514.

Beresford, N. A., & et al. (2010). Predicting the radiation exposure of terrestrial wildlife in the Chernobyl exclusion zone: an international comparison of approaches. *Journal of Radiological Protection, 30*(2), 341.

Copplestone, D., Bielby, S., Jones, S. R., Patton, D., Daniel, P., & Gize, I. (2001). *Impact Assessment of Ionising Raditaiton on Wildlife: R&D Publication 128*. Bristol: Environmental Agency.

Coughtrey, P. J., & Thorne, M. C. (1983). *Radionuclide distribution and transport in terrestrial and aquatic ecosystems. A critical review of data, Volume 5*. Rotterdam: A.A. Balkema.

ERICA. (2007). *D-ERICA: An INTEGRATED APPROACH to the assessment and management of environmental risks from ionising radiation*: Swedish Radiation Protection Authority.

FASSET. (2003a). *Dosimetric models and data for assessing radiation exposures to biota. Deliverable 3*. Stockholm: Norwegian Radiation Protection Authority.

FASSET. (2003b). *Handbook for Assessment of the Exposure of Biota to Ionising Radiation from Radionuclides in the Environment. Deliverable 5*. Stockholm: Swedish Radiation Protection Authority.

Larsson, C. M. (2004). The FASSET Framework for assessment of environmental impact of ionising radiation in European ecosystems - an overview. *Journal of Radiological Protection, 24*(4A), A1-A12.

Mendenhall, W., & Sincich, T. (2006). *Statistics for Engineering and the Sciences* (5th ed.). New Jersey: Prentice-Hall, Inc.

Smith, J. (2005). Effects of ionising radiation on biota: do we need more regulation? *Journal of Environmental Radioactivity, 82*(1), 105-122.

Smithson, M. (2000). *Statistics with Condidence*. London: SAGE Publications Ltd.

Ulanovsky, A., Pröhl, G., & Gómez-Ros, J. M. (2008). Methods for calculating dose conversion coefficients for terrestrial and aquatic biota. *Journal of Environmental Radioactivity, 99*(9), 1440-1448.

USDOE. (2004). *RESRAD-BIOTA: A Tool for Implementing a Graded Approach to Biota Dose Evaluation*. Washington D.C.

Vives i Batlle, J., Balonov, M., Beaugelin-Seiller, K., Beresford, N., Brown, J., Cheng, J. J., et al. (2007). Inter-comparison of absorbed dose rates for non-human biota. *Radiation and Environmental Biophysics, 46*(4), 349-373.

Yankovich, T. L., & et al. (2010). An international model validation exercise on radionuclide transfer and doses to freshwater biota. *Journal of Radiological Protection, 30*(2), 299.

Chapter 4

Model comparisons with environmental measurements

4.1 Introduction

In recent years, there have been a number of studies which have compared the models and approaches to estimate either the activity concentration or radiation doses in non-human biota. The FASSET and ERICA models have been used predict radionuclide transfer to a range of terrestrial animals within the Chernobyl exclusion zone (Beresford, Wright et al. 2005; Beresford, Wright et al. 2005; Beresford, Wright et al. 2005; Beresford, Gaschak et al. 2008). The ERICA model has also been used to predict the background exposure dose rates to terrestrial wildlife in England and Wales (Beresford, Barnett et al. 2008), and the radionuclide transfer at Sellafield coastal sand dunes (Wood, Marshall et al. 2008). The model-model comparison studies to estimate either radionuclide transfer and radiation doses to non-human biota (Vives i Batlle, Balonov et al. 2007; Beresford, Balonov et al. 2008; Beresford, Barnett et al. 2008) have already been discussed in Chapter 3. In addition to model-data comparisons, studies of the radiation exposure of terrestrial wildlife in the Chernobyl exclusion zone (Beresford and et al. 2010) and doses to freshwater biota in Perch Lake, Canada (Yankovich and et al. 2010) also provided model-model intercomparison.

In this chapter, a model-data comparison study to estimate radiation doses in aquatic organisms (pelagic fish, benthic fish and crustacean) is described. The 5 different models (FASSET, ERICA, R&D128, RESRAD and D-Max model) were used to calculate the internal and external radiation doses from Cs-137 and Sr-90 in aquatic biota in two lakes (Svyatoye and Perstok) in Belarus. The characteristics of these lakes have been described in Chapter 1 Section 1.5. The model predictions are compared with each other, and against field data from these lakes.

4.2 Method

This study used measurements of water, sediment and fish tissue activity concentrations obtained from a review of data on the two lakes held by the Institute of Geological Sciences of the National Academy of Sciences of Belarus. These data were primarily obtained during a European project INTAS-2001-0556 [Radio-Ecological Study of the Chernobyl Cooling POND and options for remediation (RESPOND). The details of these data will be described in the following.

Nine undrained lakes; Tyumenskoye (#1), Svyatoye (#3), Svyatoye (#5), Kolpino (#6), Svyatoye (#7), Stoyacheye (#8), Perstok (#15), Vigoda (#16) and Dvorishche (#17) in contaminated areas of Belarus were investigated during this study (Kudelsky, Pashkevich et al. 2005). The general characteristics of each lake, including morphometry, origin, hydrology, hydrochemistry, bottom sediments and state of lakes were described. Also, the fish, zooplankton, phytoplankton population and the level of Cs-137 and Sr-90 (for Perstok) concentration activity of water, bottom sediment and fish were provided in the report.

For chemical analysis of the water, the value of O_2, CO_2, NH_4^+, H_2S, pH and Eh were measured in the field. The bottom sediments for most lakes were collected by using a grab sampler, whilst more detailed bottom sediment samples from Svyatoye#3 lake were using Mackereth corer and Russian corer. The composition, content of organic matter, moisture content and Cs-137 activity concentration of sediment were determined. Fish samples were obtained by gill netting using nets of various sizes. The species identification, determination of age, size and sex was carried out before preparation of the fish sample for radioactivity analysis. Measurement of Cs-137 activity concentration of fish, bottom sediment and water were determined by using gamma spectrometry system (NaI detector) with standard error of measurements ±1.5-13.8% and using beta scintillation spectrometry for Sr-90 with standard error ±20-35%.

In this study we used measurements of fish tissue concentration and that of the surrounding medium (water, sediment) from Svyatoye#3 and Perstok lakes to predict the internal and external dose of biota. These two lakes had the highest Cs-137 deposition of all lakes in Belarus following the Chernobyl accident. Cs-137 concentration in the watershed was 1.3681×10^9 and 3.7×10^9 kBq km^{-2} respectively in 1997 (1.754×10^9 and 4.744×10^9 kBq km^{-2} respectively in 1986) (Kudelsky, Pashkevich

et al. 2005). At Svyatoe lake, there were only data of Cs-137 activity concentration in fish, sediments and water, whilst for Perstok, there were data of both Cs-137 and Sr-90 activity concentration There are no data of Sr-90 in Svyatoye lake because the distribution of Sr-90 significantly decreased with the distance from Chernobyl NPP (Mück, Pröhl et al. 2002): the distance of Svyatoye lake from ChNPP is 225 km, whilst the distance of Perstok lake from ChNPP is 13 km.

In addition to activity concentration measurements, the concentration of potassium and calcium was taken into account for the prediction of fish tissue activity concentration for D-MAX model. The D-MAX model can predict the Cs-137 activity concentration in fish from the potassium concentration in water (Smith, Kudelsky et al. 2000; Smith, Kudelsky et al. 2002) and the Sr-90 activity concentration in fish from the calcium concentration in water (Smith, Sasina et al. 2009).

4.2.1 The prediction of the internal dose to fish

Depending on the available measurement data, there are two methods to calculate the internal dose in fish. Firstly, the measured tissue activity concentration can be used or, secondly (if no tissue measurements are available) by using the water activity concentration. For the first approach, the internal dose rate is calculated by using tissue activity concentration and DCC_{int} as shown in equation 4.1 (FASSET 2003; ERICA 2007).

$$D_{int} = C_t \times DCC_{int} \quad (4.1)$$

where D_{int} is the internal dose in µGy hr^{-1},

C_t is the tissue activity concentration in fish in Bq kg^{-1} (wet weight) and

DCC_{int} is the Internal Dose Conversion Coefficient in µGy hr^{-1} per Bq kg^{-1}.

In cases in which tissue activity concentrations are not known, the models can determine the fish activity concentration by using water activity concentration and Concentration Ratio (CR) in l kg^{-1} as shown in Equation 4.2 (Smith, Kudelsky et al. 2000; Smith 2005; Smith, Voitsekhovitch et al. 2005; ERICA 2007; Beresford, Barnett et al. 2008).

$$CR = \frac{C_t}{C_w} \quad (4.2)$$

where C_w is the water activity concentration in Bq l^{-1}

The CR values depend on the organism type. In this case, the data available for Svyatoye and Perstok lakes show three types of aquatic biota; pelagic fish, benthic fish and crustaceans. The internal and external doses of pelagic fish are calculated from the water activity concentration, as it is assumed that they are shielded from external dose from the sediment. The benthic fish and crustaceans are assumed to live on or close to the sediment surface and so receive the majority of their external dose from the sediment. But the tissue concentration and hence internal dose of those organisms is calculated from water activity concentration using the concentration ratio. The comparison of the default CR value in each model is shown in **Table 4.1**.

Table 4.1 Comparison of CR values for the different models (Smith, Kudelsky et al. 2000; U.S.DOE 2002; Copplestone, Wood et al. 2003; FASSET 2003; Smith, Sasina et al. 2009).

Organism type	Radionuclide	Concentration Ratio (l kg^{-1})				
		FASSET	ERICA	RESRAD	R&D128	D-MAX
Pelagic	Cs-137	10200	7100	22000	11000	Svyatoye, Cs-137 1446(p), 708(np), Perstok, Cs-137 784(p), 160(np), Sr-90 151
	Sr-90	25	17	320	43	
Benthic	Cs-137	12200	6300	22000	11000	
	Sr-90	n/d	17	320	43	
Crustacean	Cs-137	n/d	10400	22000	$5200^{(10g)}$ $630^{(1kg)}$	
	Sr-90	n/d	200	320	270	

Note p is predatory fish, np is non-predatory fish

For D-MAX model, Concentration Factor (CR) in l kg^{-1} fresh weight can be calculated by using potassium concentration (mg l^{-1}) in the water. The CR is calculated by following equations (Smith, Kudelsky et al. 2000).

For predatory/omnivorous fish (perch and pike),

$$\mathrm{CR\ (predatory)} = \frac{4880}{[K^+]} \tag{4.3}$$

And non-predatory fish (Roach, Rudd, Verkhovka, Bitterling, Goldfish, Bream)

$$\mathrm{CR\ (non\text{-}predatory)} = \frac{2390}{[K^+]} \tag{4.4}$$

For the best estimation value, the uncertainty range is estimated to be 0.5-2 times (Smith, Kudelsky et al. 2000).

For the estimation of internal dose of Sr-90 in fish, CR can be predicted by using calcium concentration in water as in the following equation (Smith, Sasina et al. 2009).

$$\mathrm{CR\ (muscle)} = \frac{181}{[Ca]^{1.2}} \tag{4.5}$$

$$\mathrm{CR\ (bone)} = \frac{16317}{[Ca]^{1.2}} \tag{4.6}$$

Assuming wet weigh of bony parts of fish is 23% that gives a whole fish CR as the following equation (Smith, Sasina et al. 2009).

$$\mathrm{CF\ (whole\ fish)} = \frac{3850}{[Ca]^{1.2}} \tag{4.7}$$

The uncertainty range is estimated to be 0.33-3 times (Smith, Sasina et al. 2009) the best estimate value. From Equation 4.7, CR of whole fish can be calculated from calcium concentration which can be used to estimate the tissue concentration of fish and internal exposure of Sr-90 in fish.

The different methods for calculating the internal dose by using fish tissue activity concentration and water activity concentration are illustrated in **Figure 4.1**. The internal dose rates in fish for Cs-137 in Svyatoye lake and for Cs-137 and Sr-90 in Perstok lake are calculated for each of the models using both methods.

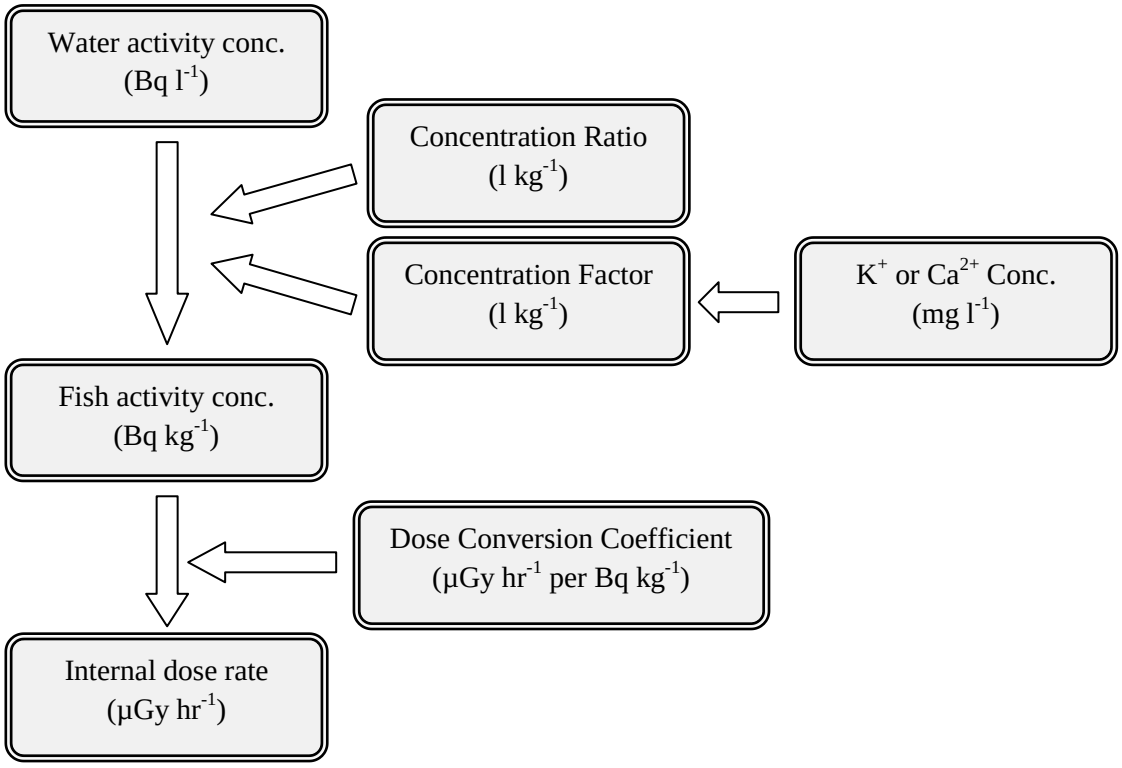

Figure 4.1 Illustrate the method for calculating the internal dose rate

4.2.2 The prediction of the external dose

The internal dose rate for pelagic fish was calculated by using water activity concentration and DCC_{ext} as shown in Equation 4.8 (FASSET 2003; ERICA 2007).

$$D_{ext} = C_w \times DCC_{ext} \quad (4.8)$$

For the benthic fish and crustaceans, the dose rate was calculated by using water activity concentration and sediment activity concentration because those organisms are exposed by both water and sediment. The equation for calculating the internal dose rate for benthic fish and crustacean is shown in Equation 4.9 (FASSET 2003).

$$D_{ext} = (0.5C_w + 0.5C_d) \times DCC_{ext} \quad (4.9)$$

where D_{ext} is the external dose rate in µGy hr^{-1},

C_d is sediment activity concentration in Bq kg^{-1} and

DCC_{ext} is the External Dose Conversion Coefficient in µGy hr^{-1} per Bq kg^{-1}.

As can be seen from Equation (4.9), it is assumed that the organism lives on the sediment-water interface, receiving half its dose from the sediment and half from the

water. Sediment and water are both assumed to be semi-infinite media of homogeneously distributed activity concentration.

4.2.3 The prediction of total (internal and external) dose

The total dose rate of aquatic organism was calculated directly by using the summation of the internal dose rate and the external dose rate as show in equation 4.10 (FASSET 2003).

$$D_{total} = D_{int} + D_{ext} \quad (4.10)$$

Where D_{total} is the total dose in μGy hr^{-1},
D_{int} is the internal dose in μGy hr^{-1} and
D_{ext} is the external dose rate in μGy hr^{-1}

4.2.4 Available data from the study lakes

Syatoye lake

Svyatoye lake is an undrained lake located 237 km in the northeast from ChNPP. The Cs-137 contamination was more than 1,368.1 kBq m^{-2} (Kudelsky, Pashkevich et al. 2005) at the time of the Chernobyl accident. A site description was given in Chapter 1, Section 1.5.1.

Sediment concentration

Five sediment cores were taken in the sites of the lake (**Figure 4.2**). There are two main texture types of the bottom sediments in Svyatoye lake: fine sand and silty loam (**Table 4.2**). The distribution of Cs-137 with depth in the sediment profile is shown in Tables 4.3 and 4.4. The highest activity concentration of Cs-137 in the solid phase of fine sand is 80250 Bq kg^{-1} at 2-4 cm layer (**Table 4.3**) whilst the highest concentration level of Cs in solid phase of slit loam is 107200 Bq kg^{-1} in the surface 0-2 cm layer (**Table 4.4**). For the model predictions, we assumed a worst case scenario for calculating radiation doses to biota. So, this study used the maximum observed value of 107200 Bq kg^{-1} for the silt loam sediment concentration for Cs-137. Also, more aquatic biota lives in the silt loam than the sand because the slit loam has more vegetation than the sand. No such sediment concentration for Sr-90 has shown in the report: as discussed previously, this is likely due to the low deposition of Sr-90 at this site.

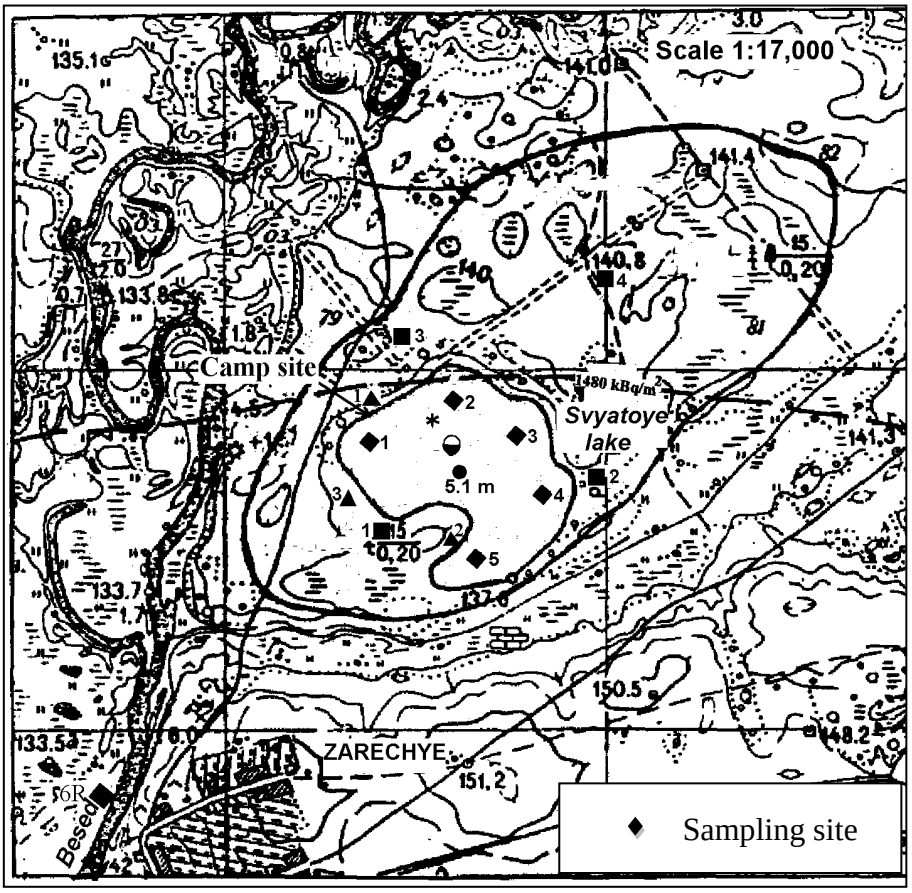

Figure 4.2 Illustration of the sketch map showing the sampling sites of the Svyatoye No.3 lake (Kudelsky, Pashkevich et al. 2005).

Table 4.2 Content of different granulometric fractions in the bottom sediments (Kudelsky, Pashkevich et al. 2005).

Sample	Layer cm	Rock and mineral fragments > 2 mm	Very coarse sand 2-1 mm	Coarse sand 1-0.5 mm	Medium sand0.5-0.25 mm	Fine sand 0.25-0.1 mm	Very fine sand 0.1-0.05 mm	Coarse silt, 0.05-0.01 mm	Fine silt and clay <0.01 mm	Textural class
1	0-12	0.07	0.25	2.32	4.30	6.51	3.44	1.23	79.24	Fine sand
4	0-12	0.02	0.69	8.95	24.02	50.05	6.27	2.97	7.03	Silt loam

Sample 1: 56.32 % of fine and very fine sand (>50 %); 9.64 % of coarse and very coarse sand (< 25 %); Sample 4: 80.47 % of silt, 16.82 % of sand.

Table 4.3 Concentrations of Cs in the solid phase ($ACs_{s.ph.}$) and pore water ($ACs_{p.w.}$) of fine sand and the distribution coefficients (K_d). Point 1. 16.02.2000 (Kudelsky, Pashkevich et al. 2005).

Layer, cm	Sample	$ACs_{s.ph.}$, Bq kg^{-1}	$ACs_{p.w.}$, Bq l^{-1}	Kd, l kg^{-1}
0-2	Blue-green algae with	60810±3650	135±11	450±64
2-4	admixture of organic silt	80250±500	267±18	300±37
4-6	Fine-grained sand	46530±2750	430±28	108±13
6-8	(top layers with	32600±1920	322±22	101±13
8-10	admixture of algae)	33380±1940	287±20	116±15
10-12		29220±1690	196±14	149±19
12-14		14360±850	82.7±7.0	174±25
14-16	Fine-grained sand	3880±230	39.8±4.1	97±16
16-18		1870±110	9.3±0.9	200±30
18-20	Fine-grained sand with	1230±70	4.4±0.6	280±60
20-22	admixture of organic silt	793±48	3.4±0.4	235±45
22-24		571±34	6.0±0.7	95±17
24-26		392±28	4.0±0.7	98±24
26-28		336±27	3.6±0.6	94±23

Water concentration

Svyatoye lake had previously (in 1998) been chosen for an experiment to reduce the bioaccumulation of radiocaesium (Cs-137) in fish which was contaminated by Chernobyl accident (Smith, Kudelsky et al. 2003). The concentration of Cs-137 in the water was changed by the experiment. The concentration of Cs-137 in the water depends on the concentration of the potassium chloride salt. During 1996-1997, the content of potassium was in the range 0.95 to 1 mg l^{-1} and the Cs-137 concentration was in the range 3.8 to 4.9 Bq l^{-1}. In 1998, KCl was added to the water in an experiment to reduce the uptake of Cs-137 in fish. The concentration of potassium was increased to 10 mg l^{-1} and the concentration of Cs-137 increased up to 10.6-12.36 Bq l^{-1} (Kudelsky, Pashkevich et al. 2005). The concentration of Cs-137 in the water increased as a result of remobilisation of activity from bed sediments by ion-exchange with the

increased potassium (Smith, Kudelsky et al. 2003). The subsequent studies in 2001-2004 have shown that the concentration of potassium and Cs-137 varied, with a tendency to slightly decrease (**Table 4.5**).

Table 4.4 Activity concentration of ^{137}Cs in the solid phase ($ACs_{s.ph.}$) and pore water ($ACs_{p.w.}$) of silt loam* and the coefficient K_d. Point 2. 25.02.1999 (Kudelsky, Pashkevich et al. 2005).

Layer, cm	$ACs_{s.ph.}$, Bq kg^{-1}	$ACs_{p.w.}$, Bq l^{-1}	Kd, l kg^{-1}
0-2	107200±7980	58.6±6.1	1830±330
2-4	60410±4590	45.7±4.8	1320±240
4-6	34860±2680	40.1±4.0	870±160
6-8	29510±2270	40.2±4.2	730±130
8-10	23050±1750	39.7±4.1	580±100
10-12	20730±1600	38.7±4.1	540±100
12-14	11640±870	31.6±3.6	370±70
14-16	9530±730	33.2±4.0	290±60
16-18	6890±460	28.5±3.7	240±50
18-20	5000±445	17.5±3.2	290±80
20-24	3860±260	10.7±1.8	360±90
24-28	1840±170	6.7±1.5	280±90
28-32	2090±100	4.8±1.7	230±100
32-36	930±93	3.6±1.5	260±130

* OM content— 47 – 48 %; water capacity (quantity of water retained by 100 g of solid phase) of the samples is 1000 – 1690.

In the present study we used measurements of Cs-137 and fish from the year 2003 to test the different dose models, as shown in **Table 4.6**. The measurements from 2003 were used because there were more available fish tissue concentration measurements for 2003 than the other years, allowing improved statistical analysis.

Table 4.5 Concentration of potassium and Cs-137 in water from 1996 – 1998 and 2001 – 2004 (Kudelsky, Pashkevich et al. 2005).

Year	K^+ concentration (mg l^{-1})	Cs-137 concentration (Bq l^{-1})
1996 – 1997	0.95 – 1	3.8 – 4.9
1998	10	10.6 – 12.36
2001	7 – 8.5	5.2 – 14.47
2002	6.75 – 8.7	5.11 – 17.58
2003	4.98 – 10.0	4.96 – 17.54
2004	4.98 – 5.36	9.60 – 14.24

Table 4.6 Concentration of Cs-137 and Potassium in water (2003) (Kudelsky, Pashkevich et al. 2005)

Year	K^+ concentration (mg l^{-1})	Cs-137 concentration (Bq l^{-1})
2003	6.75	9.94

Fish tissue concentration

In 2003, three types of aquatic biota were caught in Svyatoye lake: Pelagic fish, Benthic fish and crustaceans. There were nine species of pelagic fish: Pike (Esox lucius L.), Roach (Rutilus rutilus L.), Rudd (Scardinius erythrophthalmus L.), Verkhovka (Leucaspius delineates Heck.), Bitterling (Rhodeus sericeus amarus Bloch.), Gold fish (Carassius auratus gibelio Bloch.), Bream (Abramis brama L.), Perch (Perca fluviatilus L.) and Ruffe (Gymnocephalus cernuss L.) whilst two species of benthic fishes were caught: Tench (Tinca tinca L.) and Gudgeon (Gobio gobio L.) and only one species of crustacean: Crayfish (Decapoda L.). The data of the activity of Cs-137 in all fishes was from the whole body (muscular and bone tissue). The Cs-137 activity concentrations of whole fish that were used for calculating internal doses are shown in **Table 4.7**.

Table 4.7 Cs-137 activity of fish in Svyatoye lake 2003 (Kudelsky, Pashkevich et al. 2005).

Fish	Age (year)	Weight (g)	Cs-137 in fish (Bq kg^{-1}) w.w.
Pelagic fish			
Pike	9	956	9653.6
	7	543.3	4980.9
Roach	4	46.2	6676.1
	3	12.6	6327.1
Rudd	5	36.8	4668.9
	4	13.6	4406.4
Verkhovka	3	3	3070.9
	1	3.1	5149.0
Bitterling	2	1.75	5315.2
Gold fish	9	781	5302.5
Bream	1	2.6	7644.2
Perch	6	455.7	20744.1
	5	275.75	17409.7
	4	82.9	12658.2
	3	35.9	8597.0
Rudd	3	9.6	1535.6
	2	3.6	4602.0
Benthic fish			
Tench	6	130.1	3372.1
	1	8.7	6131.6
Gudgeon	4	12.2	5461.8
	2	2.8	5763.5
Crustacean			
Crayfish		19.4	4246.3

Perstok lake

Perstok lake is an undrained flood plain lake (periodically flooded during spring with approximate frequency once every five years). The lake is located 13 km to the northwest of the ChNPP. The Cs-137 and Sr-90 contamination was more than 3,700 kBq m^{-2} and 110 kBq m^{-2} respectively (Kudelsky, Pashkevich et al. 2005). Further details of the lake were presented in Chapter 1 Section 1.5.2.

Sediment concentration

A sediment sample was taken at a depth of 2 m in the sites of the lake (**Figure 4.2**) by using the bottom sediment sampler (the sample column 12 cm and the area of sampling 256 cm^2) (Kudelsky, Pashkevich et al. 2005). The bottom sediment of Perstok lake is high content of organic matter slit. The sediment activity of Cs-137 and Sr-90 were 55,066 and 92,200 Bq kg^{-1} dry weight respectively in 2002 (**Table 4.8**) (Kudelsky, Pashkevich et al. 2005).

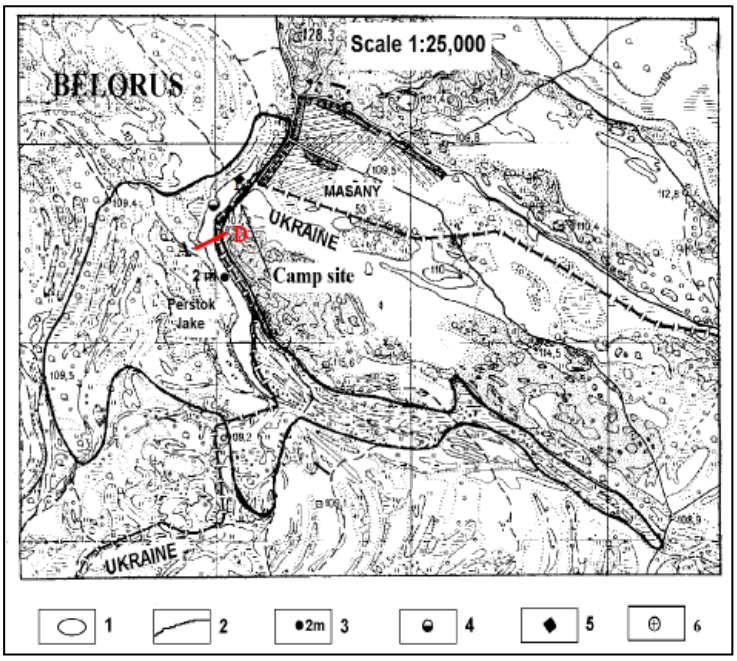

General description of the territory: 1-lake; 2-catchment boundaries; 3-lake depth,m

Sites of sample collection: 4- water sampling; 5-bottom sediment

Figure 4.3 Illustration of the sketch map showing the sampling sites of Perstok lake (Kudelsky, Pashkevich et al. 2005).

Table 4.8 The sediment activity of Cs-137 and Sr-90 (Kudelsky, Pashkevich et al. 2005).

Bottom sediment (Bq kg^{-1} d.w.)	Cs-137	Sr-90
High organic slit From 0 – 0.2 m layer	55,066	92,200

Water concentration

Water sampling had been carried out in the sites of the lake shown in **Figure 4.2**. The water activity concentration of Cs-137 in Perstok lake had been studied from 2002-2004 whilst, the only data available for Sr-90 was from 2002. The water activity concentration of Cs-137 was 14.1, 19.23 and 21.9 Bq l^{-1} in 2002, 2003 and 2004 respectively (Kudelsky et al., 2005). The activity concentration of Sr-90 in water was 22 Bq l^{-1} in 2002 (Kudelsky et al., 2005). The potassium concentration in the water was 6.1, 7.45 and 5.00 mg l^{-1} in 2002, 2003 and 2004 respectively whilst; there was only a data for the calcium concentration (which was 26.45 mg l^{-1}) in 2002. The data of Cs-137, Sr-90, K^+ and Ca^{2+} concentration in water are summarised in **Table 4.9**.

Table 4.9 Measurements of Cs-137, Sr-90, K^+ and Ca^{2+} concentration in water (Kudelsky, Pashkevich et al. 2005). There are not enough data to estimate standard deviations of measured values, or standard errors of mean values, but the data give an indication of the range in values for Cs-137, K^+ and Ca^{2+} concentrations in water.

Year	Cs-137 (Bq l^{-1})	Sr-90 (Bq l^{-1})	K^+ (mg l^{-1})	Ca^{2+} (mg l^{-1})
2002	14.1	22	6.1	26.45
2003	19.23	n/d	7.45	n/d
2004	21.9	n/d	5.00	n/d

Tissue concentration

Five species of pelagic fish were caught in Perstok lake in 2002: Roach, Rudd, Verkhovka, Bream and Perch. The activity of Cs-137 in fish tissue varied from 4977.96

to 9537.5 Bq kg^{-1} (**Table 4.10**). The activity of Sr-90 in fish tissue varied from 2400 to 10806 Bq kg^{-1}. The data of the activity of Sr-90 in Bream was from the muscular tissue whilst measurements for other species were whole body (muscular and bone tissue).

Table 4.10 The activity of Cs-137 and Sr-90 concentration in fish tissue (Kudelsky, Pashkevich et al. 2005).

Fish	Age (year)	Weight (g)	Cs-137 in fish (Bq kg^{-1}) w.w.	Sr-90 in fish (Bq kg^{-1}) w.w.
Pelagic fish				
Roach	3	11.2	7010.8	9094
Rudd	3	12.2	4977.96	10806
Verkhovka	2	3.5	6170.6	2400
Bream	5	204.5	6303.2	257*
Perch	3	9.1	9537.5	5848
	2	3	7938.9	4646

*****muscular tissue (in the other case, muscular and osseous tissue)

4.2.5 Statistical analysis

The "Z-score" was recommended by the 1993 Harmonized Protocol for the conversion of participant's results and is widely used in various applications for model proficiency testing (Michael, Stephen et al. 2006). Z-score was used to analyse estimated dose rates in the international comparison exercise (Vives i Batlle, Balonov et al. 2007; Beresford and et al. 2010; Yankovich and et al. 2010). In this case, Z-score is used to compare model predictions for individual organisms. Z-score measures how many standard deviation units away from the mean a particular data values lies as given in the following equation (Smithson 2000; Mendenhall and Sincich 2006):

$$Z = \frac{\text{predicted dose rate} - \text{mean dose rate}}{\text{Standard Deviation}} \qquad (4.11)$$

Z-values between 0 and 2 in absolute value are considered satisfactory, the results are more biased when Z-values is between 2 and 3 in absolute value and the results are highly biased when Z-value ≥ 3 in absolute value (Vives i Batlle, Balonov et al. 2007; Beresford and et al. 2010; Yankovich and et al. 2010). Note that Z-score is not used to

judge any prediction or to identify any outliers that right or wrong (Vives i Batlle, Balonov et al. 2007; Beresford and et al. 2010; Yankovich and et al. 2010). The D-MAX model were not included in the statistical evaluation for the external dose rate comparison because D-MAX model is used to predict the maximum total and internal dose rate so it is not appropriate to apply a Z factor.

Z-values may not always be useful for model comparisons. They assume that data are normally distributed, but there are not always sufficient data points to know the statistical distribution of measurements. Also, for assessments of radiation dose to biota, it is usually necessary to give a conservative estimate so that doses and effects are not under-estimated.

4.3 Results

The results in this study will be divided into three sections; the prediction of the internal dose rate, the prediction of the external dose rate and the total (internal plus external) dose rate.

4.3.1 The prediction of the internal dose rate

As described in the Methods section, there are two ways to calculate the internal dose rate: firstly by using actual fish tissue activity concentration and secondly (where direct measurements of radionuclides in fish are not available) on the basis of the water activity concentration.

Svyatoye lake

Lake Svyatoye, the comparisons of the fish tissue concentration between the actual values and the model predictions of the models are shown in **Table 4.11**. The Z-scores for the tissue concentration from the model prediction in Svyatoye Lake are shown in **Table 4.12**. The prediction of the tissue concentration between the models in pelagic fish, benthic fish and crustaceans did not show bias ($Z \leq 2$). The RESRAD model was the furthest away from measured values ($Z=1.7017$ in pelagic fish, $Z=1.4653$ in benthic fish and $Z=1.3532$ in crustaceans) of the prediction of the tissue concentration between the models. From the measured and estimated fish tissue concentrations presented in **Table 4.11**, the internal dose rate can be estimated using the DCC. The internal dose rates estimated by the two different methods for each model are shown in **Table 4.13**, and **Figures 4.4, 4.5** and **4.6**. The Z-score for the internal dose rates predicted from water

concentration in each model are shown in **Table 4.14**. The prediction of the internal dose rates between the models in pelagic fish, benthic fish and crustacean did not show bias ($Z \leq 2$). The RESRAD model was the furthest away from the average of all the models (Z=1.6750 in pelagic fish, Z=1.8234 in benthic fish and Z=1.4073 in crustacean) of the prediction of the internal dose rate between the models.

Table 4.11 The comparison of the tissue concentration between the actual and the prediction of the models.

Fish	Age (year)	Weight (g)	Actual tissue conc. (Bq kg^{-1})	Tissue conc. From the model prediction (Bq kg^{-1})				
				FASSET	ERICA	RESRAD	R&D128	D-MAX
Pelagic fish								
Pike	9	956	9653.6	101388	70574	218680	109340	14372.5
	7	543.3	4980.9	101388	70574	218680	109340	14372.5
Roach	4	46.2	6676.1	101388	70574	218680	109340	7038.99
	3	12.6	6327.1	101388	70574	218680	109340	7038.99
Rudd	5	36.8	4668.9	101388	70574	218680	109340	7038.99
	4	13.6	4406.4	101388	70574	218680	109340	7038.99
Verkhovka	3	3	3070.9	101388	70574	218680	109340	7038.99
	1	3.1	5149.0	101388	70574	218680	109340	7038.99
Bitterling	2	1.75	5315.2	101388	70574	218680	109340	7038.99
Goldfish	9	781	5302.5	101388	70574	218680	109340	7038.99
Bream	1	2.6	7644.2	101388	70574	218680	109340	7038.99
Perch	6	455.7	20744.1	101388	70574	218680	109340	14372.5
	5	275.75	17409.7	101388	70574	218680	109340	14372.5
	4	82.9	12658.2	101388	70574	218680	109340	14372.5
	3	35.9	8597.0	101388	70574	218680	109340	14372.5
Ruffe	3	9.6	1535.6	101388	70574	218680	109340	7038.99
	2	3.6	4602.0	101388	70574	218680	109340	7038.99
Benthic fish								
Tench	6	130.1	3372.1	121268	62622	218680	109340	7038.99
	1	8.7	6131.6	121268	62622	218680	109340	7038.99
Gudgeon	4	12.2	5461.8	121268	62622	218680	109340	7038.99
	2	2.8	5763.5	121268	62622	218680	109340	7038.99
Crustacean								
Crayfish		19.4	4246.3	n/d	103376	218680	51688	n/d

Table 4.12 The Z-score for the tissue concentration from the model prediction in Svyatoye Lake.

organism	Z-score					
	FASSET	ERICA	R&D128	RESRAD	D-MAX (predatory)	D-MAX (non-predatory)
Pelagic fish	0.1871	0.2108	0.2898	1.7017	0.9366	1.0313
Benthic fish	0.2229	0.5250	0.0708	1.4653	n/d	1.2339
Crustacean	n/d	0.0896	0.4768	1.3532	n/d	n/d

Table 4.13 The comparison of the internal dose rate in μGy hr^{-1} between the prediction from the tissue concentration and the prediction from the water concentration for each model.

Fish	FASSET		ERICA		RESRAD		R&D128		D-MAX	
	Tissue conc.	Water Conc.	Tissue conc.	Water Conc.	Tissue conc.	Water Conc.	Tissue conc.	Water Conc.	Tissue conc.	Water Conc.
Pelagic fish										
Pike	1.54	16.22	1.74	14.30	1.69	42.92	1.70	21.00	4.51	6.71
	0.80	16.22	0.90	14.30	0.87	42.92	0.87	21.00	2.32	6.71
Roach	1.07	16.22	1.20	14.30	1.17	36.38	1.20	21.00	3.12	3.28
	1.01	16.22	1.14	14.30	1.11	36.38	1.10	21.00	2.95	3.28
Rudd	0.75	16.22	0.84	14.30	0.82	36.38	0.82	21.00	2.18	3.28
	0.71	16.22	0.79	14.30	0.77	36.38	0.77	21.00	2.06	3.28
Verkhovka	0.49	16.22	0.55	14.30	0.54	36.38	0.54	21.00	1.43	3.28
	0.82	16.22	0.93	14.30	0.90	36.38	0.90	21.00	2.40	3.28
Bitterling	0.85	16.22	0.96	14.30	0.93	36.38	0.93	21.00	2.48	3.28
Goldfish	0.85	16.22	0.95	14.30	0.93	42.92	0.93	21.00	2.47	3.28
Bream	1.22	16.22	1.38	14.30	1.34	36.38	1.30	21.00	3.57	3.28
Perch	3.32	16.22	3.73	14.30	3.63	42.92	3.60	21.00	9.68	6.71
	2.79	16.22	3.13	14.30	3.05	42.92	3.00	21.00	8.12	6.71
	2.03	16.22	2.28	14.30	2.22	36.38	2.20	21.00	5.91	6.71
	1.38	16.22	1.55	14.30	1.50	36.38	1.50	21.00	4.01	6.71
Ruffe	0.25	16.22	0.28	14.30	0.27	36.38	0.27	21.00	0.72	3.28
	0.74	16.22	0.83	14.30	0.80	36.38	0.80	21.00	2.15	3.28
Benthic fish										
Tench	0.61	21.83	0.61	11.90	0.59	49.58	0.59	19.00	1.57	3.28
	1.10	21.83	1.10	11.90	1.08	49.58	1.10	19.00	2.86	3.28
Gudgeon	0.98	21.83	1.08	11.90	0.95	49.58	0.95	19.00	2.55	3.28
	1.04	21.83	1.10	11.90	1.01	49.58	1.00	19.00	2.69	3.28
Crustacean										
Crayfish	0.38	n/d	0.41	9.92	0.74	49.58	0.42	5.10	1.98	n/d

Table 4.14 The Z-score for the internal dose rates predicted from water concentration in each model in Svyatoye Lake.

	Z-score						
organism	FASSET	ERICA	R&D128	RESRAD (10g)	RESRAD (1kg)	D-MAX (predatory)	D-MAX (non-predatory)
Pelagic fish	0.2861	0.4272	0.0650	1.1946	1.6750	0.9847	1.2366
Benthic fish	0.0456	0.5906	0.1357	1.8234	n/d	n/d	1.1428
Crustacean	n/d	0.5827	0.8246	1.4073	n/d	n/d	n/d

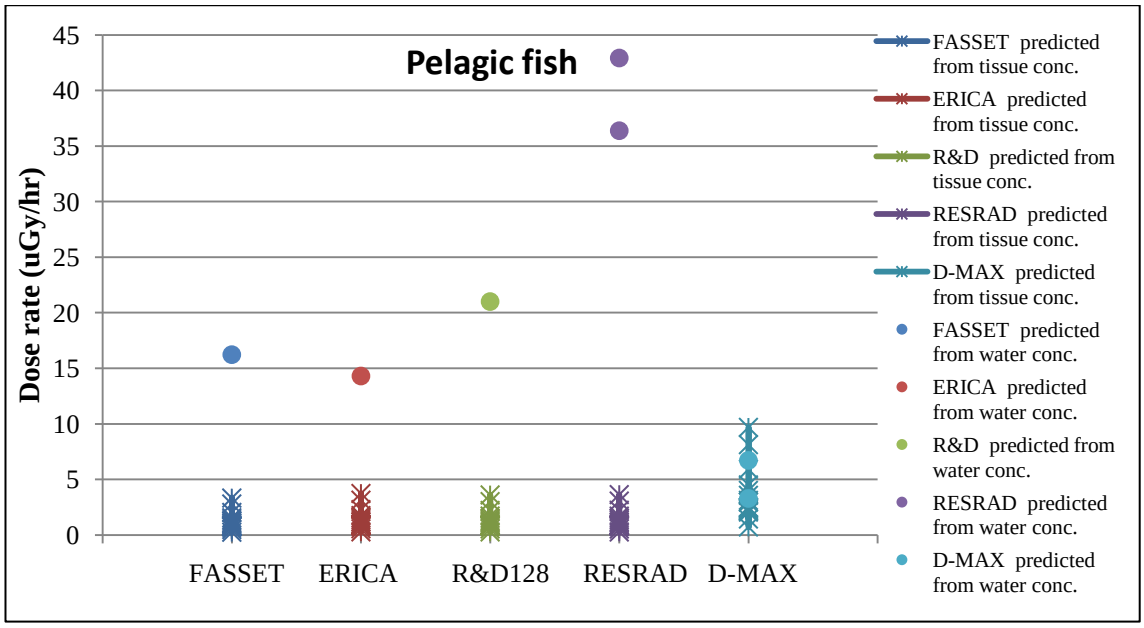

Figure 4.4 The internal dose rate of pelagic fish from Cs-137 in Svyatoe Lake: comparison between the prediction from tissue concentration and the prediction from the water concentration.

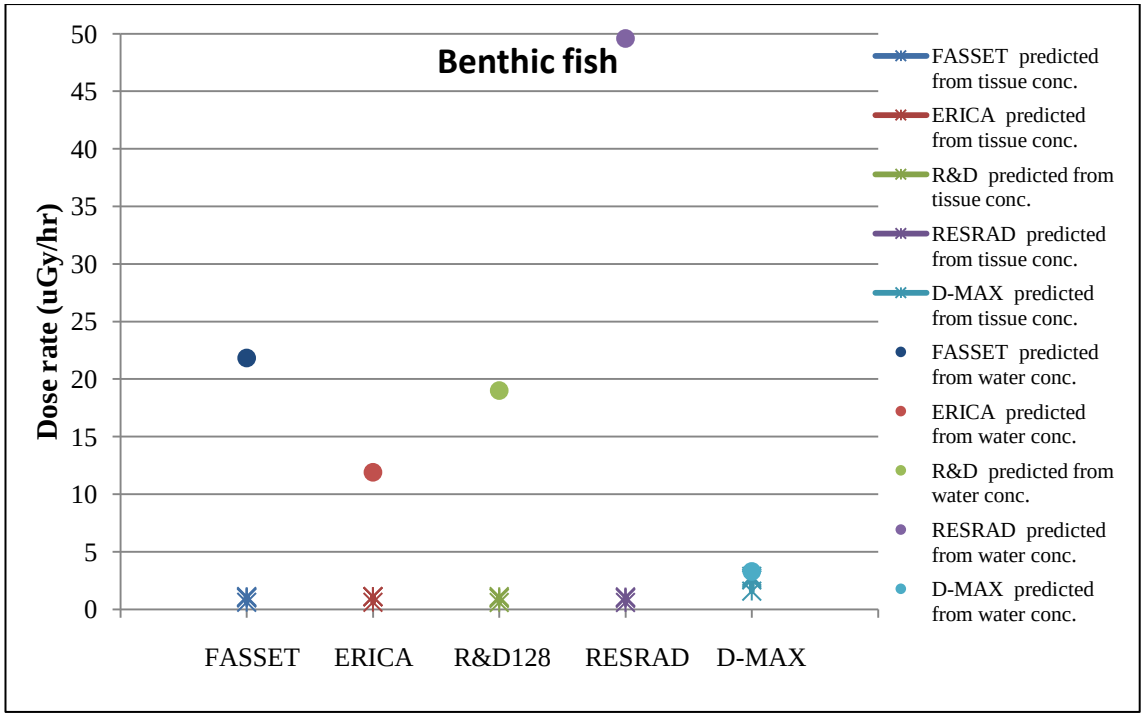

Figure 4.5 The internal dose rate of benthic fish from Cs-137 in Svyatoe Lake: comparison between the prediction from tissue concentration and the prediction from the water concentration.

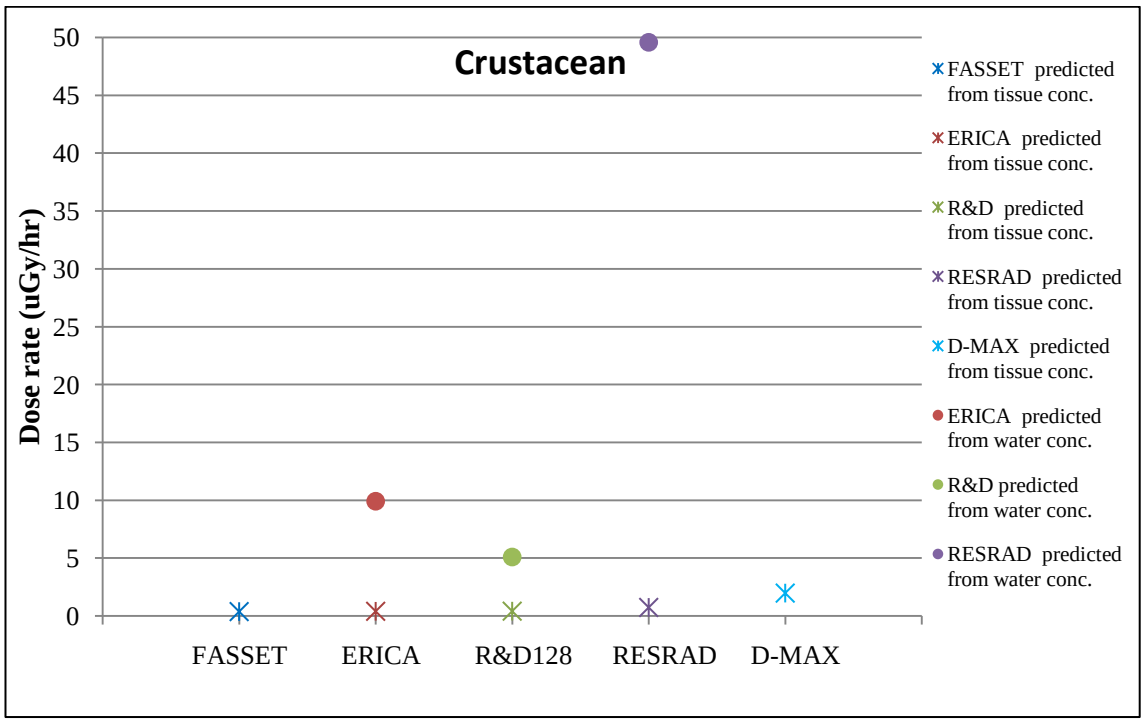

Figure 4.6 The internal dose rate of crustaceans from Cs-137 in Svyatoe Lake: comparison between the prediction from tissue concentration and the prediction from the water concentration.

Perstok lake

The comparison of the fish tissue concentration between the actual values and the prediction of the models in Perstok Lake is shown in **Table 4.15**. The Z-score for the tissue concentration from the model predictions for aquatic organisms in Perstok Lake are shown in **Table 4.16**. The prediction of the tissue concentration for Cs-137 and Sr-90 between the models did not show bias ($Z \leq 2$). The RESRAD model was the furthest away from the average of all the models (Z=1.7066 for Cs-137 and Z=1.6233 for Sr-90) of the prediction of the tissue concentration between the models. From the fish tissue concentration in **Table 4.15**, the internal dose rate can also be determined by using the DCC. The comparison of the internal dose rate determined between the prediction from the tissue concentration and the prediction from the water concentration in each model in Perstok lake is shown in **Table 4.17**, **Figures 4.7** and **4.8**. The Z-score for the internal dose rates predicted from water concentration in each model are shown in **Table 4.18**. The prediction of the internal dose rates for Cs-137 and Sr-90 between the models did not show bias ($Z \leq 2$). The RESRAD model was the furthest away from the mean prediction of other models (Z=1.6626 for Cs-137 and Z=1.4065 for Sr-90) of the prediction of the internal dose rate between the models.

Table 4.15 The comparison of the tissue concentration between the actual and the prediction of the models in Perstok Lake.

Fish	Age (year)	Weight (g)	Actual tissue conc. (Bq kg^{-1})	Tissue conc. From the prediction of the model (Bq kg^{-1})				
				FASSET	ERICA	RESRAD	R&D128	D-MAX
Cs-137								
Roach	3	11.2	7010.8	143820	100110	310200	155100	11048.9
Rudd	3	12.2	4977.96	143820	100110	310200	155100	11048.9
Verkhovka	2	3.5	6170.6	143820	100110	310200	155100	11048.9
Bream	5	204.5	6303.2	143820	100110	310200	155100	11048.9
Perch	3	9.1	9537.5	143820	100110	310200	155100	22560
	2	3	7938.9	143820	100110	310200	155100	22560
Sr-90								
Roach	3	11.2	9094	550	374	7040	946	3326.62
Rudd	3	12.2	10806	550	374	7040	946	3326.62
Verkhovka	2	3.5	2400	550	374	7040	946	3326.62
Bream	5	204.5	257	550	374	7040	946	156.394
Perch	3	9.1	5848	550	374	7040	946	3326.62
	2	3	4646	550	374	7040	946	3326.62

Table 4.16 The Z-score for the tissue concentration from the model prediction in Perstok Lake.

radionuclide	Z-score					
	FASSET	ERICA	R&D128	RESRAD	D-MAX (predatory)	D-MAX (non-predatory)
Cs-137	0.1832	0.2170	0.2865	1.7066	0.9270	1.0324
Sr-90	0.6706	0.7328	0.5307	1.6233	n/d	0.3108

Table 4.17 The comparison of the internal dose rate between in μGy hr^{-1} the prediction from the tissue concentration and the prediction from the water concentration in each model.

Fish	FASSET		ERICA		RESRAD		R&D128		D-MAX	
	Tissue conc.	Water Conc.	Tissue conc.	Water Conc.	Tissue conc.	Water Conc.	Tissue conc.	Water Conc.	Tissue conc.	Water Conc.
Cs-137										
Roach	1.12	23.01	1.26	16.80	1.23	42.92	1.20	27.00	3.27	5.16
Rudd	0.80	23.01	0.90	16.80	0.87	42.92	0.87	27.00	2.32	5.16
Verkhovka	0.99	23.01	1.11	16.80	1.08	42.92	1.10	27.00	2.88	5.16
Bream	1.01	23.01	1.13	16.80	1.10	50.83	1.10	27.00	2.94	5.16
Perch	1.53	23.01	1.72	16.80	1.67	42.92	1.70	27.00	4.45	10.53
	1.27	23.01	1.43	16.80	1.39	42.92	1.40	27.00	3.70	10.53
Sr-90										
Roach	5.55	0.34	5.73	0.24	5.71	4.10	5.70	0.58	5.91	2.16
Rudd	6.59	0.34	6.81	0.24	6.79	4.10	6.70	0.58	7.02	2.16
Verkhovka	1.46	0.34	1.51	0.24	1.50	4.10	1.50	0.58	1.56	2.16
Bream	0.16	0.34	0.16	0.24	0.16	4.42	0.16	0.58	0.17	0.10
Perch	3.57	0.34	3.68	0.24	3.67	4.10	3.60	0.58	3.80	2.16
	2.83	0.34	2.93	0.24	2.92	4.10	2.90	0.58	3.02	2.16

Table 4.18 The Z-score for the internal dose rates predicted from water concentration in each model in Perstok Lake.

organism	Z-score						
	FASSET	ERICA	R&D128	RESRAD (10g)	RESRAD (1kg)	D-MAX (predatory)	D-MAX (non-predatory)
Cs-137	0.1406	0.5431	0.1181	1.1499	1.6626	0.9494	1.2975
Sr-90	0.9389	0.9964	0.8010	1.2225	1.4065	n/d	0.1073

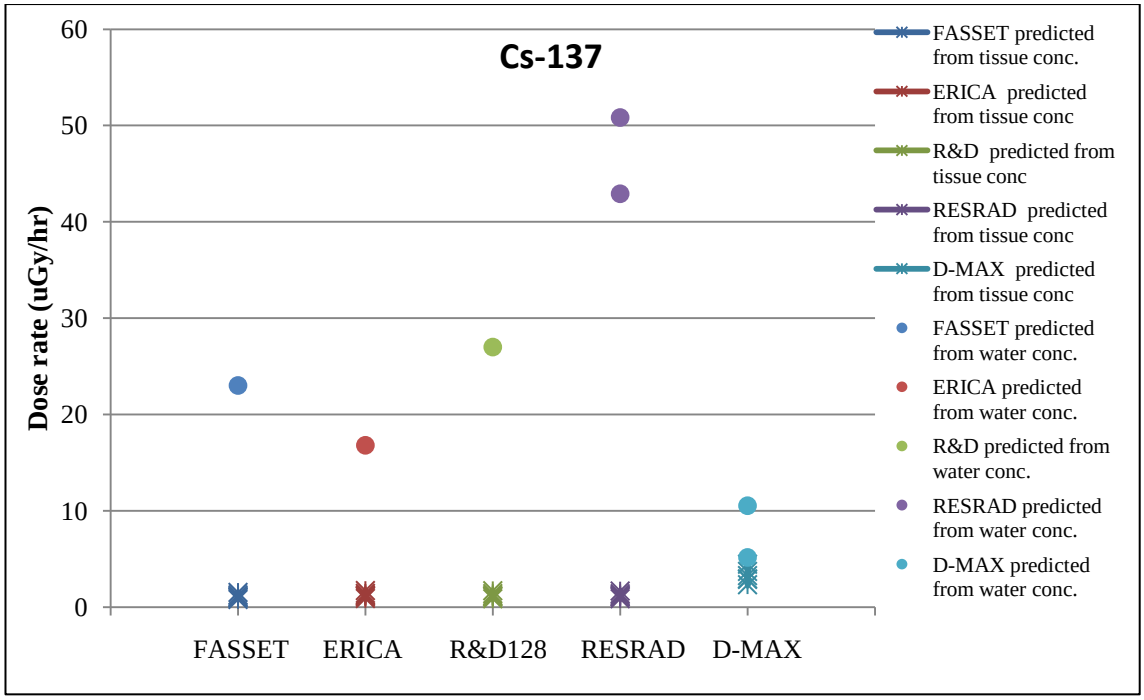

Figure 4.7 Cs-137 internal dose rate of pelagic fish in Perstok Lake: comparison between the prediction from tissue concentration and the prediction from the water concentration.

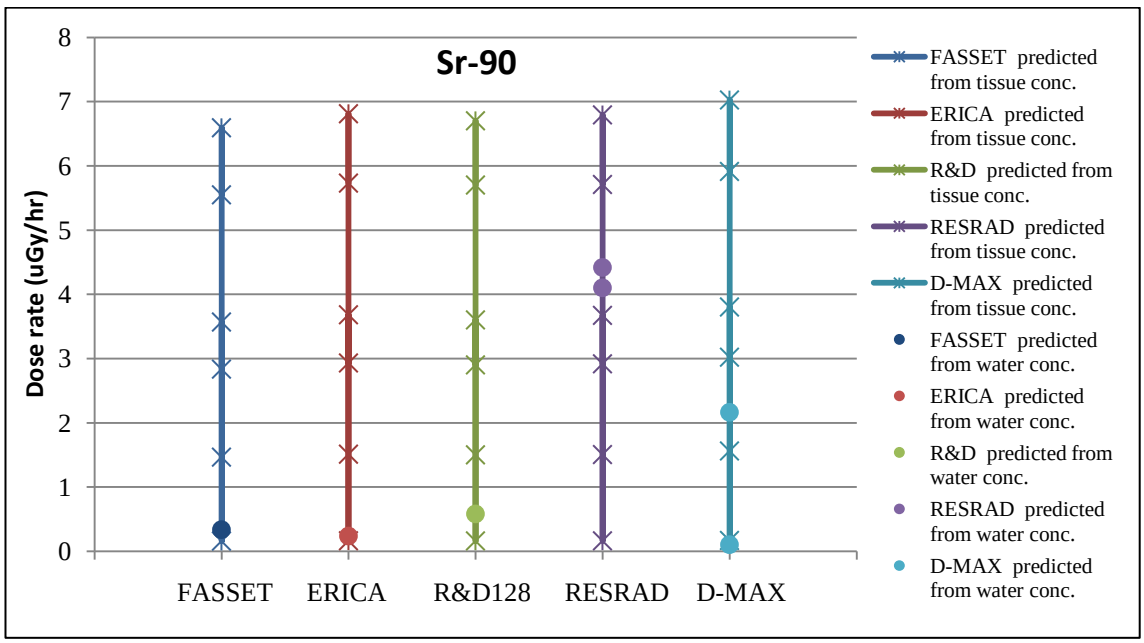

Figure 4.8 The internal dose rate of pelagic fish from Sr-90 in Perstok Lake: comparison between the prediction from tissue concentration and the prediction from the water concentration.

4.3.2 The prediction of external dose rate

As described in the method section, the calculation of the external dose rate of pelagic fish can be determined by using water activity concentration and DCC_{ext} whilst, benthic fish and crustacean can be determined by using the combination of water activity concentration, sediment activity concentration and DCC_{ext}. The predictions of the external dose rate were given for two lakes; Svayatoye and Perstok. As for the internal dose predictions, for Svyatoye lake, measurements were available to test predictions of three organism types: (pelagic fish, benthic fish and crustaceans) whilst, for Perstok measurements were available only for pelagic fish. As discussed previously, for Lake Perstok, both Cs-137 and Sr-90 were measured whilst only measurements of Cs-137 were available for Svyatoye.

Svatoye lake

The model comparisons of the external dose rate for pelagic fish, benthic fish and crustaceans for Svyatoye lake are shown in **Table 4.19**. For pelagic fish, each model can calculate the external dose rate by using the water activity concentration (9.94 Bq l^{-1}) and DCC_{ext}. The RESRAD model is able to calculate the external dose rate for a range of biota sizes. The model separates the organism size into 8 geometries; (1) 0.00001 kg, (2) 0.001 kg, (3) 0.01 kg, (4) 1 kg, (5) 10 kg, (6) 100 kg, (7) 500 kg, (8) 1000 kg. In this case, the measurements show that the size of fish caught from Svyatoye Lake varied between 1.75 to 956 g. It should be noted that the size of the fish that caught from the lake is not fully representative of the fish size in an actual fish population because the small fish size cannot be caught by the net. The fish were therefore put into two representative size categories of the RESRAD model, 10g and 1 kg. The size of the benthic fish varied between 2.8 g to 130.1 g whilst there was only one sample for crustaceans of weight 19.4 g. The predictions of the benthic fish and crustaceans for the RESRAD model were calculated by using a reference weight of 0.01 kg. Only the RESRAD model can choose the fish size for the assessment, whilst the other models use the default size (shown in Chapter 2 Section 2.4). From the data in **Table 4.19**, the comparison of the external dose rate between the models in Svyatoye lake is illustrated in **Figure 4.9**. The Z-score for the external dose rates predicted between the models in pelagic fish, benthic fish and crustacean as shown in **Table 4.20** did not show bias ($Z \leq 2$). The worst agreement of the prediction of the external dose rate

between the models for pelagic fish (Z=1.6917) was RESRAD model. For benthic fish (Z=1.4172) and for crustacean (Z=1.3941) the worst agreement was for R&D128.

Table 4.19 The comparison of external dose rate predictions between the models in Svyatoye lake.

Water conc. ($Bq\ l^{-1}$)	Sediment conc. ($Bq\ kg^{-1}$)	External Dose rate ($\mu Gy\ hr^{-1}$)					
		FASSET	ERICA	RESRAD (10 g)	RESRAD (1 kg)	R&D128	D-MAX
Pelagic fish							
9.94	107200	2.98E-03	2.88E-03	3.17E-03	2.90E-03	2.90E-03	4.64E-03
Benthic fish							
9.94	107200	15.5	15	15.6	n/d	6.3	50
Crustacean							
9.94	107200	20.4	19.8	15.6	n/d	7.9	50

Table 4.20 The Z-score for the external dose rates predicted by each model in Svyatoye Lake.

organism	Z-score				
	FASSET	ERICA	R&D128	RESRAD (10g)	RESRAD (1kg)
Pelagic fish	0.1278	0.7169	0.5513	1.6917	0.5513
Benthic fish	0.5332	0.4134	1.4972	0.5506	n/d
Crustacean	0.7730	0.6739	1.3949	0.0519	n/d

The predicted external dose rate for pelagic fish is significantly lower than for the benthic fish and crustaceans because it uses only the water activity concentration for the prediction of the external dose rate. The prediction of the external dose rate for the D-MAX model is higher than the other models because the D-MAX model gives the total (internal + external) dose based on conservative assumptions.

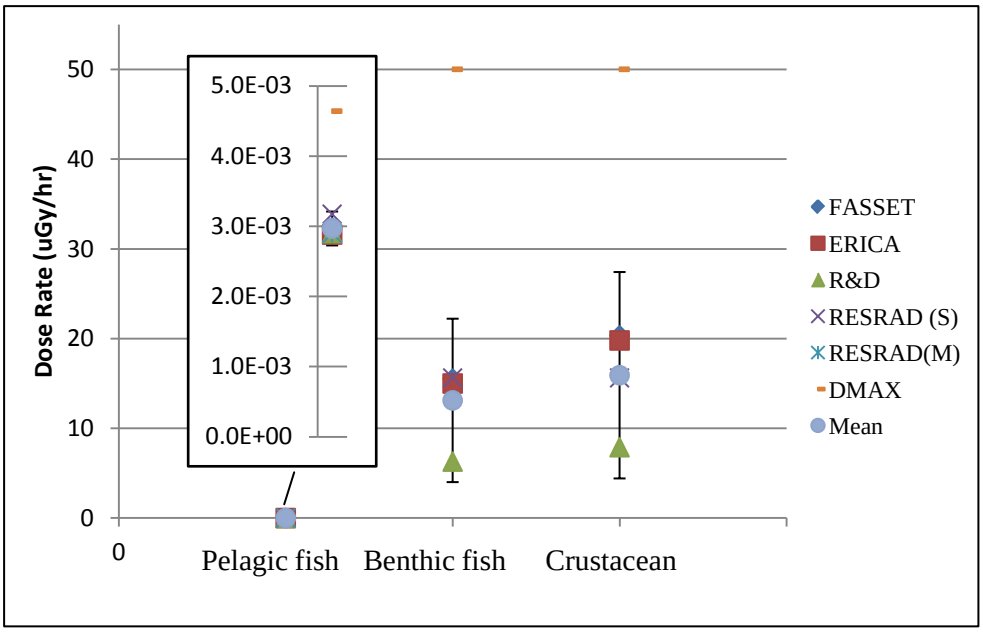

Figure 4.9 The external dose rate from Cs-137: comparison between the models in Svyatoye lake

Perstok lake

The comparison of the Cs-137 and Sr-90 external dose rate for pelagic fish between the models for Perstok Lake is shown in **Table 4.21**. For Perstok Lake, there is only the data of pelagic fish, but there are data of the water activity concentration of Cs-137 and Sr-90, so external doses can be calculated. As for Svyatoye lake, the RESRAD model was run for two different size classes; 10 g and 1 kg. From the data in **Table 4.21**, the comparison of the external rate between the models in Perstok lake can be illustrated in **Figure 4.10**. The Z-score for the external dose rates predicted between the models for Cs-137 and Sr-90 as shown in **Table 4.22** did not show bias ($|Z| \leq 2$). The RESRAD model produced the least satisfactory (Z=1.6733 for Cs-137 and Z=1.6279 for Sr-90) predictions of the external dose rate compared with the other models.

Table 4.21 The comparison of external dose rate between the models for data from Perstok lake.

Water conc. ($Bq\ l^{-1}$)	External Dose rate ($\mu Gy\ hr^{-1}$)					
	FASSET	ERICA	RESRAD (10 g)	RESRAD (1 kg)	R&D128	D-MAX
Cs-137						
14.1	4.23E-03	4.09E-03	4.50E-03	4.12E-03	4.20E-03	6.58E-03
Sr-90						
22	9.24E-04	5.28E-04	1.49E-03	4.88E-04	6.60E-04	1.43E-02

Table 4.22 The Z-score for the external dose rates predicted in each model in Perstok Lake.

organism	Z-score				
	FASSET	ERICA	R&D128	RESRAD (10g)	RESRAD (1kg)
Cs-137	0.0164	0.8428	0.1677	1.6733	0.6792
Sr-90	0.2590	0.7031	0.3824	1.6279	0.8014

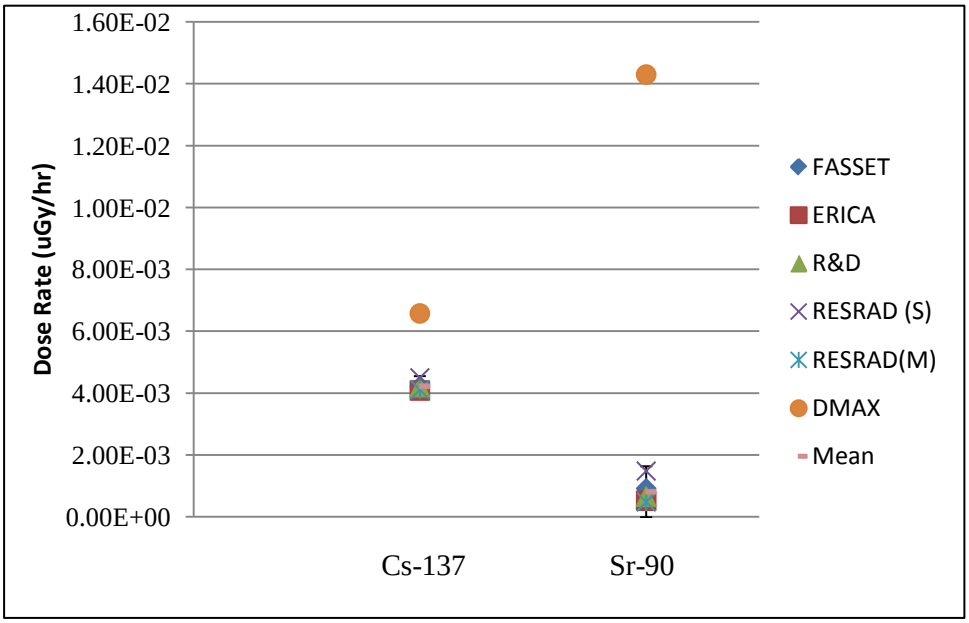

Figure 4.10 The external dose rate from Cs-137 and Sr-90: comparison between the models in Perstok lake.

4.3.3 The prediction of the total (internal plus external) dose rate

The total (internal plus external) dose rate for each lake can be determined in two ways; (1) from the summation of the external dose rate and the internal dose predicted from the activity concentration of the medium (for pelagic fish using water activity concentration and for benthic fish and crustaceans using water and sediment activity concentration) and (2) from the summation of the external dose rate plus the internal dose rate predicted from fish tissue activity concentration.

Svyatoye lake

The comparison of the total dose rate between the models by using the medium activity concentration of pelagic fish, benthic fish and crustacean in Svyatoye lake is shown in **Table 4.23**. For pelagic fish, there are two different values of the total dose rate from the RESRAD model; for 0.01 kg and 1 kg reference organisms. For benthic fish and crustaceans, as above, only results for a 0.01 kg reference organism were calculated. The total dose rate for the D-MAX model can be separated into two categories; predatory and non-predatory fish. The D-MAX model assumes the maximum activity either in tissue or the external medium for calculating the total dose rate. For pelagic fish, the external dose rate predicted from water activity concentration is much lower than the internal dose rate (predicted from tissue activity concentration using the K^+ concentration of the water). Therefore, the total dose rate for pelagic fish predicted by using the D-MAX model is based on the internal dose rate predicted from the K^+ concentration. For benthic fish and crustaceans, the sediment activity concentration is higher than the predicted fish tissue activity concentration. Therefore, the total dose rate for the benthic and crustacean predicted by using the D-MAX model used the external dose rate.

The comparison between the models of the total dose rate by using the fish tissue activity concentration of pelagic fish, benthic fish and crustacean in Svyatoye lake is shown in **Table 4.24**.

Table 4.23 The comparison between the models of the total dose rate calculated on the basis of the medium activity concentration in Svyatoye lake.

Total Dose rate (μGy hr^{-1})						
FASSET	ERICA	RESRAD (10 g)	RESRAD (1kg)	R&D	D-MAX predatory	D-MAX non-predatory
Pelagic fish						
16.2	14.3	36.4	42.9	21	6.71	3.28
Benthic fish						
37.3	26.9	65.2	n/d	25.3	n/d	50.0
Crustacean						
20.4	29.7	65.2	n/d	13.0	n/d	50.0

Table 4.24 The comparison between the models of the total dose rate calculated on the basis of the fish tissue activity concentration in Svyatoye lake.

Tissue Conc.	Total Dose rate (μGy hr^{-1})				
	FASSET	ERICA	RESRAD	R&D128	D-MAX
Pelagic fish					
9653.6	1.5476	1.7429	1.6904	1.7029	4.5050
4980.9	0.7999	0.8999	0.8737	0.8729	2.3244
6676.1	1.0712	1.2029	1.1698	1.2029	3.1155
6327.1	1.0153	1.1429	1.1115	1.1029	2.9526
4668.9	0.7500	0.8439	0.8198	0.8229	2.1788
4406.4	0.7080	0.7959	0.7740	0.7729	2.0563
3070.9	0.4943	0.5559	0.5407	0.5429	1.4331
5149.0	0.8268	0.9299	0.9032	0.9029	2.4029
5315.2	0.8534	0.9599	0.9323	0.9329	2.4804
5302.5	0.8514	0.9569	0.9321	0.9329	2.4745
7644.2	1.2261	1.3829	1.3407	1.3029	3.5673
20744.1	3.3220	3.7329	3.6323	3.6029	9.6806
17409.7	2.7885	3.1329	3.0490	3.0029	8.1245
12658.2	2.0283	2.2829	2.2198	2.2029	5.9072
8597.0	1.3785	1.5529	1.5073	1.5029	4.0119
1535.6	0.2487	0.2789	0.2719	0.2729	0.7166
4602.0	0.7393	0.8309	0.8073	0.8029	2.1476
Benthic fish					
3372.1	16.1524	15.6070	16.2167	6.8900	50.0267
6131.6	16.6491	16.1000	16.7000	7.4000	50.0267
5461.8	16.5286	16.0800	16.5792	7.2500	50.0267
5763.5	16.5829	16.1000	16.6333	7.3000	50.0267
Crustacean					
4246.3	20.7521	20.2080	16.3667	8.3200	50.0267

From **Table 4.23** and **4.24**, the comparison of the total dose rate of pelagic fish predicted from (a) the water activity concentration and from (b) the fish tissue activity concentration is illustrated in **Figure 4.11**. For benthic fish and crustaceans, the total dose rate is illustrated in **Figures 4.12** and **4.13** respectively.

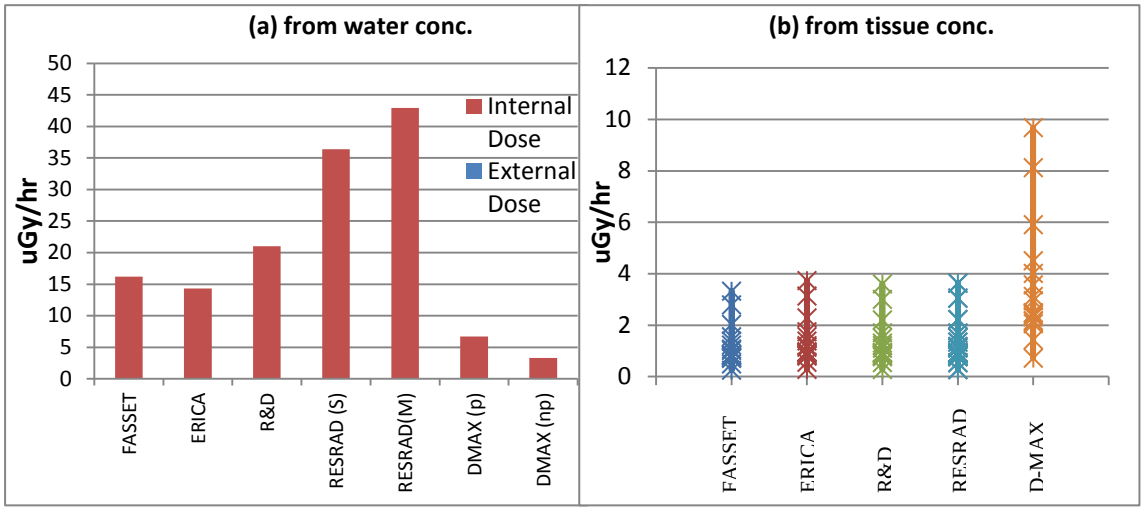

Figure 4.11 The comparison of the total dose rate to pelagic fish (Svyatoye Lake) predicted from (a) the water activity concentration and from (b) the fish tissue activity concentration.

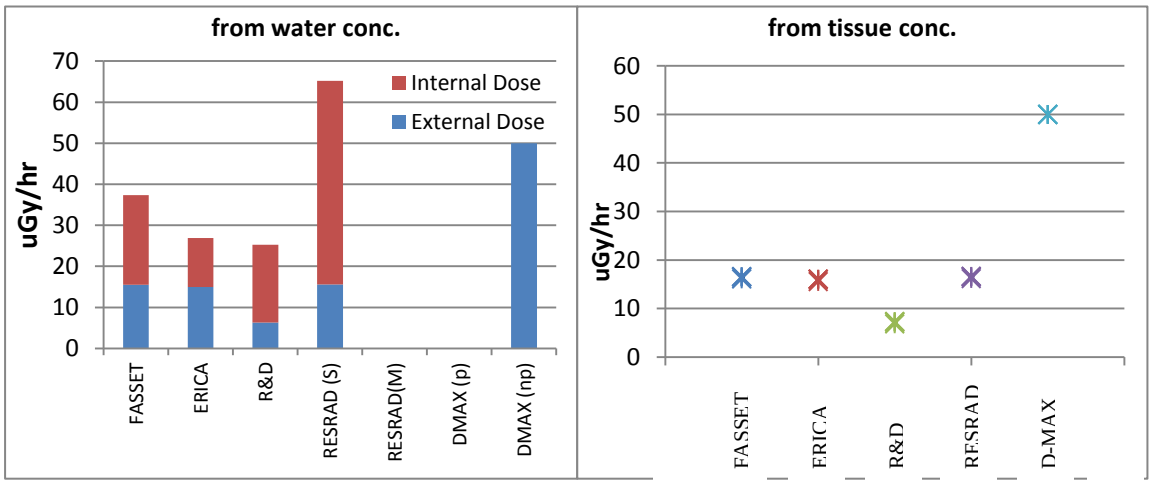

Figure 4.12 The comparison of the total dose rate to benthic fish (Svyatoe Lake) predicted from (a) the water activity concentration and from (b) the fish tissue activity concentration.

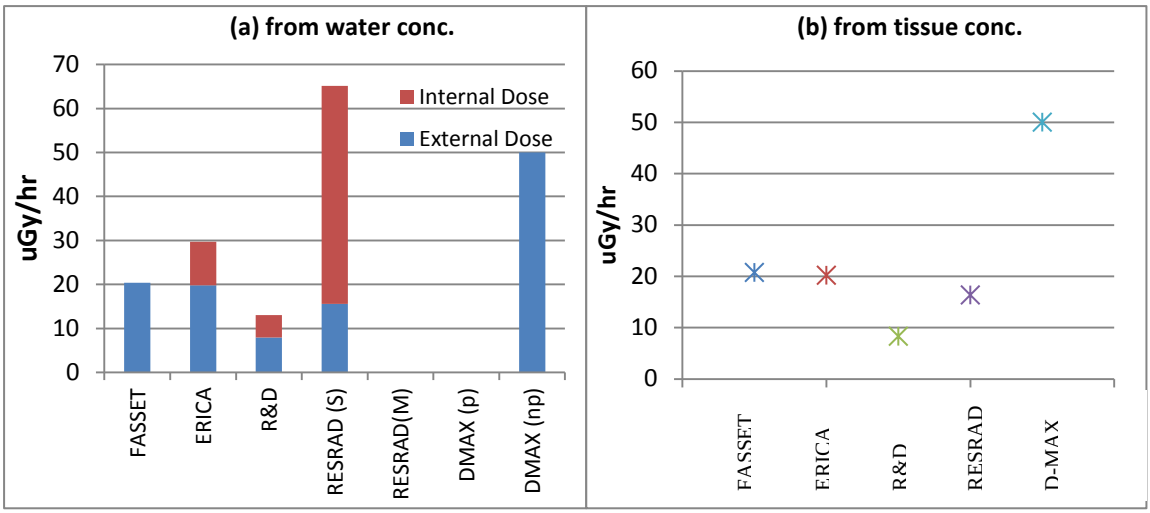

Figure 4.13 The comparison of the total dose rate to crustaceans (Svyatoe Lake) predicted from (a) the water activity concentration and from (b) the fish tissue activity concentration.

Perstok lake

The comparison between the models of the Cs-137 and Sr-90 total dose rate to pelagic fish based on the water activity concentration in Svyatoye lake is shown in **Table 4.25**. In Perstok lake, there were only measurement data available for pelagic fish. The comparison between the models of the Cs-17 and Sr-90 total dose rate by using the fish tissue activity concentration of pelagic fish in Perstok lake is shown in **Table 4.26**.

Table 4.25 The comparison between the models of the total dose rate calculated on the basis of the water activity concentration in Perstok lake.

Total Dose rate (μGy hr^{-1})						
FASSET	ERICA	RESRAD (0.01kg)	RESRAD (1kg)	R&D	D-MAX predatory	D-MAX non-predatory
Cs-137						
23.01	16.80	42.92	50.84	27.00	10.53	5.16
Sr-90						
0.34	0.24	4.10	4.42	0.58	2.17	0.12

Table 4.26 The comparison between the models of the total dose rate calculated on the basis of the fish tissue activity concentration in Perstok lake.

Tissue Conc.	Total Dose rate (μGy hr^{-1})				
	FASSET	ERICA	RESRAD	R&D128	D-MAX
Cs-137					
7010.8	1.1260	1.2641	1.2295	1.2042	3.2717
4977.96	0.8007	0.9001	0.8753	0.8742	2.3230
6170.6	0.9915	1.1141	1.0837	1.1042	2.8796
6303.2	1.0127	1.1341	1.1087	1.1042	2.9415
9537.5	1.5302	1.7241	1.6753	1.7042	4.4508
7938.9	1.2745	1.4341	1.3920	1.4042	3.7048
Sr-90					
9094	5.5483	5.7305	5.7098	5.7007	5.9111
10806	6.5926	6.8105	6.7932	6.7007	7.0239
2400	1.4649	1.5105	1.5057	1.5007	1.5600
257	0.1577	0.1625	0.1627	0.1607	0.1671
5848	3.5682	3.6805	3.6723	3.6007	3.8012
4646	2.8350	2.9305	2.9182	2.9007	3.0199

From the data presented in **Tables 4.25** and **4.26**, the comparison of the Cs-137 and Sr-90 total dose rate to pelagic fish predicted from (a) the water activity concentration and from (b) the fish tissue activity concentration are illustrated in **Figures 4.14** and **4.15** respectively.

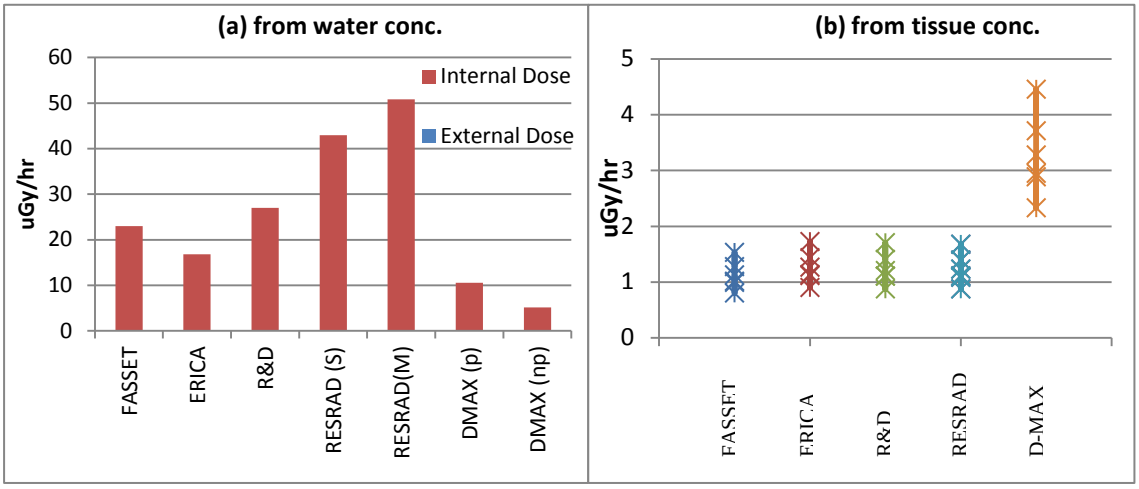

Figure 4.14 The comparison of the Cs-137 total dose rate (pelagic fish, Perstok Lake) predicted from (a) the water activity concentration and from (b) the fish tissue activity concentration.

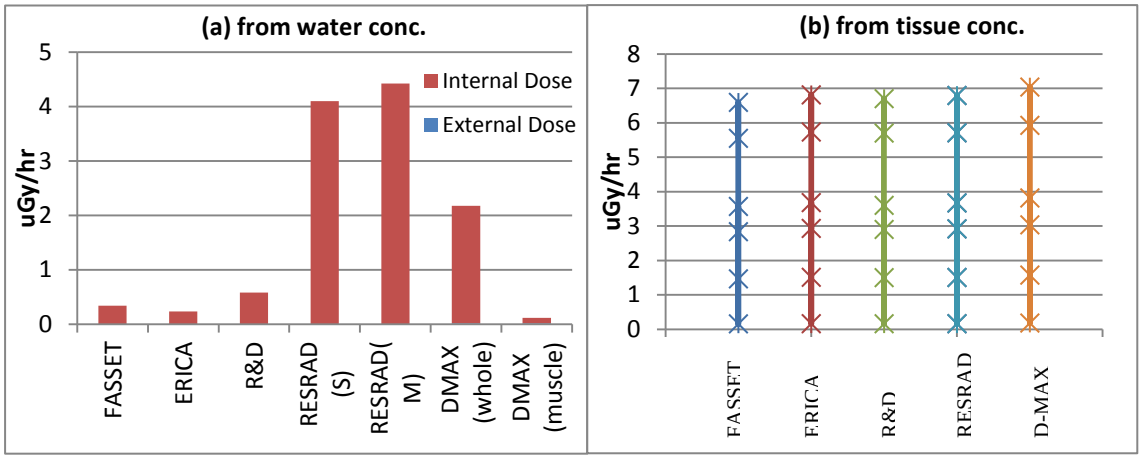

Figure 4.15 The comparison of the Sr-90 total dose rate (pelagic fish, Perstok Lake) predicted from (a) the water activity concentration and from (b) the fish tissue activity concentration.

4.4 Discussion

4.4.1 The prediction of internal dose rate

Dose Conversion Coefficient (DCC)

As described in the Methods (Section 4.2.1), the internal dose rate can be calculated either by using fish tissue activity concentration or using a concentration ratio approach to estimate tissue concentrations from the water concentration. When calculating the internal dose directly from measured fish tissue activity concentration, the internal dose rate depends only on the DCC_{int} in each model (**Table 4.27**). This summary of the the DCC_{int} for each model shows that they have quite similar values, explaining the similar predicted values for the different models observed in this study when tissue activity concentration measurements are used as the basis for predictions (**Figures 4.4 -4.8**) This is in accordance with the finding of Vives i Batlle et al., 2007 that model dose rate predictions are in good agreement (Vives i Batlle, Balonov et al. 2007). Only the D-Max model for Cs-137 gives significantly different (higher) predictions than the other models because this simple screening model assumes no escape of gamma radiation from the organism.

The DCC_{int} for the RESRAD model depends on the fish weight: as illustrated in Chapter 3, the DCC_{int} increases as the organism weight increased due to the higher absorbed fractions of radiation (Taranenko and et al. 2004). The DCC_{int} of pelagic fish of the RESRAD model (1 kg weight) is closer to the other models than 0.01 kg approach because the reference pelagic fishes in the other models are close to 1 kg (FASSET 2003) (Copplestone, Bielby et al. 2001). For the RESRAD model, the user can choose only terrestrial animal, terrestrial plant, riparian animal and aquatic animal, so specific organisms such as benthic fish or crustacean are not given as default values. The DCC_{int} of RESRAD model therefore uses the same value for pelagic fish, benthic fish and crustacean whilst the other models use different DCC_{int} values between pelagic fish, benthic fish and crustaceans. However, it can be seen from **Table 4.27** that the DCC_{int} of pelagic fish and benthic fish are very close, since their assumed sizes are similar. For example, for Cs-137, the DCC_{int} for pelagic fish and benthic fish are $1.6x10^{-4}$ and $1.8x10^{-4}$ for FASSET model, $1.8x10^{-4}$ and $1.9x10^{-4}$ for ERICA model and $1.74x10^{-4}$ and $1.7x10^{-4}$ for R&D. For Sr-90 shows the same result as the Cs-137. However, the DCC_{int} for crustacean in all models are lower than the DCC_{int} for pelagic fish and benthic fish because of their lower assumed size.

All models used the same basic approach that average energy deposited at any point in the object to calculate the DCC_{int}. The slight differences in DCCint in the different models are due to the organism size and the occupancy factor used in each model.

Table 4.27 A comparison of DCC_{int} in pelagic fish, benthic fish and crustacean between the models (Copplestone, Bielby et al. 2001; FASSET 2003; ERICA 2009; U.S.DOE 2009)

Model	DCC_{int} ($\mu Gy\ hr^{-1}$ per $Bq\ kg^{-1}$)					
	Pelagic fish		Benthic fish		Crustacean	
	Cs-137	Sr-90	Cs-137	Sr-90	Cs-137	Sr-90
FASSET	$1.6x10^{-4}$	$6.1x10^{-4}$	$1.8x10^{-4}$	$6.3x10^{-4}$	$9.0x10^{-5}$	$1.9x10^{-4}$
ERICA	$1.8x10^{-4}$	$6.3x10^{-4}$	$1.9x10^{-4}$	$6.3x10^{-4}$	$9.6x10^{-5}$	$2.0x10^{-4}$
RESRAD(10 g)	$1.48x10^{-4}$	$5.82x10^{-4}$	$1.48x10^{-4}$	$5.82x10^{-4}$	$1.48x10^{-4}$	$5.82x10^{-4}$
RESRAD (1kg)	$1.75x10^{-4}$	$6.28x10^{-4}$	$1.75x10^{-4}$	$6.28x10^{-4}$	$1.75x10^{-4}$	$6.28x10^{-4}$
R&D128	$1.74x10^{-4}$	$6.2x10^{-4}$	$1.7x10^{-4}$	$6.2x10^{-4}$	$9.8x10^{-5}$	$2.2x10^{-4}$

*****DCC_{int} for ERICA and RESRAD are taken from the model program

Concentration Ratio (CR)

When estimating internal dose on the basis of water activity concentration, the internal dose rate depends on the CR and DCC_{int} in each model. From the CR values in each model in **Table 4.1**, the CR for Cs-137 is much higher than the CR for Sr-90 (around 20 -400 times depending on the models). In Perstok Lake, for example, the tissue activity concentration for Cs-137 was higher than Sr-90 even though the water concentration of Cs-137 (14.1 Bq l^{-1}) was lower than Sr-90 (22 Bq l^{-1}) because of higher CR values.

Tissue Activity Concentration

For Cs-137, the tissue activity concentration predicted from the models in all organisms (pelagic fish, benthic fish and crustacean) showed the higher estimates than the measured tissue activity concentration (**Table 4.11** and **4.15**), with the exception of the D-MAX model because the D-MAX model predict the tissue activity concentration from the potassium concentration in the water rather than using a generic value (Smith, Kudelsky et al. 2000). The D-MAX model gave the best prediction for the tissue activity concentration. The RESRAD model showed the worst agreement of the prediction of the tissue concentration between the models.

For Sr-90, the tissue activity concentration predicted by the models showed under-estimation compared with the measured tissue activity concentration (**Table 4.15**), again with the exception of the D-MAX model. This model predicts the tissue concentration from the calcium concentration in the water rather than using a generic value (Smith, Sasina et al. 2009). This was also found in an international model validation exercise on radionuclide transfer and doses to freshwater biota in Perch Lake. In this study, the D-MAX model again gave a good prediction for the tissue activity concentration to within approximately two-fold of the measured values (Yankovich and et al. 2010). In the Perch Lake study, the RESRAD model was also close to the measured value, whilst ERICA and R&D128 under-predicted because the CR value were based on the measured edible fish tissue (muscle) rather than whole-body (Yankovich and et al. 2010). Even though, for Sr-90, the RESRAD model showed the worst agreement of the prediction of the tissue concentration between the models but the RESRAD model predicted the tissue concentration better than the FASSET, ERICA and R&D128. In general, as found here for Perstok Lake, the prediction of the tissue activity concentration for Sr-90 from the models was close to the measured tissue

activity concentration and the model using site specific water chemistry (D-MAX model) was the most close to the measured data (Yankovich and et al. 2010).

It can be concluded that the model using water chemistry based to predict tissue concentration (D-MAX) is much closer to the measured tissue concentration for both Cs-137 and Sr-90. Even though the RESRAD model shows the worst agreement for Sr-90 prediction, this model is closer to the measured tissue concentration because the other models (FASSET, ERICA and R&D128) used the muscle tissue to predict the tissue concentration rather than the whole tissue. Therefore, the RESRAD model is "right for the wrong reason". This is a well known difficulty of model comparison exercises which sometimes only focus on predicted dose. But in this study, we have analysed both tissue concentration predictions, and dose predictions, allowing identification of this problem with the RESRAD model.

Dose rates

In general, when the organism sizes are much smaller than the radiation range in the medium, the internal dose rate tends to zero because of the escape of radiation from the body and when the organism sizes are much larger than the radiation range in the medium, the internal dose approximates D_∞ (Ulanovsky and Pröhl 2006; Ulanovsky, Pröhl et al. 2008) because a large amount of the energy is absorbed by the large size of organism (Amiro 1997);

$$D_\infty(E) = 5.76 \times 10^{-4} E \quad (\mu Gy\ h^{-1}\ Bq\ kg^{-1}) \qquad (4.12)$$

where E is the energy in MeV of a mono-energetic source

For Cs-137, the internal dose rates predicted from the water activity concentration were about an order of magnitude higher than the internal dose rate predicted from the tissue activity concentration (**Table 4.13** and **4.17** and **Figures 4.4, 4.5, 4.6** and **4.7**) with the exception of the D-MAX model. The D-MAX model showed good predictions for the internal dose rate in pelagic fish and benthic fish (**Table 4.13** and **Figure 4.4** and **4.5**) whilst the R&D model showed the closest prediction for crustaceans (**Table 4.13** and **Figure 4.6**). The D-MAX model does not calculate doses to crustaceans. In the case that the tissue activity concentration is not known, the D-MAX model can predict the tissue activity concentration for Cs-137 using a concentration ratio estimated from the K^+ concentration in the water (Smith 2005) and the tissue activity concentration for Sr-90

from Ca^{2+} concentration in the water (Smith, Sasina et al. 2009). The RESRAD model predicted much higher internal dose (based on water activity concentration) than the other models: the internal dose for pelagic fish was estimated to be approximately twice as high as the prediction of FASSET, ERICA and R&D128 and four to five times higher than for D-Max. This is obviously due to a more conservative choice of CR value in the model.

For Sr-90, the internal dose rates predicted from the water concentration were within the range of those predicted from the tissue concentration, but showed under-estimation (**Table 4.17** and **Figure 4.8**) with the exception of the D-MAX and RESRAD models. Even though the RESRAD model showed the worst agreement of the prediction of the internal dose rate between the models for Sr-90, the RESRAD model predicted the internal dose rate better than the FASSET, ERICA and R&D128.

4.4.2 The external dose rate

Dose Conversion Coefficient (DCC)

As described in the Methods (Section 4.2.2), the external dose rate can be calculated by using medium activity concentration (water or sediment) and DCC_{ext}. The DCC_{ext} values in each model are quite similar (See **Table 4.28**), though The DCC_{ext} for the RESRAD model depends on the fish weight, the DCC_{ext} for 10g weight of organism being higher than 1 kg weight of organism since the DCC_{ext} decreases when the organism weight increased due to the increased self-shielding effect (Taranenko and et al. 2004). The DCC_{ext} of pelagic fish of the RESRAD model 1 kg approach is closer to the other models than 10 g approach because the weight is similar to the other models.

External dose rates

In general, when the organism sizes are much smaller than the radiation range in the medium, the external dose rate approaches D_{∞} and when the organism sizes are much larger than the radiation range in the medium, the external dose approximates zero (Ulanovsky and Pröhl 2006; Ulanovsky, Pröhl et al. 2008). The prediction of the external dose rate near the surface of the organism overestimates the whole body dose especially in large organisms (Amiro 1997). Alpha-particles can be ignored for the external dose rate because weakly penetrating short-range radiation can be stopped by the outer protective layer of skin but α-particles are taken into account for the internal

dos rate (Amiro 1997; Ulanovsky and Pröhl 2006; Ulanovsky, Pröhl et al. 2008). The external dose rate for pelagic fish depends on the DCC_{ext} and the water activity concentration (Equation 4.8), whilst the external dose rate for benthic fish and crustacean depends on DCC_{ext} and medium (water and sediment) activity concentration (Equation 4.9).

Table 4.28 The comparison of DCC_{ext} in pelagic fish, benthic fish and crustacean between the models (Copplestone, Bielby et al. 2001; FASSET 2003; ERICA 2009; U.S.DOE 2009).

Model	DCC_{ext} (μGy hr^{-1} per Bq kg^{-1})					
	Pelagic fish		Benthic fish		Crustacean	
	Cs-137	Sr-90	Cs-137	Sr-90	Cs-137	Sr-90
FASSET	$3x10^{-4}$	$4.2x10^{-5}$	$2.9x10^{-4}$	$2.7x10^{-5}$	$3.8x10^{-5}$	$4.7x10^{-4}$
ERICA	$2.9x10^{-4}$	$2.4x10^{-5}$	$2.8x10^{-4}$	$2.1x10^{-5}$	$3.7x10^{-5}$	$4.5x10^{-4}$
RESRAD (0.01kg)	$3.18x10^{-4}$	$6.77x10^{-5}$	$3.18x10^{-4}$	$6.77x10^{-5}$	$3.18x10^{-4}$	$6.77x10^{-5}$
RESRAD (1kg)	$2.92x10^{-4}$	$2.21x10^{-5}$	$2.92x10^{-4}$	$2.21x10^{-5}$	$2.92x10^{-4}$	$2.21x10^{-5}$
R&D128	$2.95x10^{-4}$	$2.99x10^{-5}$	$2.95x10^{-4}$	$2.99x10^{-5}$	$3.71x10^{-5}$	$4.34x10^{-4}$

*****DCC_{int} for ERICA and RESRAD are taken from the model program

For Cs-137, the predicted external dose rates of benthic fish and crustaceans were approximately four orders of magnitude higher than pelagic fish (**Figure 4.9**) because the sediment activity concentration was much higher than the water activity concentration. The external dose rates of pelagic fish, benthic fish and crustaceans in Svyatoye lake, and pelagic fish in Perstok lake from all models (FASSET, ERICA, R&D128 and RESRAD) showed similar predictions to each other. The D-MAX model gives the maximum dose rate to any organism in a particular medium, so predicts significantly (approximately a factor of 2) higher dose than the other models.

For Sr-90 in Perstok lake, there are only data in pelagic fish. The external dose rate of Sr-90 was lower than the external dose rate of Cs-137 because the beta-emitting Sr-90 is less penetrating than the gamma-emisssions of Cs-137 (**Figure 4.10**) even though the water concentration of Sr-90 (22 Bq l^{-1}) was higher than the water concentration of Cs-

137 (14.1 Bq l^{-1}). The external dose rate from all model showed similar predictions. The RESRAD model at 10 g approach showed the most difference to other models whilst the model for 1 kg fish was closer to the other models.

4.4.3 The total dose rate

The analysis above has allowed the relative importance of the external and internal dose in determining overall dose rate to fish to be assessed. The total dose rate in pelagic fish was mostly from the internal dose rate because the external dose from low activity concentrations in water was very low. The external dose played a much more important part in forming the total dose rate for benthic fish and crustaceans because of the high Cs-137 activity concentration in sediment (**Figures 4.11 a, b, 4.12 a, b** and **4.13 a, b**). For example, the range in Cs-137 activity concentration in fish in Svyatoye Lake was 1536 -20744 Bq kg^{-1} whilst the activity concentration in sediment was 107200 Bq kg^{-1}. In Perstok Lake, there were only tissue activity concentration data for pelagic fish, so it was not possible to accurately estimate internal doses to benthic fish and crustaceans in Perstok. It is expected, though that the sediment Cs-137 would also play an important role in dose formation for benthic fish and crustaceans in Perstok. The total dose of Sr-90 to pelagic fish was also mainly from the internal dose: it is likely that this would also apply to benthic fish and crustaceans as the external dose from beta-emitting Sr-90 would be less important.

For pelagic fish, the predicted dose for Sr-90 was lower than the Cs-137 dose even though the Sr-90 water activity concentration was higher than the Cs-137 because the CR value of the Sr-90 was quite low in comparison with Cs-137 (**Table 4.1**). This is expected to be true for most lakes, except when calcium concentrations are very low but potassium concentrations are high. The total dose rate predicted on the basis of the water concentration from FASSET, ERICA and R&D128 model was lower than the total dose rate predicted from tissue concentration because the predicted internal dose from water concentration was lower, whist the total dose rate predicted on the basis of the water concentration from RESRAD and D-MAX model was closer to the total dose rate predicted from tissue concentration than FASSET, ERICA and R&D128 model.

4.4.4 Comparison with regulatory values

The (more accurate) total dose rate predicted from the tissue concentration was used to compare with the dose limit to protect the organism from the effects of ionising radiation. The England and Wales dose limit (40 μGy hr^{-1}) is used for this comparison. The dose limit is based on the dose limit of 1 mGy d^{-1}.

For Svyatoye Lake, there was only one radionuclide (Cs-137) which contributed significantly to the total dose rate. All models predicted the total dose rate for pelagic fish to be lower than the dose limit. The D-MAX model (a screening model) predicted two times higher dose rates than the other models for pelagic fish. For the benthic fish and crustacean, D-MAX model predicted the total dose rate (around 50 μGy hr^{-1}) over the dose limit, whilst the prediction from the other models was below the dose limit. For Perstok Lake, two radionuclides (Cs-137 and Sr-90) contributed to the total dose rate. The combined total dose rate (Cs-137 plus Sr-90) was below the dose limit. The D-MAX model showed the highest prediction than the other models for Cs-137, whilst there was a good agreement between the models for Sr-90.

For the dose assessment, doses estimated from tissue concentrations of radionuclides were used, because this is obviously the most accurate method. If no tissue concentration data were available, predictions would have been made only on the basis of the CR value and the medium (water) activity concentration. In this case, doses would have been predicted to have been greater than the limit (40 μGy hr^{-1}) by the D-MAX (benthic fish and crustaceans) and RESRAD (all species) models.

4.5 Summary

Using monitoring data of radioactivity in water, fish and sediments, the models for dose assessments have been compared in Svyatoye and Perstok Lakes. For predicting internal dose rates using measured tissue concentrations the models all give similar values, but the D-MAX screening model gives approximately two times higher estimates than the other models. The similarity between the models for internal dose rates was also observed from their DCC_{int} values as discussed in Chapter 3. For estimating doses in cases where tissue measurements are not available, the models are more varied. This is because the assumed CR is different. The model where CR is estimated depending on water chemistry gives the best prediction in this case. For benthic organisms, external

dose from sediments is very important, so the assumption of habitat (in sediment, on sediment, or in water) is important in predicting the dose to these organisms.

Based on the findings of this thesis, it can be recommended that inclusion of water chemistry relationships to improve prediction of fish-water concentration ratio will significantly improve model dose predictions. These relationships could be included in the ERICA model, which gives more accurate DCCs than D-Max, to give a generic best model to assess doses to fish from radiocaesium and radiostrontium.

The dose rates to fish in Svyatoye and Perstok lakes are near the 40 μGy h^{-1} limit for possible impacts from radiation, but the models (except the conservative D-MAX model) do not predict the doses to be over the limit. But it is important to state that the estimates have only used the available fish activity concentration data. Doses to different fish sizes, or to different life cycle stages, may be different to the estimates made here. This will be discussed further in the next Chapter.

4.6 Reference

Amiro, B. D. (1997). Radiological dose conversion factors for generic non-human biota used for screening potential ecological impacts. *Journal of Environmental Radioactivity, 35*(1), 37-51.

Beresford, N., Wright, S., Barnett, C., Wood, M., Gaschak, S., Arkhipov, A., et al. (2005). Predicting radionuclide transfer to wild animals: an application of a proposed environmental impact assessment framework to the Chernobyl exclusion zone. *Radiation and Environmental Biophysics, 44*(3), 161-168.

Beresford, N. A., Balonov, M., Beaugelin-Seiller, K., Brown, J., Copplestone, D., Hingston, J. L., et al. (2008). An international comparison of models and approaches for the estimation of the radiological exposure of non-human biota. *Applied Radiation and Isotopes, 66*(11), 1745-1749.

Beresford, N. A., Barnett, C., Brown, J., Cheng, J., Copplestone, D., Filistovic, V., et al. (2008). Inter-comparison of models to estimate radionuclide activity concentrations in non-human biota. *Radiation and Environmental Biophysics, 47*(4), 491-514.

Beresford, N. A., Barnett, C. L., Jones, D. G., Wood, M. D., Appleton, J. D., Breward, N., et al. (2008). Background exposure rates of terrestrial wildlife in England and Wales. *Journal of Environmental Radioactivity, 99*(9), 1430-1439.

Beresford, N. A., & et al. (2010a). Assessment of risk to wildlife from ionising radiation: can initial screening tiers be used with a high level of confidence? *Journal of Radiological Protection, 30*(2), 265.

Beresford, N. A., & et al. (2010b). Predicting the radiation exposure of terrestrial wildlife in the Chernobyl exclusion zone: an international comparison of approaches. *Journal of Radiological Protection, 30*(2), 341.

Beresford, N. A., Gaschak, S., Barnett, C. L., Howard, B. J., Chizhevsky, I., Strømman, G., et al. (2008). Estimating the exposure of small mammals at three sites within the Chernobyl exclusion zone - a test application of the ERICA Tool. *Journal of Environmental Radioactivity, 99*(9), 1496-1502.

Beresford, N. A., Wright, S. M., Barnett, C. L., Hingston, J. L., Batlle, J. V. i., Copplestone, D., et al. (2005). A case study in the Chernobyl zone Part 2: Predicting radiation induced effects in biota. *Radioprotection, 40*(Suppl. 1), S299-S305.

Beresford, N. A., Wright, S. M., Barnett, C. L., Wood, M. D., Gaschak, S., Arkhipov, A., et al. (2005). A case study in the Chernobyl zone Part I: Predicting radionuclide transfer to wildlife. *Radioprotection, 40*(Suppl. 1), S291-S297.

Copplestone, D., Bielby, S., Jones, S. R., Patton, D., Daniel, P., & Gize, I. (2001). *Impact Assessment of Ionising Raditaiton on Wildlife: R&D Publication 128*. Bristol: Environmental Agency.

Copplestone, D., Wood, M. D., Bielby, S., Jones, S. R., Vives, J., & Beresford, N. A. (2003). *Habitats regulations for Stage 3 assessments: radioactive substances authorisations*. Bristol: Environment Agency.

ERICA. (2007). *D-ERICA: An INTEGRATED APPROACH to the assessment and management of environmental risks from ionising radiation*: Swedish Radiation Protection Authority.

ERICA. (2009). ERICA Assessment Tool: ERICA.

FASSET. (2003a). *Dosimetric models and data for assessing radiation exposures to biota. Deliverable 3*. Stockholm: Norwegian Radiation Protection Authority.

FASSET. (2003b). *Handbook for Assessment of the Exposure of Biota to Ionising Radiation from Radionuclides in the Environment. Deliverable 5*. Stockholm: Swedish Radiation Protection Authority.

FASSET. (2003c). *Transfer Factor and Dose Conversion Coefficient Look-up Tables. Handbook for Assessment of the Exposure of Biota to Ionising Radiation from Radionuclides in the Environment. Deliverable 5 Appendix 1*. Stockholm: Swedish Radiation Protection Authority.

Kudelsky, A. V., Pashkevich, V. I., Yankov, A. I., Samodurov, V. P., Savchik, S. F., & Rudemok, A. A. (2005). *Radio-ecological study of the Chernobyl Cooling Pond and options for remediation*. Minsk: National Academy of Science of Belarus.

Mendenhall, W., & Sincich, T. (2006). *Statistics for Engineering and the Sciences* (5th ed.). New Jersey: Prentice-Hall, Inc.

Michael, T., Stephen, L. R. E., & Roger, W. (2006). The International Harmonized Protocol for the proficiency testing of analytical chemistry laboratories (IUPAC Technical Report). *Pure & Applied Chemistry, 78*(1), 145-196.

Mück, K., Pröhl, G., Likhtarev, I., Kovgan, L., Meckbach, R., & Golikov, V. (2002). A Consistent Radionuclide Vector After the Chernobyl Accident. *Health Physics, 82*(2), 141-156.

Smith, J. (2005). Effects of ionising radiation on biota: do we need more regulation? *Journal of Environmental Radioactivity, 82*(1), 105-122.

Smith, J. T., Kudelsky, A. V., Ryabov, I. N., Daire, S. E., Boyer, L., Blust, R. J., et al. (2002). Uptake and elimination of radiocaesium in fish and the "size effect". *Journal of Environmental Radioactivity, 62*(2), 145-164.

Smith, J. T., Kudelsky, A. V., Ryabov, I. N., & Hadderingh, R. H. (2000). Radiocaesium concentration factors of Chernobyl-contaminated fish: a study of the influence of potassium, and "blind" testing of a previously developed model. *Journal of Environmental Radioactivity, 48*(3), 359-369.

Smith, J. T., Kudelsky, A. V., Ryabov, I. N., Hadderingh, R. H., & Bulgakov, A. A. (2003). Application of potassium chloride to a Chernobyl-contaminated lake: modelling the dynamics of radiocaesium in an aquatic ecosystem and decontamination of fish. *The Science of The Total Environment, 305*(1-3), 217-227.

Smith, J. T., Sasina, N. V., Kryshev, A. I., Belova, N. V., & Kudelsky, A. V. (2009). A review and test of predictive models for the bioaccumulation of radiostrontium in fish. *Journal of Environmental Radioactivity, 100*(11), 950-954.

Smith, J. T., Voitsekhovitch, O. V., Konoplev, A. V., & Kudelsky, A. V. (2005). Radioactivity in aquatic systems. In J. T. Smith & N. A. Beresford (Eds.), *Chernobyl-Catastrophe and Consequences* (pp. 139-189). Berlin: Praxis Publishing Ltd.

Smithson, M. (2000). *Statistics with Condidence*. London: SAGE Publications Ltd.

Taranenko, V., & et al. (2004). Absorbed dose rate conversion coefficients for reference terrestrial biota for external photon and internal exposures. *Journal of Radiological Protection, 24*(4A), A35.

U.S.DOE. (2002). *A Graded Approach for Evaluating Radiation Doses to Aquatic and Terrestrial Biota*. Washington D.C.: U.S.DOE.

U.S.DOE. (2009). RESRAD-BIOTA for Windows (Version 1.5): U.S. Department of Energy.

Ulanovsky, A., & Pröhl, G. (2006). A practical method for assessment of dose conversion coefficients for aquatic biota. *Radiation and Environmental Biophysics, 45*(3), 203-214.

Ulanovsky, A., Pröhl, G., & Gómez-Ros, J. M. (2008). Methods for calculating dose conversion coefficients for terrestrial and aquatic biota. *Journal of Environmental Radioactivity, 99*(9), 1440-1448.

Vives i Batlle, J., Balonov, M., Beaugelin-Seiller, K., Beresford, N., Brown, J., Cheng, J. J., et al. (2007). Inter-comparison of absorbed dose rates for non-human biota. *Radiation and Environmental Biophysics, 46*(4), 349-373.

Wood, M. D., Marshall, W. A., Beresford, N. A., Jones, S. R., Howard, B. J., Copplestone, D., et al. (2008). Application of the ERICA Integrated Approach to the Drigg coastal sand dunes. *Journal of Environmental Radioactivity, 99*(9), 1484-1495.

Yankovich, T. L., & et al. (2010). An international model validation exercise on radionuclide transfer and doses to freshwater biota. *Journal of Radiological Protection, 30*(2), 299.

Chapter 5

Measurement of the external dose to aquatic organisms

5.1 Introduction

The major radioactive nuclides released from the Chernobyl Nuclear Power Plant were I-131, caesium radioisotopes, Sr-90, plutonium radioisotopes and noble gasses (IAEA, 2006a, 2006b). Large amounts of short half-life radioactive nuclides, for example I-131, I-133 and Te-132 were released, whilst long half-lives radioactive nuclides, for example Pu-239, Pu-240 and Pu-242 were released in small amounts (**Table 5.1**) (IAEA, 2006b). In the early phase, the radioactive nuclide of most concern was I-131 because it was released in large quantities and has high radiotoxicity, especially when concentrated in the thyroid. After the short half-life radioactive nuclides had decayed away, Cs-137 and Sr-90 were of most concern. Cs-137 is more volatile than Sr-90 (IAEA, 2006b) so, the Sr-90 was distributed mainly in hot particles close to the Chernobyl Nuclear Power Plant, whilst the Cs-137 spread over a much larger area (J. T. Smith & Beresford, 2005).

Table 5.1 Half-life and amounts of radionuclides released from Chernobyl accident (IAEA, 2006b).

radionuclides	Half-life	Released (PBq)
Short half-lives radioactive nuclides		
I-131	8.04 d	~1760 PBq
I-133	20.8 h	2,500 PBq
Te-132	3.26 d	~1,150 PBq
Long half-lives radioactive nuclides		
Pu-239	24,065 years	0.013 PBq
Pu-240	6,537 years	0.018 PBq
Pu-242	376,000 years	0.00004 PBq

The radioactive fallout was deposited in both aquatic and terrestrial environments. In the terrestrial environment, radionuclides deposited to the soil surface then migrated deeper into the soil by advection and dispersion. A proportion of deposited radioactivity migrated to the water bodies such as rivers or lakes by rainwater runoff (Jim T. Smith, Voitsekhovitch, Konoplev, & Kudelsky, 2005). There were two main types of the accumulation of radionuclides in the aquatic environment; (1) from direct deposition to the water surface and (2) from the transportation of radionuclides from the catchment (Jim T. Smith, et al., 2005). In closed lake systems, such as Svyatoye and Perstok Lakes, which have no or minor inflow and outflow of water, the bed sediment is the main factor which controls activity concentration in the water (IAEA, 2006b; Jim T. Smith, et al., 2005). The Cs-137 and Sr-90 activity concentration in water in closed lake system is therefore significantly higher than rivers and open lake systems (Jim T. Smith, et al., 2005).

In the present study, models will be used to determine the radiation doses to biota from radionuclides deposited in bottom sediments. In-situ measurements in water and sediment depth profile of both beta and gamma radiation will be measured using Thermoluminescent dosimeters (TLDs) in the two closed lakes, Svyatoye and Perstok. The in-situ measurements in water and sediment surface will be used to estimate radiation doses to aquatic biota in these lakes. In addition, the measured dose rate-depth profile will be compared with the sediment profile distribution calculation. This will test a new method of in-situ measurement to determine both beta and gamma doses and estimate maximum doses in the sediment depth profile and above the sediment surface of each lake. These studies will support previous studies of radiation effects on aquatic organisms (e.g. (Cailes, 2006) and (Tumnoi, 2006)) as previously discussed in Chapter 1, Section 1.7.

5.2 The use of TLD measurements to determine the radiation dose to biota.

As discussed in Chapter 1, TLDs are one of the most effective methods to determine cumulative radiation doses. In the past, TLDs have been used to determine the radiation dose in biota, in sediments and in terrestrial environments.

A literature search found that before the Chernobyl accident, only a few studies had used TLDs to determine radiation doses in the environment. One of the first studies to use in-situ TLD measurements determined radiation doses to Plaice (*Pleuronectes*

platessa) in the Irish Sea off Sellafield (Woodhead, 1973). These measurements were made by tagging the fish with TLDs which were then released and recaptured. The work was able to estimate the dose rates to their gonads to be a maximum of 18μGy/h. In 1974, TLDs were used placed on the mud-water interface to estimate the dose rates from contaminated sediments at Gable Mountain Pond, USA. There was a good agreement between dose rates and sediment concentrations that higher Cs-137 activity concentration in sediment observed in deeper water (C.E.Cushing & D.G.Watson, 1974). TLDs have also been used to determine radiation doses received by small mammals inhabiting a dry radioactive leaching pond on the Idaho National Engineering Laboratory Site in southeastern Idaho (Halford & Markham, 1978). In this study (Halford & Markham, 1978), the TLDs were surgically implanted in 3 species; white-footed deer mouse (*Peromyscus maniculatus*), least chipmunk (*Eutamias minimus*), and Ord's kangaroo rat (*Dipodomys ordii*). The deer mice received a mean dose equivalent rate of 1600 μSv d^{-1}, whilst least chipmunks and Ord's kangaroo rats received the mean dose equivalent of 170 μSv d^{-1} and 60 μSv d^{-1} respectively.

After the Chernobyl accident, TLDs were widely used to determine radiation doses in humans, the environment and biota. For example, TLDs were used to determine the external radiation doses to the population from the Chernobyl fall-out in contaminated territories of Ukraine. The dose rate was about 1.1 mSv yr^{-1} in 1996-1997 (Chumak, Likhtarev, & Pavlenko, 1999). In the south eastern part of Norway, the highest dose in first month and first year were 0.29 and 1.7 mSv respectively (Strand, Stranden, & Rudjord, 1987). TLDs also were used in environmental stations for environmental monitoring. TLDs were used at King George Island, South Shetland Archipelago (Godoy, et al., 1998) and the Hungarian Nuclear Power Plant (NPP) at Paks (Szabó, Fehér, & Germán, 1990) for environmental monitoring.

For the determination of the external dose to biota, TLDs were mounted in collar in Yellow-necked mouse (*Apodemus flavicollis*), Bank vole (*Clethrionomys glareolus*) and Vole species (*Microtus spp.*) to measure the external dose rate comparing with the predicted dose rate in the Chernobyl exclusion zone. There was poor agreement between predicted and measured dose rate because soil samples taken in the study were insufficient (Beresford, et al., 2008). TLDs also placed on small mammals (*Microtus Oeconomus*) in the exclusion zone around Chernobyl reactor. The work showed that the external doses were 1-2 orders of magnitude higher than the internal dose (Chesser, et

al., 2000). TLDs were put in animal phantom (frog) to measure the external dose comparing with the calculated dose in wetland contaminated area. The measured doses were lower than the calculated dose (Stark & Pettersson, 2008).

Furthermore, TLDs were used to relate the sediment surface activity concentration to radiation doses in Pond A, a former cooling pond of the R-reactor, at the Savannah River site in the USA (Abraham, Whicker, Hinton, & Rowan, 2000). Sub-surface in-situ measurement of gamma dose rate from Cs-137 was also measured in the Chernobyl Exclusion Zone using TLDs placed at different depth intervals in the soil (Timms, Smith, Coe, Kudelsky, & Yankov, 2005). To our knowledge, however, TLD's have not yet been used to measure in situ dose profiles in and above radioactively contaminated sediments. This study used TLDs for in-situ measurement of both beta and gamma radiation in water and lake sediment.

5.3 Methods

The design of the vertical TLD array that was used for the in-situ measurements has previously been discussed in Chapter 2, Section 2.2. In addition to the TLD measurements, sediment cores were also taken at 3 points in Svyatoye, Perstok and Dvorishche lakes next to the TLD sampling locations and near the bank.

5.3.1 Pilot study of TLD measurement method

The pilot study was performed to check the feasibility of the method before the main research was carried out. The pilot study was performed in two lakes; Svyatoye and Perstok Lake: the general description of these lakes was discussed in Chapter 1, Sections 1.51 and 1.5.2 respectively. TLD arrays were placed between 6 June and 6 September 2007 (92 days) in Svyatoye Lake (**Figure 5.1**) and between 8 June and 12 September 2007 (96 days) in Perstok Lake (**Figure 5.2**). After that period of time, the TLDs were returned to DSTL Alverstoke to measure the beta and gamma doses according to the method described in Chapter 2, Section 2.2. Six transit control TLDs (3 TLDs for total dose and 3 TLDs for gamma dose) were left outside the contaminated zone for the same period to measure the additional dose due to the transportation of the TLDs from the laboratory to the field site (in this case, transit control TLDs were kept in Minsk) and back again, as well as natural background exposure. The dose rates from the transit control dose rate were subtracted from the doses measured at the study sites.

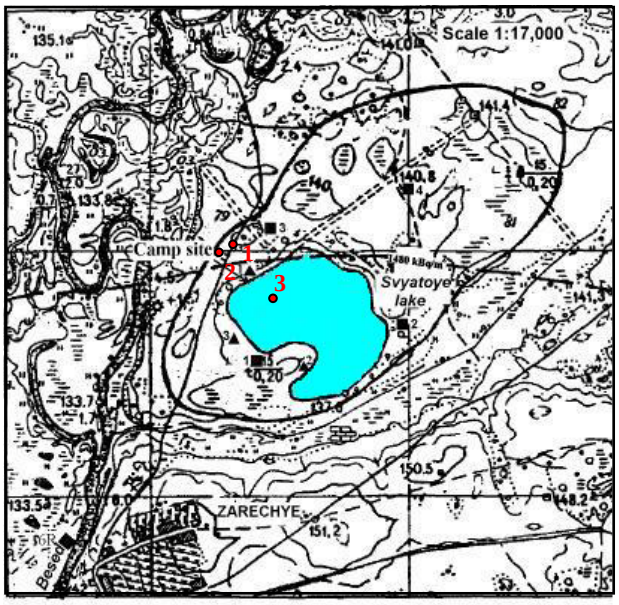

Figure 5.1 The locations of three TLD arrays that were positioned in Svyatoye lake.

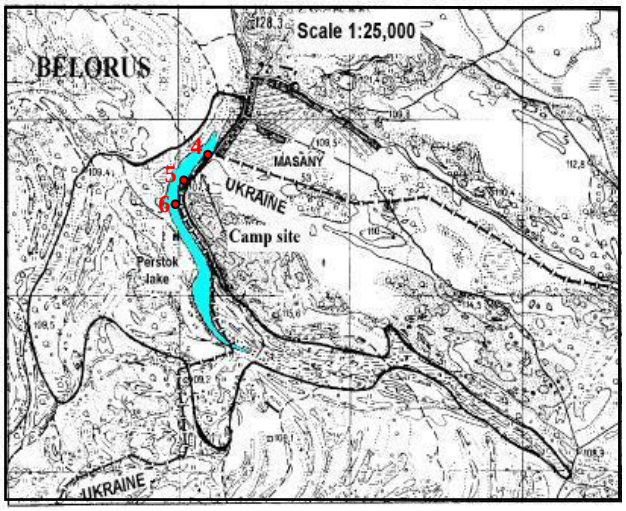

Figure 5.2 The locations of three TLD arrays that were positioned in Perstok lake.

5.3.2 Main study of TLD measurement

The pilot study and the main study were used the same design of TLD array but, for the main study, a stainless steel sleeve (**Figure 5.3**) was used to protect from smearing of the sediment in each section when TLD was driven into the sediment.

Figure 5.3 The stainless steel sleeve with (above) and without (below) TLD array.

Following the pilot study in 2007 and using the modified TLD design described above, the main study was performed to measure the in-situ external dose rate in three lakes; Svyatoye, Perstok and Dvorische lake. The additional studies at Dvorische lake were to provide a comparison with a lake of low contamination. The TLD array and the method have been described in Chapter 2, Section 2.2. TLD arrays were placed between 9 July and 8 October 2008 (91 days) in Svyatoye lake (**Figure 5.4**), 11 July and 10 October 2008 (91 days) in Perstok lake (**Figure 5.5**) and 11 July and 10 October 2008 (91 days) in Dvorische lake (**Figure 5.6**). The TLD arrays were placed near the bank in the littoral zone, which provides a key habitat for aquatic organisms. The TLD array was put into the sleeve and driven into the sediment together. After driving the apparatus in to an appropriate level, the sleeve was removed from the TLD array. As for the pilot study, six transit control TLDs (3 TLDs for total dose and 3 TLDs for gamma dose) were left in Minsk for the same period for the transit control dose rate. The dose rates from the transit control dose rate were subtracted from the doses measured at the study sites.

After that period of time, the TLDs were recovered and sent back to measure beta and gamma doses. As for the pilot study, the TLDs were provided and measured by Defence Science and Technology Laboratory (DSTL), Alverstoke according to the method described in Chapter 2, Section 2.2.

Figure 5.4 The TLD array was placed in Svyatoye lake.

Figure 5.5 The TLD array was placed in Perstok lake.

Figure 5.6 The TLD array was placed in Dvorishche lake

5.3.3 The measurement of the sediment activity concentration

Following the removal of the TLD arrays, three sediment samples were taken in each lake by workers at the Institute of Geochemistry and Geophysics in Belarus. Sediment samples were collected on 8 October 2008, 10 October 2008 and 10 October 2008 for Svyatoye, Perstok and Dvorishche lake respectively. Sediment cores were taken at 3 locations in each lake (already discussed in Chapter 2, Section 2.2) using a 35 mm internal diameter tube. The sampling points were taken close to the position of the TLD array near the lake bank in the littoral zone of the lake. The sediment samples were collected in each 5 cm vertical depth profile from sediment surface until 25 cm depth. It was not possible to export the sediment samples to the UK for analysis. Therefore, the sediment sampling analysis was carried out by Belarusian scientists according to the agreed protocol described in Chapter 2, Section 2.2. The Cs-137 activity concentrations in sediment were analysed by using Ge-Li gamma spectrometry. The Sr-90 activity concentrations in sediment were analysed by using an alpha-beta gas flow counter.

5.3.4 The dose rate from the sediment activity concentration

The beta dose rate

For the beta radiation, the sediment activity concentrations could be directly converted to a beta dose rate because the beta range in sediment is only a few centimetres. So, approximately all of the beta energy is absorbed by the sediment in each 5 cm layer. For strontium, the total average beta energy of Sr-90 and Y-90 (daughter of Sr-90) was used because Sr-90 disintegrates 0.182 MeV of beta to Y-90 and then Y-90 disintegrates 0.760 MeV of beta to Zr-90 stable nuclide (KAERI, 2000). The total average beta energy from Sr-90/Y-90 is 0.942 MeV. For Cs-137, there are two beta energies emitted from Cs-137 (0.174 MeV at 94.4% and 0.416 at 5.6%) (KAERI, 2000). Average beta energy of 0.187552 MeV was used for Cs-137 beta decay. From the average beta energy, the beta dose rate was calculated from Equation 5.1 (J. Smith, 2005).

$$E = C \times 1.6 \times 10^{-19} \Sigma_i \varepsilon_i \qquad (5.1)$$

where E is the beta dose rate (Gy s^{-1}), C is activity concentration (Bq kg^{-1}, w.w.),

ε_i is the mean energy of electron volt ($1eV=1.6x10^{-9}J$), of the i th radiation emitted when the radionuclide undergoes decay

The gamma dose rate

For gamma radiation, the sediment activity concentrations cannot be directly converted to a gamma dose rate because the gamma range in sediment is long (of order 20 cm for 0.662 MeV radiation) and so the gamma dose is dispersed into other sections of sediment. The gamma dose rate was calculated using a simple model based on the models used in ERICA, RESRAD and D-MAX.

For the gamma dose rate above the sediment, the simple estimation of dose rate assumed that the dose rate decreased with distance above the sediment according to linear attenuation of gamma energy. This leads to an over-estimate of dose rate because, in reality, the beam is not collimated since most emitted photons do not travel directly upwards. This means that attenuation in reality will be greater than that estimated by a simple linear attenuation model.

The gamma dose rate above the sediment was estimated from the estimated dose rate on the sediment surface using the known relationship of the linear attenuation of photon energy in water with distance. The dose rate on the sediment surface was estimated by using the model for benthic fish from FASSET (and ERICA), which assumes a semi-infinite distribution of radioactivity below the sediment surface:

$$D_{SS} = DCC_{ext} * [0.5.C_{water} + 0.5.C_{sed}] \quad (5.2)$$

where D_{ss} is the external dose rate on sediment surface (μGy hr^{-1}),
DCC_{ext} is the External Dose Conversion Coefficient (μGy hr^{-1} per Bq kg^{-1}),
C_{water} is water concentration (Bq l^{-1}) and
C_{sed} is sediment concentration (Bq kg^{-1} w.w.)

The Cs-137 DCC_{ext} for the infinite medium (0.662 MeV gamma only) was calculated from Equation 5.1 to be $3.81x10^{-4}$ μGy hr^{-1} per Bq kg^{-1}. In a closed lake system such as Svyatoye and Perstok lake, the water concentration declines only at a slow rate due to slow out flow rate of water from the system (Jim T. Smith, et al., 2005) and so the data from 2002-04 can be used to estimate activity concentrations in 2008. For Svyatoye, the Cs-137 concentration in water was 10.74, 9.94 and 9.77 Bq l^{-1} in 2002, 2003 and 2004 respectively (Kudelsky, et al., 2005). For Perstok, the Cs-137 concentration in water was 14.09, 19.23 and 21.94 Bq l^{-1} in 2002, 2003 and 2004 respectively (Kudelsky, et al., 2005). The average Cs-137 concentration during 2002-2004 was used in Equation 5.2 because there was no available data of the Cs-137 concentration in water in 2008. The average Cs-137 concentration in water was 10.15 and 18.42 Bq l^{-1} for Svyatoye and Perstok lake respectively. For Dvorische lake, there was only one measurement (5.02 Bq l^{-1}) of Cs-137 concentration in water in 2004 (Kudelsky, et al., 2005). For sediments, as a conservative assumption, the maximum sediment concentration in each depth profile was used in Equation 5.2. The water concentration is quite low when compared with the sediment concentration because of high Cs-137 transfer to bed sediment (Jim T. Smith, et al., 2005), so, as found in Chapter 4, the water plays no significant role in forming the external dose to benthic organisms.

The dose rate above the sediment surface was estimated from Equation 5.3

$$D_i = D_{ss}\, e^{-\mu_{en}/\rho.\rho.x_i} \quad (5.3)$$

where D_i is the dose rate above the sediment of i th position (μGy hr^{-1}),
D_{ss} is the external dose rate on sediment surface (μGy hr^{-1}),
μ_{en}/ρ is mass energy-absorption coefficient in water at 0.662 MeV (0.0326 cm^2 g^{-1}) (Hubbell & Seltzer, 2010),
ρ is density of water (1 g cm^{-3}) (Elert, 2010) and
x_i is distance from the sediment surface (cm)

The dose rate below the sediment surface was estimated from Equation 5.4

$$D_{BS} = DCC_{ext} . C_{sed} \quad (5.4)$$

where D_{BS} is the dose rate below the sediment surface (μGy hr^{-1})

The dose rate below and above the sediment surface was calculated in two ways: from both maximum sediment concentration and average sediment activity concentration in the top 15 cm.

5.4 Results

The results are divided into 4 sections; the pilot study of the TLD measurement method, the main study of TLD measurement, the sediment activity concentration measurements and the beta and gamma dose rate estimated from the sediment activity concentrations.

5.4.1 The pilot study

The pilot study was performed in two lakes (Svyatoye and Perstok) in 2007 to test the new method of beta and gamma sub surface measurement. Three TLD arrays were placed in each lake.

Svyatoye lake

The beta and gamma dose rates (after subtraction of the transit control dose rate) as a function of depth are shown in **Table 5.2** and **Figure 5.7**. The transit control dose rate for total dose (beta and gamma) and gamma dose was 1.15±0.08 and 1.09±0.05 μGy hr^{-1} respectively. **Figure 5.7** plots the beta and gamma dose rate in μGy hr^{-1} against the

depth (cm) in different sampling sites. In the depth profile, the zero point is the sediment surface. From zero point up to 25 cm is above the sediment surface, whilst from zero point down to -25 is below sediment surface. There were three different sampling sites in Svyatoye lake. The sediment types in site 1 and site 2 were silty loam, whilst site 3 was fine sand (from observation). The beta dose rate in the depth profile was quite low and there was no clear pattern of dose rate in depth profile. The negative values of beta dose rate showed that the beta dose rate was lower than the transit control dose rate. For gamma dose rate, the maximum dose rate was 2.22, 1.72 and 1.76 µGy hr^{-1} in site 1, 2 and 3 respectively at 5 cm below the sediment surface. The gamma dose rate approached zero at 25 cm above the sediment surface and increased gradually with depth to 5 cm below the sediment surface. The gamma dose rate decreased gradually from the 5 cm below the sediment surface to 25 cm below the sediment surface. In contrast, the gamma dose rate did not reach zero below the sediment. Zero gamma dose rate is expected in the very deep sediment. In the case of the dose rate in sub surface soil, the zero or negative value of dose rate was found at depths of 40-50 cm (Timms, et al., 2005).

Table 5.2 The pilot study of the beta and gamma measured dose rate after subtraction of the transit control dose rate in Svyatoye lake.

Distance (cm)	Dose rate Site 1 (µGy hr^{-1})		Dose rate Site 2 (µGy hr^{-1})		Dose rate Site3 (µGy hr^{-1})	
	Beta	Gamma	Beta	Gamma	Beta	Gamma
25	0.43	0.18	-0.02	0.08	0.01	0.09
15	0.03	0.42	-0.23	0.32	0.14	0.16
5	0.06	0.98	-0.19	0.78	-0.02	0.69
0	0.19	1.53	0.01	1.09	0.09	1.08
-5	0.13	2.22	0.08	1.72	0.03	1.76
-10	-0.17	2.20	0.30	1.54	0.37	1.60
-15	0.14	1.38	0.16	1.07	0.29	1.09
-20	0.13	0.87	0.31	0.47	0.23	0.61
-25	0.21	0.55	0.23	0.29	0.26	0.31

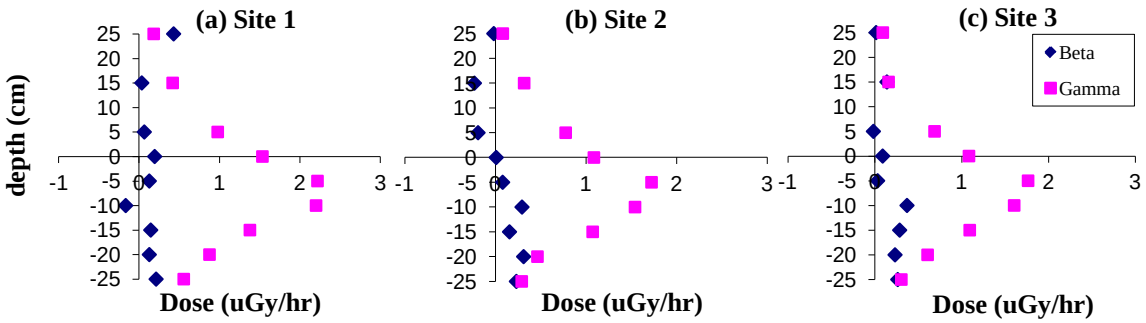

Figure 5.7 The pilot study of the dose rate in depth profile of beta and gamma radiation contamination at 3 different sites in Svyatoye lake; (a) site 1, (b) site2 and (c) site 3.

Perstok lake

For Perstok lake, the beta and gamma dose rates after subtraction of the transit control dose rate are shown as a function of depth in **Table 5.3** and **Figure 5.8**. **Figure 5.8** plots the beta and gamma dose rate in µGy hr^{-1} against the depth (cm) at the three different sampling sites. The sediment types in sites 1, 2 and 3 were silts with a high content of organic matter covered with vegetation (Kudelsky, et al., 2005). The beta dose rate in the depth profile was not quite low as in Svyatoye lake but there was again no clear pattern of dose rate with depth. For gamma dose rate, the maximum dose rate was 1.31, 0.53 and 3.64 µGy hr^{-1} in site 4, 5 and 6 respectively at the sediment surface. The gamma dose rate approached zero at 25 cm above the sediment surface and increased gradually with depth closer to the sediment surface. The gamma dose rate decreased gradually from the sediment surface to 25 cm below the sediment surface. In contrast with the Svyatoye lake, the gamma dose rate reached to zero below the sediment at site 5.

The pattern of gamma dose rate of Svyatoye and Perstok lakes was quite clear in the depth profile, which was nearly zero at 25 cm above the sediment and then increased gradually with depth to the maximum of 5 or 10 cm below the sediment surface. After that, the gamma dose rate decreased gradually to 25 cm below the sediment surface. The peak of the gamma dose rate comes from the Cs-137 accumulated at that position which transferred the gamma decay energy to the TLD. If the Cs-137 concentrations are highly accumulated, the gamma dose rate evaluated by the TLD will be high. Thus, the peak of the maximum gamma dose rate was observed at the point that there were highest accumulation concentrations of Cs-137. The dose rate profile is more spread out with depth than the profile of Cs-137 because of the several centimetres penetration of

the 0.661 MeV gamma ray in water. The pattern of beta dose rate of both lakes was not so clear in the depth profile. It should be the same as the modelled beta dose rate pattern, and the distribution of Cs-137 and Sr-90 with depth because of the low penetration of beta particles in water. But, the maximum beta dose rate in the depth profile was not found in the same position: this depends on the sediment type (this will be discussed Section 5.5.2).

Table 5.3 The pilot study of the beta and gamma measured dose rate after subtraction of the transit control dose rate in Perstok lake.

Distance (cm)	Dose rate Site 1 (µGy hr^{-1})		Dose rate Site 2 (µGy hr^{-1})		Dose rate Site3 (µGy hr^{-1})	
	Beta	Gamma	Beta	Gamma	Beta	Gamma
25	0.07	0.30	0.05	0.09	0.09	0.46
15	0.11	0.73	-0.01	0.19	2.16	1.18
5	0.37	1.12	0.17	0.53	0.04	2.63
0	0.18	1.31	0.18	0.52	1.16	3.64
-5	0.10	1.00	0.39	0.28	1.83	3.13
-10	0.24	0.66	0.31	0.16	0.96	1.72
-15	0.21	0.39	0.33	0.06	1.23	0.90
-20	1.10	0.23	0.27	0.04	2.26	0.49
-25	0.45	0.16	0.21	0.00	2.46	0.31

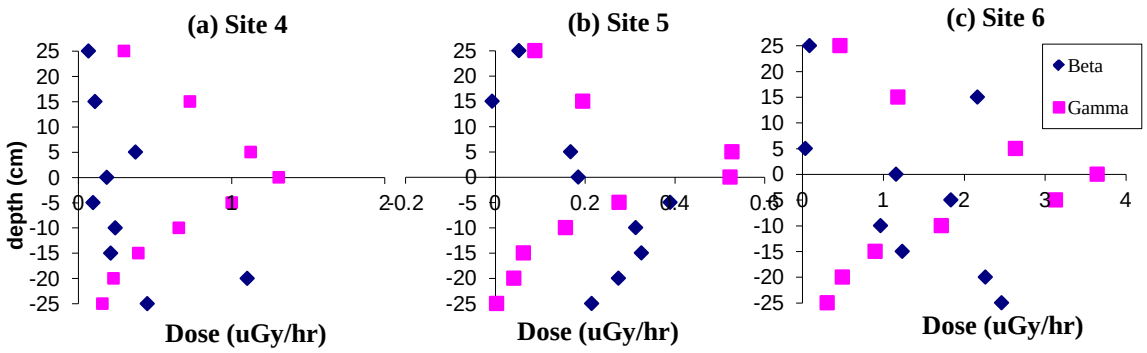

Figure 5.8 The pilot study of the dose rate depth profile of beta and gamma radiation contamination at 3 different sites in Perstok lake; (a) site 4, (b) site 5 and (c) site 6.

5.4.2 The main Study

After the pilot study, as discussed in Chapter 2, Section 2.2, the main study improved the method to drive the TLD array into the sediment by using a stainless steel sleeve to protect from smearing. It was believed that smearing of sediment may have caused the lack of any clear beta dose profile with depth in the sediment since the beta dose rate would be affected by smeared sediment close to the TLDs. The main study was performed in three lakes; Svyatoye, Perstok and Dvorische in 2008.

Svyatoye lake

The beta and gamma dose rates (after subtraction of the transit control) are shown as a function of depth in Table 5.4 and Figure 5.9. The transit control dose rate for total dose (beta and gamma) and gamma dose was 0.39±0.03 and 0.40±0.01 μGy hr^{-1} respectively. **Figure 5.9** plots the beta and gamma dose rate in μGy hr^{-1} against depth (cm) at the three different sampling sites. The sediment types at sites 1 and 2 were silty loam, whilst site 3 was fine sand (from observation). The beta dose rate in the depth profile was again quite low with no clear pattern of the dose rate as a function of depth. Negative values from the beta dose rate showed that the beta dose rate was lower than the transit control dose rate. For gamma dose rate, the maximum dose rate was 2.25 μGy hr^{-1} at 15 cm below the sediment surface at site 1, 1.56 μGy hr^{-1} at 10 cm below sediment surface at site 2 and 1.88 μGy hr^{-1} at 5 cm below the sediment surface at site 3. The gamma dose rate approached zero at 25 cm above the sediment surface and increased gradually with depth to the maximum dose rate below the sediment surface. The gamma dose rate decreased gradually from the maximum dose rate below the sediment surface to 25 cm below the sediment surface.

Table 5.4 The main study of the beta and gamma measured dose rate after subtraction of the transit control dose rate in Svyatoye lake.

Distance (cm)	Dose rate Site 1 (µGy hr^{-1})		Dose rate Site 2 (µGy hr^{-1})		Dose rate Site3 (µGy hr^{-1})	
	Beta	Gamma	Beta	Gamma	Beta	Gamma
25	-0.02	0.10	-0.03	0.07	0.01	0.14
15	-0.07	0.37	-0.04	0.21	-0.06	0.33
10	0.01	0.48	-0.01	0.36	-0.08	0.52
5	0.05	0.70	0.00	0.55	0.07	0.78
0	0.15	1.02	-0.16	0.89	0.00	1.37
-5	0.14	1.74	0.11	1.31	0.14	1.88
-10	0.62	1.85	-0.17	1.56	0.67	1.58
-15	-0.33	2.25	0.16	1.29	-0.06	1.62
-20	0.33	1.35	0.30	0.71	0.03	0.87
-25	0.00	1.40	0.10	0.45	0.11	0.68

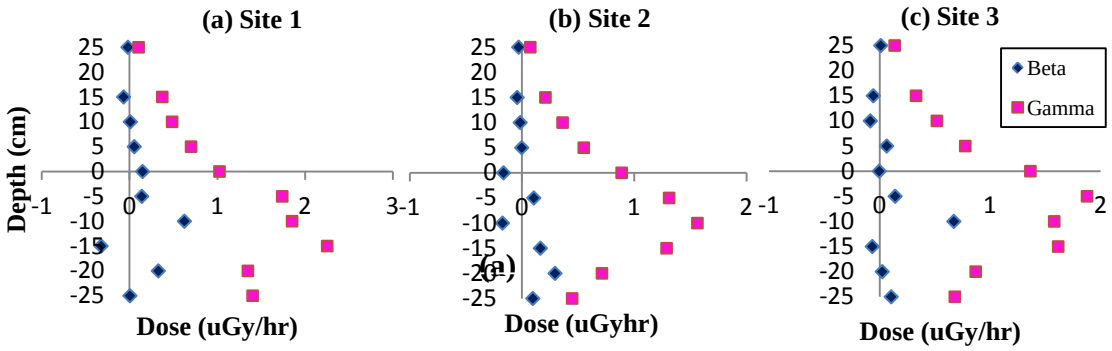

Figure 5.9 The main study of the dose rate of beta and gamma radiation as a function of depth at 3 different sites in Svyatoye lake; (a) site 1, (b) site2 and (c) site 3.

Perstok lake

For Perstok lake, the beta and gamma dose rates (after subtraction of the transit control dose rate) are shown as a function of depth in **Table 5.5** and **Figure 5.10**. **Figure 5.10** plots the beta and gamma dose rate in µGy hr^{-1} against the depth (cm) in the three

different sampling sites. The sediments at sites 4, 5 and 6 were silt with a high content of organic matter covered with vegetation (Kudelsky, et al., 2005). The beta dose rate as a function of depth was quite low, as in Svyatoye lake. There was no clear pattern of dose rate in the depth profile. For gamma dose rate, the maximum dose rate was 0.91 μGy hr^{-1} at 15 cm below the sediment surface at site 4, 1.35 μGy hr^{-1} at the sediment surface at site 5 and 2.32 μGy hr^{-1} at 5 cm below the sediment surface at site 6. The gamma dose rate did not approach zero at 25 cm above the sediment surface because the water level had decreased to 20 cm above the sediment surface when the TLD arrays were taken back, reducing the shielding effect at 25cm. The gamma dose rate increased gradually towards the sediment surface to the maximum dose rate below the sediment surface and then decreased gradually from the maximum dose rate to 25 cm below the sediment surface. In contrast, the gamma dose rate did not reach zero below the sediment except at site 5. Zero gamma dose rate is expected in the deeper sediment.

Table 5.5 The main study of the beta and gamma measured dose rate after subtraction of the transit control dose rate in Perstok lake.

Distance (cm)	Dose rate Site 1 (μGy hr^{-1})		Dose rate Site 2 (μGy hr^{-1})		Dose rate Site3 (μGy hr^{-1})	
	Beta	Gamma	Beta	Gamma	Beta	Gamma
25	0.07	0.21	0.20	0.50	0.13	0.65
15	0.03	0.18	0.06	0.55	0.08	0.81
10	-0.02	0.16	-0.03	0.67	-0.19	1.11
5	0.00	0.29	0.13	0.95	-0.47	1.61
0	-0.06	0.43	-0.04	1.35	0.00	2.17
-5	0.10	0.61	-0.03	0.93	0.34	2.32
-10	-0.06	0.82	-0.02	0.52	-0.21	2.04
-15	0.16	0.91	-0.04	0.27	-0.04	1.45
-20	0.31	0.71	-0.04	0.15	-0.01	0.83
-25	0.14	0.57	0.02	0.07	0.03	0.45

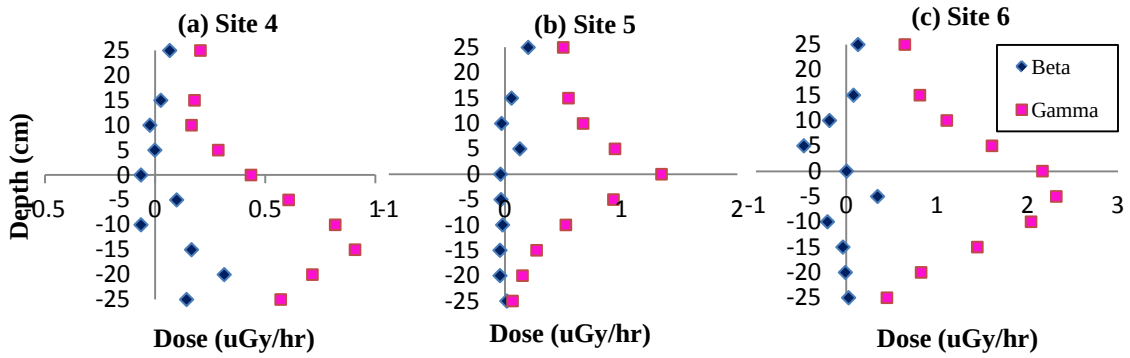

Figure 5.10 The main study of the dose rate of beta and gamma radiation as a function of depth at 3 different sites in Perstok lake; (a) site 4, (b) site 5 and (c) site 6.

Dvorishche lake

The beta and gamma dose rate for Dvorische lake was expected to be relatively low compared to the other lakes according to the data of the Cs-137 contamination density in watershed area in 1997 which was 1.368×10^9, 3.7×10^9 and 1.85×10^8 kBq km^2 in Svyatoye, Perstok and Dvorishche lake respectively (Kudelsky, et al., 2005). All the measured dose rates were lower than the transit control dose rate.

5.4.3 The measurement of the sediment activity concentration

In 2008, when the TLD arrays were recovered, three sediment cores were taken at each lake near to the position that the TLD arrays were placed. Cs-137 and Sr-90 activity concentration were analysed in each depth profile (5cm intervals) according to the methods outlined in Chapter 2, Section 2.2.

Svyatoye lake

The Cs-137 and Sr-90 sediment activity concentrations (Bq kg^{-1} d.w.) as a function of depth are shown in **Table 5.6** and **Figure 5.11**. For Cs-137, the maximum activity concentration was 83,200±2,600 Bq kg^{-1} at 0-5 cm depth at site 1, 37,300±1,200 Bq kg^{-1} at 0-5 cm depth at site 2 and 37,500±1,200 Bq kg^{-1} at 0-5 cm depth at site 3, followed by an exponential decline at greater depths. At all sites, the peak sediment activity concentration was found at 0-5 cm depth, and Site 1 showed the highest peak activity concentration compared with sites 2 and 3. For Sr-90, the maximum activity

concentration was 220±40 Bq kg^{-1} at 0-5 cm depth at site 1, 860±40 Bq kg^{-1} at 0-5 cm depth at site 2 and 100±40 Bq kg^{-1} at 5-10 cm depth at site 3, followed by an exponential decline. Site 2 showed the highest peak activity concentration depth compared with sites 1 and 3.

The Cs-137 and Sr-90 sediment activity concentration per unit volume (Bq cm^{-3}) in the depth profile are shown in **Table 5.7** and **Figure 5.12**. For Cs-137, the maximum activity concentration per unit volume was 12.82 Bq cm^{-3} at 5-10 cm depth at site 1, 14.09 Bq cm^{-3} at 0-5 cm depth at site 2 and 32.83 Bq cm^{-3} at 0-5 cm depth at site 3, followed by an exponential decline. The peak sediment activity concentration per volume was found at 5-10 cm depth at site 1 and 0-5 cm depth at site 2 and 3. The percentage of Cs-137 activity concentration found in the top 15 cm of sediment with 84.5%, 97.6% and 97.8% at sites 1, 2 and 3 respectively. For Sr-90, the maximum activity concentration per unit volume was 0.048 Bq cm^{-3} at 5-10 cm depth at site 1, 0.326 Bq cm^{-3} at 0-5 cm depth at site 2 and 0.079 Bq cm^{-3} at 5-10 cm depth at site 3, followed by an exponential decline. The percentage of Sr-90 activity concentration found in the top 15 cm of sediment was 87.2%, 92.4% and 72.4% at sites 1, 2 and 3 respectively. Site 2 showed the highest peak activity concentration per unit volume. Water content decreased and the solids density increased with sediment depth, explaining why peaks in activity per unit dry weight did not always coincide with peaks in activity per unit volume. The Sr-90 activity concentrations in sediment approximately 2 orders of magnitude lower than the Cs-137 concentrations.

From Table 5.6 and 5.7, the maximum activity concentration of the Cs-137 and Sr-90 sediment activity concentrations and the Cs-137 and Sr-90 sediment activity concentration per unit volume were at 0-5 cm depth or 5-10 cm depth and then followed by an exponential decline. However, the concentrations slightly increased again at the deepest depth, possibly because of the pre-Chernobyl accident activities; most likely nuclear weapons testing. Or, it could be due to a change in sediment type – if more clay minerals were found at this depth, a peak could be produced by accumulation of migrating Cs-137 from the surface.

Table 5.6 The Cs-137 and Sr-90 sediment activity concentration in Bq kg^{-1} d.w. as a function of depth for different sites in Svyatoye lake.

Depth (cm)	Site 1		Site 2		Site 3	
	Cs-137 Activity con. (Bq kg^{-1})	Sr-90 Activity con. (Bq kg^{-1})	Cs-137 Activity con. (Bq kg^{-1})	Sr-90 Activity con. (Bq kg^{-1})	Cs-137 Activity con. (Bq kg^{-1})	Sr-90 Activity con. (Bq kg^{-1})
0-5	83200±2600	220±40	37300±1200	860±40	37500±1200	64±6
5-10	25800±800	96±14	630±20	30±4	16700±500	100±10
10-15	2960±100	14±3	195±6	8±2	443±14	10±2
15-20	425±14	4±1	86±3	8±2	467±15	12±2
20-25	2540±80	5±1	172±6	12±3	166±5	13±2
25-30					231±7	23±4

Table 5.7 The Cs-137 and Sr-90 sediment activity concentration per unit volume (Bq cm^{-3}) as a function of depth for different sites in Svyatoye lake.

Depth (cm)	Site 1		Site 2		Site 3	
	Cs-137 Activity con. (Bq cm^{-3})	Sr-90 Activity con. (Bq cm^{-3})	Cs-137 Activity con. (Bq cm^{-3})	Sr-90 Activity con. (Bq cm^{-3})	Cs-137 Activity con. (Bq cm^{-3})	Sr-90 Activity con. (Bq cm^{-3})
0-5	5.76	0.015	14.09	0.326	32.83	0.056
5-10	12.82	0.048	0.71	0.033	13.17	0.079
10-15	3.97	0.019	0.24	0.010	0.75	0.017
15-20	0.58	0.005	0.14	0.012	0.51	0.013
20-25	3.55	0.007	0.25	0.018	0.22	0.016
25-30					0.28	0.028

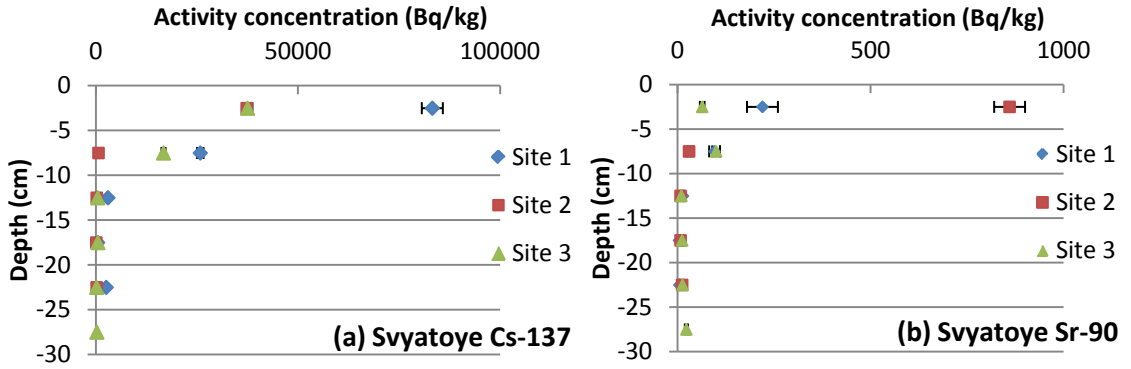

Figure 5.11 The sediment activity concentration in Bq kg^{-1} d.w. as a function of depth for different sites in Svyatoye lake; (a) Cs-137 and (b) Sr-90.

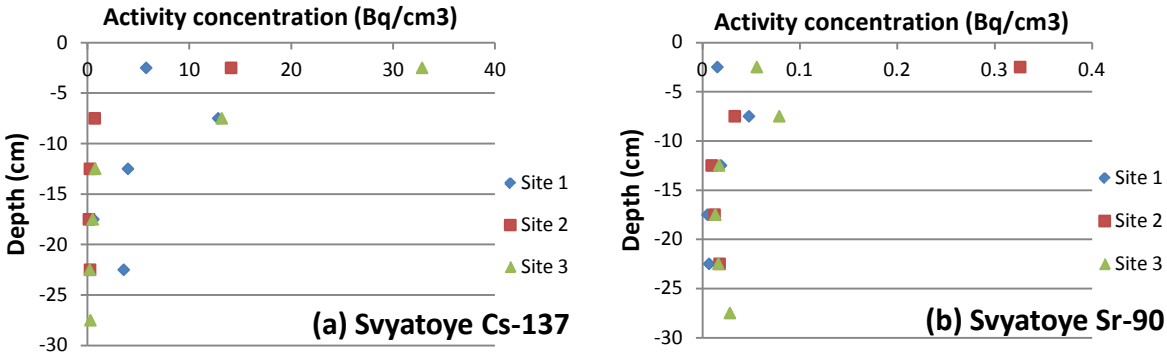

Figure 5.12 The sediment activity concentration per unit volume (Bq cm^{-3}) as a function of depth for different sites in Svyatoye lake; (a) Cs-137 and (b) Sr-90.

Perstok lake

The Cs-137 and Sr-90 sediment activity concentration (Bq kg^{-1} d.w.) as a function of depth are shown in **Table 5.8** and **Figure 5.13**. For Cs-137, the maximum activity concentration was 11,500±400 Bq kg^{-1} at 0-5 cm depth at site 4, 27,000±800 Bq kg^{-1} at 0-5 cm depth at site 5 and 27,100±900 Bq kg^{-1} at 5-10 cm depth at site 6, followed by an exponential decline. The peak sediment activity concentration was found at 0-5 cm depth at site 4 and 5, whilst at site 6 the peak was found at 5-10 cm depth. For Sr-90, the maximum activity concentration was 1,640±70 Bq kg^{-1} at 0-5 cm depth at site 4, 1,890±80 Bq kg^{-1} at 0-5 cm depth at site 5 and 1,780±70 Bq kg^{-1} at 5-10 cm depth at

site 6, followed by an exponential decline. Site 5 showed the highest peak activity concentration (at 0-5 cm depth) compared with the other sites.

The Cs-137 and Sr-90 sediment activity concentration per unit volume (Bq cm^{-3}) as a function of depth are shown in **Table 5.9** and **Figure 5.14**. For Cs-137, the maximum activity concentration per unit volume was 13.69 Bq cm^{-3} at 0-5 cm depth at site 4, 12.80 Bq cm^{-3} at 0-5 cm depth at site 5 and 17.45 Bq cm^{-3} at 5-10 cm depth at site 6, followed by an exponential decline. The percentage of Cs-137 activity concentration found in the top 15 cm of sediment was 98.8%, 98.8% and 98.5% in sites 4, 5 and 6 respectively. For Sr-90, the maximum activity concentration per unit volume was 1.957 Bq cm^{-3} at 0-5 cm depth (site 4), 0.894 Bq cm^{-3} at 0-5 cm depth (site 5) and 1.149 Bq cm^{-3} at 5-10 cm depth (site 6), followed by an exponential decline. The Sr-90 inventory in the top 15 cm of sediment was 99.3%, 99.2% and 98.6% in sites 4, 5 and 6 respectively. Water content decreased and the solids density increased with the sediment depth in Site 6. The water content approximately remained stable in Site 4 and fluctuated in Site 5. The Sr-90 concentrations in sediment were approximately 1 order of magnitude lower than Cs-137 concentration.

Table 5.8 The Cs-137 and Sr-90 sediment activity concentration in Bq kg^{-1} d.w. as a function of depth for different sites in Perstok lake.

Depth (cm)	Site 4		Site 5		Site 6	
	Cs-137 Activity con. (Bq kg^{-1})	Sr-90 Activity con. (Bq kg^{-1})	Cs-137 Activity con. (Bq kg^{-1})	Sr-90 Activity con. (Bq kg^{-1})	Cs-137 Activity con. (Bq kg^{-1})	Sr-90 Activity con. (Bq kg^{-1})
0-5	11500±400	1640±70	27000±800	1890±80	23800±800	1590±60
5-10	3230±100	1110±40	1860±60	61±6	27100±900	1780±70
10-15	213±7	91±9	397±12	10±2	1050±30	120±20
15-20	47±2	8±2	84±3	4±1	382±12	18±4
20-25	150±5	14±3	320±10	15±4	84±3	10±2

Table 5.9 The Cs-137 and Sr-90 sediment activity concentration per unit volume (Bq cm^{-3}) as a function of depth for different sites in Perstok lake.

Depth (cm)	Site 4		Site 5		Site 6	
	Cs-137 Activity con. (Bq cm^{-3})	Sr-90 Activity con. (Bq cm^{-3})	Cs-137 Activity con. (Bq cm^{-3})	Sr-90 Activity con. (Bq cm^{-3})	Cs-137 Activity con. (Bq cm^{-3})	Sr-90 Activity con. (Bq cm^{-3})
0-5	13.69	1.957	12.80	0.894	11.01	0.667
5-10	3.78	1.303	1.87	0.061	17.45	1.149
10-15	0.26	0.110	0.30	0.007	0.77	0.089
15-20	0.06	0.009	0.04	0.002	0.38	0.017
20-25	0.16	0.015	0.14	0.006	0.08	0.009

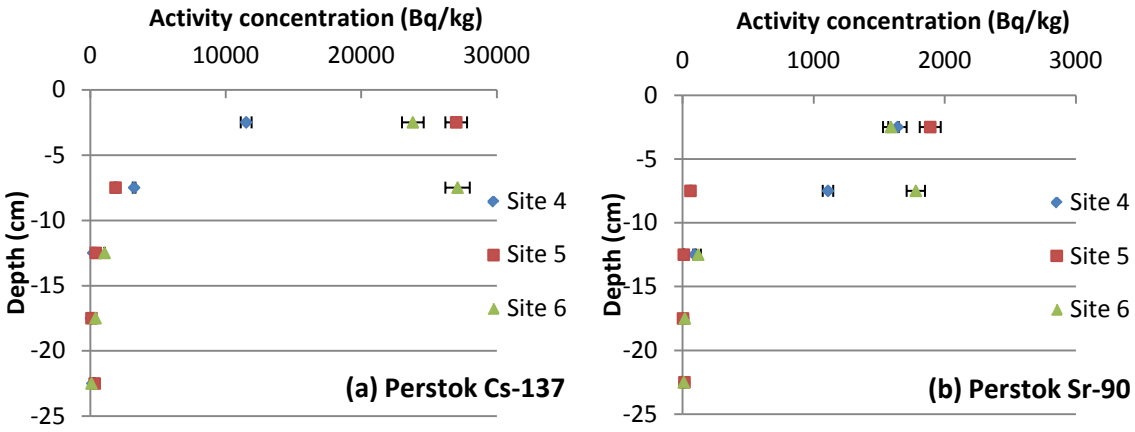

Figure 5.13 The sediment activity concentration in Bq kg^{-1} d.w. as a function of depth for different sites in Perstok lake; (a) Cs-137 and (b) Sr-90.

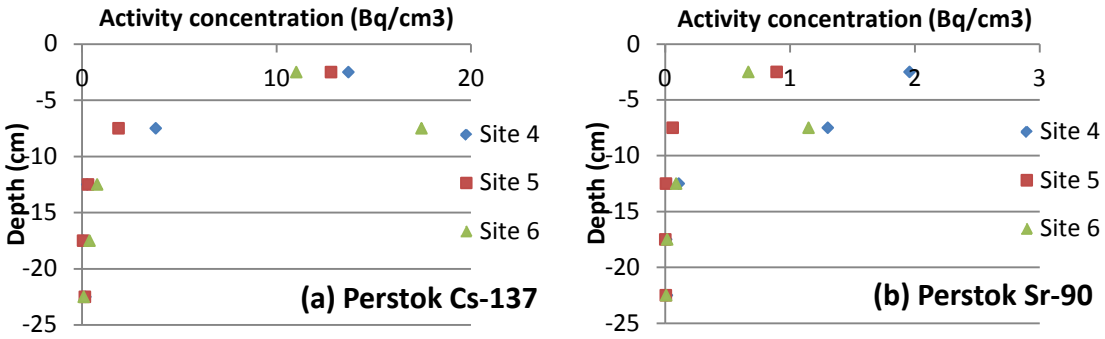

Figure 5.14 The sediment activity concentration per volume (Bq cm^{-3}) as a function of depth for different sites in Perstok lake; (a) Cs-137 and (b) Sr-90.

Dvorische Lake

The Cs-137 and Sr-90 sediment activity concentration (Bq kg^{-1} d.w.) as a function of depth are shown in **Table 5.10** and **Figure 5.15**. For Cs-137, the maximum activity concentration was 750±20 Bq kg^{-1} at 0-5 cm depth at site 7, 1,050±30 Bq kg^{-1} at 5-10 cm depth at site 8 and 1,410±40 Bq kg^{-1} at 0-5 cm depth at site 9, followed by an exponential decline. The peak sediment activity concentration was found at 0-5 cm depth at site 7 and 9, whilst at site 8 the peak was found at 5-10 cm depth. Site 9 showed the highest peak activity concentration (at 0-5 cm depth) compared with site 7 and 8. For Sr-90, the maximum activity concentration was 11±3 Bq kg^{-1} at 0-5 cm depth (site 7), 260±50 Bq kg^{-1} at 0-5 cm depth in site 8 and 18±7 Bq kg^{-1} at 0-5 cm depth (site 9), followed by an exponential decline. Site 8 showed a very high peak activity concentration (at 0-5 cm depth) compared with sites 7 and 9. The Sr-90 sediment concentration was quite low compared with the other lakes. The activity reached to zero in the deep sediment.

The Cs-137 and Sr-90 sediment activity concentration per unit volume (Bq cm^{-3}) as a function of depth are shown in Table 5.11 and Figure 5.16. For Cs-137, the maximum activity concentration per unit volume was 0.59 Bq cm^{-3} at 0-5 cm depth (site 7), 0.15 Bq cm^{-3} at 0-5 cm depth (site 8) and 0.10 Bq cm^{-3} at 0-5 cm depth (site 9), followed by an exponential decline. The peak sediment activity concentration per unit volume was found at 0-5 cm depth in all sites. The Cs-137 activity found in the top 15 cm of sediment was 99.2%, 79% and 85% in sites 7, 8 and 9 respectively. For Sr-90, the maximum activity concentration per unit volume was 0.009 Bq cm^{-3} at 0-5 cm depth

(site 7), 0.044 Bq cm^{-3} at 0-5 cm depth (site 8) and 0.001 Bq cm^{-3} at 0-5 cm depth (site 9), followed by an exponential decline. The Sr-90 activity found in the top 15 cm of sediment with almost 100% at all sites. Site 8 showed the highest peak activity concentration per unit volume (at 0-5 cm depth) compared with sites 7 and 9. The Sr-90 concentrations in sediment were approximately 1 order of magnitude lower than Cs-137 concentrations.

Table 5.10 The Cs-137 and Sr-90 sediment activity concentration in Bq kg^{-1} d.w. as a function of depth for different sites in Dvorische lake.

Depth (cm)	Site 7		Site 8		Site 9	
	Cs-137 Activity con. (Bq $kg^{-1)}$	Sr-90 Activity con. (Bq kg^{-1})	Cs-137 Activity con. (Bq kg^{-1})	Sr-90 Activity con. (Bq kg^{-1})	Cs-137 Activity con. (Bq kg^{-1})	Sr-90 Activity con. (Bq kg^{-1})
0-5	750±20	11±3	840±30	260±50	1410±40	18±7
5-10	570±20	4±1	1050±30	32±10	870±30	
10-15	106±3	5±1	790±30		890±30	<0.9
15-20	8.3±0.3	<0.6	580±20	12±4	177±6	
20-25	15.7±0.6		440±20		104±3	

Table 5.11 The Cs-137 and Sr-90 sediment activity concentration per unit volume (Bq cm^{-3}) as a function of depth for different sites in Dvorische lake.

Depth (cm)	Site 7		Site 8		Site 9	
	Cs-137 Activity con. (Bq cm^{-3})	Sr-90 Activity con. (Bq cm^{-3})	Cs-137 Activity con. (Bq cm^{-3})	Sr-90 Activity con. (Bq cm^{-3})	Cs-137 Activity con. (Bq cm^{-3})	Sr-90 Activity con. (Bq cm^{-3})
0-5	0.59	0.009	0.15	0.044	0.10	0.001
5-10	0.38	0.003	0.12	0.003	0.06	
10-15	0.04	0.002	0.04		0.08	<0.001
15-20	0.01	<0.001	0.07	0.002	0.03	
20-25	0.01		0.01		0.01	

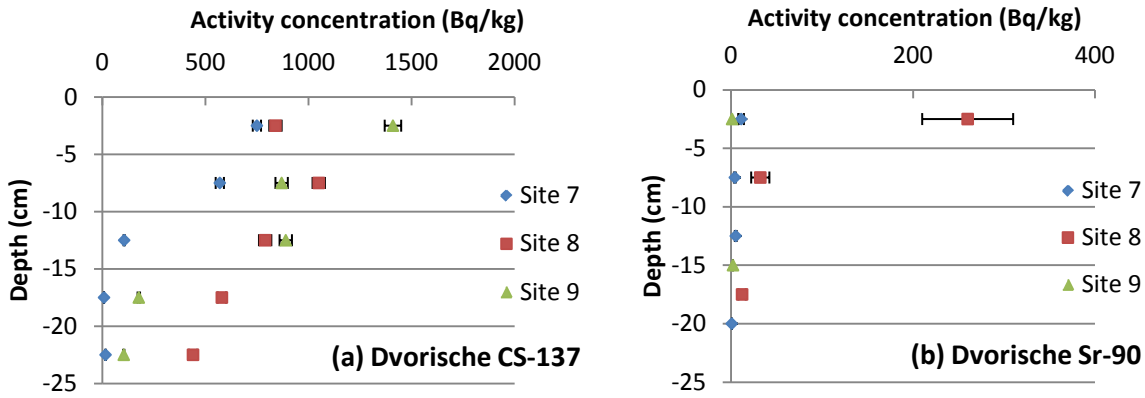

Figure 5.15 The sediment activity concentration in Bq kg^{-1} d.w. as a function of depth for different sites in Dvorische lake; (a) Cs-137 and (b) Sr-90.

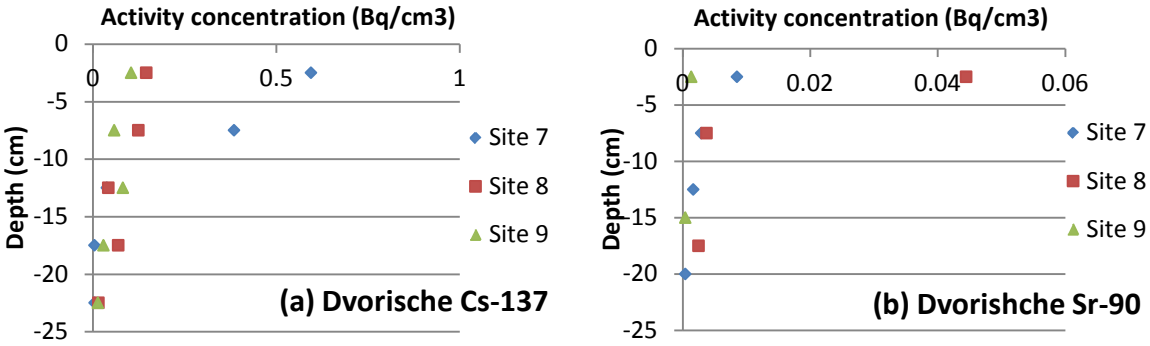

Figure 5.16 The sediment activity concentration per volume (Bq cm^{-3}) as a function of depth for different sites in Dvorische lake; (a) Cs-137 and (b) Sr-90.

5.4.4 The beta and gamma dose rate estimated from sediment activity concentration.

From the results of the Cs-137 and Sr-90 sediment activity concentrations, the gamma and beta dose rate were predicted for comparison with the dose-rate measurements. As described in the Methods Section, the beta dose rate can be directly calculated from the sediment activity concentration. The gamma dose rate can be estimated by using the DCC and FASSET/ERICA model assumptions.

Estimation of the beta dose rate

The total beta dose rate was calculated from the Sr-90 and Cs-137 beta dose rate. The beta dose rate was performed in three lakes; Svyatoye, Perstok and Dvorische.

Svyatoye lake

The beta dose rate predicted from sediment activity concentration (Bq kg^{-1} w.w.) as a function of depth at different sites is shown in **Table 5.12** and **Figure 5.17**. **Figure 5.17** plots the beta dose rate from Sr-90, Cs-137 and total dose against the depth (cm) at the different sampling sites. The beta dose rate from Sr-90 was lower than the beta dose rate from Cs-137 even though the beta energy from Sr-90 (1.18 MeV) is higher than Cs-137 (0.187552 MeV) because the amount of Cs-137 contained in the sediment was much higher than Sr-90. Therefore the total beta dose rate mostly came from the Cs-137 beta. The peak beta dose rate was 1.368 µGy hr^{-1} at 5-10 cm depth at Site 1, 1.434 µGy hr^{-1} at 0-5 cm depth at Site 2 and 2.219 µGy hr^{-1} at 0-5 cm depth at Site 3.

Table 5.12 The estimated beta dose rate as a function of depth at different sites in Svyatoye lake.

Depth (cm)	Site 1 (µGy hr^{-1})			Site 2 (µGy hr^{-1})			Site 3 (µGy hr^{-1})		
	Sr-90	Cs-137	Total	Sr-90	Cs-137	Total	Sr-90	Cs-137	Total
-2.5	0.016	1.161	1.177	0.146	1.258	1.405	0.019	2.196	2.215
-7.5	0.025	1.338	1.363	0.012	0.051	0.063	0.024	0.811	0.835
-12.5	0.006	0.242	0.248	0.003	0.017	0.020	0.004	0.039	0.043
-17.5	0.002	0.037	0.039	0.004	0.008	0.012	0.005	0.040	0.046
-22.5	0.002	0.226	0.228	0.006	0.016	0.022	0.005	0.013	0.018
-27.5							0.009	0.019	0.028

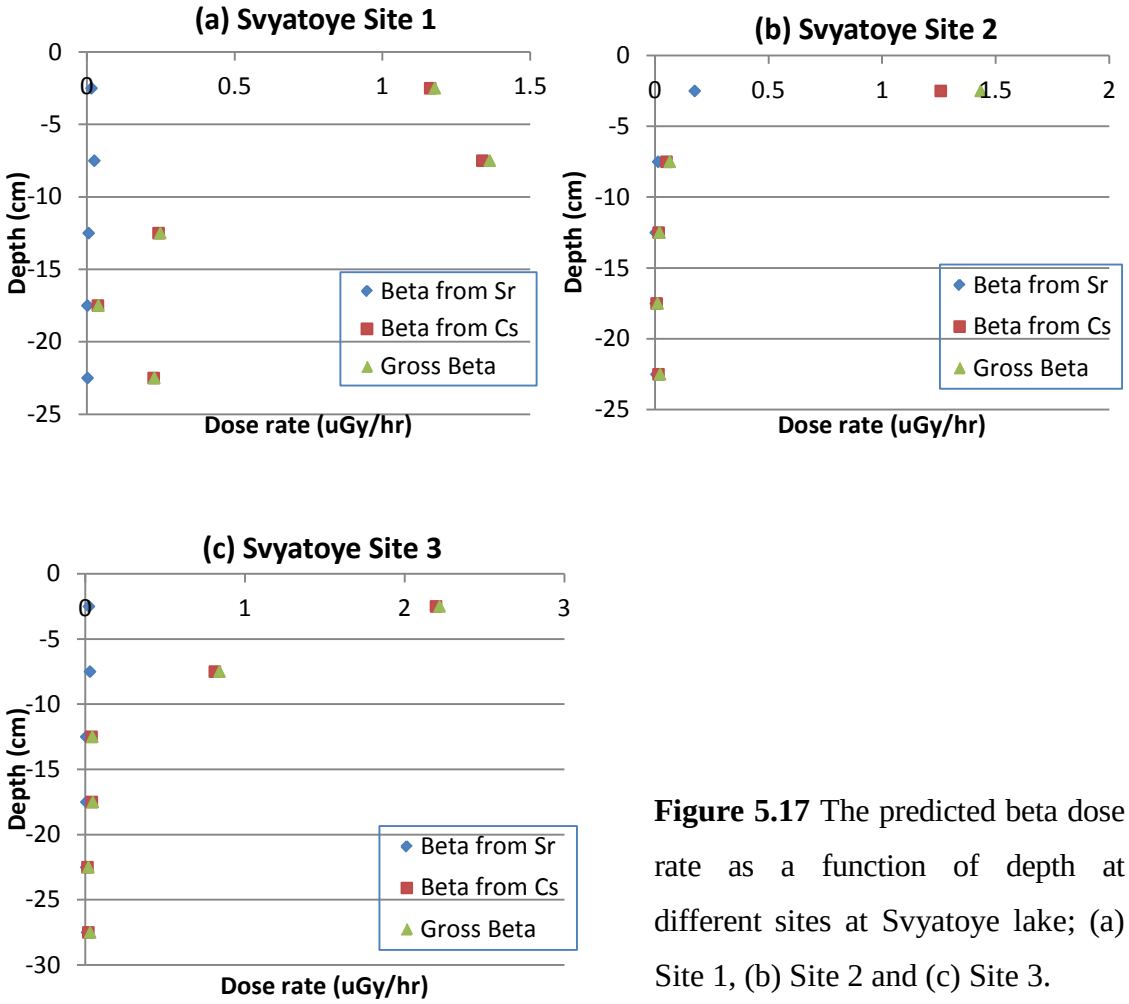

Figure 5.17 The predicted beta dose rate as a function of depth at different sites at Svyatoye lake; (a) Site 1, (b) Site 2 and (c) Site 3.

Perstok lake

The beta dose rate predicted from sediment activity concentration (Bq kg^{-1} w.w.) in the depth profile at different sites is shown in **Table 5.13** and **Figure 5.18**. The peak beta dose rate was predicted to be 1.379 µGy hr^{-1} at 0-5 cm depth (Site 4), 1.428 µGy hr^{-1} at 0-5 cm depth (Site 5) and 1.895 µGy hr^{-1} at 5-10 cm depth (Site 6).

Table 5.13 The estimated beta dose rate as a function of depth at different sites in Perstok lake.

Depth (cm)	Site 4 (µGy hr^{-1})			Site 5 (µGy hr^{-1})			Site 6 (µGy hr^{-1})		
	Sr-90	Cs-137	Total	Sr-90	Cs-137	Total	Sr-90	Cs-137	Total
-2.5	0.532	0.741	1.273	0.352	1.005	1.358	0.303	0.997	1.300
-7.5	0.426	0.246	0.673	0.023	0.138	0.160	0.449	1.357	1.805
-12.5	0.038	0.018	0.056	0.004	0.029	0.032	0.043	0.073	0.116
-17.5	0.003	0.004	0.008	0.001	0.005	0.006	0.007	0.032	0.040
-22.5	0.006	0.012	0.018	0.003	0.014	0.017	0.004	0.007	0.011

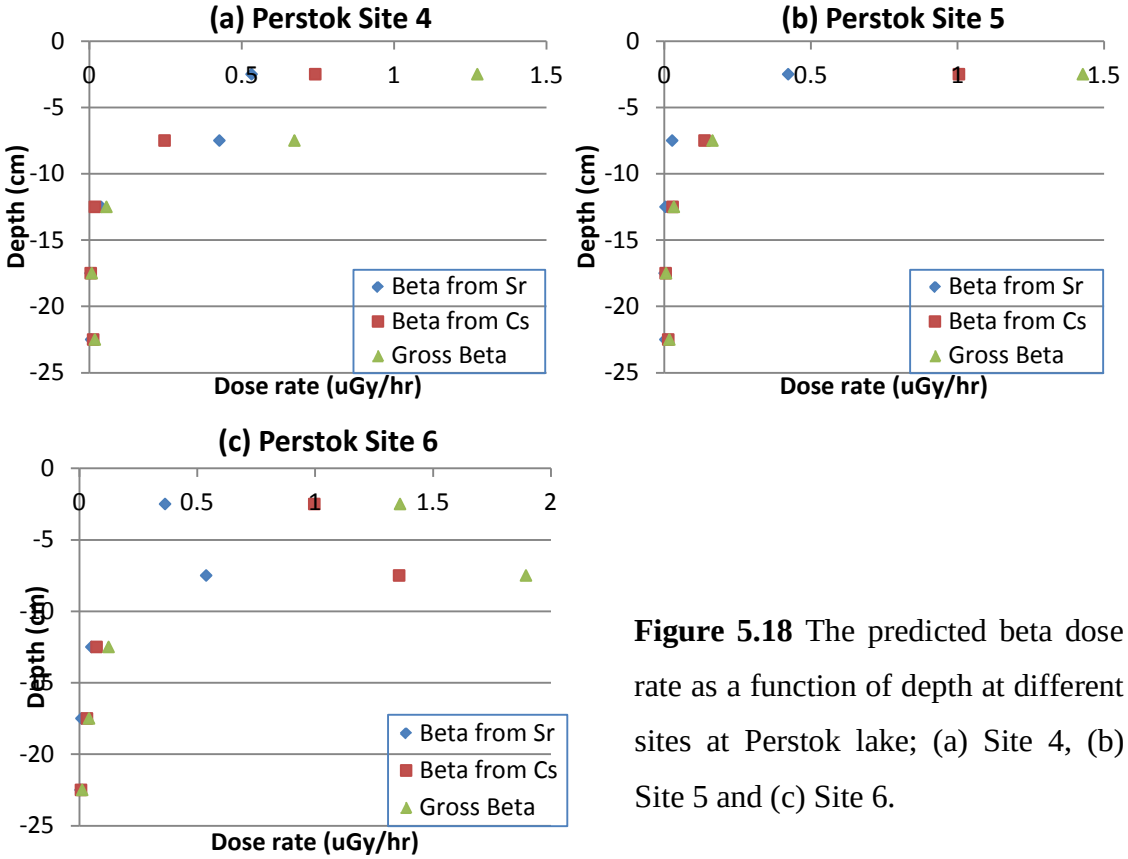

Figure 5.18 The predicted beta dose rate as a function of depth at different sites at Perstok lake; (a) Site 4, (b) Site 5 and (c) Site 6.

Dvorische lake

The beta dose rate predicted from the sediment activity concentration (Bq kg^{-1} w.w.) in the depth profile at different sites is shown in **Table 5.14** and **Figure 5.19**. The peak beta dose rate was 0.049 µGy hr^{-1} at 0-5 cm depth in Site 7, 0.146 µGy hr^{-1} at 0-5 cm depth in Site 8 and 0.022 µGy hr^{-1} at 0-5 cm depth in Site 9. As expected from the much lower Sr-90 and Cs-137 activity concentrations, the beta dose rate in Dvorische

lake is very low in comparison with Svyatoye and Perstok lake because of the rainfall pattern during the accident.

Table 5.14 The estimated beta dose rate as a function of depth at different sites in Dvorische lake.

Depth (cm)	Site 7 (μGy hr^{-1})			Site 8 (μGy hr^{-1})			Site 9 (μGy hr^{-1})		
	Sr-90	Cs-137	Total	Sr-90	Cs-137	Total	Sr-90	Cs-137	Total
-2.5	0.003	0.045	0.048	0.079	0.051	0.131	0.001	0.021	0.022
-7.5	0.001	0.034	0.035	0.005	0.030	0.035		0.015	
-12.5	0.001	0.004	0.005		0.010		0.002	0.018	0.012
-17.5		0.000		0.001	0.012	0.012		0.007	
-22.5	0.000	0.001	0.001		0.007			0.004	

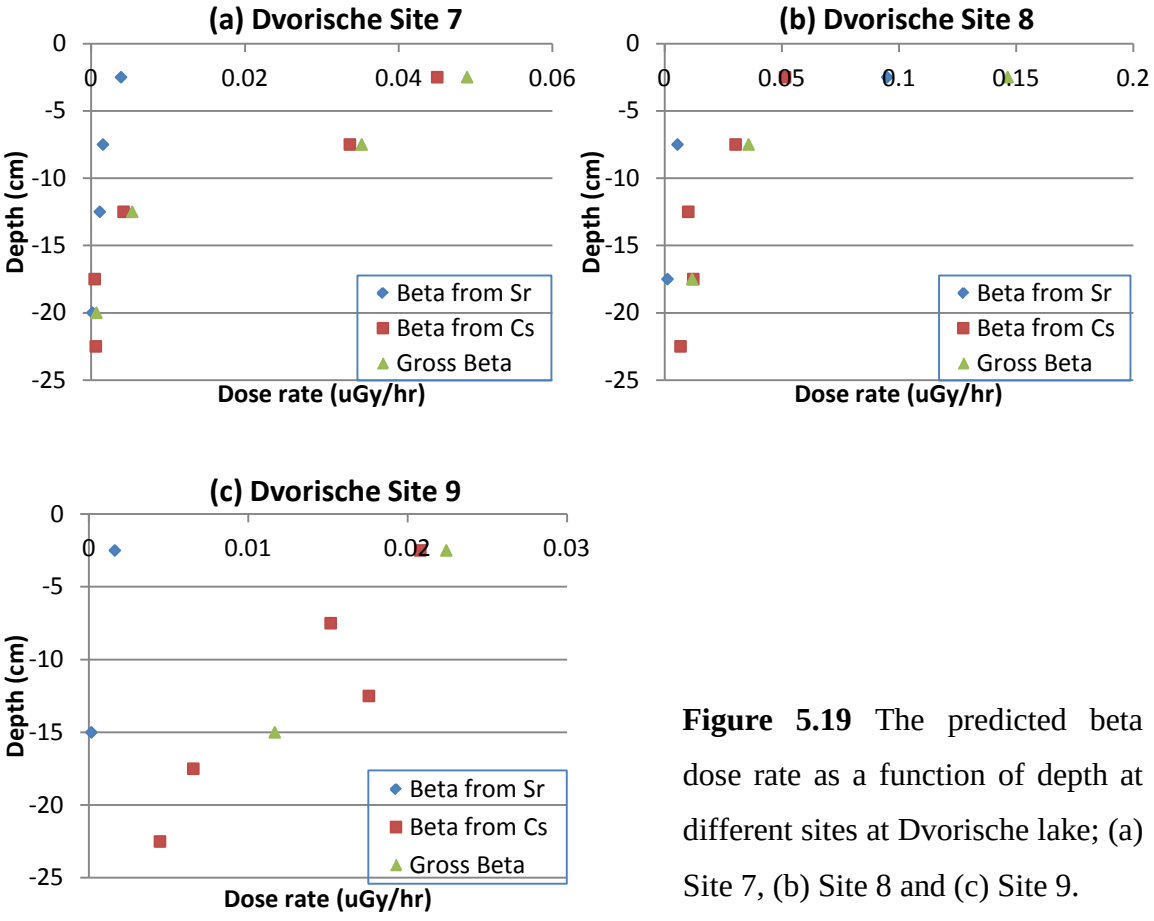

Figure 5.19 The predicted beta dose rate as a function of depth at different sites at Dvorische lake; (a) Site 7, (b) Site 8 and (c) Site 9.

The gamma dose rate

The gamma dose rate above the sediment surface was predicted from the attenuation function from the dose rate on the sediment surface , whilst the gamma dose rate on the sediment surface was predicted from the water and sediment concentration (Bq kg^{-1} w.w.) assuming a semi-infinite distribution of activity in water and sediment. The gamma dose rate above, on and below the sediment surface was calculated using both the maximum and the average top 15 cm sediment concentration (Bq kg^{-1} w.w.). This gave information on whether, for assessments, it would be better to use the maximum measured activity concentration, or the average. The gamma dose rate estimate was performed in three lakes; Svyatoye, Perstok and Dvorische lake.

Svyatoye lake

The gamma dose rates above the sediment, on the sediment and below the sediment (maximum and average sediment concentration) in different sites are shown in **Figure 5.20** which plots the dose rate in µGy hr^{-1} against depth in cm. The gamma dose rate on the sediment surface in Svyatoye lake was estimated to be between 2.2 and 3.9 µGy hr^{-1} for the maximum sediment concentration and 0.8 and 1.8 µGy hr^{-1} for the average sediment concentration. The highest estimated gamma dose rate on the sediment surface was on Site 3 (3.9 µGy hr^{-1}). The gamma dose rate above the sediment surface declined with the distance from the sediment surface. The gamma dose rate below the sediment surface predicted based on the maximum sediment concentration was between 4.4 to 7.8 µGy hr^{-1}.

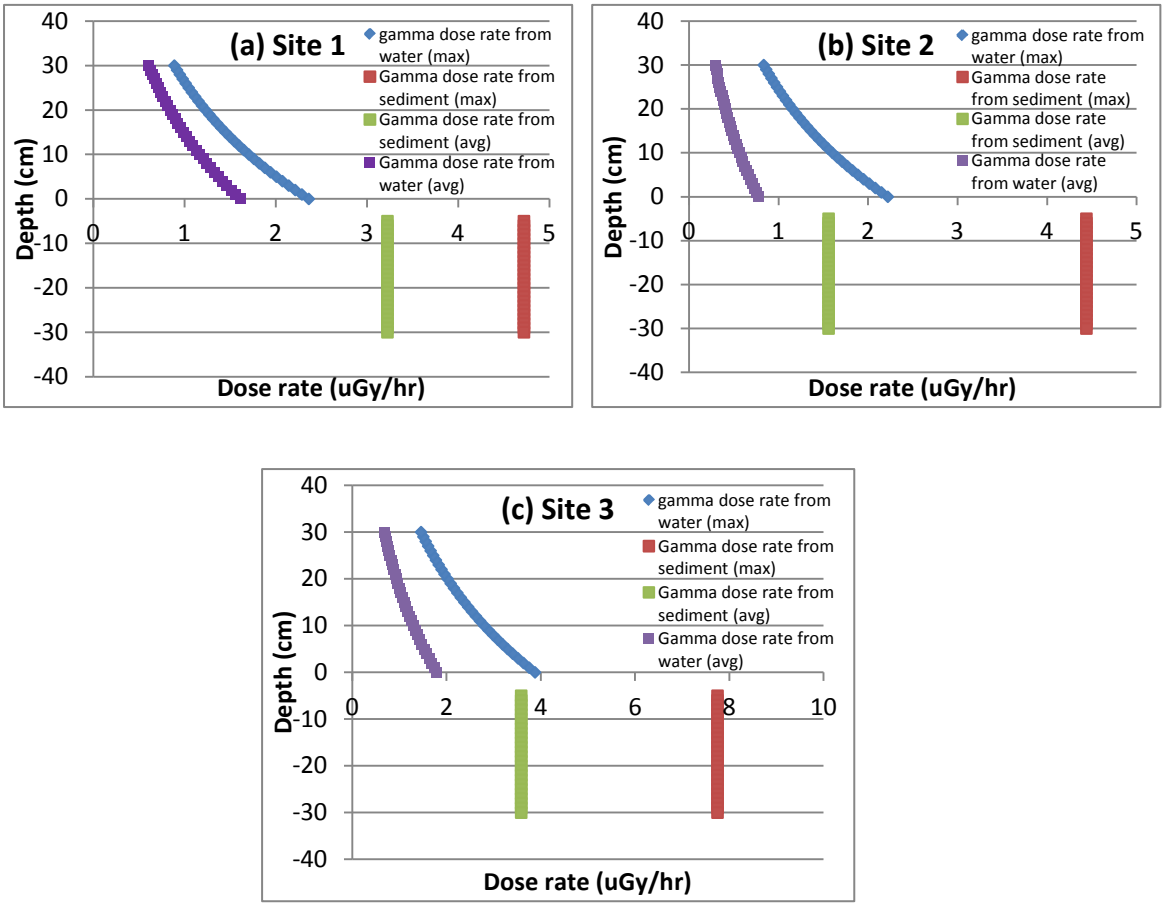

Figure 5.20 The predicted gamma dose rate for sediment and water (maximum and average) as a function of depth at different sites at Svyatoye lake; (a) Site 1, (b) Site 2 and (c) Site 3.

Perstok Lake

The gamma dose rates above the sediment, on the sediment and below the sediment (maximum and average sediment concentration) in different sites are shown in **Figure 5.21** which plots the dose rate in µGy hr^{-1} against depth in cm. The gamma dose rate on the sediment surface in Perstok lake was estimated to be between 1.3 and 2.4 µGy hr^{-1} for the maximum sediment concentration and 0.6 and 1.4 µGy hr^{-1} for the average sediment concentration. The highest gamma dose rate on the sediment surface was at Site 6 (2.4 µGy hr^{-1}). The gamma dose rate above the sediment surface declined with the distance from the sediment surface. The gamma dose rate below the sediment surface predicted from the maximum sediment concentration was between 2.62 and 4.79 µGy hr^{-1} at the three different sites.

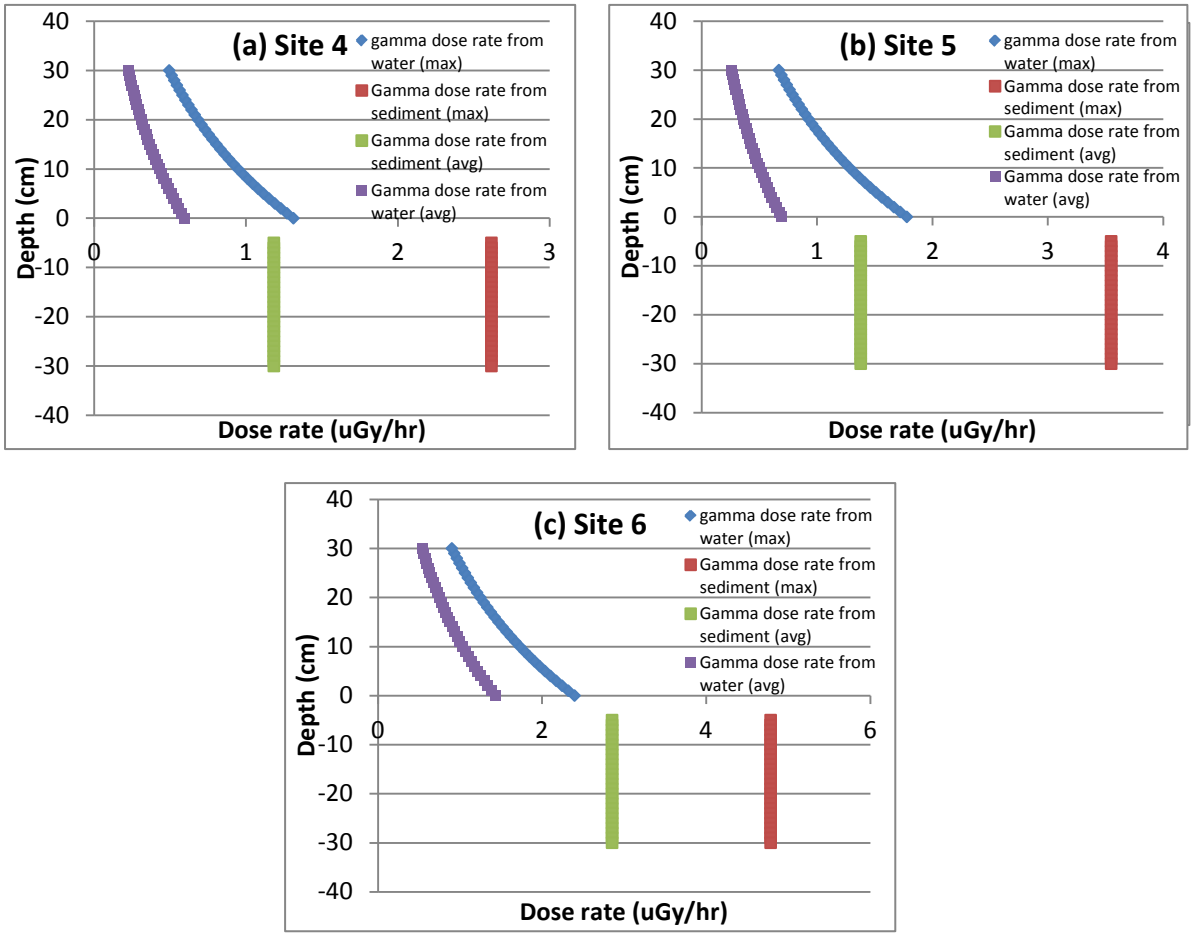

Figure 5.21 The predicted gamma dose rate for sediment and water (maximum and average) as a function of depth at different sites at Perstok lake; (a) Site 4, (b) Site 5 and (c) Site 6.

Dvorische Lake

The gamma dose rates above the sediment, on the sediment and below the sediment (maximum and average sediment concentration) at different sites are shown in **Figure 5.22** which plots the dose rate in µGy hr^{-1} against depth in cm. The gamma dose rate on the sediment surface in Dvorische lake was between 0.04 and 0.09 µGy hr^{-1} for the maximum sediment concentration and 0.03 and 0.06 µGy hr^{-1} for the average sediment concentration. The predicted gamma dose rate above the sediment surface declined with distance from the sediment surface. The gamma dose rate below the sediment surface predicted using the maximum sediment concentration was between 0.07 to 0.18 µGy hr^{-1}.

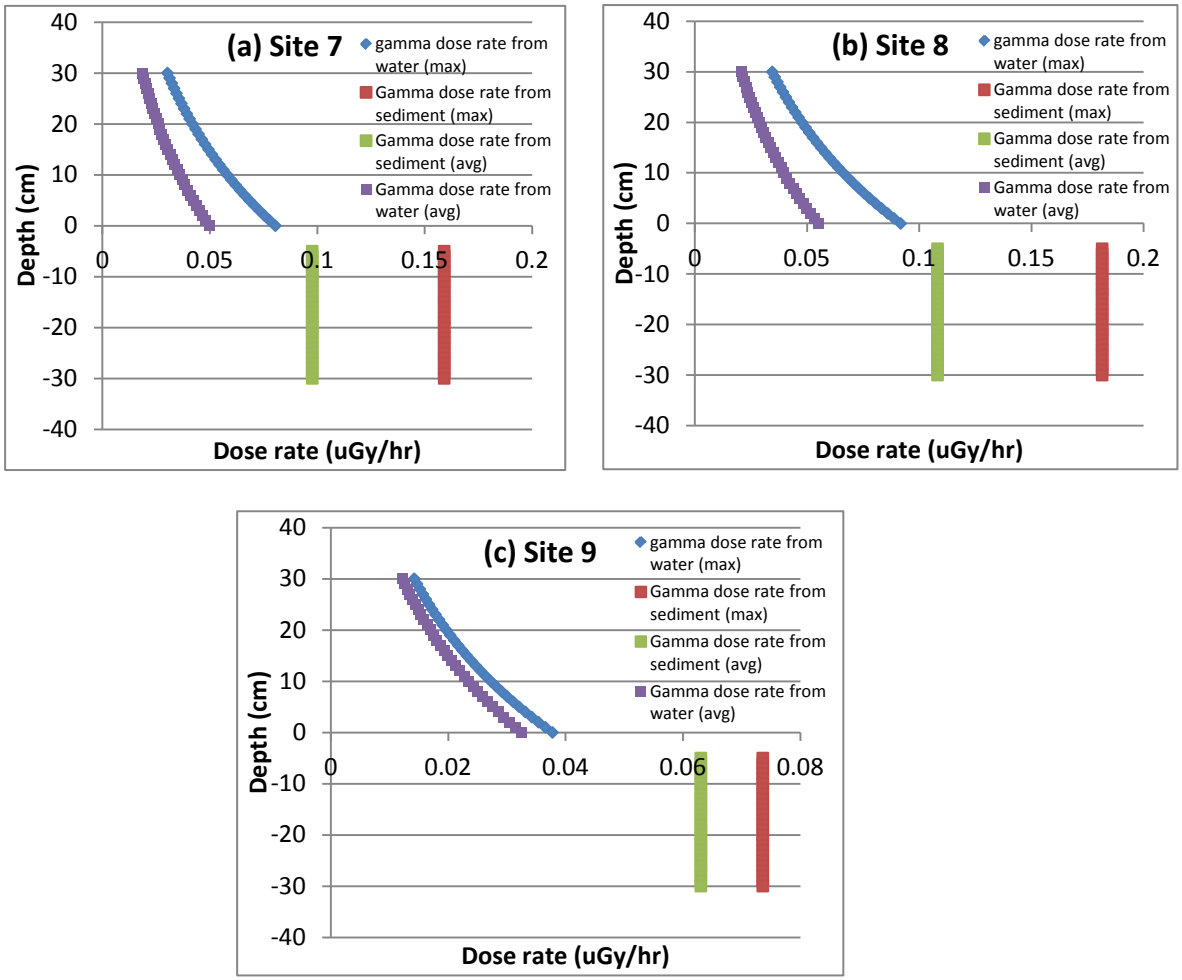

Figure 5.22 The predicted gamma dose rate for sediment and water (maximum and average) as a function of depth at different sites at Dvorische lake; (a) Site 7, (b) Site 8 and (c) Site 9.

5.5 Discussion

5.5.1 The measured in situ gamma and beta dose rate as a function of depth

A literature review found that few studies have used TLDs to determine the radiation dose on/below the sediment. Abraham, et al., (2000) calculated the exposure rate from the sediment of Pond A, a former Savannah River Site cooling pond for R-reactor, which was contaminated with Cs-137. These workers used two types of TLDs (UD-802 and CaF_2) and compared the measurements with the mean exposure dose rate calculated from sediment data. The mean exposure dose rate calculated from the sediment (69 µR hr^{-1}) was over-estimated in comparison with the estimation from the UD-802 (40 µR hr^{-1}) and CaF_2 (64 µR hr^{-1}) because the core sampling bias formed by a high density of

tree stamps and roots (Abraham, et al., 2000). In a literature search, no studies were found which measured the beta dose rate in the sediment depth profile.

The pilot study carried out in 2007 at three different sites in Svyatoye and Perstok lakes found that the maximum gamma dose rates were at 5 cm depth below the sediment surface in Svyatoye lake and at the sediment surface in Perstok lake. The maximum gamma dose rates in Svyatoye lake were approximately 2 μGy hr^{-1}, whilst the maximum gamma dose rates at Perstok Lake were more variable (around 0.6 – 4 μGy hr^{-1}). The beta dose rates, in contrast to the gamma dose, did not show any clear pattern with depth and were much lower. For Perstok lake, the beta dose rates were higher than the beta dose rates from Svyatoye lake (as expected from the distance from Chernobyl, (Mück, et al., 2002)) but still did not show a consistent pattern with depth. The beta dose rates were scattered and disordered along the depth profile (**Figure 5.8**).

From the pilot study, the scattered pattern of the beta dose rate was observed. To prevent the scatter of the beta dose, the main study was performed in summer 2008 using the same design of TLD arrays but with the stainless steel sleeve to protect the smearing when drive the TLD arrays to the sediment (discussed in Chapter 2, Section 2.2). The main study was performed at three different sites in three lakes; Svyatoye, Perstok and Dvorische. Dvorische lake was used for the control lake because of low contamination density in watershed area (Kudelsky, et al., 2005). The measurement of beta dose rates in all three lakes was not successful even following the improvement of instrument used in the main study. The beta dose rates still did not show any clear pattern with depth for several reasons; 1). The beta dose rates were quite low and close to the background dose rate. This may be because of the low beta dose rate in the lake sediment, as shown by the calculated beta dose rates. It would have been better to change the type of the TLDs to calcium based TLDs because they are more sensitive than the lithium based TLDs (Furetta, 2003; IAEA & ANSTO, 2004; McKinlay, 1981). 2) The problem of design of the instrument. The TLD array was designed to make holes with 1 cm depth for measuring beta dose rates. Beta radiation, which is short range, cannot travel to the TLD in some directions because of the collimating effect of the TLD array. It would have been better to have made separate TLD arrays for gamma and beta measurement. The thickness of the beta TLD array should be thin as possible to prevent the collimating effect 3) The TLD did not have proper contact with the sediment. This may be because bubbles in the shield holes were produced when the

TLD array was driven to the sediment. The solution is the same as 2: a thinner array. 4) The failure of the dosimetry method underwater. The measurement of beta dose rate using TLDs may have failed because the protective plastic sachet, necessary to make the TLDs waterproof, is also shielding for beta.

For the gamma dose rate, the maximum dose rates (approximately 2 μGy hr^{-1}) were found between 5 and 15 cm depth below the sediment surface in Svyatoye lake. The maximum dose rates in Perstok lake were more variable than Svyatoye lake (1 – 2 μGy hr^{-1}) at 0 – 15 cm depth below the sediment surface. The maximum gamma dose rates and the vast majority of Cs-137 contamination were found in the top 15 cm depth sediment surface in both lakes. The gamma dose rate approached to zero in the deeper sediment. There is uncertainty over the position of the zero point in the depth profiles, since high vegetation above the sediment surface was found in some sites (Site 1 and 2 in Svyatoye lake and all sites in Perstok lake). This may have caused wrong mapping of the TLDs array position compared to the activity-depth profile. TLDs are an effective way for measuring in situ dose without the medium (soil or sediment) sampling and modelling calculation (Timms, et al., 2005). This study is the first in situ beta and gamma measurement of dose rates below the sediment surface. The estimation of the maximum gamma dose rate was found in the top 15 cm depth in both lakes. But, further work on the method of measurement of beta dose rate is needed. TLDs can also be used to predict the vertical migration of radionuclide. Therefore, TLDs can be used to estimate spatial pattern of radionuclide (Abraham, et al., 2000).

5.5.2 The Cs-137 and Sr-90 sediment concentration depth profile

The depth profile of sediment concentration in activity per unit dry weight (Bq kg^{-1}) and activity per unit volume (Bq cm^{-3}) are different. The sediment activity concentration in Bq kg^{-1} is dependent on the dry weight of sediment material in the layer. The top 5 cm layer of the sediment surface in some sites was vegetation which has low weight per unit volume. The sediment concentration is high when calculated in Bq kg^{-1}. In some sites, the peak concentration in Bq kg^{-1} is at 0-5 cm layer but the peak concentration per volume is at 5-10 cm layer, showing the influence of different sediment density with depth. In this study, the peak concentration per volume was compared between the sites.

Svyatoye lake

Site 1 and Site 2 are silty loam covering with the vegetation, whilst Site 3 is fine sand (Kudelsky, et al., 2005). The mass of dry sediment in the top 5 cm layer was different at the different sites (3.33 g at Site 1, 18.19 g at Site 2 and 42.14 g at Site 3). At Sites 1 and 2, the peak in the Sr-90 activity concentration was in the same depth layer as Cs-137, suggesting similar migration. At Site 3 which is fine sand, the vertical migration of Sr-90 is higher than Cs-137. The vertical the migration of Sr-90 has been shown in some studies to be more rapid than Cs-137 due to the higher K_d for Cs-137 ($3.2x10^4$ l kg^{-1}) than Sr-90 ($1.2x10^3$ l kg^{-1}) (Whicker, Iii, Bowling, Alberts, & Brisbin, 1990). It is likely that the higher mobility of Sr-90 in Site 3 is due to the lower absorption of Sr-90 to sandy sediments since the Cation Exchange Capacity of sandy sediments is low (Yasuda & Uchida, 1993).

The Cs-137 activity found in the top 15 cm layer was between 84.5 to 97.8 % at the three sites whilst the Sr-90 activity concentration in the top 15 cm layer was between 72.4 to 92.4 %. So, vertical transport of these radionuclides has been very slow in the 22 years since deposition. Since the maximum activity concentration was in the surface layers (either 0-5 or 5-10 cm), this also suggests very low sedimentation rate, probably because they are shallow (meaning sediments are mixed) and there are no outside inputs of sediment in these closed lakes. From the sediment samples, the Cs-137 inventory in watershed area was 1,340±40, 770±30 and 2,390±80 kBq m^{-2} at Site 1, 2 and 3 respectively. The average Cs-137 inventory in watershed area was 1,500±94 kBq m^{-2}, whilst the Cs-137 inventory calculated from the Radio-Ecological Study of the Chernobyl Cooling POND Report by Belarusian Scientist was 1,067 kBq m^{-2} (Kudelsky, et al., 2005). The measured Cs-137 inventory was higher than the calculation from the Report. The Cs-137 inventory in Site3 was quite high (2,390 kBq m^{-2}) comparing with the other sites resulting to the average Cs-137 inventory. The measured Cs-137 inventory will close to the report when take more samples.

Perstok lake

The type of sediment is silt with a high content of organic matter in all sites (Kudelsky, et al., 2005). The Cs-137 maximum concentration was at 0-5 cm depth in Site 4 and 5 and at 5-10 cm depth in Site 6 (**Figure 5.14 a**). The Sr-90 maximum concentration was at 0-5 cm depth in Site 4 and 5 and at 5-10 cm depth Site 6 (**Figure 5.14 b**). This shows

the good agreement between Cs-137 and Sr-90 migration in the lake. The percentage of Cs-137 activity found in the top 15 cm layer was between 98.5 and 98.8 %. The Sr-90 activity found in the top 15 cm layer was between 98.6 and 99.2 %. It shows that there was almost no vertical migration of Sr-90 and Cs-137 in Perstok lake below the top 15 cm depth layer, as observed in the silt sediments of Svyatoye lake.

From the sediment samples, the Cs-137 inventory was 900±30, 760±30 and 1,490±50 kBq m^{-2} in Sites 4, 5 and 6 respectively with an average inventory of 1,050±66 kBq m^{-2}. The estimated inventory for the watershed of the lake was more than twice as high as this: 2,886 kBq m^{-2} (Kudelsky, et al., 2005). It is likely that this was because the samples taken were from the shallow littoral zone of the lake. It is known that the Cs-137 sediment inventory increases with increased water depth because of the continual transport from shallower to deeper sediment area (Abraham, et al., 2000; Blakar, Hongve, & Njåstad, 1992; Kansanen, Jaakkola, Kulmala, & Suutarinen, 1991; Whicker, et al., 1990).

Dvorische lake

The sediment consists of fine sand and lacustrine silts with high organic content (Kudelsky, et al., 2005). The Cs-137 sediment concentration in this lake was approximately 1 order of magnitude lower than Perstok lake, whilst the Sr-90 sediment concentrations were approximately 2 order of magnitude lower than Perstok lake. The Cs-137 and Sr-90 maximum concentrations were at 0-5 cm depth at all sites (Figure 5.16 a and b). The percentage of Cs-137 activity found in the top 15 cm layer was between 79 to 99.2 % and for Sr-90 this was between 95 and 100 %. As with the other lakes, the silt sediments do not show higher migration of Sr-90 than Cs-137.The limit of detection of Sr-90 is about 0.6 Bq kg^{-1}.

The Cs-137 inventory in the sediments was 51±2, 19.7±0.7 and 14.2±0.5 kBq m^{-2} at Sites 7, 8 and 9 respectively. The average Cs-137 inventory in the three sites was 28.3±2.1 kBq m^{-2}, compared to the estimated Cs-137 inventory in the watershed of 140.6 kBq m^{-2} (Kudelsky, et al., 2005). Again, this may be due to erosion of sediment from shallower to deeper areas of the lake.

5.5.3 The beta and gamma dose rates estimated from sediment activity concentrations

The beta and gamma dose rates predicted from the sediment concentration were calculated using simple equations as discussed in Section 5.3.4. As discussed in Section 5.5.1, the in situ beta dose measurement was not a successful experiment as there was no clear pattern of beta dose with depth. So, the dose measurements did not compare with the activity-depth profiles of the nuclides in the sediment. This may have been due to problems of sediment smearing, even with the improved equipment, or to problems in reading the beta dose from the dosimeters. The problem with beta dose measurements is not, however, so important because they can be quite simply calculated from measurements of radionuclide activity concentration in sediments.

For the calculated beta dose rate, the results of the total beta dose rate (from Cs-137 and Sr-90) showed that the beta dose rate from Sr-90 was not so important in Svyatoye and Dvorische lake compared with Cs-137 because the concentration of Cs-137 (11,649-20,329 and 193-417 Bq kg^{-1} w.w. in Svyatoye and Dvorische respectively) in sediment was so much higher than Sr-90 (45-270 and 3-146 Bq kg^{-1} w.w.). For Perstok lake, both beta dose rates from Cs-137 and Sr-90 were important because the Sr-90 concentration in sediment was high (650-980 Bq kg^{-1} w.w.). The maximum beta dose rates occurred near the sediment surface (0-5 cm depth) except Site 1 in Svyatoye lake and Site 6 in Perstok lake, then decreased exponentially. The maximum beta dose rates were in the range of 1.36-2.22, 1.27-1.80 and 0.02-0.13 μGy hr^{-1} in Svyatoye, Perstok and Dvorische lakes respectively.

For the gamma dose rate, the dose above the sediment surface, on the sediment surface and below the sediment surface are predicted by using the simple method described above. The gamma dose rate above the sediment surface was decreased exponentially with the distance from the sediment surface because the water activity concentration was 2-3 orders of magnitude lower than the sediment activity concentration (2 orders of magnitude in Dvorische lake and 3 orders in Svyatoye and Perstok lake). The gamma dose rate above, on and below the sediment surface was calculated using two different scenarios; the maximum Cs-137 and the average Cs-137 in the top 15 cm of depth.

The gamma dose rate at 30 cm above the sediment was 0.836-1.46, 0.403-0.901 and 0.014-0.035 μGy hr^{-1} in Svyatoye, Perstok and Dvorische lake respectively using the maximum sediment concentration at each site. Using the average of the top 15 cm of

sediment, the gamma dose rate was estimated to be 0.294-0.674, 0.224-0.538 and 0.012-0.021 μGy hr^{-1} in Svyatoye, Perstok and Dvorische lake respectively. The gamma dose rate at the sediment surface was 2.22-3.88, 1.31-2.40 and 0.04-0.09 μGy hr^{-1} in Svyatoye, Perstok and Dvorische lake respectively using the maximum sediment concentration at each site. Using the average of the top 15 cm of sediment, the gamma dose rate was estimated to be 0.782-1.793, 0.595-1.431 and 0.032-0.055 μGy hr^{-1} in Svyatoye, Perstok and Dvorische lake respectively.

The gamma dose rate below the sediment surface was estimated to be 4.44-7.75, 2.62-4.79 and 0.073-0.181 μGy hr^{-1} in Svyatoye, Perstok and Dvorische lake respectively using the maximum sediment concentration at each site. Using the average of the top 15 cm of sediment, the gamma dose rate was estimated to be 1.56-3.22, 1.18-2.85 and 0.063-0.108 μGy hr^{-1} in Svyatoye, Perstok and Dvorische lake respectively.

5.5.4 Comparison of the in situ gamma dose rate and calculated gamma dose rate

The comparison of the in situ measured and calculated gamma dose rates are shown in **Figure 5.23** for Svyatoye lake and **Figure 5.24** for Perstok lake. For Svyatoye lake, the predicted gamma dose rate on the sediment surface and above the sediment surface are higher than the measured dose rate by a factor of two. The estimation of the gamma dose rate on the sediment and above the sediment in Perstok lake is closer to the measured dose rate than Svyatoye lake. As discussed above, the calculated gamma dose rate is expected to be an over estimate because the photon beam is not collimated: the majority of photons do not travel directly upwards.

For the calculated gamma dose rates above and below the sediment surface, the calculation based on maximum Cs-137 activity concentration shows an over prediction by a factor of two to four, whilst the average gamma dose rate predicts a dose closer to the in situ measurement. For the sediment below the 5 cm sediment surface layer, the calculation assumes an infinite medium, all energy produced from the gamma are absorbed by the medium. On the sediment surface, the calculation assumes a semi-infinite medium because the medium can absorb only half of the emitted photons; the others escape from the medium. For the layer between 0-5 cm below the sediment, the gamma dose rate can be predicted by the extrapolation from the gamma dose rate on the sediment surface.

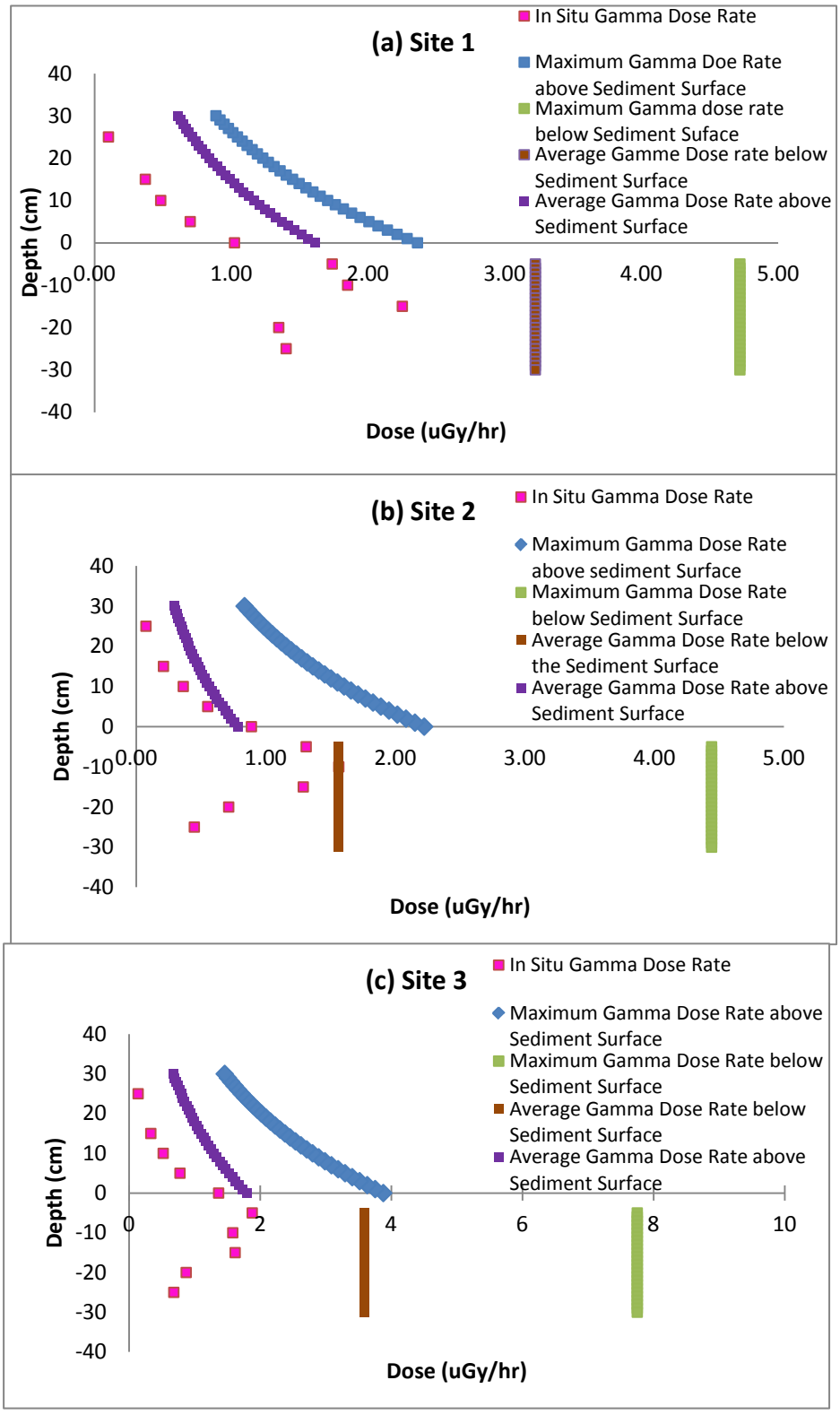

Figure 5.23 The comparison of in situ measured gamma dose rate and calculated gamma dose rate in different sites at Svyatoye lake; (a) Site 1, (b) Site 2 and (c) Site 3.

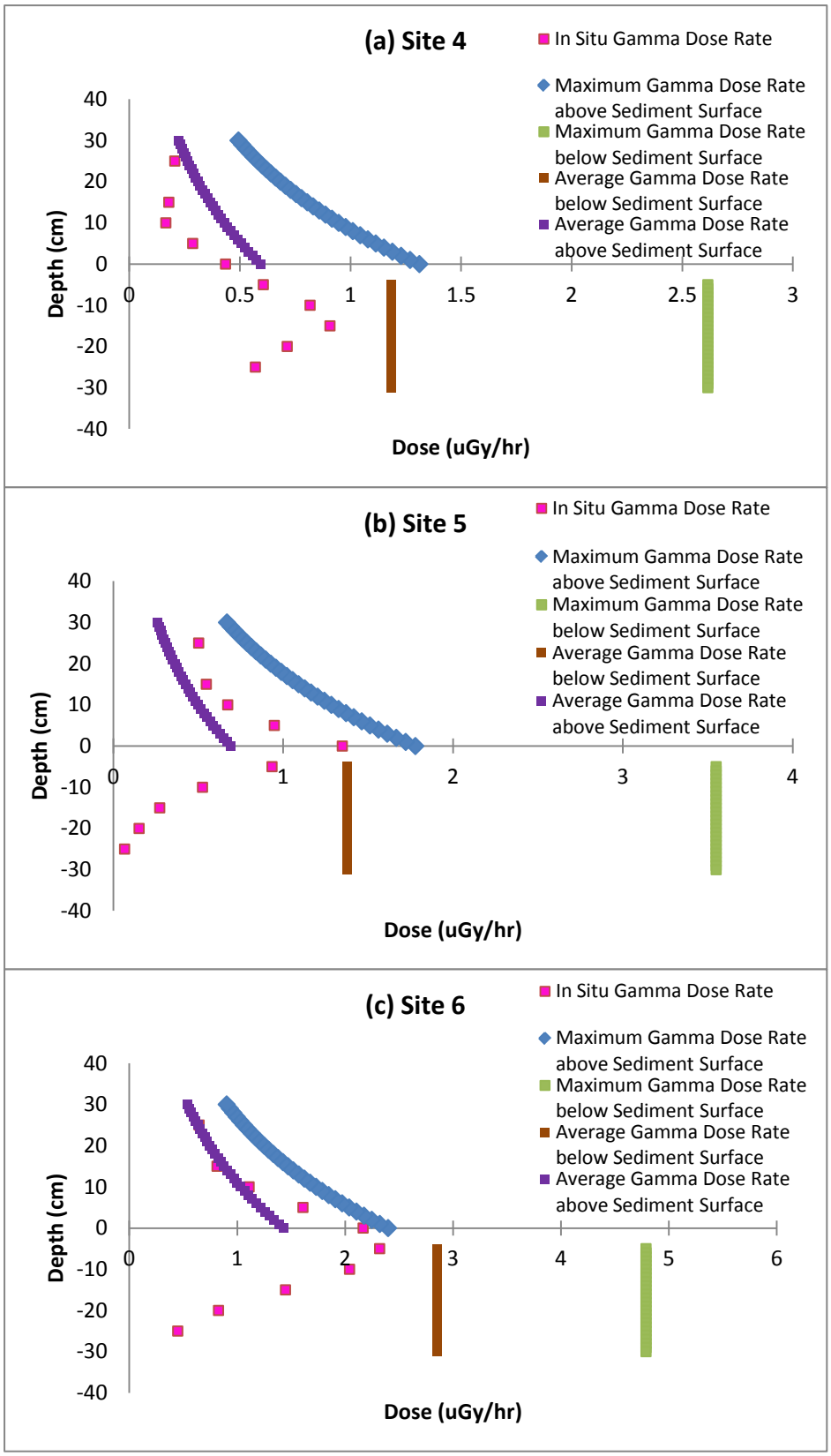

Figure 5.24 The comparison of in situ measured gamma dose rate and calculated gamma dose rate in different sites at Perstok lake; (a) Site 4, (b) Site 5 and (c) Site 6.

5.5.5 The prediction of total external dose rate to biota

The total (beta and gamma) external dose rate was estimated by (1) in situ measurement and (2) calculated dose rate. In this study, the gamma in situ measurement gave good results, whilst the beta in situ measurement needs more experimentation to improve the method further. To make an estimate of external doses to biota, the highest dose rate site of each lake was selected to represent the highest risk. A position 25 cm above the sediment surface was used to represent the received dose rate point of pelagic fish. The position 0 cm (on the sediment surface) was assumed to represent the received dose rate point of benthic fish. The maximum dose rate below the sediment surface was assumed to represent the received dose rate point of some insects and their larvae (which live in the sediment). The predicted external dose rate for pelagic fish, benthic fish and insect larvae in Svyatoye, Perstok and Dvorische lake is shown in **Table 5.15** and **Figure 5.25**.

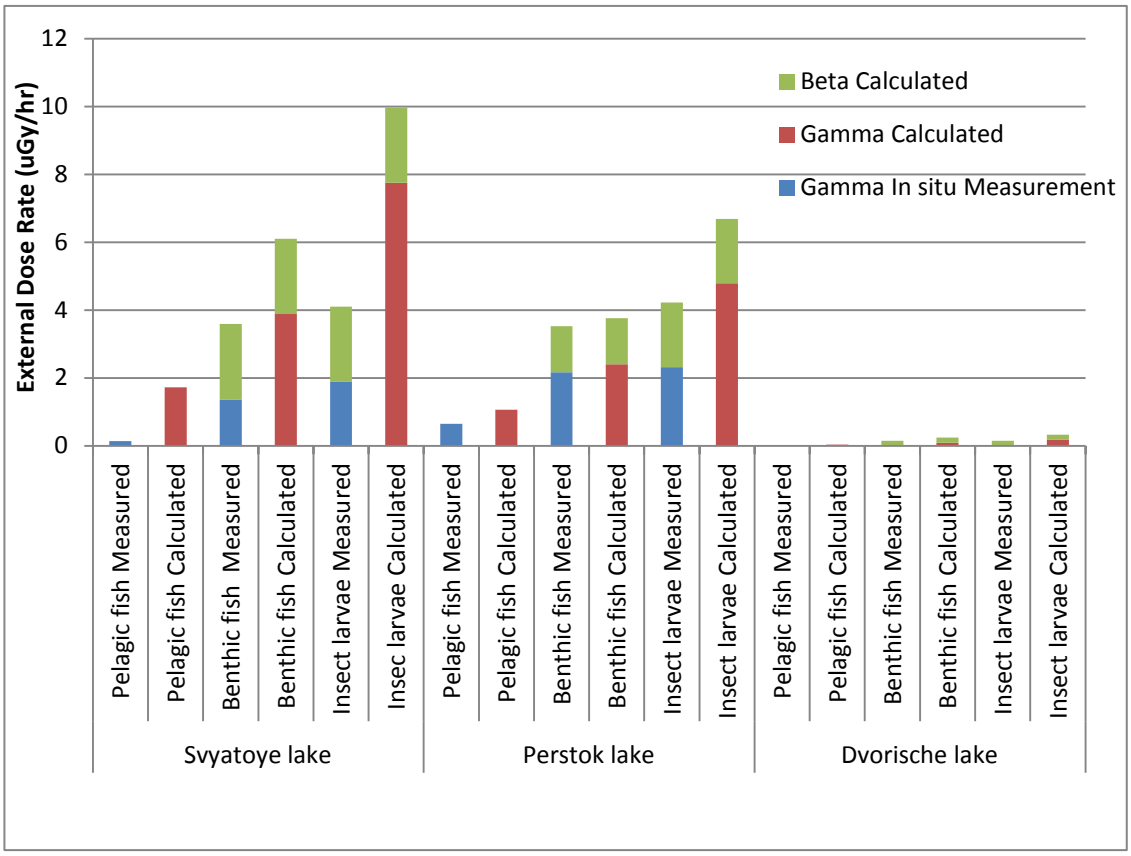

Figure 5.25 The predicted external dose rate for pelagic fish, benthic fish and insect larvae in Svyatoye, Perstok and Dvorische lake showing the proportion of dose from beta and gamma radiation.

Table 5.15 The predicted external dose rate for pelagic fish, benthic fish and insect larvae in Svyatoye, Perstok and Dvorishche lake

Biota	Svyatoye lake (µGy hr^{-1})					Perstok lake (µGy hr^{-1})					Dvorische lake (µGy hr^{-1})				
	(1) Gamma in situ	(2) Gamma calculated	(3) Beta calculated	Total dose (1)+(3)	Total dose (2)+(3)	(1) Gamma in situ	(2) Gamma calculated	(3) Beta calculated	Total dose (1)+(3)	Total dose (2)+(3)	(1) Gamma in situ	(2) Gamma calculated	(3) Beta calculated	Total dose (1)+(3)	Total dose (2)+(3)
Pelagic fish	0.14	1.72	0	0.14	1.72	0.65	1.06	0	0.65	1.06	n.d.	0.04	0	-	0.04
Benthic fish	1.37	3.88	2.22	3.59	4.10	2.17	2.40	1.36	3.53	3.76	n.d.	0.09	0.15	-	0.24
Insect larvae	1.88	7.75	2.22	4.1	9.97	2.32	4.79	1.90	4.22	6.69	n.d.	0.18	0.15	-	0.33

Note Beta external dose in the water assumed to be zero because Cs-137 and Sr-90 concentration in water were very low.

Overall, the calculated dose rate is approximately 1-2 times higher than the measured dose rate. This is expected because of the conservative simplifying assumptions in the model. The external dose rate of insect larvae is the highest because it lives in the sediment which has a much higher activity concentration than the water, whilst the external dose rate of pelagic fish is the lowest because it lives in the water column. The external dose rate in Svyatoye is higher than Perstok lake because Cs-137 activity concentrations in sediments are higher, whilst Dvorische shows the lowest external dose rate. None of the estimated external dose rates are higher than 10 μGy hr^{-1}.

5.6 Summary

In summary, the simple model for gamma dose rate with depth above and below the sediment surface gives reasonable agreement with measured values. Although the model tends to over-estimate dose rates, this is not a serious problem for radiological assessments. The method of using the average activity concentration in the top 15 cm layer gave more accurate estimates (less over-estimation) of dose rate, so this approach could be used for assessments.

The measurement of beta dose in situ was not successful despite the improved apparatus used in the main field study. This may have been because of sediment smearing, because the beta dosimeters did not have proper contact with sediment, because of the design of the apparatus or because of failure of the dosimetry method underwater. This would need further investigation by changing the TLD type or improving the design of the apparatus to improve the contact between the sediment and the dosimeter since it is possible that poor contact led to the low doses measured.

The sediment activity-depth profiles in each lake showed that 20 years after Chernobyl, most of the Cs-137 and Sr-90 were still in the surface 15 cm of sediment. This shows strong absorption of these radionuclides to the sediments (except, for Sr-90 to the fine sand sediment of Svyatoye lake) and not much burial of sediment layers. This means that, in these closed lakes, external dose rates to benthic biota are still important at this long time after the Chernobyl accident.

5.7 References

Abraham, J. P., Whicker, F. W., Hinton, T. G., & Rowan, D. J. (2000). Inventory and spatial pattern of 137Cs in a pond: a comparison of two survey methods. *Journal of Environmental Radioactivity, 51*(2), 157-171.

Beresford, N. A., Gaschak, S., Barnett, C. L., Howard, B. J., Chizhevsky, I., Strømman, G., et al. (2008). Estimating the exposure of small mammals at three sites within the Chernobyl exclusion zone - a test application of the ERICA Tool. *Journal of Environmental Radioactivity, 99*(9), 1496-1502.

Blakar, I. A., Hongve, D., & Njåstad, O. (1992). Chernobyl cesium in the sediments of Lake Høysjøen, Central Norway. *Journal of Environmental Radioactivity, 17*(1), 49-58.

C.E.Cushing, & D.G.Watson. (1974). *Aquatic Studies of Gable Mountain Pond*. Virginia: Pacific Northwest Laboratories.

Cailes, C. R. (2006). *Phenotypic and genetic effects of Chernobyl-derived radionuclide contamination on the red-eyed damselfly Erythromma Najas (Odonata, Coenagrionidae).* University of Plymouth, Plymouth.

Chesser, R. K., Sugg, D. W., Lomakin, M. D., Bussche, R. A. v. d., DeWoody, J. A., Jagoe, C. H., et al. (2000). Concentrations and dose rate estimates of 134, 137cesium and 90 strontium in small mammals at chornobyl, Ukraine. *Environmental Toxicology and Chemistry, 19*(2), 305-312.

Chumak, V. V., Likhtarev, I. A., & Pavlenko, J. V. (1999). Monitoring of Individual Doses of Populations Residing in the Territories Contaminated after Chernobyl Accident. *Radiation Protection Dosimetry, 85*(1-4), 137-139.

Elert, G. (2010). Density of Water. *The Physics Factbook* Retrieved 10 October, 2010, from http://hypertextbook.com/facts/2007/AllenMa.shtml

Furetta, C. (2003). Handbook of Thermoluminescence Available from http://site.ebrary.com/lib/portsmouth/Doc?id=10085582&ppg=124

Godoy, J. M., Schuch, L. A., Nordemann, D. J. R., Reis, V. R. G., Ramalho, M., Recio, J. C., et al. (1998). 137Cs, 226, 228Ra, 210Pb and 40K concentrations in Antarctic soil,

sediment and selected moss and lichen samples. *Journal of Environmental Radioactivity, 41*(1), 33-45.

Halford, D. K., & Markham, O. D. (1978). Radiation Dosimetry of Small Mammals Inhabiting a Liquid Radioactive Waste Disposal Area. *Ecology, 59*(5), 1047-1054.

Hubbell, J. H., & Seltzer, S. M. (2010). Tables of X-Ray Mass Attenuation Coefficients and Mass Energy-Absorption Coefficients. *Physical Reference Data* Retrieved 10 October, 2010, from http://physics.nist.gov/PhysRefData/XrayMassCoef/ComTab/water.html

IAEA. (2006a). *Chernobyl's Legacy: Health, Environmental and Socio-Economic Impacts and Recommendations to the Governments of Belarus, the Russian Federation and Ukraine*. Vienna: IAEA.

IAEA. (2006b). *Environmental Consequences of the Chernobyl Accident and Their Remediation: Twenty years of Experience (Report of the Chernobyl Forum Expert Group 'Environment')*. Vienna: IAEA.

IAEA, & ANSTO. (2004). Radiation Protection Distance Learning Project.

KAERI. (2000). Table of Nuclides. Retrieved 10 October, 2010, from http://atom.kaeri.re.kr/

Kansanen, P. H., Jaakkola, T., Kulmala, S., & Suutarinen, R. (1991). Sedimentation and distribution of gamma-emitting radionuclides in bottom sediments of southern Lake Päijänne, Finland, after the Chernobyl accident. *Hydrobiologia, 222*(2), 121-140.

Kudelsky, A. V., Pashkevich, V. I., Yankov, A. I., Samodurov, V. P., Savchik, S. F., & Rudemok, A. A. (2005). *Radio-ecological study of the Chernobyl Cooling Pond and options for remediation*. Minsk: National Academy of Science of Belarus.

McKinlay, A. F. (1981). *Thermoluminescence dosimetry*. Bristol: Adam Hilger Ltd.

Mück, K., Pröhl, G., Likhtarev, I., Kovgan, L., Meckbach, R., & Golikov, V. (2002). A Consistent Radionuclide Vector After the Chernobyl Accident. *Health Physics, 82*(2), 141-156.

Smith, J. (2005). Effects of ionising radiation on biota: do we need more regulation? *Journal of Environmental Radioactivity, 82*(1), 105-122.

Smith, J. T., & Beresford, N. A. (2005). Introduction. In J. T. Smith & N. A. Beresford (Eds.), *Chernobyl-Catastrophe and Consequences* (pp. 1-34). Berlin: Praxis Publishing Ltd.

Smith, J. T., Voitsekhovitch, O. V., Konoplev, A. V., & Kudelsky, A. V. (2005). Radioactivity in aquatic systems. In J. T. Smith & N. A. Beresford (Eds.), *Chernobyl-Catastrophe and Consequences* (pp. 139-189). Berlin: Praxis Publishing Ltd.

Stark, K., & Pettersson, H. (2008). External radiation doses from 137Cs to frog phantoms in a wetland area: in situ measurements and dose model calculations. *Radiation and Environmental Biophysics, 47*(4), 481-489.

Strand, T., Stranden, E., & Rudjord, A. L. (1987). External Radiation Doses to the Norwegian Population from the Chernobyl Fall-out. *Radiation Protection Dosimetry, 20*(4), 231-236.

Szabó, P. P., Fehér, I., & Germán, E. (1990). Environmental Monitoring around Nuclear Installations using TL Dosemeters. *Radiation Protection Dosimetry, 34*(1-4), 191-194.

Timms, D. N., Smith, J. T., Coe, E., Kudelsky, A. V., & Yankov, A. I. (2005). In situ measurements of the sub-surface gamma dose from Chernobyl fallout. *Applied Radiation and Isotopes, 62*(6), 923-930.

Tumnoi, Y. (2006). *The effects of chronic radiation dose on the fitness and genetic diversity of Roach (Rutilus rutilus L.) in the Chernobyl region.* University of Portsmouth.

Whicker, F. W., Iii, J. E. P., Bowling, J. W., Alberts, J. J., & Brisbin, I. L., Jr. (1990). Distribution of Long-Lived Radionuclides in an Abandoned Reactor Cooling Reservoir. *Ecological Monographs, 60*(4), 471-496.

Woodhead, D. S. (1973). The radiation dose received by plaice (Pleuronectes platessa) from the waste discharged into the north-east Irish Sea from the fuel reprocessing plant at Windscale. *Health Physics, 25*(2), 115-121.

Yasuda, H., & Uchida, S. (1993). Statistical approach for the estimation of strontium distribution coefficient. *Environmental Science & Technology, 27*(12), 2462-2465.

Chapter 6

Monte Carlo method to estimate uncertainty in internal dose rates to fish

6.1 Introduction

The Monte Carlo method is a technique for using random numbers to solve a statistical or mathematical solution (Rubinstein, 1981). Its name was inspired by the gambling casino at Monte Carlo city in Monaco (Jacoboni & Lugli, 1989). It was first used as mathematical method to develop the atomic bomb in Los Alamos in the 1940s (Kalos & Whitlock, 1986). However, it has also been used in many other applications in physics, biology and chemistry (Jain, 1992). In the past, Monte Carlo simulation required the writing of very complicated computer code to simulate the data but currently, there are many useful software packages for generating random numbers to simulate data, and run Monte Carlo models, such as SPSS and Excel. This, together with the introduction of high-speed personal computers, has made the Monte Carlo method a common way of estimating uncertainty in environmental models. After the Chernobyl accident, the Monte Carlo method was used to predict the area in west Cumbria where the radiocaesium contaminated in lamb meat would require the enforcement of restrictions (Wright, Smith, Beresford, & Scott, 2003). For the prediction of the internal dose rate in the real environment, key factors such as fish mass and radionuclide activity concentration are varied, so the internal radiation exposure of a fish will be uncertain. But, the variation of fish mass and radionuclide activity concentration can be evaluated by using Monte Carlo Simulation. The new versions of RESRAD (Version 1.5) and ERICA (1.0 May 2009) model also have probabilistic functions of media activity concentrations simulated by Monte Carlo method to predict the dose rate (Beresford, Barnett, Howard, et al., 2008; Brown, et al., 2008; Hosseini, Thørring, Brown, Saxén, & Ilus, 2008; U.S.DOE, 2009).

The new versions of RESRAD and ERICA models, the internal dose rate predicted from radionuclide activity concentration in water can be generated by using Monte Carlo calculation. User can set type of distribution (normal, exponential, etc.) and then put the mean and standard deviation to generate the internal dose rate. Those new version models (with the probabilistic function) have just launched in 2009. This study is based on the previous version which have no the probabilistic function.

Chapter 3 has described the predicted internal dose rates per Bq kg^{-1} (Dose Conversion Coefficient, DCC) which are determined by using 5 different models (FASSET, ERICA, R&D 128, RESRAD and D-MAX). Equations to predict DCC for Cs-137 and Sr-90 as a function of mass of organism were developed. The internal dose rates can be calculated from those equations by using mass and tissue concentration of organism. These equations will be used to assess the effect of variability in animal shape and size on dose rates and the effect this has on uncertainty in model predictions.

Variability represents the diversity or heterogeneity in a population. Basically, variability is a property of nature, for example, fish size, fish mass, habitat and media activity concentration. Variability usually cannot be reduced by further measurement or study. Uncertainty is different from variability and represents biased ignorance or lack of perfect data about poorly characterised phenomena or models. Basically, uncertainty is a property of the risk analyst, for example, the uncertainty of the model prediction. Unlike variability, uncertainty can be reduced by further measurement or study ("Science and Decisions : Advancing Risk Assessment," 2008).

This chapter will investigate the uncertainty in estimates of the internal dose of fish in two contaminated lakes in Belarus (Lakes Perstok and Svyatoye) by using data of fish mass and radionuclide activity concentration in fish. The variation in predicted DCC will be assessed by the Monte Carlo method and can be compared with the DCCs predicted by the 5 models. The internal dose determined from measured activity concentrations in fish can also be compared between that predicted by the Monte Carlo method and the 5 different models. This study allows an evaluation of the effect of variability in fish mass and radionuclide activity concentration on the uncertainty of internal dose.

6.2 Methods

6.2.1 The method to calculate internal dose rate

In general, models can be used to calculate the internal dose rate of fish in each radionuclide by using radionuclide activity concentration in fish per unit mass (Bq kg^{-1}) and DCC for each model. For cases where the radionuclide activity concentration in fish are unknown (they have not been measured), the models can predict the radionuclide activity concentration in fish by using radioactivity concentration in water and concentration factor in each model. This is then multiplied by the DCC to calculate the internal dose rate. Moreover, from Chapter 3, DCC can be determined from a generalised function of mass, using the fitted equation for Cs-137 (D = 7.79E-6 Ln(m) + 1.80E-4 when D is Dose rate in μGy hr^{-1} per Bq kg^{-1} or DCC and m is weight of organism in kg) and fish mass. This DCC is then multiplied by radionuclide activity concentration in fish to calculate internal dose.

In summary, there are three ways to calculate the internal dose rate, depending on the available data:

1. By using radionuclide activity concentration in fish and DCC to calculate the internal dose rate
2. By using fitted equation from the previous chapter and fish mass to calculate DCC and then use DCC and radionuclide activity concentration in fish to calculate the internal dose rate
3. By using radioactivity concentration in water and concentration factor to calculate radionuclide activity concentration in fish and then use radionuclide activity concentration in fish and DCC to calculate the internal dose rate

The ways to calculate the internal dose rate are illustrated in **Figure 6.1**.

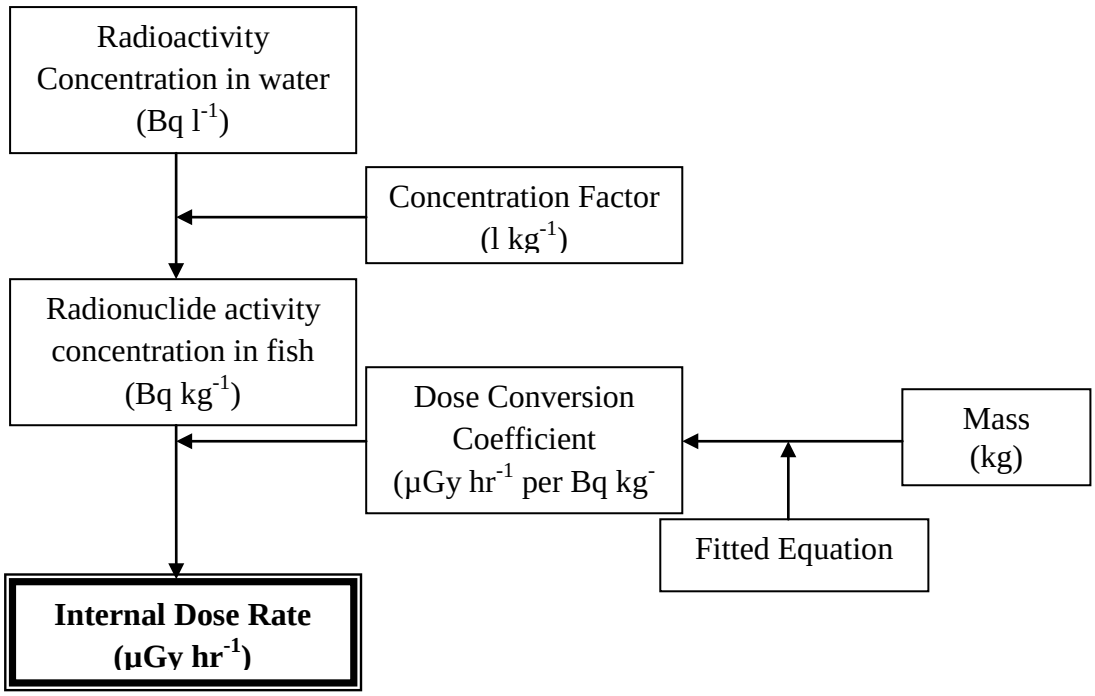

Figure 6.1 The ways to calculate the Internal Dose Rate

6.2.2 The available data of fish mass and radionuclide activity concentration in fish

The report on the results of the Project INTAS-2001-0556 (Radio-Ecological Study of the Chernobyl Cooling POND and options for remediation (RESPOND)) (Kudelsky, et al., 2005) was used as the source of the data of fish mass and radionuclide activity concentration in fish. The data of the two most important nuclides: Cs-137 and Sr-90 in the report were used for the analysis.

For Cs-137 in Svyatoye lake, the data of fish mass and radionuclide activity concentration in fish of 9 species of pelagic fish (Pike, Roach, Rudd, Verkhvoka, Bitterling, Gold fish, Bream, Perch and Ruff) which were caught between 1997 and 2004 used for the Monte Carlo calculation. Whilst it is known (J. T. Smith, Kudelsky, Ryabov, & Hadderingh, 2000) that over this period radioactivity concentrations in fish are likely to have declined slowly, such temporal changes over this period are small in comparison with the overall variation in fish activity concentrations (1,536-117,790 Bq kg^{-1}). The total number of data of fish mass and radionuclide activity concentration in fish were 294. For Cs-137 in Perstok lake, the data of fish mass and radionuclide activity concentration in fish of 9 species of pelagic fish (Pike, Roach, Rudd, Verkhvoka, Tench, Gold fish, Bream, Perch and Ruff) which were caught between 1998

and 2004 used for Monte Carlo calculation. The total number of the data of fish mass and radionuclide activity concentration in fish are 35. The summary of the number of fish in each species for Svyatoye and Perstok lake that were used for the Monte Carlo calculation is shown in **Table 6.1**. The summary of fish mass and radionuclide activity concentration in Svyatoye and Perstok lake is shown in **Table 6.2**.

Table 6.1 Summary of the number of fish data of each species for Svyatoye and Perstok lake.

Lake	Fish species (number of data)
Svyatoye	Pike(22), Roach(70), Rudd(39), Verkhvoka(10), Bitterling(3), Gold fish(27), Bream(1), Perch(100) and Ruff(22)
Perstok	Pike(3), Roach(9), Rudd(5), Verkhvoka(3), Tench(1), Gold fish(2), Bream(5), Perch(6) and Ruff(1)

Table 6.2 Summary of fish mass and radionuclide activity concentration in Svyatoye and Perstok lake

	Svyatoye lake		Perstok lake	
	Fish mass (kg)	Fish concentration (Bq kg^{-1})	Fish mass (kg)	Fish concentration (Bq kg^{-1})
Average	0.2165	20,629.47	0.1398	7,949.65
Standard Deviation	0.4033	21,101.46	0.3169	3,228.96
Minimum	0.00175	1,535.6	0.003	2,761.6
Maximum	3.995	117,790	1.841	17,900.6

The histograms of log scale of fish mass and radionuclide activity concentration in fish in Svyatoye lake are shown in **Figures 6.2** and **6.3** respectively. The histograms on a log scale of fish mass and radionuclide activity concentration in fish in Perstok lake are shown in **Figures 6.4** and **6.5** respectively.

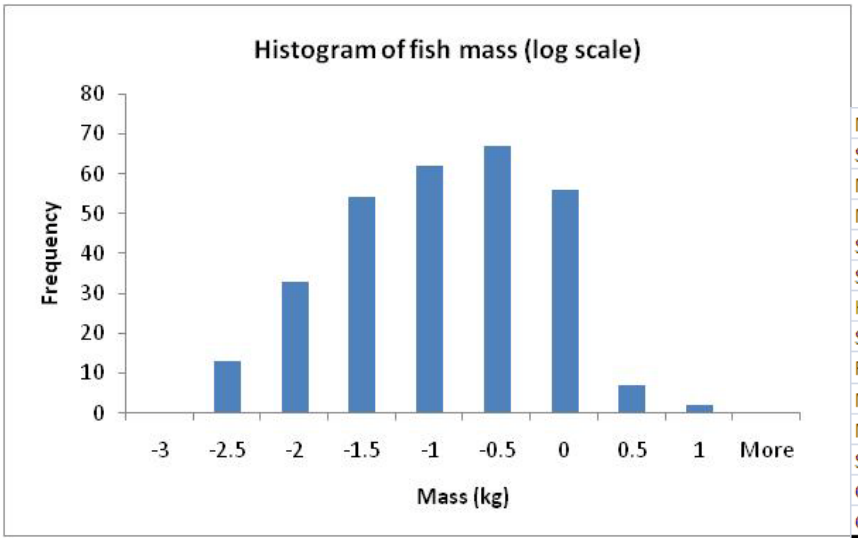

Mean	-1.171
Standard Error	0.042802
Median	-1.16133
Mode	-0.21183
Standard Deviation	0.733893
Sample Variance	0.538599
Kurtosis	-0.85657
Skewness	-0.13173
Range	3.358479
Minimum	-2.75696
Maximum	0.601517
Sum	-344.274
Count	294
Confidence Level(9	0.084237

Figure 6.2 Histogram and descriptive statistics of fish mass (log scale) in Svyatoye lake.

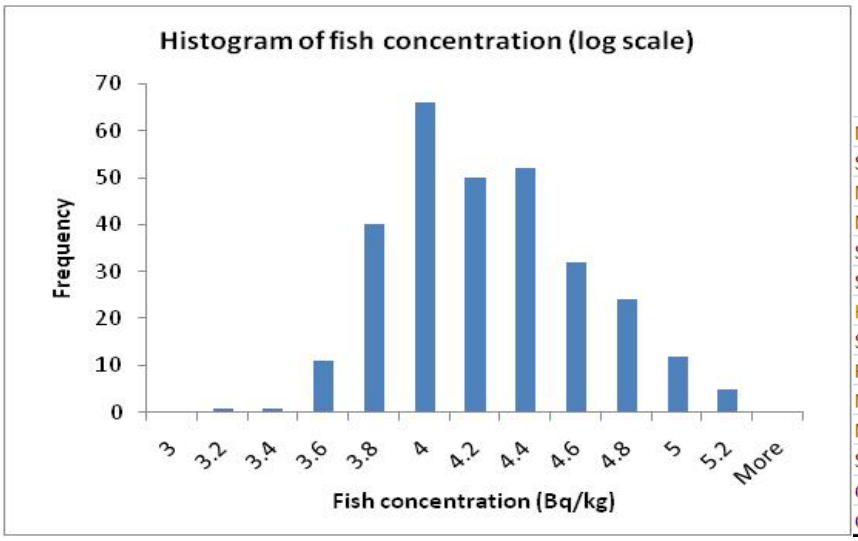

Mean	4.144235
Standard Error	0.0218
Median	4.105851
Mode	4.211654
Standard Deviation	0.373786
Sample Variance	0.139716
Kurtosis	-0.47827
Skewness	0.380837
Range	1.88483
Minimum	3.186278
Maximum	5.071108
Sum	1218.405
Count	294
Confidence Level(9	0.042904

Figure 6.3 Histogram and descriptive statistics of radionuclide activity concentration in fish (log scale) in Svyatoye lake.

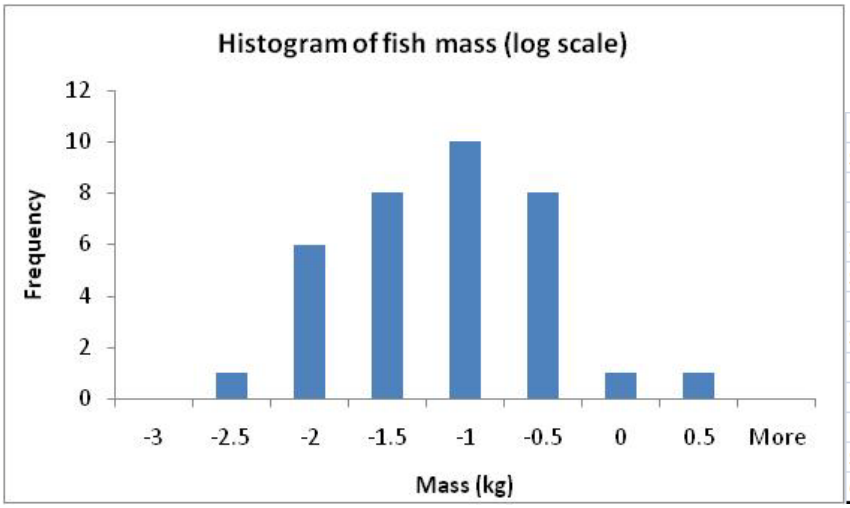

Mean	-1.3677
Standard Error	0.113412
Median	-1.2233
Mode	-1.91364
Standard Deviation	0.670955
Sample Variance	0.450181
Kurtosis	-0.60039
Skewness	0.293458
Range	2.787933
Minimum	-2.52288
Maximum	0.265054
Sum	-47.8694
Count	35

Figure 6.4 Histogram and descriptive statistics of fish mass (log scale) in Perstok lake.

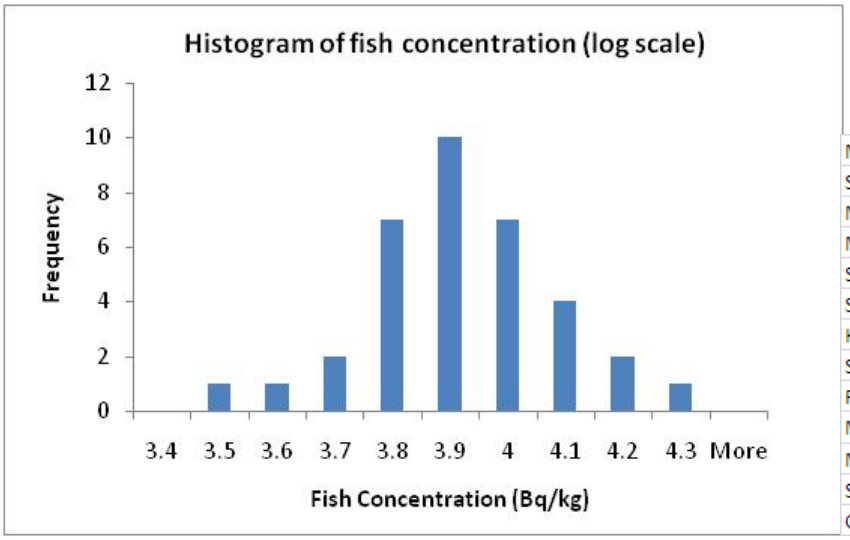

Mean	3.868599
Standard Error	0.028415
Median	3.828022
Mode	3.793609
Standard Deviation	0.168103
Sample Variance	0.028259
Kurtosis	0.791762
Skewness	-0.00421
Range	0.813282
Minimum	3.439585
Maximum	4.252868
Sum	135.401
Count	35

Figure 6.5 Histogram and descriptive statistics of radionuclide activity concentration in fish (log scale) in Perstok lake.

For Sr-90 in Svyatoye lake, there are no such data for Sr-90 radionuclide activity concentration in fish because Sr-90 is only radiologically significant in areas close to the Chernobyl nuclear power plant. For Sr-90 in Perstok lake, the data of fish mass and radionuclide activity concentration in fish are not enough for Monte Carlo calculation

(only 6 measurements). Therefore, the comparison between the predicted equation and the 5 different models of the DCCs and internal dose rates of Sr-90 in fish are discussed, but Monte Carlo analysis is not carried out.

The above histograms (**Figures 6.2, 6.3, 6.4** and **6.5**) of fish mass and Cs-137 concentration in fish in Svyatoye and Perstok lake show the variation in observed fish mass and Cs-137 concentration in fish. For the fish mass, mean and standard deviation is -1.1710±0.7339 and -1.3677±0.6710 kg (log scale) in Svyatoye and Perstok respectively. For the Cs-137 concentration, mean and standard deviation is 4.1442±0.3738 and 3.8686±0.1681 Bq kg^{-1} (log scale) in Svyatoye and Perstok respectively.

In this Chapter, Cs-137 activity concentration in fish and fish mass data will be generated using the Monte Carlo method implemented using Microsoft Excel. The Random Number Generation function in the Data Analysis Tool in the Excel spread sheet is used to generate the random data. For this study, 1000 model runs were made. It was assumed that the data were lognormally distributed. The summary of parameters in each lake for the generation of the random numbers for fish mass and Cs-137 activity concentration in fish are shown in **Table 6.3**.

6.2.3 The comparison of DCC_{int} of Cs-137 and the Cs-137 internal dose predicted by the Monte Carlo method and the 5 models

By using above Monte Carlo method, a thousand random values of fish mass and Cs-137 activity concentration in fish were generated based on the distribution of observed data (**Table 6.3**). A thousand random predicted DCC_{int} can also be calculated by using the fitted equation (D = 7.79E-6 Ln(m) + 1.80E-4 when D is Dose rate in μGy hr^{-1} per Bq kg^{-1} or DCC and m is weight of organism in kg) with randomly generated fish mass and presented in a histogram. This will allow comparison of predicted DCCs from the 5 models and DCCs derived from the Monte Carlo distributions using the observed mass data. The variation in internal dose rate of Cs-137 in fish determined using the Monte Carlo method will also be compared with the predictions of the 5 models.

Table 6.3 Summary of parameters in Svyatoye and Perstok lake for the generation of data for the Monte Carlo model.

	Svyatoye lake		Perstok lake	
	Fish mass	Cs-137 activity concentration in fish	Fish mass	Cs-137 activity concentration in fish
No. of variable	1	1	1	1
No. of random number	1000	1000	1000	1000
Distribution	Lognormal	Lognormal	Lognormal	Lognormal
Mean	-1.1710	4.1442	-1.3677	3.8686
Standard deviation	0.7339	0.3738	0.6710	0.1681

6.2.4 The effect of fish mass, radionuclide activity concentration in fish and DCC on the internal dose

The study of the effect of fish mass, radionuclide activity concentration in fish and DCC on the variability in predicted internal dose rate can be compared by using 3 different scenarios; 1) Vary fish mass, radionuclide activity concentration in fish and DCC, i.e. all parameters varied, 2) Vary fish mass and radionuclide activity concentration in fish but use mean of DCC) and 3) Vary fish mass and DCC (use mean of radionuclide activity concentration in fish). The approach of varying one parameter, whilst giving the others their mean value was previously used by CROUT et al to study the importance of various parameters to prediction of Cs-137 uptake by crops (Cox, et al., 2006).

For variation of fish mass and fish concentration, the fish mass and fish concentration were generated by using Monte Carlo method. The parameters that were used in Svyatoye and Perstok lakes for the generation of data are shown in **Table 6.3**. For variation of DCCs, the fitted equation (D = 7.79E-6 Ln(m) + 1.80E-4) and generated fish mass data were used to generate the DCCs. From the variation of DCC and radionuclide activity concentration in fish, the mean DCC and radionuclide activity concentration in fish were calculated. The effect of fish mass, radionuclide activity concentration in fish and DCC in predicted internal dose rate was shown as a histogram of the internal dose rate. The different scenarios show the effect of variation in different

model parameters (fish size, Cs-137 activity concentration) on DCC. If the distribution of the histogram of variation in DCC depends strongly on a particular parameter, this will be shown in the difference in outputs for the different scenarios. If a narrow distribution of the DCC histogram (low standard deviation) of the internal dose rate is shown in Scenario 2, the DCC is the most important factor for the internal dose rate. If a narrow histogram of the internal dose rate is observed in Scenario 3, the radionuclide activity concentration in fish (which is not varied in Scenario 3) is the most important factor for the internal dose rate. As shown in **Figure 6.9 c** and **6.10 c**, the variation in radionuclide concentration in fish is the most important factor causing variation in predicted dose.

6.2.5 The Cs-137 internal dose rate predicted by using radionuclide concentration in water

If direct measurements of radionuclides in biota are not available, the FASSET, ERICA, R&D and RESRAD models can predict the internal dose rate by using Cs-137 concentration in water, concentration ratio (CR) in l kg^{-1} and DCC from each model. The DMAX model can use K^+ Concentration in water to predict Concentration ratio (CR). The details of this relationship have been described in Chapter 2, Section 2.5.5. The summary of average potassium concentrations and Cs-137 concentrations in water in Svyatoye and Perstok lake are shown in **Table 6.4**. The summary of Concentration Ratio and DCC assumed in each model in Svyatoye and Perstok lake are shown in **Table 6.5**. The variation of the predicted internal dose rate from Monte Carlo method can be compared with the predicted internal dose rate from the different models.

Table 6.4 The summary of average potassium concentrations and Cs-137 concentrations in water in Svyatoye and Perstok lake (Kudelsky, et al., 2005).

Year	Svyatoye lake		Perstok lake	
	Average K^+ (mg l^{-1})	Average Cs-137 (Bq l^{-1})	Average K^+ (mg l^{-1})	Average Cs-137 (Bq l^{-1})
1997-2004 for Svyatoye 1998-2004 for Perstok	7.79±2.03	11.17±3.98	5.95±1.14	13.17±7.72

Table 6.5 Summary of Concentration Ratio and DCC of Cs-137 in each model in Svyatoye and Perstok lakes (Copplestone, et al., 2003; ERICA, 2009; FASSET, 2003; J. Smith, 2005; U.S.DOE, 2002).

Model	Concentration Ratio (l kg^{-1})	DCC (μGy hr^{-1} per Bq kg^{-1})
FASSET	10200	$1.6x10^{-4}$
ERICA	7100	$1.8x10^{-4}$
RESRAD	22000	$1.48x10^{-4}$
R&D128	11000	$1.74x10^{-4}$
D-MAX	Svyatoye: 1253(p), 614(np) Perstok: 1640(p), 803(np)	$4.67x10^{-4}$

Note p – predatory, np – nonpredatory

6.2.6 The prediction of DCCs and internal dose rate of Sr-90 in fish using different models

Unlike Cs-137, there are not many data of Sr-90 activity concentration in fish (only 6 data in Perstok lake and no such data in Svyatoye lake). The estimation of fish mass and fish concentration by using the Monte Carlo method is not possible because of high uncertainty: there are not enough data to determine accurate probability distributions. For Sr-90, it was only possible to carry out a comparison of DCCs and the internal dose rate between the models. The DCCs can be compared between the DCCs predicted by the 5 models and the DCCs from the fitted Equation (D = 5.46E-5 Ln(m) + 7.95E-4 when D is Dose rate in μGy hr^{-1} per Bq kg^{-1}, or DCC, and m is weight of organism in kg). If direct measurements of Sr-90 activity concentration in fish are not available, FASSET, ERICA, R&D and RESRAD models can predict the internal dose rate by using Sr-90 concentration in water, concentration ratio (CR, l kg^{-1}) and DCC from each model. The DMAX model can use Ca^{2+} concentration in water to predict Concentration Ratio (CR). The details of this relationship have been described in Chapter 2, Section 2.5.5. A summary of average calcium concentrations and Sr-90 concentrations in water in Perstok lake is shown in **Table 6.6**. The summary of Concentration Ratios and DCCs used in each model in Svyatoye and Perstok lake are shown in **Table 6.7**.

Table 6.6 The summary of average calcium concentrations and Sr-90 concentrations in water in Svyatoye and Perstok lake (Kudelsky, et al., 2005).

Year	Perstok lake	
	Average Ca^{2+} ($mg\ l^{-1}$)	Average Sr-90 ($Bq\ l^{-1}$)
1998-2004	26.45±1.32	22.0

Table 6.7 The summary of Concentration Ratios and DCCs of Sr-90 in each model in Perstok lake (Copplestone, et al., 2003; ERICA, 2009; FASSET, 2003; J. Smith, 2005; U.S.DOE, 2002).

Model	Concentration Ratio ($l\ kg^{-1}$)	DCC ($\mu Gy\ hr^{-1}$ per $Bq\ kg^{-1}$)
FASSET	25	$6{,}20x10^{-4}$
ERICA	17	$6.30x10^{-4}$
RESRAD	320	$5.82x10^{-4}$
R&D128	43	$6.22x10^{-4}$
D-MAX	227	$6.50x10^{-4}$
Fitted Equation	-	$5.38x10^{-4}$±$5.22\ x10^{-5}$

6.3 Results

6.3.1 The comparison of DCCs for Cs-137 predicted by the Monte Carlo method with those predicted by the 5 models

The predicted DCCs for Cs-137 can be calculated by using the randomly generated values of fish mass in the fitted equations (D = 7.79E-6 Ln(m) + 1.80E-4) relating fish mass to DCC_{int}. The uncertainty of the fitted equation is 8%. The uncertainty was calculated from the standard deviation of residual of the fitted equation predicted and the models predicted. The comparison of the variation in predicted DCC by the Monte Carlo method and the DCC predicted by the 5 models for Svyatoye and Perstok lake are shown in **Figures 6.6** and **6.7** respectively.

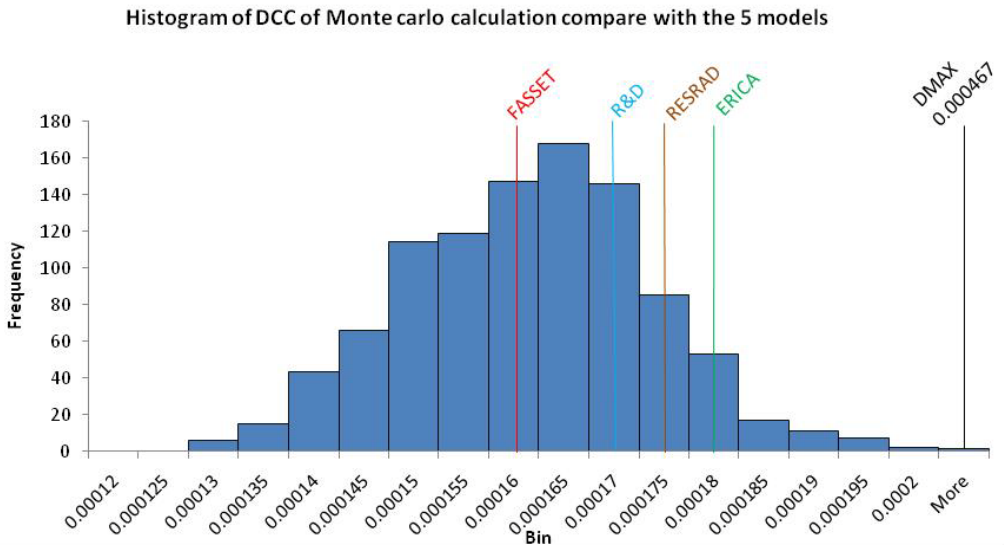

Figure 6.6 The variation in predicted DCC by the Monte Carlo method and the DCC predicted by the 5 models for Svyatoye lake.

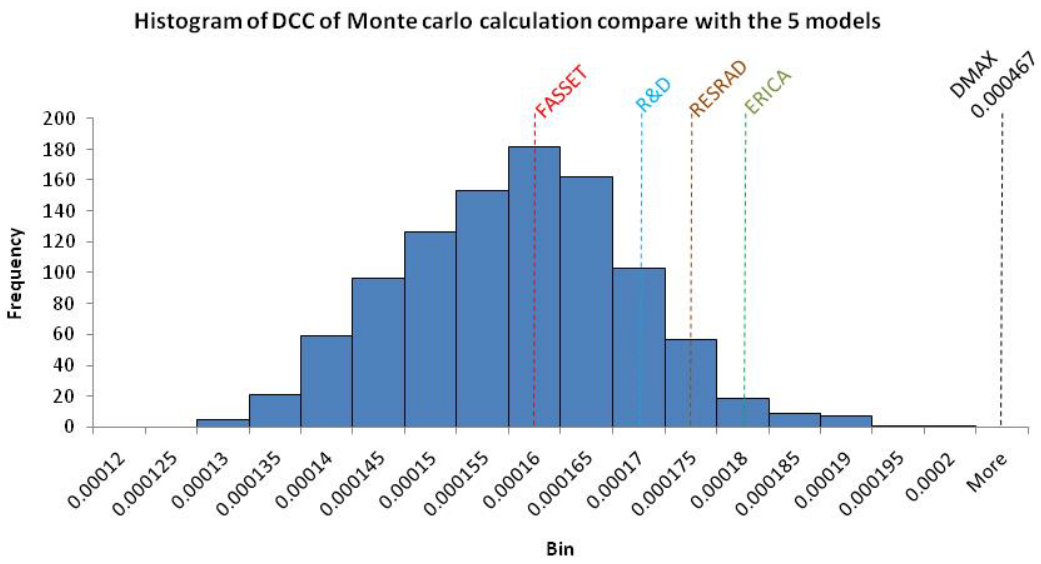

Figure 6.7 the variation in predicted DCC by the Monte Carlo method and the DCC predicted by the 5 models for Perstok lake.

For Svyatoye lake, the DCCs predicted by the FASSET, R&D128, RESRAD, ERICA and DMAX models were $1.6x10^{-4}$, $1.7x10^{-4}$, $1.75x10^{-4}$, $1.8x10^{-4}$ and $4.67x10^{-4}$ µGy hr^{-1} per Bq kg^{-1} respectively. The predicted DCCs by the Monte Carlo method was normally distributed with mean and standard deviation $1.59x10^{-4}\pm1.22x10^{-5}$ µGy hr^{-1} per Bq kg^{-1}. The range of values within two standard deviations of the mean was $1.346x10^{-4}$ to

$1.834x10^{-4}$ μGy hr^{-1} per Bq kg^{-1}. This range includes all of the DCCs predicted by the models except the DMAX model: this model aims to give a conservative maximum exposure.

For Perstok lake, the predicted DCCs by the Monte Carlo method were normally distributed with mean and standard deviation $1.56x10^{-4}\pm1.11x10^{-5}$ μGy hr^{-1} per Bq kg^{-1}. The range of values within two standard deviations of the mean was $1.338x10^{-4}$ to $1.782x10^{-4}$ μGy hr^{-1} per Bq kg^{-1}. This range includes all of the DCCs predicted by the models except the D-MAX model.

6.3.2 Monte Carlo prediction of the variation of Cs-137 internal dose rate compared with the five models

The internal dose rate determined from measurements of radionuclide activity concentration in fish can also be also compared between the Monte Carlo assessment of variability and the five models. In this case, for the Monte Carlo model randomly generated fish mass data were used (based on the measured variability in fish mass), the fitted equation (D = 7.79E-6 Ln(m) + 1.80E-4) and randomly generated radionuclide activity concentration in fish (based on the measured variability in radionuclide activity concentration in each lake). These data were used to calculate the variation in internal dose rate.

For the five models, using DCCs and the observed radionuclide activity concentration in fish, the internal dose rate was predicted for each sample. The comparisons of the internal dose rate estimated by each model in Svyatoye and Perstok lakes are shown in **Table 6.8** and **Figure 6.8**. The results show that the prediction of the internal dose rates in each model are within the range of values predicted by the Monte Carlo model in both Svyatoye and Perstok lake except for the D-Max model which tends to give an upper bound estimate of dose. The standard deviation of the estimated internal dose rates from Perstok lake is smaller than Svyatoye lake because the variation of radioactivity concentration in Perstok lake is less than in Svyatoye lake (**Table 6.2**).

Table 6.8 The predicted internal dose rate and z-score in each model in Svyatoye and Perstok lake.

Model	Internal dose rate (μGy hr^{-1}) and (z-score)	
	Svyatoye lake	Perstok lake
Monte Carlo method	3.16±3.31 (z=1.32)	1.27±0.50 (z=1.02)
FASSET	3.30±3.38 (z=0.70)	1.27±0.51 (z=0.99)
ERICA	3.71±3.80 (z=1.12)	1.43±0.58 (z=1.23)
R&D	3.51±3.59 (z=0.23)	1.35±0.55 (z=0.12)
RESRAD	3.61±3.69 (z=0.67)	1.39±0.57 (z=0.67)
D-MAX	10.34±10.55	3.97±1.61

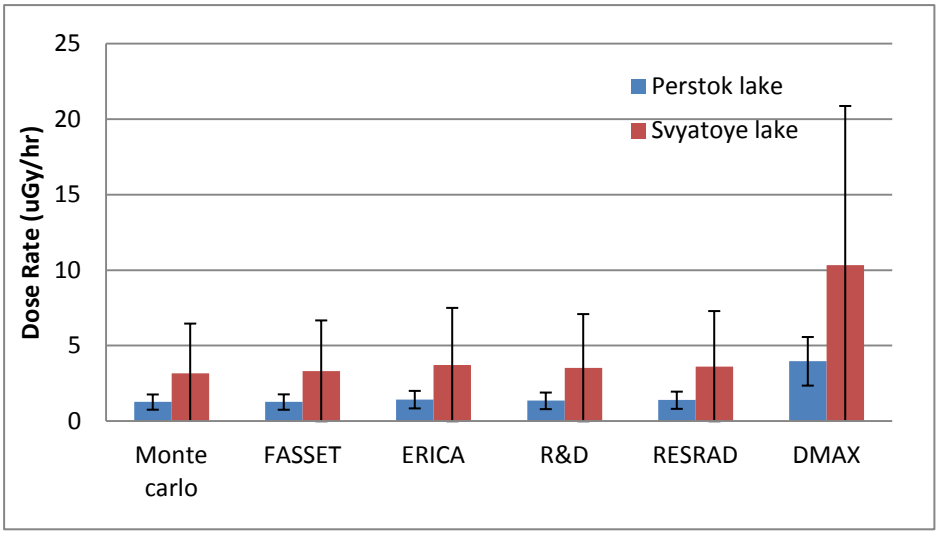

Figure 6.8 The comparison of the mean and variation in predicted internal dose rate for each model in Svyatoye and Perstok lake.

6.3.3 The effect of variability of fish mass, radionuclide activity concentration in fish and DCC on the predicted internal dose

The histograms of the variation of internal dose rate under three scenarios (1) fish mass, fish concentration and DCC all varied; 2) fish mass, fish concentration varied mean of DCC and 3) fish mass and DCC varied and use mean of fish concentration) are shown in **Figure 6.9** and **6.10** respectively.

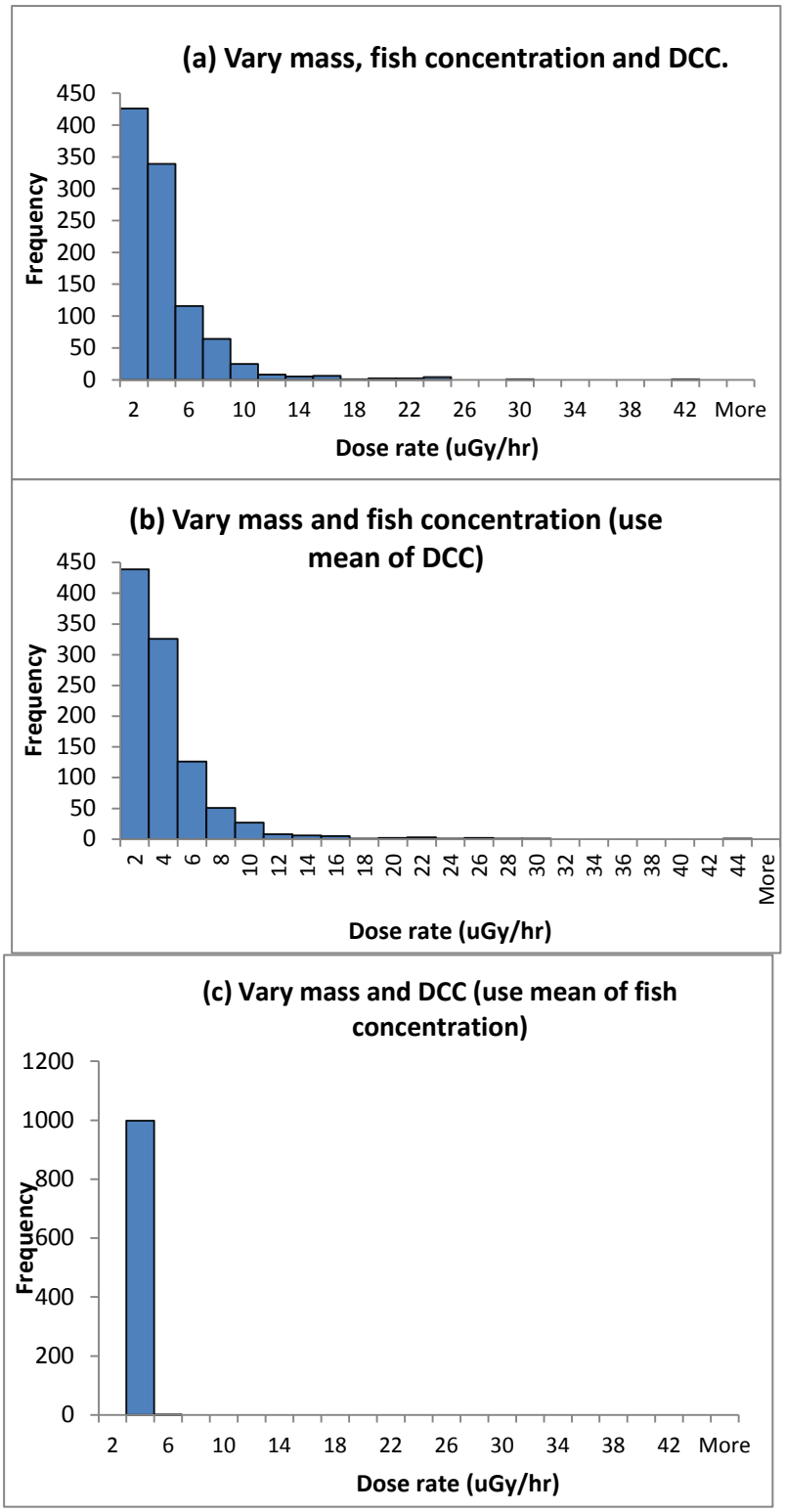

Figure 6.9 The effect of variation in fish mass, radionuclide activity concentration in fish and DCC on the predicted internal dose rate in Svyatoye lake; a) Fish mass, radionuclide activity concentration in fish and DCC all varied, b) Fish mass and radionuclide activity concentration in fish are varied, c) Fish mass and DCC are varied.

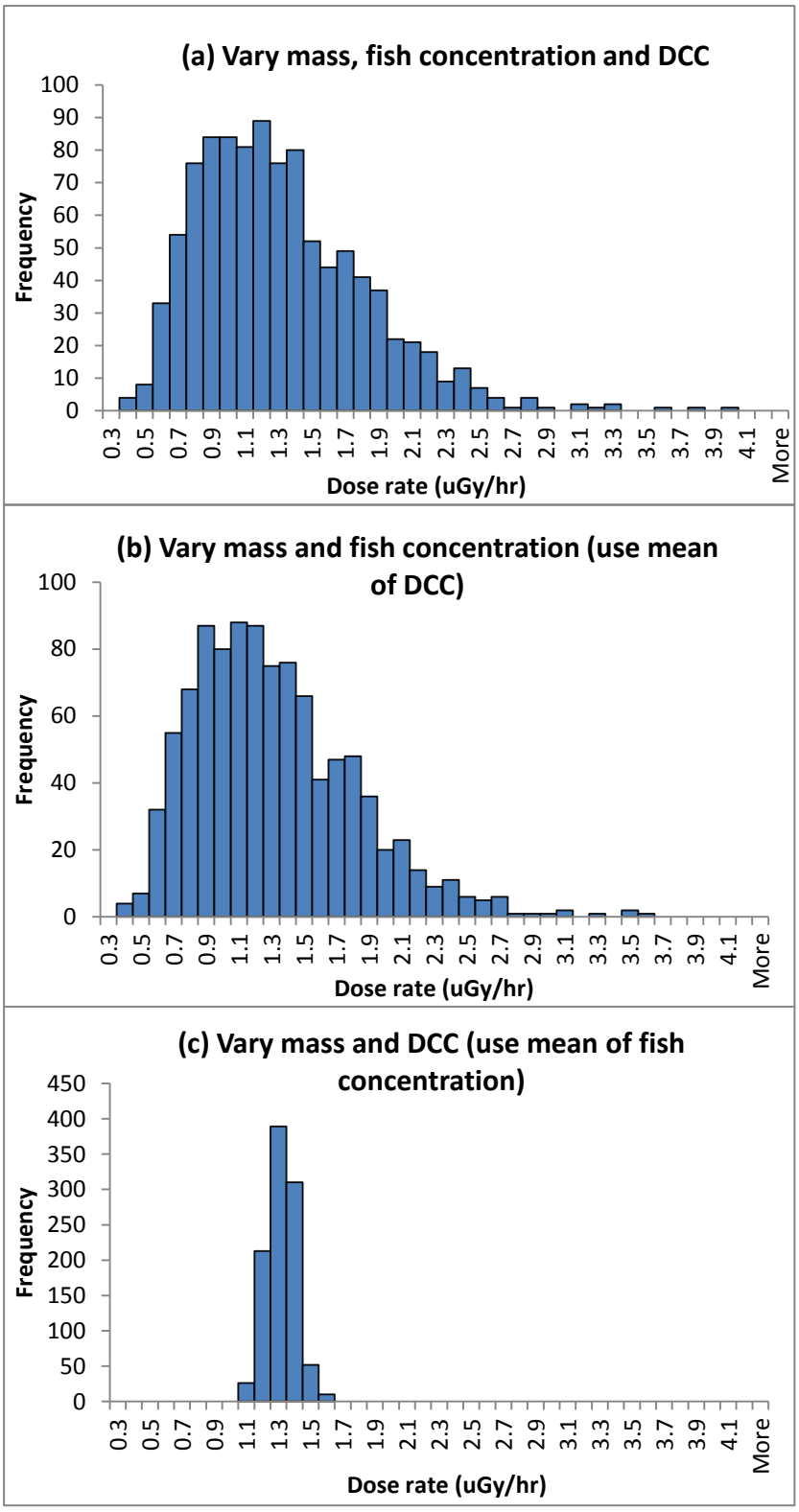

Figure 6.10 The effect of fish mass, radionuclide activity concentration in fish and DCC to the internal dose rate in Perstok lake; a) Vary fish mass, radionuclide activity concentration in fish and DCC, b) Vary fish mass and radionuclide activity concentration in fish, c) Vary fish mass and DCC.

From **Figure 6.9** and **6.10**, Scenario 1, the internal dose rate was distributed with mean and standard deviation 3.1617±3.3081 μGy hr^{-1} in Svyatoye lake and 1.2680±0.5047 μGy hr^{-1} in Perstok lake. For Scenario 2, the internal dose rate was distributed with mean and standard deviation 3.1851±3.4152 μGy hr^{-1} in Svyatoye lake and 1.2678±0.4943 μGy hr^{-1} in Perstok lake. For Scenario 3, the internal dose rate was distributed with mean and standard deviation 3.1851±0.2468 μGy hr^{-1} in Svyatoye lake and 1.2678±0.0912 μGy hr^{-1} in Perstok lake. Scenario 3 shows that, for the sampled distribution of fish, DCC and fish mass are not so important factors contributing to variation in internal dose rate. The most important factor is radionuclide activity concentration in fish because the standard deviation of the internal dose rate is high when varying the radionuclide activity concentration and low when the mean of measured values was used.

6.3.4 The internal dose rate predicted by using radionuclide concentration in water

The predicted dose rates from the different models compared with the variation of the predicted dose rate using the Monte Carlo Method (based on the measurements of Cs-137 in fish) are shown in **Table 6.9**, **Figure 6.11** (Svyatoye lake) and **6.12** (Perstok lake). **Figure 6.11** and **6.12** show the over prediction of the internal dose rate based on from Cs-137 concentration in water by using FASSET, ERICA, R&D and RESRAD models while DMAX model shows the closer prediction than the other models because it uses the K^+ concentration in water to predict the internal dose rate.

Table 6.9 Comparison of the predicted dose rate from the different models and the variation of the predicted dose rate using the Monte Carlo Method.

Model	Internal Dose Rate (μGy hr^{-1})	
	Svyatoye lake	Perstok lake
FASSET	18.23	21.5
ERICA	14.3	16.8
RESRAD	36.38	43
R&D128	21	25
D-MAX	6.53 (predatory) 3.2 (non-predatory)	10.08 (predatory) 4.94 (non-predatory)
Monte Carlo	3.16±3.30	1.26±0.50

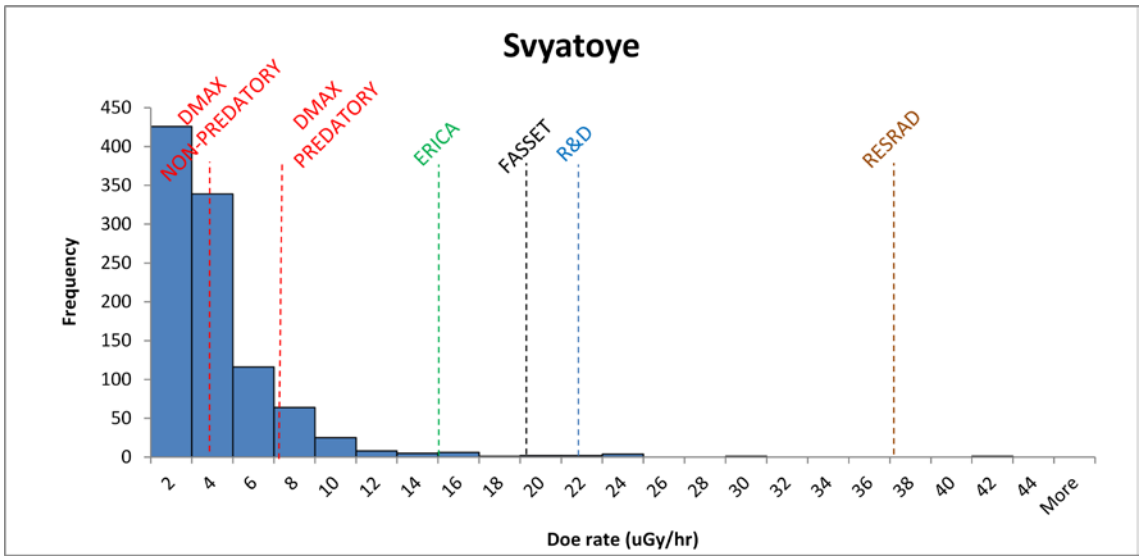

Figure 6.11 The predicted internal dose rate from the different models and the variation of the predicted dose rate based on measurements using the Monte Carlo Method in Svyatoye lake.

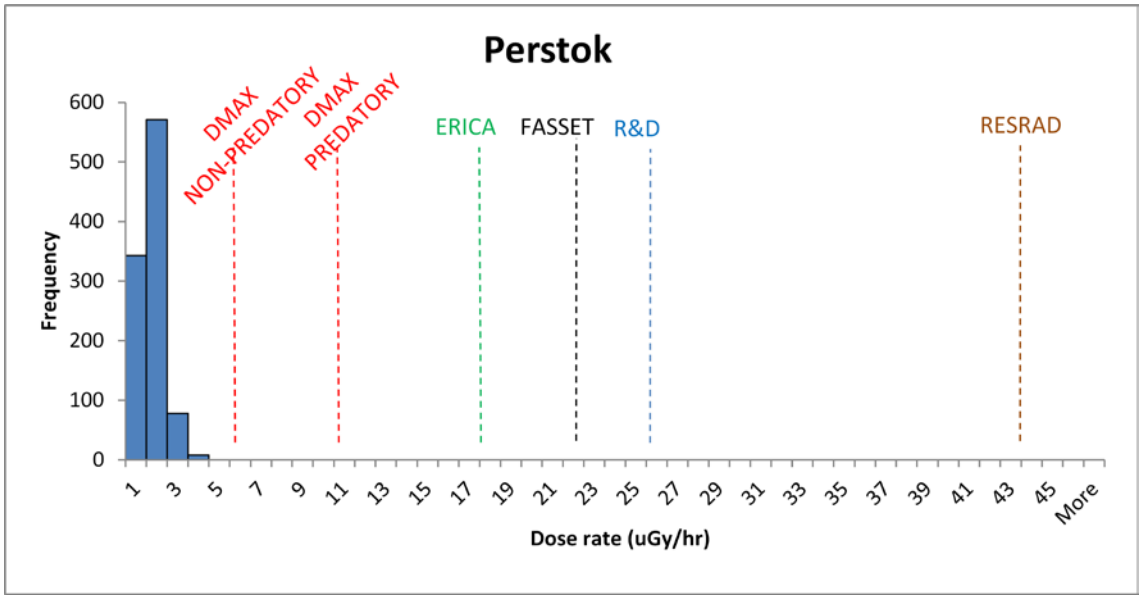

Figure 6.12 The predicted internal dose rate from the different models and the variation of the predicted dose rate form Monte Carlo Method in Perstok lake.

6.3.5 The prediction of DCCs and internal dose rates of Sr-90 in fish using different models

The comparison of DCC in different models

The predicted DCC of Sr-90 in pelagic fish by using the fitted Equation (D = 5.46E-5 Ln(m) + 7.95E-4) can be compared with the DCC predicted by the five models, as shown in **Table 6.10** and **Figure 6.14**. It shows slight differences in DCCs between the models (z<2). The results show the very low variation in DCC between the different models.

Table 6.10 The comparison of DCC_{int} for Sr-90 and z-score in each model compared with the range in DCC_{int} values estimated using the variability in fish mass in the samples from Perstok Lake.

Model	DCC_{int} (µGy hr^{-1} per Bq kg^{-1})	z-score
FASSET	$6.20x10^{-4}$	0.32
ERICA	$6.30x10^{-4}$	0.57
R&D	$6.22x10^{-4}$	0.37
RESRAD	$5.820x10^{-4}$	0.62
D-MAX	$6.50x10^{-4}$	1.06
Fitted Equation (Based on mass)	$5.38x10^{-4}\pm5.22x10^{-5}$	1.71

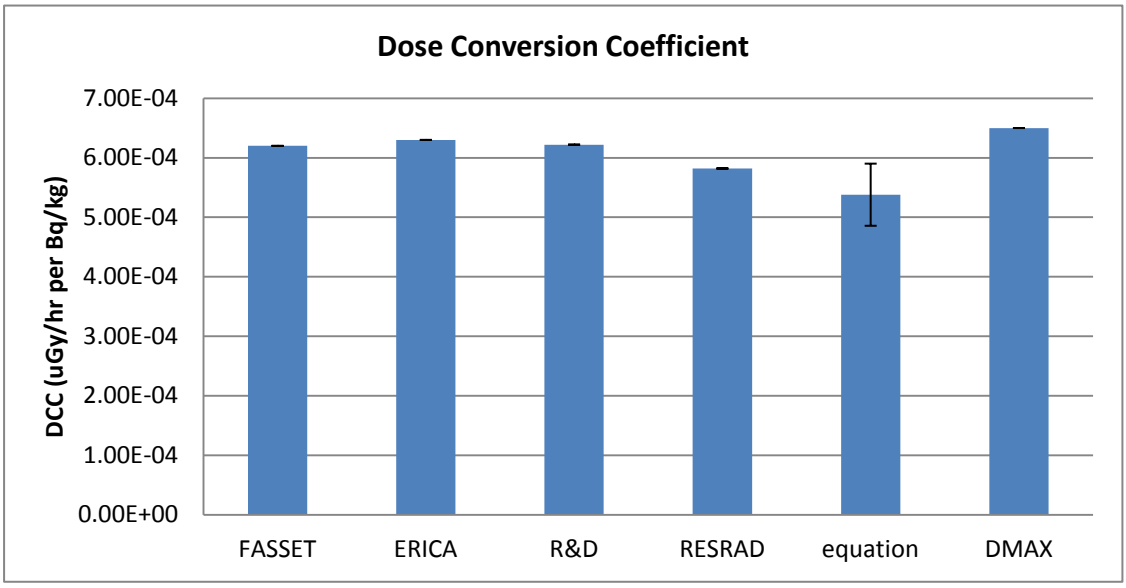

Figure 6.13 Comparison of the DCCs of Sr-90 in each model

The comparison of the internal dose rate in different models

The internal dose rate determined from tissue concentration can be compared between the five models and the fitted Equation. FASSET, ERICA, RESRAD and R&D models can predict the internal dose rate by using Sr-90 concentration in water and for the D-MAX model can use Ca^{2+} concentration in water to predict the internal dose rate. The predicted internal dose rate determined from tissue concentration in comparison with the predicted internal dose rate determined from Sr-90/Ca^{2+} concentration in water is shown in **Table 6.11** and **Figure 6.14**.

Table 6.11 The comparison of the internal dose rate for Sr-90 and z-score in each model.

Model	Internal dose rate (µGy hr^{-1}) and (z-score)	
	From tissue concentration	From water concentration
FASSET	4.07±2.10 (z=0.33)	0.34 (z=0.75)
ERICA	4.13±2.14 (z=0.57)	0.24 (z=0.80)
R&D	4.08±2.11 (z=0.38)	0.59 (z=0.61)
RESRAD	3.82±1.97 (z=0.59)	4.10 (z=1.31)
DMAX	4.26±2.20 (z=1.05)	3.24 (z=0.84)
Fitted Equation	3.51±1.98 (z=1.73)	-

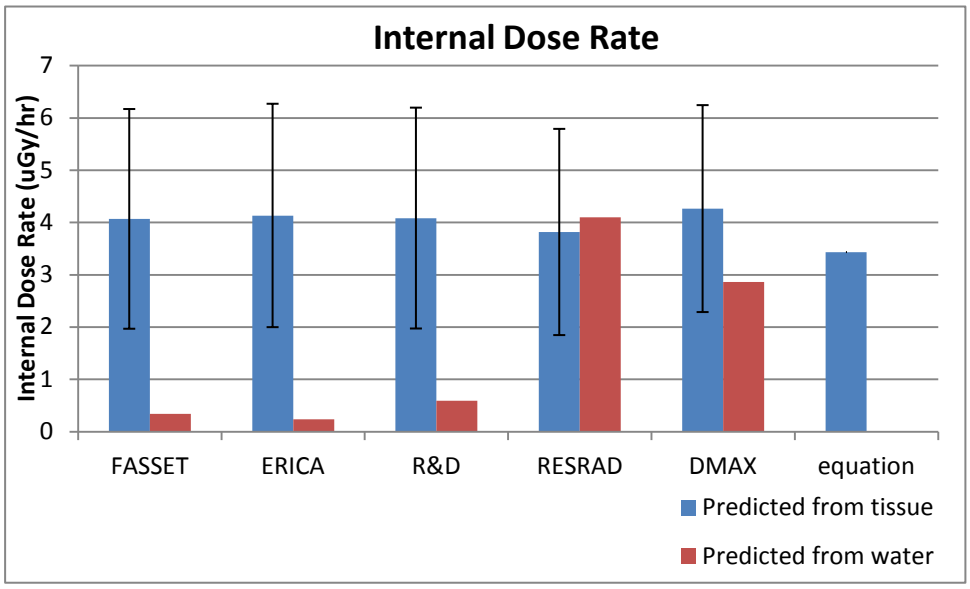

Figure 6.14 The comparison of the internal dose rate predicted from tissue concentration and Sr-90/Ca^{2+} concentration in water in each model.

The internal dose rate predicted by tissue concentration shows slight differences between the models while the internal dose rate predicted by Sr-90/Ca^{2+} concentration in water shows under prediction except RESRAD and D-MAX models which give predictions within the range of doses estimated from tissue Sr-90 concentrations.

6.4 Discussion

6.4.1 The frequency distribution of fish mass and radioactivity concentration in fish

In an actual environment, the variation of fish mass and radioactivity concentration in fish are found resulting in uncertainty of the internal dos rate in fish. The variation of fish mass was found to be 0.2165±0.4033 kg and 0.1398±0.3169 kg in Svyatoye and Perstok lakes respectively (**Table 6.2**). The variation of Cs-137 activity concentration was found to be 20,629±21,101 and 7,950±3,229 in Svyatoye and Perstok lakes respectively (**Table 6.2**). The frequency distribution of fish mass and Cs-137 activity concentration were found to be not normally distributed, as indicated by the high standard deviations in data. However, the frequency distribution of fish mass and Cs-137 activity concentration on a log scale were close to the normal distribution. A number of radiocaesium studies have reported that Cs-137 activity concentration is not normally distributed in varies species (e.g. green treefrogs (*Hyla cinerea*) (Dapson & Kaplan, 1975) and fish (Oleksyk, et al., 2002; Ugedal, Forseth, Jonsson, & Njastad, 1995)) but often lognormal distributed (Oleksyk, et al., 2002; Schubert, Brodsky, & Tyler, 1967; Ugedal, et al., 1995). The frequency distribution of activity concentrations in mammals have been found to be more skewed than fish (Oleksyk, et al., 2002). The frequency distribution of Cs-137 activity concentration in Perstok lake (skewness -0.0042) was closer to a log-normal distribution than Svyatoye lake (skewness 0.3808), whist the frequency distribution of fish mass in Svyatoye lake (skewness -0.1317) was closer to a log-normal distribution than Perstok lake (skewness 0.2935). The better shape of the frequency distribution of fish mass and Cs-137 activity concentration in log scale can be tested by using more fish sample and more fish size. The fish size used in this study was limited by the net size.

6.4.2 The comparison of DCCs and the internal dose rates for Cs-137

The Monte Carlo method was used to generate the variation of fish mass and Cs-137 activity concentration in fish (based on measured data) by assuming these parameters are log-normally distributed. The $DCCs_{int}$ were generated by the Monte Carlo method (based on the fitted Equation 3.3 and fish mass) which were then compared with the five models. The variation of the predicted DCCs by the Monte Carlo method was normally distributed with $1.59x10^{-4}\pm1.22x10^{-5}$ and $1.56x10^{-4}\pm1.11x10^{-5}$ μGy hr^{-1} per Bq kg^{-1} in Svyatoye and Perstok lakes, whilst the DCCs predicted by the five models were distributed within these ranges. The exception to this was the DMAX model which gives a conservative maximum exposure.

The predicted internal dose rates were compared between the five models and the Monte Carlo method using the Z-score. There was a good agreement ($z<2$) between the models to predict the internal dose rate. It should be noted that in both lakes all of the models except the conservative D-MAX model underpredicted internal dose rates to some fish (see **Figures 6.6** and **6.7**). So, the reference organism approach gave good estimates of average dose to fish, but gave underestimates for some fish.

6.4.3 The effect of fish mass, radionuclide activity concentration and DCC

The study of the effect of fish mass, radionuclide activity concentration in fish and DCC to the internal dose showed that the most important factor in determining variability in internal dose was radionuclide activity concentration in fish. The other factors (fish mass and DCC) were not so important. The shape of the frequency distribution of the internal dose rate was more dependent on the input function of the radionuclide activity concentration than the other factors. The size of the fish is also important to the internal dose as already discussed in Chapter 3. In an early phase of Chernobyl fall out, the Cs-137 concentration in fish decreased with age because younger age feed more contaminated food than older age (Kryshev & Ryabov, 2000). After the initial phase, the highest feeding and growth rates fish (young fish) showed the lowest Cs-137 concentration (Kryshev & Ryabov, 2000; Ugedal, et al., 1995) because the radioactivity concentration in water decreased by deposition to the sediment, resulting in reduction of radioactivity concentration in the new generation of fish (Kryshev & Ryabov, 2000). The Cs-137 activity concentration increased with fish size (Elliott, et al., 1992;

Koulikov & Ryabov, 1992; Ugedal, et al., 1995) because large animals (high body mass) may accumulate the radionuclide over the period of time (Oleksyk, et al., 2002). However, the Cs-137 concentration in fish depends on the increasing age rather than size (McCreedy, Jagoe, Glickman, & Brisbin, 1997), though the feeding behaviour (predatory/non-predatory) is also important.

It should be noted that when analysing fish data, the fishing method should be taken into account. The size of nets used affect the distribution of fish caught (Carol & García-Berthou, 2007). The gill nets used in this study had a minimum mesh size of approximately 1 cm. So, fish below this size could not be sampled. So, the probability distribution of fish size and Cs-137 activity concentration shows the distribution for the caught samples. The distribution of fish size and activity concentration in the lakes is expected to be different. This will not affect the large fish sizes, which have higher activity concentration, so the higher dose rates are represented in the analysis. But, it is expected that smaller and very young fish could not be sampled, so the lower doses to these fish are not seen in the probability distributions.

6.4.4 The comparison of the internal dose rate predicted by using water activity concentration

The frequency distribution of the internal dose rate was compared with the internal dose rate predicted by using the Cs-137 activity concentration in water. The comparison showed the same result as the comparison in Chapter 4. The internal dose rate predicted by using the water activity concentration showed an over-prediction compared with the frequency distribution of the internal dose rate. The prediction of the internal dose rate of the D-MAX model was closer to the frequency distribution of the internal dose rate (in comparison to the other models) because this model used the potassium concentration in water to predict the internal dose rate (J. T. Smith, et al., 2002). But, the D-MAX model under-estimated the dose to some fish, so the uncertainty in D-MAX predictions needs to be accounted for when applying it as a conservative screening model. The RESRAD model showed the worst prediction of the internal dose rate when used to predict doses based on the Cs-137 concentration in water. In this case, the model using site specific chemistry (potassium concentration) showed closer prediction to the measured data rather than the other models (Yankovich, et al., 2010). The results showed that the variability of the prediction of radionuclide transfer to the biota is the

most important factor resulting the variability in the dose rate in biota, as found in previous studies (Beresford, Barnett, Brown, et al., 2008; Beresford, et al., 2010; Vives i Batlle, et al., 2007; Yankovich, et al., 2010).

6.4.5 The comparison of DCCs and the internal dose rate for Sr-90

For Sr-90, there were no enough data for the fish mass and radioactivity concentration to generate probability distributions by using the Monte Carlo method. The sample sizes need to be large enough for statistical analysis of the data. The comparison of the DCCs between the models showed that there was a good agreement between the models ($z<2$). The comparison of the internal dose rate between the prediction from tissue concentration and the prediction from the water concentration showed an over-prediction of the internal dose rate from the water concentration which is the same result as was found in Chapter 4, but this chapter showed the variation of the internal dose rate. The RESRAD model showed a good prediction of the internal dose rate comparing with the other models (Yankovich, et al., 2010). The type of fish (predatory or non-predatory) also affects the concentration factor of Sr-90 and so the internal dose rates since non-predatory fish have a higher Sr-90 concentration factor than predatory fish (Kryshev, 2006; Outola, Saxén, & Heinävaara, 2009).

6.5 Summary

In summary, significant variation of fish mass and fish concentration is found in real environments, resulting in uncertainty in estimation of the internal dose. The Monte Carlo method was used to estimate the uncertainty in internal dose rate caused by uncertainty of the data. Some of the models have probabilistic function for the internal dose rate such as ERICA and RESRAD model. Those models can generate the internal dose rate by using mean and standard deviation of radionuclide activity concentration in water. Many factors affect the uncertainty in the internal dose rate; in this study the variability in fish mass, age, radioactivity concentration and DCCs was studied. It was found that variability in Cs-137 activity concentration in different fish was the most important factor in the uncertainty of predictions of internal dose rate. The age and the size of the fish also affect predictions but are less important.

The model comparison with variability in fish in real lakes has shown the limitations of the reference organism approach used in models. It was found that the models using this

approach gave generally good estimates of average dose rate to fish from Cs-137, but they underestimated dose to a part of the fish population of the lake, because some fish had size significantly greater than the size of the reference organism.

It is also necessary to consider for dose assessments the dose to different stages of the life cycle of fish. In this study, because of the gill-net sampling method, we could not study very young, small fish. It is expected that their internal dose would be lower than the range of internal doses estimated by the Monte Carlo method used because activity concentrations in small fish are lower than in bigger fish. But the external dose to small fish, fertilized eggs and roe might be greater than estimated by models, especially in cases where part of the life cycle is spent on the sediment surface.

6.6 References

Beresford, N. A., Barnett, C., Brown, J., Cheng, J., Copplestone, D., Filistovic, V., et al. (2008). Inter-comparison of models to estimate radionuclide activity concentrations in non-human biota. *Radiation and Environmental Biophysics, 47*(4), 491-514.

Beresford, N. A., Barnett, C. L., Brown, J. E., Cheng, J. J., Copplestone, D., Gaschak, S., et al. (2010). Predicting the radiation exposure of terrestrial wildlife in the Chernobyl exclusion zone: an international comparison of approaches. *Journal of Radiological Protection, 30*(2), 341.

Beresford, N. A., Barnett, C. L., Howard, B. J., Scott, W. A., Brown, J. E., & Copplestone, D. (2008). Derivation of transfer parameters for use within the ERICA Tool and the default concentration ratios for terrestrial biota. *Journal of Environmental Radioactivity, 99*(9), 1393-1407.

Brown, J. E., Alfonso, B., Avila, R., Beresford, N. A., Copplestone, D., Pröhl, G., et al. (2008). The ERICA Tool. *Journal of Environmental Radioactivity, 99*(9), 1371-1383.

Carol, J., & García-Berthou, E. (2007). Gillnet selectivity and its relationship with body shape for eight freshwater fish species. *Journal of Applied Ichthyology, 23*(6), 654-660.

Copplestone, D., Wood, M. D., Bielby, S., Jones, S. R., Vives, J., & Beresford, N. A. (2003). *Habitats regulations for Stage 3 assessments: radioactive substances authorisations*. Bristol: Environment Agency.

Cox, G. M., Gibbons, J. M., Wood, A. T. A., Craigon, J., Ramsden, S. J., & Crout, N. M. J. (2006). Towards the systematic simplification of mechanistic models. *Ecological Modelling, 198*(1-2), 240-246.

Dapson, R. W., & Kaplan, L. (1975). Biological Half-Life and Distribution of Radiocesium in a Contaminated Population of Green Treefrogs Hyla cinerea. *Oikos, 26*(1), 39-42.

Elliott, J. M., Hilton, J., Rigg, E., Tullett, P. A., Swift, D. J., & Leonard, D. R. P. (1992). Sources of Variation in Post-Chernobyl Radiocaesium in Fish from Two Cumbrian Lakes (North-West England). *Journal of Applied Ecology, 29*(1), 108-119.

ERICA. (2009). ERICA Assessment Tool: ERICA.

FASSET. (2003). *Dosimetric models and data for assessing radiation exposures to biota. Deliverable 3*. Stockholm: Norwegian Radiation Protection Authority.

Hosseini, A., Thørring, H., Brown, J. E., Saxén, R., & Ilus, E. (2008). Transfer of radionuclides in aquatic ecosystems - Default concentration ratios for aquatic biota in the Erica Tool. *Journal of Environmental Radioactivity, 99*(9), 1408-1429.

Jacoboni, C., & Lugli, P. (1989). The Monte Carlo Method for Semiconductor Device Simulation Available from http://books.google.co.uk/books?id=3cWnyhKmACEC&pg=PP9&dq=the+monte+carlo+method&lr=&source=gbs_selected_pages&cad=5#v=onepage&q=&f=false

Jain, S. (1992). *Monte Carlo Simulations of Disordered Systems*. Singapore: World Scientific Publishing Co. Pte. Ltd.

Kalos, M. H., & Whitlock, P. A. (1986). *Monte Carlo methods* (Vol. Volume I: Basics). New York: John Wiley & Sons, Inc.

Koulikov, A. O., & Ryabov, I. N. (1992). Specific cesium activity in freshwater fish and the size effect. *Science of The Total Environment, 112*(1), 125-142.

Kryshev, A. I. (2006). 90Sr in fish: A review of data and possible model approach. *Science of The Total Environment, 370*(1), 182-189.

Kryshev, A. I., & Ryabov, I. N. (2000). A Dynamic model of 137Cs accumulation by fish of different age classes. *Journal of Environmental Radioactivity, 50*(3), 221-233.

Kudelsky, A. V., Pashkevich, V. I., Yankov, A. I., Samodurov, V. P., Savchik, S. F., & Rudemok, A. A. (2005). *Radio-ecological study of the Chernobyl Cooling Pond and options for remediation*. Minsk: National Academy of Science of Belarus.

McCreedy, C. D., Jagoe, C. H., Glickman, L. T., & Brisbin, I. L. (1997). Bioaccumulation of cesium-137 in yellow bullhead catfish (Ameiurus natalis) inhabiting an abandoned nuclear reactor reservoir. *Environmental Toxicology and Chemistry, 16*(2), 328-335.

Oleksyk, T. K., Gashchak, S. P., Glenn, T. C., Jagoe, C. H., Peles, J. D., Purdue, J. R., et al. (2002). Frequency distributions of 137Cs in fish and mammal populations. *Journal of Environmental Radioactivity, 61*(1), 55-74.

Outola, I., Saxén, R. L., & Heinävaara, S. (2009). Transfer of 90Sr into fish in Finnish lakes. *Journal of Environmental Radioactivity, 100*(8), 657-664.

Rubinstein, R. Y. (1981). *Simulation and the Monte Carlo Method*. New York: John Wiley & Sons, Inc.

Schubert, J., Brodsky, A., & Tyler, S. (1967). The Log-Normal Function As a Stochastic Model of the Distribution of Strontium-90 and Other Fission Products in Humans. *Health Physics, 13*(11), 1187-1204.

Science and Decisions : Advancing Risk Assessment. (2008). Available from http://site.ebrary.com/www/lib/portsmouth/docDetail.action?docID=10286194

Smith, J. (2005). Effects of ionising radiation on biota: do we need more regulation? *Journal of Environmental Radioactivity, 82*(1), 105-122.

Smith, J. T., Kudelsky, A. V., Ryabov, I. N., Daire, S. E., Boyer, L., Blust, R. J., et al. (2002). Uptake and elimination of radiocaesium in fish and the "size effect". *Journal of Environmental Radioactivity, 62*(2), 145-164.

Smith, J. T., Kudelsky, A. V., Ryabov, I. N., & Hadderingh, R. H. (2000). Radiocaesium concentration factors of Chernobyl-contaminated fish: a study of the influence of potassium, and "blind" testing of a previously developed model. *Journal of Environmental Radioactivity, 48*(3), 359-369.

U.S.DOE. (2002). *A Graded Approach for Evaluating Radiation Doses to Aquatic and Terrestrial Biota Module 1: Principles and Application*: U.S.DOE.

U.S.DOE. (2009). RESRAD-BIOTA for Windows (Version 1.5): U.S. Department of Energy.

Ugedal, O., Forseth, T., Jonsson, B., & Njastad, O. (1995). Sources of Variation in Radiocaesium Levels Between Individual Fish from a Chernobyl Contaminated Norwegian Lake. *Journal of Applied Ecology, 32*(2), 352-361.

Vives i Batlle, J., Balonov, M., Beaugelin-Seiller, K., Beresford, N., Brown, J., Cheng, J. J., et al. (2007). Inter-comparison of absorbed dose rates for non-human biota. *Radiation and Environmental Biophysics, 46*(4), 349-373.

Wright, S., Smith, J., Beresford, N., & Scott, W. (2003). Monte-Carlo prediction of changes in areas of west Cumbria requiring restrictions on sheep following the Chernobyl accident. *Radiation and Environmental Biophysics, 42*(1), 41-47.

Yankovich, T. L., Batlle, J. V. i., Vives-Lynch, S., Beresford, N. A., Barnett, C. L., Beaugelin-Seiller, K., et al. (2010). An international model validation exercise on radionuclide transfer and doses to freshwater biota. *Journal of Radiological Protection, 30*(2), 299.

Chapter 7

General Conclusions

On 26 April 1986, the worst nuclear accident in the history of the nuclear industry occurred at Unit 4 of the Chernobyl nuclear power plant (ChNPP) in the Ukraine (at that time a Republic of the Soviet Union) (Anspaugh, Catlin, & Goldman, 1988; IAEA, 2006a, 2006b; Smith & Beresford, 2005; UNSCEAR, 2000). A large amount of radioactive nuclides were released into the environment (IAEA, 2006b; UNSCEAR, 1996) and large areas of Ukraine, Belarus and Russia were badly contaminated (IAEA, 2006a, 2006b; OECD/NEA, 2002). Now, twenty years on, only isotopes with half lives exceeding a decade remain in the environment in significant quantities. Cs-137 (half life =30.17 y) and Sr-90 (half life = 28.8 y) remain the contaminants of greatest importance whereas over the longer term (hundreds to thousands of years) the long half life contaminants of plutonium isotopes and americium-241 will remain (IAEA, 2006b).

The effect of ionizing radiation from radioactive nuclides (particularly Cs-137 and Sr-90) released from the accident is still important. The freshwater aquatic environments of the 30 km Exclusion Zone around Chernobyl present a unique opportunity to quantify the effects of chronic radiation doses from ionising radiation on biota (IAEA, 2006b). Few studies have been able to assess the effects of chronic radiation exposure on animal and plant life in its natural environment. In order to assess the effects of chronic radiation on biota, it is necessary to develop effective methods of estimating radiation doses. The purpose of the present study was to further compare and test models for estimating radiation doses to biota in the natural environment. In addition to carrying out further model intercomparison and testing against empirical data, this research will also support previous work on the effects of radiation on aquatic biota (e.g. (Cailes, 2006) and (Tumnoi, 2006)) by accurately measuring the dose in the littoral zone of the lakes.

Five models (RESRAD, FASSET, ERICA, R&D128 and the D-Max models) were used in this thesis for estimating both internal and external radiation doses to biota. The testing and critical analysis of these models was carried out to give a better understanding of the prediction of internal and external dose by the models and of the influence of variation in organism size, organism shape, Dose Conversion Coefficient (DCC) and radionuclide concentration on doses.

External radiation dose can also be determined by in situ measurement. Thermoluminescent Dosimeters (TLDs) were used for testing a new in situ measurement for the prediction of external gamma and beta radiation doses. TLDs were chosen for in situ measurement because they are passive dosimeters (they keep a cumulative record until the evaluation), suitable for the selected environment (water and sediment), small and reliable (Timms, Smith, Coe, Kudelsky, & Yankov, 2005). For comparing model predicted external doses with measured values, the activity concentration of Cs-137 and Sr-90 in environmental media samples (sediment, and water concentration) in Svyatoye, Perstok and Dvorishche lakes were used to predict the external dose rates.

Variation of predicted dose with size and shape of organism

The comparison of model predictions for different weights of organisms can be divided into two categories; the internal dose and the external dose. For the internal dose, the variation of organism shape did not significantly affect the results; because there was not much variation in dose around the fitted dose-mass relationships (see Chapter 3). So, the variation in organism mass is more important than variation in the organism shape. The deviation of the internal dose predicted for different organisms of Cs-137 seems to be uniform as a function of weight, whilst the deviation of the internal dose of Sr-90 (a pure beta emitter) is high in low weight organisms but quite low in high weight organisms. All of the simple model fits give reasonably good estimates of the dose to the different reference organisms used in the models. These are within 20% deviation for Cs-137 (a beta and gamma emitter) and 40% deviation for Sr-90 (beta emitter). For the external dose, the comparison of the external dose rate is more variable than the internal dose rate. The most important factor determining the external dose for biota predicted by the models appears to be occupancy factor. All models give predictions which are within 30% deviation of the dose-mass relationship (for Cs-137) and almost 50% deviation (for Sr-90) from the trend lines. The deviation of the external dose of Cs-137 and Sr-90 seems to be uniform in low and heavy weight organisms.

Model-data comparisons for internal dose

Model-data comparisons were carried out by estimating radiation doses from Cs-137 and Sr-90 in aquatic organisms (pelagic fish, benthic fish and crustacean) in two lakes (Svyatoye and Perstok) in Belarus. For predicting internal dose rates using measured

tissue concentrations the models all give similar values, but the D-MAX screening model gave approximately two times higher estimates than the other models. The similarity between the models for internal dose rates was also observed from an analysis of their DCC_{int} values. For estimating doses in cases where tissue measurements are not available, the models give much more varied predictions. The most important factor for the variability of the dose estimation is the radionuclide transfer to biota (CR), as found in other studies of models (Beresford, et al., 2008; Beresford, et al., 2010; Vives i Batlle, et al., 2007; Yankovich, et al., 2010). This is because the assumed CR is very different for different models. The model where CR is estimated depending on water chemistry gives the most accurate predictions as found in the previous Perch Lake study (Yankovich, et al., 2010).

For pelagic fish, internal dose plays the most significant role in dose formation in the study lakes. For benthic organisms, external dose from sediments is very important, so the assumption of habitat (in sediment, on sediment, or in water) and habitat occupancy is important in predicting the dose to these organisms.

For the dose assessment, doses estimated from tissue concentrations of radionuclides were used, because this was the most accurate method. The internal dose rates to fish in Svyatoye and Perstok lakes are near the dose limit (40 μGy h^{-1}), but the models (except the conservative D-MAX model for benthic organisms) do not predict the doses to be over the limit. If no tissue concentration data were available, the doses estimated from CR values (based on water activity concentration) were used. In this case, the predicted doses would have been over the 40 μGy h^{-1} limit by the D-MAX (benthic fish and crustaceans) and RESRAD (all species) models.

Uncertainty in estimates of fish internal dose rate in a real environment.

The uncertainty in estimates of the internal dose of fish in two contaminated lakes in Belarus (Lakes Perstok and Svyatoye) was studied by using data of fish mass and radionuclide activity concentration in fish. In an actual environment, variation of fish mass and fish concentration is seen, resulting in uncertainty in the estimation of the internal dose. The DCCs and the internal dose rates can be predicted by using Monte Carlo method to show the effects of variation in the data on predictions of dose rate. The DCCs of the 5 models were distributed within the normally distributed range of DCCs predicted by the Monte Carlo method apart from the DMAX model which over-

estimated doses. This model(DMAX) gives a conservative maximum exposure. There was also a good agreement ($z<2$) between the models to predict the internal dose rate.

The study of the effect of variation in fish mass, radionuclide activity concentration in fish and DCC to the internal dose showed that the most important factor was variation in radionuclide activity concentration in fish. The other factors (fish mass and DCC) were not such important sources of variation as the radionuclide activity concentration.

Assessment of external doses to biota in Lakes Svyatoye and Perstok

The external dose rate predicted from water and sediment activity concentrations was compared with in-situ measurements using Thermoluminescent dosimeters (TLDs) in the two closed lakes, Svyatoye and Perstok. A simple model for gamma dose rate with depth above and below the sediment surface gives reasonable agreement with measured values. The method of using the average activity concentration in the top 15 cm layer is more suitable to use for assessments than the maximum value because it gave more accurate estimates (less over-estimation) of dose rate. The measurement of in situ beta dose rate was not successful. The beta dose rates measured in all sites did not show any clear pattern with depth, but the measured Cs-137 and Sr-90 activity concentrations did show a clear pattern In addition, the beta dose rates predicted from the measured activity concentrations were much higher than the dose rates measured by the TLDs. The method of in situ beta dose rate measurement needs further investigation.

Twenty years after Chernobyl accident, most of the Cs-137 and Sr-90 in these lakes was still in the surface 15 cm of sediment. The calculated external gamma dose rates are in the range 1-2 times higher than the measured dose rate because of the conservative simplifying assumptions in the model. The external dose rate to insect larvae is the highest because they live in or on the sediment which has a much higher activity concentration than the water. The external dose rate is lowest to pelagic fish because they live in the water column. None of the estimated external dose rates were higher than 10 $\mu Gy\ hr^{-1}$.

Total (internal plus external) dose rates to aquatic organisms

The results of this study allow identification of the organisms in lakes which are likely to be exposed to the highest dose rates from two key gamma and beta-emitting radionuclides, Cs-137 and Sr-90. In the long term, both radionuclides are mainly found

in the sediments of lakes: activity concentrations in the water are much lower and not important for external dose. For Cs-137, the highest dose rates are expected to be to large fish (which have high uptake and absorb most of the internal gamma energy) and benthic organisms which receive a high external dose from sediments. For Sr-90, the organisms with high bioaccumulation (such as molluscs which have high calcium uptake for their shell) will have high doses. In addition, very small benthic organisms (size << than mean beta range in tissue) will receive high external Sr-90 doses from sediments.

It can be concluded that the external dose rates to benthic biota and large fish in these closed lakes are still significant at this long time after the Chernobyl accident. But, radiation effects on these organisms may not be clearly seen, since the dose rates are below or close to guideline limits.

References

Anspaugh, L. R., Catlin, R. J., & Goldman, M. (1988). Global impact of the Chernobyl reactor accident. *Journal Name: Science (Washington, D.C.); (United States); Journal Volume: 242:4885*, Medium: X; Size: Pages: 1513-1519.

Beresford, N. A., Barnett, C., Brown, J., Cheng, J., Copplestone, D., Filistovic, V., et al. (2008). Inter-comparison of models to estimate radionuclide activity concentrations in non-human biota. *Radiation and Environmental Biophysics, 47*(4), 491-514.

Beresford, N. A., Barnett, C. L., Brown, J. E., Cheng, J. J., Copplestone, D., Gaschak, S., et al. (2010). Predicting the radiation exposure of terrestrial wildlife in the Chernobyl exclusion zone: an international comparison of approaches. *Journal of Radiological Protection, 30*(2), 341.

Cailes, C. R. (2006). *Phenotypic and genetic effects of Chernobyl-derived radionuclide contamination on the red-eyed damselfly Erythromma Najas (Odonata, Coenagrionidae).* University of Plymouth, Plymouth.

IAEA. (2006a). *Chernobyl's Legacy: Health, Environmental and Socio-Economic Impacts and Recommendations to the Governments of Belarus, the Russian Federation and Ukraine*. Vienna: IAEA.

IAEA. (2006b). *Environmental Consequences of the Chernobyl Accident and Their Remediation: Twenty years of Experience (Report of the Chernobyl Forum Expert Group 'Environment')*. Vienna: IAEA.

OECD/NEA. (2002). *Chernobyl Assessment of Radiological and Health Impacts*. Paris: OECD.

Smith, J. T., & Beresford, N. A. (2005). Introduction. In J. T. Smith & N. A. Beresford (Eds.), *Chernobyl-Catastrophe and Consequences* (pp. 1-34). Berlin: Praxis Publishing Ltd.

Timms, D. N., Smith, J. T., Coe, E., Kudelsky, A. V., & Yankov, A. I. (2005). In situ measurements of the sub-surface gamma dose from Chernobyl fallout. *Applied Radiation and Isotopes, 62*(6), 923-930.

Tumnoi, Y. (2006). *The effects of chronic radiation dose on the fitness and genetic diversity of Roach (Rutilus rutilus L.) in the Chernobyl region.* University of Portsmouth.

UNSCEAR. (1996). *Sources and effects of ionising radiation*. New York: United Nations.

UNSCEAR. (2000). *Sources and effects of ionising radiation. Volume II: Effect*. New York: United Nations.

Vives i Batlle, J., Balonov, M., Beaugelin-Seiller, K., Beresford, N., Brown, J., Cheng, J. J., et al. (2007). Inter-comparison of absorbed dose rates for non-human biota. *Radiation and Environmental Biophysics, 46*(4), 349-373.

Yankovich, T. L., Batlle, J. V. i., Vives-Lynch, S., Beresford, N. A., Barnett, C. L., Beaugelin-Seiller, K., et al. (2010). An international model validation exercise on radionuclide transfer and doses to freshwater biota. *Journal of Radiological Protection, 30*(2), 299.